3-25-2014 12:00 AM

Indoleamine 2,3-dioxygenase confers resistance to chemotherapy and γ radiation to cancer cells, independent of direct immune involvement

Saman Maleki Vareki
The University of Western Ontario

Supervisor
Dr. James Koropatnick
The University of Western Ontario

Graduate Program in Microbiology and Immunology
A thesis submitted in partial fulfillment of the requirements for the degree in Doctor of Philosophy

Indoleamine 2,3-dioxygenase confers resistance to chemotherapy and γ radiation to cancer cells, independent of direct immune involvement

(Thesis format: Monograph)

by

Saman Maleki Vareki

Graduate Program in Microbiology & Immunology

A thesis submitted in partial fulfillment
of the requirements for the degree of
Doctor of Philosophy

The School of Graduate and Postdoctoral Studies
The University of Western Ontario
London, Ontario, Canada

Abstract

Indoleamine 2,3-dioxygenase-1 (IDO) is an immunosuppressive molecule expressed by most human tumours. IDO levels correlate with poor prognosis in cancer patients and IDO inhibitors are under investigation to enhance endogenous anticancer immunosurveillance. Little is known regarding the immune-independent functions of IDO relevant to cancer therapy. In this thesis I show, for the first time, that IDO mediates human tumour cell resistance, in a cell-autonomous fashion, to single and combination treatment with a diverse group of chemotherapy drugs and γ radiation. These drugs include a PARP inhibitor (olaparib), a DNA cross-linking agent (cisplatin), a folate antimetabolite (pemetrexed), a nucleoside analogue (gemcitabine), a base excision repair inhibitor (methoxyamine), an NAD^+ inhibitor (FK866) and combined treatments with olaparib and radiation and methoxyamine and pemetrexed in the absence of immune cells. Antisense-mediated reduction of IDO, alone and (in a synthetic lethal approach) in combination with antisense to the DNA repair protein BRCA2 sensitizes human lung cancer cells to olaparib and cisplatin. Antisense-mediated reduction of IDO (in a synthetic lethal approach) in combination with antisense to thymidylate synthase sensitizes human lung cancer cells to pemetrexed and 5FUdR. Antisense reduction of IDO decreased NAD^+ in human tumour cells. NAD^+ is essential for PARP activity and these data suggest that IDO mediates treatment resistance independent of its well-established immunomodulatory effects, and at least partially due to a previously unrecognized role for IDO in DNA repair. Furthermore, increased IDO levels correlated with the accumulation of tumour cells in G_1 and depletion of cells in the G_2/M phases of the cell cycle, suggesting that the effects of IDO on the cell cycle may also modulate sensitivity to radiation and chemotherapeutic agents. IDO is a potentially valuable therapeutic target in cancer treatment, independent of immune function and in combination with other therapies.

Keywords:

Indoleamine 2,3-dioxygenase (IDO), cancer, breast cancer type-2 susceptibility protein (BRCA2), Thymidylate synthase (TS), DNA repair, chemotherapy, γ radiation, olaparib, cisplatin, pemetrexed, 5FUdR, gemcitabine, FK866, methoxyamine

Co-Authorship Statement

Experiments presented in Figure 4.63 were conducted by Christine Di Cresce (PhD program, Dept. of Microbiology and Immunology, Schulich School of Medicine and Dentistry, Western University). Experiments presented in Figure 4.66 were carried out by Mateusz Rytelewski (PhD program, Dept. of Microbiology and Immunology, Schulich School of Medicine and Dentistry, Western University). Di Chen (PhD program, Dept. of Pathology, Schulich School of Medicine and Dentistry, Western University) was involved in counting cancer cells in data presented in Figures 4.35, 4.36, 4.37, 4.47, 4.48, and 4.49.

Acknowledgments

Apart from my own efforts, the successful completion if this dissertation depends on the encouragement and guidance of many others. I would like to express my gratitude to all those who helped me during my Ph.D. studies.

Above all, I would like to express my special appreciation and thanks to my supervisor Dr. James Koropatnick, you have been a tremendous mentor for me. I would like to thank you for encouraging my research and for allowing me to grow as a research scientist. Your advice on both research as well as on my career have been priceless.

I would also like to thank my committee members Dr. Joseph Mymryk, Dr. Rodney DeKoter and Dr. Wei-ping Min for serving as my committee members even at hardship. Also special thanks to Dr. Joseph Mymryk for reading this thesis.

I would especially like to thank my friends Mateusz Rytelewski, Christine Di Cresce, Dr. Peter J Ferguson, Rene Figueredo, Dr. Reza Mazaheri and Dr. Julio Masabanda for supporting and helping me during my Ph.D.

I would like to thank my beautiful wife, Solmaz, for love, kindness, and support she has shown me during my PhD studies.

This thesis is dedicated to all international students who left their loved ones behind to follow their dreams; to those who did not quit in the face of tremendous challenges or even hostilities they experienced and finally finished their journey.

Table of Contents

1.1 Introduction synopsis 1

1.2 General Introduction 2

1.3 Major Non-Surgical Methods of Cancer Treatment 3

1.3.1 Chemotherapy 3

1.3.2 Radiation 6

1.3.3 Immunotherapy 6

1.3.4 Combination treatments of cancer 8

1.4 Cancer Treatment Resistance 9

1.4.1 Resistance to Chemotherapy 9

1.4.2 Resistance to Radiation 11

1.4.3 Resistance to Immunotherapy 12

1.5 Indoleamine 2,3-dioxygenase 12

1.5.1 IDO and the Immune System 13

1.5.2 IDO and Cancer 20

1.5.3 IDO Inhibitors 23

1.5.4 IDO Inhibition to Improve Chemotherapy and Radiation 25

1.6 DNA Repair 28

1.7 Base Excision Repair 28

1.7.1 Base Excision Repair and Cancer 32

1.7.2 Base Excision Repair Inhibition in Cancer Treatment 32

1.8 Homologous Recombination Repair 33

1.9 PARPs and DNA Repair 36

1.9.1 PARP-1 and XRCC1 39

1.9.2 PARP-2 and XRCC1 39

1.9.3 PARP-1 and Homologous Recombination Repair 39

1.9.4 Inhibiting PARP in Cancer Treatment 40

1.10 Nicotinamide Adenine Dinucleotide 40

1.10.1 *De Novo* NAD^+ Biosynthesis 40

1.10.2 Salvage Pathway of NAD^+ Biosynthesis 44

1.11 NAD^+ and DNA Repair 44

1.12 NAD^+ Inhibition as a Strategy for Cancer Treatment 45

1.13 Thymidylate Synthase 46

1.13.1 TS Inhibition in Cancer 46

1.14 Targeting mRNA with RNA Interference 47

2 Thesis Hypotheses: 49

2.1 Thesis Objectives 49

2.2 Thesis Overview 50

3 Materials and Methods 54

3.1 Cell Culture 54

3.2 Cytotoxic Drugs 54

3.3 Stable IDO Downregulation 55

3.3.1 Bacterial Strain, Growth, and Preparation of Competent Cells 55

3.3.2 Plasmid Quality Control and Diagnostic Restriction Digest 61

3.4 Transient Transfection of A549 Cells with anti-IDO shRNA or Scrambled shRNA Plasmids 63

3.5 RNA Isolation 63

3.6 IDO mRNA Detection via Conventional PCR 64

3.7 IDO mRNA Quantitation by Real-Time PCR 64

3.8 IDO, BRCA2 and TS Protein Detection and Measurement 66

3.9 NAD^+ Quantification 66

3.10 Cell Cycle Analysis 67

3.11 Olaparib Treatment 67

3.12 γ Radiation Treatment 68

3.13 Combined Treatment with Radiation and Olaparib 68

3.14 Cisplatin, Gemcitabine, Pemetrexed, and 5FUdR Treatment 68

3.15 Blocking NAD^+ Synthesis by FK866 Treatment 69

3.16 Blocking BER by Methoxyamine Treatment 69

3.17 Combined Treatment with Pemetrexed and MX 69

3.18 IDO siRNA Transfection 69

3.19 BRCA2 siRNA Transfection and Drug Treatment 72

3.20 TS siRNA Transfection and Drug Treatment 72

3.21 Puromycin Treatment of A549 Cells 73

3.22 Colony Forming Assay after Irradiation 73

3.23 Statistical Analysis 73

4 Results 75

4.1 IDO Induction in A549 and HeLa Cells 75
4.2 IDO mRNA Levels in H441 Cells 84
4.3 IDO siRNA Downregulation in A549 and H441 Cells 87
4.4 Plasmid Quality Control and Diagnostic Restriction Digest (anti-IDO shRNA Stable Transfection) 87
4.5 IDO mRNA Quantification in A549 and H441 Clonal Population 98
4.6 IDO Protein Levels in A549 and HeLa Clonal Populations 105
4.7 IDO Levels are Inversely Correlated with Tumour Cell Proliferation 105
4.8 IDO Effect on A549 Cell Cycle 105
4.9 IDO Downregulation Decreases Intracellular NAD^+ 116
4.10 IDO Mediates Resistance to the NAD^+ Inhibitor FK866 116
4.11 IDO in Tumour Cells Mediates Resistance to Olaparib 121
4.12 IDO Mediates Resistance to γ Radiation in Cancer Cells 136
4.13 IDO in Human Tumour Cells Mediates Resistance to Combined γ Radiation and PARP Inhibition 151
4.14 IDO in Human Tumour Cells Mediates Resistance to the Base Excision Repair Inhibitor Methoxyamine 164
4.15 IDO in Human Tumour Cells Mediates Resistance to the TS-targeting Drug Pemetrexed 164
4.16 IDO in Human Tumour Cells Mediates Resistance to Combined Treatment of Pemetrexed and Methoxyamine 177
4.17 The Effect of IDO Downregulation in Human Tumour Cells Sensitivity to other TS-targeting Drugs (5FUdR and Gemcitabine) 184
4.18 The Effect of IDO Downregulation in Human Tumour Cells' Sensitivity to Cisplatin 193
4.19 Thymidylate Synthase siRNA Downregulation in A549 Clonal Populations 208
4.20 Thymidylate Synthase siRNA Downregulation in A549 Clonal Populations after IFNγ Induction 208
4.21 TS siRNA Downregulation in A549 Clonal Populations 213
4.22 TS Downregulation Enhances the Capacity of IDO Downregulation to Sensitize A549 Cells to Pemetrexed 213
4.23 IDO Downregulation Enhances the Capacity of TS Downregulation to Sensitize A549 Cells to 5FUdR 219
4.24 BRCA2 Downregulation in A549 Clonal Populations 223

4.25 Concurrent IDO and BRCA2 Downregulation Sensitizes A549 Cells to the PARP Inhibitor Olaparib More than Knockdown of Either Gene Alone 226
4.26 Concurrent IDO and BRCA2 Downregulation Sensitizes A549 Cells to the DNA Cross-linking Agent Cisplatin More than Knockdown of Either Gene Alone 229
4.27 Concurrent IDO and BRCA2 Downregulation does not Sensitize A549 Cells to 5FUdR 229

5 Chapter 5 234

Discussion 234

5.1 IDO Induction in A549 and HeLa Cells 234
5.2 IDO siRNA Downregulation in A549 and H441 Cells 235
5.3 Stable Transfection of A549, HeLa and H441 Cells with anti-IDO shRNA 236
5.4 The Effects of IDO on the A549 Cell Cycle 236
5.5 IDO Downregulation Decreases Intracellular NAD^+ 237
5.6 IDO in Tumour Cells Mediates Resistance to the NAD^+ Inhibitor FK866 238
5.7 IDO in Tumour Cells Mediates Resistance to Olaparib 238
5.8 IDO Mediates Resistance to γ Radiation in Cancer Cells 239
5.9 IDO in Human Tumour Cells Mediates Resistance to Combined γ Radiation and PARP Inhibition 240
5.10 The Effect of IDO Downregulation on Human Tumour Cell Sensitivity to Cisplatin 240
5.11 IDO in Human Tumour Cells Mediates Resistance to the Base Excision Repair Inhibitor Methoxyamine 241
5.12 IDO in Human Tumour Cells Mediates Resistance to the TS-targeting Drug Pemetrexed 241
5.13 IDO in Human Tumour Cells Mediates Resistance to Combined Treatment of Pemetrexed and Methoxyamine 242
5.14 The Effect of IDO Human Tumour Cell Sensitivity to Other TS-targeting Drugs (5FUdR and Gemcitabine) 242
5.15 Concurrent IDO and TS Downregulation Sensitized A549 Cells to Pemetrexed More than Knocking Down Either Gene Alone 243
5.16 Concurrent IDO and TS Downregulation Sensitizes A549 Cells to 5FUdR to a Greater Degree than Reduction of Either Target Alone 244

5.17 Concurrent IDO and BRCA2 Downregulation did Not Sensitize A549 Cells to 5FUdR **244**
5.18 Concurrent IDO and BRCA2 Downregulation Sensitizes A549 Cells to the PARP Inhibitor Olaparib More than Knockdown of Either Gene Alone **245**
5.19 Concurrent IDO and BRCA2 Downregulation Sensitizes A549 Cells to Cisplatin to Greater Degree than Knockdown of Either Target Alone **245**
5.20 A new function for IDO **246**
5.21 Limitations: **246**
6 Chapter 6 ..... **248**
6.1 Significance **248**
6.2 Future Directions **249**
Refrences……..250
Appendix……..267
Curriculum Vitae…….276

List of Tables

Table 1. 1. Many human tumours express IDO.. 22
Table 1. 2. IDO inhibition increases the effectiveness of certain chemotherapeutic drugs in the presence of the immune system in a mouse model of breast cancer. 27
Table 3. 1. SureSilencing shRNA plasmid sequences. 57
Table 3. 2. IDO and GAPDH PCR primer sequences. 65
Table 3. 3. ON-Target Plus® IDO1, TS and BRCA2 siRNA target mRNA sequences. .. 71

List of Figures

Figure 1. 1. IDO function. 17
Figure 1. 2. IDO suppression of immune cells. 19
Figure 1. 3. The BER pathway. 31
Figure 1. 4. Homologous recombination repair of DSB. 35
Figure 1. 5. PARP function during DNA damage and repair. 38
Figure 1. 6. *De novo* NAD^+ production. 43
Figure 3. 1. The puromycin-resistant vector pGeneClip™ 59
Figure 4. 1. Quality of RNA isolated from A549 cells ± IFNγ (50 ng/ml). 77
Figure 4. 2. IDO mRNA levels in A549 cells ± IFNγ (25, 50 or 100 ng/ml). 79
Figure 4. 3. IDO mRNA levels in HeLa cells ± IFNγ (25, 50 or 100 ng/ml). 81
Figure 4. 4. IDO protein levels in A549 cells ± IFNγ (25 ng/ml). 83
Figure 4. 5. IDO mRNA levels in H441 cells. 86
Figure 4. 6. IDO mRNA levels in A549 cells after transfection with IDO siRNA. 89
Figure 4. 7. IDO mRNA levels in H441 cells after transfection with IDO siRNA. 91
Figure 4. 8. qPCR analysis of IDO mRNA in A549 cells following siRNA transfection. 93
Figure 4. 9. qPCR analysis of IDO mRNA in H441 cells following siRNA transfection. 95
Figure 4. 10. Pst 1 digestion to confirm the presence of IDO shRNA in the expression vector. 97
Figure 4. 11. IDO mRNA quantification in A549 clonal populations. 100
Figure 4. 12. IDO mRNA levels in selected A549 clonal cell lines. 102
Figure 4. 13. IDO mRNA quantification in H441 clonal populations. 104
Figure 4. 14. IDO protein levels in A549 clonal cell populations with and without IFNγ (25 ng/ml) treatment. 107
Figure 4. 15. IDO protein levels in HeLa clonal cells with and without IFNγ (25 ng/ml) treatment. 109
Figure 4. 16. IDO slows proliferation of A549 cells and anti-IDO shRNA attenuates the IDO-mediated reduction in proliferation. 111
Figure 4. 17. IDO slows proliferation of HeLa cells and anti-IDO shRNA attenuates IDO-mediated reduction in proliferation. 113

Figure 4. 18. IDO mediated the increased accumulation of cells in G_1 and decreased accumulation in G_2/M in A549 cells..... 115
Figure 4. 19. IDO downregulation decreased NAD^+ in A549 cells..... 118
Figure 4. 20. A549 clonal cell population sensitivity to FK866 (5 nM) before and after IDO induction. 120
Figure 4. 21. A549 clonal cell population sensitivity to low dose olaparib (1.5 μM) before and after IDO induction.. 123
Figure 4. 22. Sensitivity of clonal A549 populations to low dose olaparib (1.5 μM) before (A) and after (B) IDO induction. 125
Figure 4. 23. A549 clone sensitivity to high dose olaparib (5 μM) before and after IDO induction. 127
Figure 4. 24. Sensitivity of clonal A549 populations to high dose olaparib (5 μM) before (A) and after (B) IDO induction.. 129
Figure 4. 25. Induction of IDO in A549 clonal cell populations decreases the effectiveness of olaparib. 131
Figure 4. 26. HeLa clone sensitivity to high dose olaparib (5 μM) before and after IDO induction.. 133
Figure 4. 27. Sensitivity of clonal HeLa populations to high dose olaparib (5 μM) before (A) and after (B) IDO induction.. 135
Figure 4. 28. A549 clone sensitivity to γ radiation (4 Gy) before and after IDO induction. 138
Figure 4. 29. Sensitivity of clonal A549 populations to γ radiation (4 Gy) before (A) and after (B) IDO induction..... 140
Figure 4. 30. Induction of IDO in A549 clonal cell induces resistance to γ radiation.... 142
Figure 4. 31. Induction of IDO in A549 clonal cell induces resistance to γ radiation.... 144
Figure 4. 32. HeLa clone sensitivity to γ radiation (4 Gy) before and after IDO induction. 146
Figure 4. 33. Sensitivity of clonal HeLa populations to γ radiation (4 Gy) before (A) and after (B) IDO induction..... 148

Figure 4. 34. Induction of IDO in HeLa clonal cell populations and association with resistance to γ radiation.. 150
Figure 4. 35. A549 sensitivity to combined γ irradiation (4 Gy) and olaparib (5 μM) treatment before (A) and after (B) IDO induction. 153
Figure 4. 36. Sensitivity of clonal A549 populations to combined γ radiation (4 Gy) and olaparib (5 μM) treatment before (A) and after (B) IDO induction. 155
Figure 4. 37. Induction of IDO in A549 clonal cell induces resistance to combined γ radiation and olaparib treatment. 157
Figure 4. 38. HeLa sensitivity to combined γ irradiation (4 Gy) and olaparib (5 μM) treatment before (A) and after (B) IDO induction.. 159
Figure 4. 39. Sensitivity of clonal HeLa populations to combined γ radiation (4 Gy) and olaparib (5 μM) treatment before (A) and after (B) IDO induction. 161
Figure 4. 40. Antisense reduction of IDO in A549 clonal cell reduces resistance to combined γ radiation and olaparib treatment. 163
Figure 4. 41. A549 clone sensitivity to methoxyamine (3 mM) before and after IDO induction.. 166
Figure 4. 42. Sensitivity of clonal A549 populations to methoxyamine (3 mM) before (A) and after (B) IDO induction.. 168
Figure 4. 43. Induction of IDO in A549 clonal cell induces resistance to methoxyamine (3 mM)..... 170
Figure 4. 44. A549 clone sensitivity to pemetrexed (200 nM) before and after IDO induction. 172
Figure 4. 45. Sensitivity of clonal A549 populations to pemetrexed (200 nM) before (A) and after (B) IDO induction. 174
Figure 4. 46. Induction of IDO in A549 clonal cell induces resistance to pemetrexed (200 nM).. 176
Figure 4. 47. A549 clone sensitivity to combined pemetrexed (30 nM) and methoxyamine (3 mM) treatment before and after IDO induction..... 179
Figure 4. 48. Sensitivity of clonal A549 populations to combined pemetrexed (30 nM) and methoxyamine (3 mM) treatment before (A) and after (B) IDO induction.. ... 181

Figure 4. 49. Induction of IDO in A549 clonal cell induces resistance to combined pemetrexed (30 nM) and methoxyamine (3 mM) treatment. 183
Figure 4. 50. A549 clone sensitivity to 5FUdR (200 nM) before and after IDO induction. 186
Figure 4. 51. Sensitivity of clonal A549 populations to 5FUdR (200 nM) before (A) and after (B) IDO induction. 188
Figure 4. 52. A549 clone sensitivity to gemcitabine (10 nM) before and after IDO induction. 190
Figure 4. 53. Sensitivity of clonal A549 populations to gemcitabine (10 nM) before (A) and after (B) IDO induction. 192
Figure 4. 54. A549 clone sensitivity to cisplatin (8 μM) before and after IDO induction. 195
Figure 4. 55. Sensitivity of clonal A549 populations to cisplatin (8 μM) before (A) and after (B) IDO induction. 197
Figure 4. 56. Induction of IDO in A549 clonal cell induces resistance to cisplatin (8 μM). 199
Figure 4. 57. HeLa clone sensitivity to cisplatin (4 μM) before and after IDO induction. 201
Figure 4. 58. Sensitivity of clonal HeLa populations to cisplatin (4 μM) before (A) and after (B) IDO induction. 203
Figure 4. 59. Induction of IDO in HeLa clonal cell induces resistance to cisplatin (4 μM). 205
Figure 4. 60. H441 clone sensitivity to cisplatin (5 and 10 μM). 207
Figure 4. 61. TS siRNA transfection of A549 cells. 210
Figure 4. 62. TS siRNA downregulation in A549 cells after IFNγ (16 ng/ml) treatment. 212
Figure 4. 63. TS siRNA downregulation in A549 clonal populations. A549 clonal cells were seeded and grown overnight. 215
Figure 4. 64. Concurrent IDO and TS downregulation sensitizes A549 cells to pemetrexed more effectively than knockdown of IDO alone. 218

Figure 4. 65. Concurrent IDO and TS downregulation sensitizes A549 cells to 5FUdR more effectively than knockdown of TS alone.. 222
Figure 4. 66. siRNA downregulation of BRCA2 in A549 clones NC-3 and 2-18.. 225
Figure 4. 67. Concurrent IDO and BRCA2 downregulation sensitized cancer cells to olaparib to a greater degree than the knockdown of either gene alone..... 228
Figure 4. 68. Concurrent downregulation of IDO and BRCA2 sensitizes A549 to cisplatin in an additive fashion.. 231
Figure 4. 69. Concurrent downregulation of IDO and BRCA2 did not sensitize A549 to the TS-targeting drug 5FUdR to a greater degree than the knockdown of either gene alone. 233

List of abbreviations

Abbreviation	Meaning
1-MT	1-methyl tryptophan
5FUdR	2'-deoxy-5-fluorouridine
KMO	3-monooxygenase
PIM	4-phenylimidazole
CH_2-THF	5, 10-methylenetetrahydrofolate
5FU	5-fluorouracil
FdUMP	5-fluoro-2′-deoxyuridine-5′-monophosphate
FdUTP	5-fluoro-2′-deoxyuridine-5′-triphosphate
Ags	antigens
APCs	antigen presenting cells
AP site	apurinic or apyrmidinic site
APE1	apurinic/apyrimidinic endonuclease
Ago	Argonaute
ATR	ATM- and RAD3-related protein kinase
ABC	ATP-binding cassette
BER	Base excision repair
BCL-2	B cell lymphoma-2
BM	bone marrow
BRCP	breast cancer resistance protein
BRCA2	breast cancer type-2 susceptibility protein
CARs	chimeric antigen receptors
CN^-	cyanide ion
DMEM	Dulbecco's Modified Eagel Medium
DCs	dendritic cells
dCK	deoxycytidine kinase
dCMP	deoxycytidine monophosphate
dRP	deoxyribophosphate
dTMP	deoxythymidine-5'-monophosphate
dUMP	deoxyuridine monophosphate

DAP12	DNAX-activation protein 12
DSBs	double-strand breaks
dsDNA	double-stranded DNA
dsRNA	double-stranded RNA
FEN1	flap structure-specific endonuclease 1
FDA	US Food and Drug Administration
FOXO3	forkhead box O3
dFdCDP	gemcitabine diphosphate
dFdCTP	gemcitabine triphosphate
GCN-2	general control non-repressed-2
GST	glutathione S-transferases
GM-CSF	granulocyte-macrophage colony-stimulating factor
GVHD	graft versus host disease
Gy	Gray
HMG	high mobility group
HRR	homologous recombination repair
HER2	human epidermal growth factor 2
HAD	hydroxyanthranilate-3,4-dioxygenase
IDO	indoleamine 2,3-dioxygenase
IFNα	interferon α
IFNγ	interferon gamma
IRF-8	interferon regulatory factor-8
IL-2	interleukin-2
ICLs	interstrand crosslinks
KA	kynurenic acid
KFase	Kynurenine formamidase
L-1MT	L-stereoisomer of 1MT
MEMα	Minimal Essential Medium α
mTOR	mammalian target of rapamycin
MHC	major histocompatibility complex
mRNA	messenger RNA

MX	methoxyamine
MMR	mismatch repair
MMTV	mouse mammary tumour virus
MRP-1	multidrug resistance-associated protein-1
MDS	myelodysplastic syndrome
MDSC	myeloid-derived suppressor cell
NMDA	N-methyl-D-aspartate
NK	natural killer
NAAD	nicotinic acid adenine dinucleotide
NADS	nicotinamide adenine dinucleotide synthase
NaMN	nicotinic acid mononucleotide
NMNs	nicotinic acid mononucleotides
NAM	nicotinamide
NR	nicotinamide riboside
NA	nicotinic acid
NAD^+	nicotinamide adenine dinucleotide
NMNAT	nicotinamide mononucleotide adenylyltransferase
NHEJ	nonhomologous end-joining
NSCLC	non-small cell lung cancer
NSCLC	non-small cell lung carcinoma
NRK	nicotinamide riboside kinase
NER	nucleotide excision repair
ODNs	oligodeoxynucleotides
P-gp	permeability glycoprotein
PAR	polymer of adenosine diphosphate-ribose
PARP-1	poly(adenosine diphosphate-ribose) polymerase-1
PolB	polymerase β
PolD	polymerase δ
PloE	polymerase ε
PCNA	proliferating cell nuclear antigen
PAP	prostatic acid phosphatase

QA	quinolinic acid
QAPRT	QA phosphoribosyltransferase
RNase	ribonuclease
RR	ribonucleotide reductase
RNAi	RNA interference
RISC	RNA-induced silencing complex
RPMI	Roswell Park Memorial Institute Medium
shRNA	short hairpin RNA
SSBs	single-strand breaks
SSBR	single-strand break repair
ssDNA	single-stranded DNA
siRNA	small interfering RNA
SOCS3	suppressor of cytokine signaling 3
CTLA-4	T lymphocyte antigen 4
TH	T helper
TK	thymidine kinase
TMP	thymidine monophosphate
TS	thymidylate synthase
T_{regs}	T regulatory cells
TMZ	temozolomide
topo IIα	topoisomerase IIα
TGF-β	transforming growth factor-β
TDO	tryptophan 2,3-dioxygenase
TDLNs	tumour-draining lymph nodes
TNF-α	tumour necrosis factor (TNF)-α
UV	ultraviolet
UDG	uracil DNA glycosylase
VEGF	vascular endothelial growth factor
XRCC1	X-ray repair cross-complementing protein 1

Chapter 1

1.1 Introduction synopsis

In this chapter I briefly describe non-surgical methods common in cancer treatment, including chemotherapy, radiation, immunotherapy, and combinations utilizing more than one therapeutic approach. This review illuminates the exploration of cancer-relevant functions of the immunoregulatory molecule indoleamine 2,3-dioxygenase (IDO), a cellular enzyme potentially involved in mediating resistance to these treatments and the subject of this thesis.

In the chemotherapy section, major chemotherapeutic agents used in patient treatment (and assessed in the context of altered IDO expression in this thesis) are introduced and their mechanism of action described. Cellular mechanisms mediating resistance to major treatment methods are then described, followed by a description of IDO and its known role(s) in immune regulation and cancer.

IDO inhibitors and the effect of IDO inhibition in cancer treatment is then described as a background to understanding the strategies and experimental consequences of IDO inhibition in human tumour cell response to chemotherapy and/or radiation.

DNA repair events in tumour cells, including base excision repair (BER) and homologous recombination repair (HRR) are then reviewed as a background to understanding IDO functions proposed, in this thesis, to be associated with those repair events. Poly(adenosine diphosphate-ribose) polymerase (PARP) molecules and their role in BER and HRR is described as a basis for understanding the hypothesis that PARP activity is affected by IDO activity. Because PARP activity depends on nicotinamide adenine dinucleotide (NAD^+), and IDO mediates *de novo* NAD^+ synthesis, NAD^+ and its role in DNA repair is described; data presented in this thesis show that IDO downregulation decreases NAD^+ levels in cancer cells, and NAD^+ inhibition is proposed as a strategy to treat cancer. A role for IDO in mediating resistance to such strategies is described in this thesis.

Thymidylate synthase (TS) is introduced as a background to understanding the role of IDO downregulation in resistance to three TS-targeting drugs (pemetrexed, 5FUdR, and gemcitabine), alone or in combination with TS inhibition.

Finally, and to assist in understanding the technology used in this thesis to modulate IDO and TS in human tumour cells, antisense-mediated downregulation of messenger RNA (mRNA) as a technology to reduce specific cellular targets, both as a discovery tool and as potential therapeutic strategy, is described.

1.2 General Introduction

Malignancy in cancer cells occurs in a stepwise fashion and is enhanced by genomic instability, which is a major generator of mutations that are the basis of selection for cells by conditions existing in host organisms (availability of nutrients, growth factors or lack of them, oxygenation, sensitivity to drug treatments, capacity to evade immune detection, and others) [1]. Genetic instability in cancer was first hypothesized by Boveri, based on the consequences of aneuploidy on the growth of sea urchin embryos [2]. Because of genomic instability, individual cancer cells each harbour on the order of 10,000 mutations that distinguish them from a parental stem cell. Clinically detectable tumours contain 10^8-10^9 cells and can have more than 10^{11} mutations [3]. Because a high mutation rate and selection pressures driving Darwinian evolution are not mutually exclusive, genomic instability has the potential to enhance fitness of cells comprising tumours, such that they are well-adapted to survive and grow in their hosts [3]. However, it is likely that there is a maximum number of unrepaired DNA damage events and resulting mutations, DNA duplications, DNA translocations, and chromosomal abnormalities arising from DNA damage, that tumour cells can tolerate before reaching a limit that, when exceeded, alters cellular fitness and becomes a detriment to fitness [3]. This has been proposed as a reason, with the exception of P53 [4] and the DNA polymerase β encoding gene POLB [5], that most genes involved in DNA repair and/or DNA replication are intact in cancer cells [3]. A high mutation rate and resulting heterogeneity in tumour cell populations can also be a source of cells with resistance to chemotherapy, which could impede personalized medicine for cancer treatment [3]. Moreover, the possibility of converting a passenger mutation to a driver because of the changes in the tumour microenvironment due to selective pressure of internal and/or external factors, such as the immune system or chemotherapy, can also inhibit the effectiveness of cancer treatment [6]. This is an important phenomenon that should be

considered when proposing and testing treatments for cancer, since passenger mutations normally do not have any functional consequences such as conferring clonal growth advantage to cancer cells, but driver mutations are often selected for and they could confer growth or survival advantages to cancer cells [6].

1.3 Major Non-Surgical Methods of Cancer Treatment

1.3.1 Chemotherapy

Modern chemotherapy began in 1942, with the discovery of nitrogen mustard as an effective cancer treatment [7]. However, early observations of tumours developing resistance to chemotherapy after application of therapeutic drugs [8, 9] continue to the present day, and remain a major obstacle in the treatment of cancer patients with chemotherapy [10]. Traditionally, chemotherapy involves treatment with cytotoxic drugs that interfere with DNA synthesis and cell proliferation [11]. In the new era of chemotherapy, drugs also target many of the signaling networks that regulate cell proliferation and survival in cancer cells -- either targets that are unique to cancer cells (proteins or peptides not found in non-tumour cells) or that are preferentially expressed or depended on to mediate malignant characteristics and/or survival – in a strategy termed "targeted therapy" [7]. These drugs mainly consist of antibodies and small molecule kinase inhibitors that target specific molecules important to different signaling events, and that result in decreased cell proliferation and survival [11]. For example, Trastuzumab, a humanized monoclonal antibody that targets human epidermal growth factor 2 (HER2), in combination with common chemotherapy agents cisplatin plus capecitabine or 5-fluorouracil (5FU) is more effective than chemotherapy alone in increasing the median overall survival of gastric cancer patients [12]. Gefitinib, which is a small-molecule epidermal growth factor receptor-tyrosine kinase inhibitor, is used to treat patients with non-small cell lung cancer (NSCLC) [13].

1.3.1.1 Cisplatin

Cisplatin (cis-diammine-dichloro-platinum) is a platinum-based chemotherapy drug that is commonly used to treat various forms of solid tumours including ovarian, testicular, and head and neck [14]. Cisplatin primarily targets DNA by forming DNA-

protein and DNA-DNA interstrand and intrastrand crosslinks [15]. However, its cytotoxic function is mostly attributed to its ability to form interstrand adducts [16]. P53 plays a major role in cisplatin-induced apoptosis. Cisplatin is known to preferentially activate ATM- and RAD3-related protein kinase (ATR) that regulates the stability and transcriptional activity of P53 in cells [17]. Cisplatin-mediated induction and/or activation of P53 results in transactivation of several genes that are associated with cell cycle inhibition, DNA repair, and apoptosis including $p21^{Waf1/Clip1}$, the DNA damage-inducible *gadd45a* gene, and the pro-apoptotic gene *bax* [18]. The Gadd45a protein enhances nucleotide excision repair (NER) activity counteracting cisplatin function [19]. However, cisplatin-induced DNA damage can exceed cellular DNA repair capacity and induce apoptosis in the treated cells [14]. Translocation of the pro-apoptotic bax protein following cisplatin treatment triggers a cascade of events in the treated cells that finally results in apoptosis, including release of cytochrome c followed by the activation of caspase 9-caspase 3 pathway [20, 21].

1.3.1.2 Pemetrexed

Pemetrexed (Alimta) is an antifolate antimetabolite that targets multiple enzymes involved in both pyrimidine and purine synthesis. Those enzymes include TS, glycinamide ribonucleotide formyltransferase, dihydrofolate reductase, and aminoimidazole carboxamide ribonucleotide formyltransferase [22]. TS inhibition is the primary mechanism of action of pemetrexed, which results in decrease of available thymidine necessary for DNA synthesis [23, 24]. Pemetrexed enters the cells via the reduced folate carrier, the α-folate receptor, and proton-coupled folate transporter [25]. Inside the cell, pemetrexed has high affinity for folylpolyglutamate synthase that renders it to a polyglutamated form that is 60-fold more potent in TS inhibition [26]. Glutamation also increases the retention of pemetrexed inside the cell resulting in both extended exposure time and increased intracellular levels of it in treated cells [22]. Pemetrexed induces G_1/S cell cycle arrest arising from its antifolate activity and induces P53-independent cell death in cancer cells [22]. Combining pemetrexed with other cytotoxic agents has shown additive or synergistic effects both *in vitro* and *in vivo*. For example, combinations of pemetrexed with each of the platinum agents cisplatin, carboplatin, and

oxaliplatin results in either additive or greater than additive sensitivity of Calu-6 and H460 non-small cell lung carcinoma (NSCLC) xenografts to the treatment [27]. Moreover, pretreatment of H460 NSCLC xenografts with pemetrexed before fractionated radiation therapy delays tumour growth in mice as compared to radiation treatment alone. Therefore, combining pemetrexed to radiotherapy may increase the effectiveness of the latter [27].

1.3.1.3 5FUdR

5-Fluoro-2'-deoxyuridine (5FUdR) is a pyrimidine analog that inhibits TS, resulting in the depletion of intracellular thymidine monophosphate (TMP) [28]. This drug is approved for the treatment of a wide range of cancers including brain, colorectal, and liver [29-31]. 5FUdR is the deoxyribonucleoside derivative of 5FU [30]. It inhibits TS through 5-fluoro-2′-deoxyuridine-5′-monophosphate (FdUMP). 5FUdR enters cells via facilitated nucleoside transport systems [32]. Upon entry, 5FUdR is either phosphorylated to its active nucleotide FdUMP by thymidine kinase (TK), or cleaved to 5FU by thymidine phosphorylase [30]. In the presence of adequate amounts of TS co-substrate 5, 10-methylene-tetra hydrofolate (CH_2-THF), FdUMP and TS form a stable ternary complex that strikingly increases the extent and duration of TS inhibition resulting in enhanced antitumour activity [33].

1.3.1.4 Gemcitabine

Gemcitabine (2′, 2′-difluorodeoxycytidine) is a pyrimidine antimetabolite that is widely used to treat diverse malignancies, including pancreatic cancer, ovarian cancer, malignant mesothelioma, and NSCLC [34, 35]. Deoxycytidine kinase (dCK) phosphorylates gemcitabine to its cytotoxic nucleotides, gemcitabine diphosphate (dFdCDP) and triphosphate (dFdCTP) [36]. These phosphorylated nucleotides are retained inside cells [37]. Gemcitabine nucleotides inhibit deoxycytidine monophosphate (dCMP) deaminase and ribonucleotide reductase (RR). dCMP deaminase is responsible for production of deoxyuridine monophosphate (dUMP) from dCMP and RR is essential for the *de novo* synthesis of the deoxyribonucleotides required for DNA replication [35].

Thus, gemcitabine inhibits cellular DNA synthesis and induces DNA fragmentation and apoptosis in cells [38].

1.3.2 Radiation

Invention of the linear accelerator in 1960 was a major breakthrough that made radiotherapy an invaluable treatment modality for local and regional tumours [7]. Today, radiation is used to treat approximately 50% of all cancer patients. Patient outcome after radiation varies among different cancers and different stages of the disease. For example, patients with early stage NSCLC have a much higher survival rate after radiotherapy compared to patients with late stage NSCLC [39]. Also, and despite all the advances in radiation techniques, radioresistant tumours are common and there exists an urgent need to increase tumour responsiveness and sensitivity to radiation treatment [39].

1.3.3 Immunotherapy

The concept of cancer immunotherapy dates back to the late nineteenth century when William B. Coley tested cancer treatments involving administration of live and heat-killed bacteria and bacterial components systemically or directly into human tumours [40]. Cancer immunotherapy attempts to harness the power of the immune system to destroy cancer cells [41]. Cytokines such as interleukin-2 (IL-2) and interferon α (IFNα) are already being used in clinic to treat melanoma patients [41]. IL-2 is primarily involved in T cell proliferation and immune regulation [42]. IL-2 therapy is approved for hematological malignancies as well as renal cell carcinoma [41]. IFNα is a type I IFN with multiple functions including induction of apoptosis, as well as inhibition of proliferation and angiogenesis in treated cells [43].

Monoclonal antibodies are currently also used in clinical practice. For example, trastuzumab (Herceptin) is a monoclonal antibody that targets Her2 on the cell surface and is often used to treat breast cancer. Rituximab is another antibody that targets the B cell surface marker CD20. Rituximab is therefore approved for the treatment of B cell lymphoma [44]. These antibodies can directly induce apoptosis [41], or inhibit the proliferation of the tumour cells by blocking growth factor receptors [45]. Furthermore, monoclonal antibodies can indirectly contribute to the destruction of the tumour by

recruiting cytotoxic cells of the immune system, such as macrophages, natural killer (NK) cells and T cells to the tumour microenvironment [46, 47].

A recent advancement in the field of tumour immunotherapy is the reprograming of T lymphocytes to target specific antigens (Ags) on the surface of tumour cells by chimeric antigen receptors (CARs) [48]. CARs are genetically designed constructs consisting of an Ag-specific antibody molecule that is linked to a T cell signaling domain that can be accompanied by a co-stimulatory signal that significantly improves the activation of CAR-expressing T cells [49]. Since CAR-expressing T cells recognize their target cell in a major histocompatibility complex (MHC)-independent fashion, exploiting the antigen-specific properties of the monoclonal antibody, they are not affected by MHC downregulation at the surface of the tumour cells, a phenomenon common in most human cancers [49].

Another common immunotherapy approach is to design vaccines that could either increase tumour immune recognition or enhance T cell antitumour function [50]. Tumour vaccines include whole tumour cell lysates [51], recombinant viral vectors that encoded tumour Ags [52], dendritic cells (DCs) loaded with tumour Ags [53], DNA vectors encoding tumour Ags [54], and synthetic peptides [55]. Most cancer vaccines have failed to extend the overall survival of patients [56]. However, two new immune-based treatments -- sipuleucel-T and ipilimumab have demonstrated the capacity to achieve this endpoint – and have now been approved by the US Food and Drug Administration (FDA) for the treatment of patients with metastatic prostate cancer and melanoma, respectively, and have focused recent attention to cancer immunotherapy [57]. Sipuleucel-T is a cellular immunotherapy that relies on the patient's own antigen presenting cells (APCs) that have been activated *in vitro* with recombinant human prostatic acid phosphatase (PAP) and granulocyte-macrophage colony-stimulating factor (GM-CSF) [58]. PAP is expressed in ~95% of prostate cancers and is primarily limited to the prostate. GM-CSF, on the other hand, is a major activator of immune cells, especially of the granulocyte and macrophage lineage, and acts as an immune adjuvant [59]. Patients who received sipuleucel-T showed a 4.1 month increase in their median overall survival compared to patients receiving placebo [58]. Ipilimumab, on the other hand, is an anti-cytotoxic T lymphocyte antigen 4 (CTLA-4)-blocking antibody approved by the FDA in 2011 for the

treatment of metastatic melanoma [60]. CTLA-4 is expressed on T cells and when bound to B7 ligands (CD80 and CD86) on APCs, induces inhibitory downstream T cell receptor signaling which inhibits T cell function [61]. CTLA-4 is also expressed on the surface of $CD25^+$ $FOXP3^+$ T regulatory cells (T_{regs}) and is important to their immune suppressive function [60]. Ipilimumab-mediated blocking of CTLA-4 increases T cell function and depletes T_{regs} [62]. Since ipilimumab's mechanism of action is independent of the tumour type and is specific to T cells, this drug is also being investigated for treatment of prostate, lung, renal, and breast cancers [60].

1.3.4 Combination treatments of cancer

All three treatment modalities described above have the capacity, alone or in combination, to inhibit tumour growth partially or completely or to ablate tumours completely (temporarily or permanently). However, none is effective or curative in all cases, and its effectivness depends on histologically and molecularly defined tumour type and tissue origin. Because most human tumours develop resistance to individual therapeutic agents [63-65], combining multiple treatment methods (applied concurrently or sequentially) can at least partially reduce the risk of developing treatment resistance, and the development of new treatment combinations is an important and promising strategy to improve cancer therapy. Optimally-timed combination treatment of NSCLC cells with low dose erlotinib and paclitaxel eliminated tumour populations that were otherwise resistant to monotherapy with each drug at the same dose [66]. This is partially because combination therapy can avoid or delay the evolution of drug resistance in a given cancer cell. Moreover, applying high concentrations of a given drug to achieve fast tumour reduction rate is not necessarily the best strategy in the long term, as this could impose maximal selective pressure for evading mutations and acquiring resistance phenotypes in cancer cells. Therefore, using a combination of lower doses of multiple drugs can possibly delay the acquired resistance phenotype in a given tumour [66].

Until recently, combining chemotherapy and immunotherapy was considered antagonistic [67] for two main reasons. First, chemotherapy reduces lymphocyte counts to an abnormally low level (lymphocytopenia), which results in an overall reduction in some forms of immune function due to the treatment imposed immunodeficiency [68].

Second, it was widely accepted that most chemotherapies exert their effect by inducing apoptosis in cancer cells [69], an event that avoids immune stimulation and promotes immune quiescence and tolerance of tumour cell presence in host organisms [67]. This could negatively impact tumour immune surveillance (*i.e.*, the ability of the immune system to recognize and eliminate neoplastic cells, thereby protecting the body from cancer by functioning as an extrinsic immune suppressor) [70]. However, recent advances in our understanding of the immune system make it clear that therapy-induced inhibition and death of immune cells, and the nature of therapy-induced tumour cell death, do not necessarily exclude combined chemo- and immunotherapy. In fact, chemotherapy can, under some circumstances, both induce tumour cell death and induce strong immune responses to cancer cells [67]. For example, chemotherapy-mediated lymphocytopenia induced memory $CD8^+$ T cell proliferation and decreased T_{regs} in the patients with a positive clinical response to temozolomide (TMZ) [71]. Moreover, $CD8^+$ T cell responses against specific melanoma Ags were enhanced in patients after chemotherapy, while their virus-specific T cell responses remained the same [71]. Thus, antitumour immune activity can be maintained or even increased in the face of cytotoxic antitumour chemotherapy [72]. Furthermore, low dose radiation enhances T cell tumour infiltration by normalizing tumour vasculature in melanoma xenografts and mouse pancreatic carcinoma [73].

1.4 Cancer Treatment Resistance

Cancer cells within heterogeneous tumour cell populations harbour mutations that can provide fitness advantages to those subpopulations [74]. Under selective pressure imposed by growth conditions and/or administration of therapeutic agents in host organisms, resistant subpopulations can be selected for preferential survival and growth [74]. Some of the more common mechanisms mediating treatment resistance in cancer cells are described below.

1.4.1 Resistance to Chemotherapy

The effectiveness of chemotherapy is often limited by undesirable, off-target toxicities to normal cells, and by the ability of cancer cells to develop resistance to therapies. There are multiple ways a cancer cell becomes resistant to a given

chemotherapy drug. Here I describe some of the more common mechanisms of resistance to chemotherapy. For example, some cancer cells express a drug efflux pump also known as p-glycoprotein (P-gp), which is ATP-dependent [10]. P-gp is widely expressed among human cancer cells and is coded by the *MDR1* gene [10]. P-gp is capable of binding to a wide variety of hydrophobic drugs and then releasing them out of the cell and into the extracellular matrix. Multidrug resistance-associated protein-1 (MRP-1) is another drug efflux pump and a member of the ATP-binding cassette (ABC) transmembrane transporter superfamily that is composed of 9 proteins expressed by some cancer cells [75, 76]. Other proteins of this superfamily are all related to MRP-1 based on gene sequence. These include, among others, MRP-4, MRP-5, MRP-6, MRP-7, MRP-8, and MRP-9. MRP-7, for instance, is a lipophilic anion transporter that confers resistance to some natural anticancer agents such as docetaxel, paclitaxel, vinblastine, and vincristine [77]. MRP-8 confers resistance to nucleoside-based analogs including 5FU and 5FUdR [78]. Another important ABC family member is breast cancer resistance protein (BCRP). Even though this protein is expressed by most normal tissues including breast, lung, placenta, small intestine, and liver [79], it was first isolated from a resistant breast cancer cell line, hence its name [80]. In normal tissues, BCRP is involved in toxin and xenobiotic efflux as a defensive mechanism [81]. BCRP is expressed in a wide range of hematopoietic and solid tumours and its expression is frequently correlated with poor patient outcome and chemotherapy-resistant disease [80]. In general, cancer cells expressing efflux pumps exhibit reduced sensitivity to multiple drugs [10]. Mutations that alter cell surface molecules, such as mutations in folate binding protein and/or reduced folate transporter, reduce their ability to bind to chemotherapeutic drugs and this can also confer resistance to drugs such as methotrexate [82].

Many other mechanisms of tumour cell drug resistance have been identified in addition to those involved in drug efflux or influx. First, overexpression of glutathione and glutathione s-transferases (GST) that are involved in thiol-mediated detoxification of anticancer drugs is also a known drug resistant mechanism in many cancer cells, especially against platinum-based drugs such as cisplatin [83, 84]. Second, chemotherapy drugs exert their effects by induction of apoptosis [69]. However, some cancer cells can become resistant to apoptosis mainly by downregulation or loss of pro-apoptotic

molecules or by expressing anti-apoptotic proteins [85]. For example, increased expression of the B cell lymphoma-2 (BCL-2) anti-apoptotic protein has been attributed to resistance to many chemotherapy drugs and ionizing radiation [86]. Another major resistance mechanism that is most relevant to this thesis is the ability of cancer cells to repair their DNA after chemotherapy-induced DNA damage. DNA repair mechanisms related to this thesis will be discussed in more detail later. In addition, most DNA repair mechanisms in cancer cells also play major roles in conferring resistance to chemotherapy drugs. For example, BER plays a vital role in tumour cell resistance to the alkylating agent TMZ. DNA lesions that are induced by TMZ are mostly N-methylated bases that are normally recognized by DNA glycosylase members involved in BER. Therefore, TMZ therapeutic efficiency depends on the specific activity of BER in targeted tumour cells [87].

1.4.2 Resistance to Radiation

Radiation causes single and double strand breaks (SSBs and DSBs), damaged bases, and DNA abasic sites (*i.e.*, sites where a base has been lost). Both normal and cancer cells can repair these forms of DNA damage by BER [88, 89]. Ionizing radiation enhances the activity of BER proteins at the G_1 phase of the cell cycle. These proteins help to repair the damaged bases and inhibit radiation-induced cell killing [90]. BER proteins include human endonuclease III that removes damaged bases from DNA; DNA glycosylase that recognizes deoxyguanosine lesions; and apurinic/apyrimidinic endonuclease (APE1) that is involved in recognition and processing of abasic sites [90, 91]. A key protein in the BER pathway that is mainly involved in radioresistance is poly ADP ribose polymerase-1 (PARP-1) [92]. Radiation-induced DNA damage increases the activity of PARP-1 in cancer cells. Therefore, blocking PARP-1 activity or BER in cancer cells by treating the cells with PARP inhibitors [93] or other drugs that can block BER such as methoxyamine (MX) [94] is a strategy that enhances the radiation treatment outcome [95]. Another DNA repair mechanism that is involved in radioresistance is HRR [96]. For example, overexpression of Rad51 (an HRR protein) is associated with radiation resistance in breast cancer type-2 susceptibility protein (BRCA2)-defective cancer cells [97].

All the aforementioned DNA repair mechanisms that are involved in resistance to radiation were, in studies presented in this thesis, subjected to inhibition studies in order to sensitize cancer cells to various treatment methods [98] and are discussed in more detail below.

1.4.3 Resistance to Immunotherapy

Cancer immunotherapy, like other cancer treatment strategies, can lead to emergence of resistant cancer cells that hinder treatment effectiveness [99]. There are multiple barriers that could undermine effective immunotherapy, and the likelihood of their development is based on the nature of the immunotherapeutic approach [41]. However, some of these barriers are more common; for example, the presence of T_{regs} in the tumour microenvironment and tumour draining lymph nodes (TDLNs) [100] can effectively suppress tumour-specific $CD8^+$ T cells at TDLNs, thus suppressing the mounting antitumour response even after adoptive transfer of tumour-primed $CD4^+$ T cells in mice [101]. Another common mechanism that contributes to the failure of cellular immunotherapy or tumour vaccination is the loss of MHC class I on the surface of cancer cells. $CD8^+$ T cells recognize their targets by examining the MHC-peptide complex on cell surfaces; however, cancer cells have evolved to lose their MHC molecules as a common mechanism of immune evasion [101]. Fortunately, this phenomenon can be avoided by using CAR-expressing T cells for adoptive transfer as described earlier [73]. Tumour cells also develop abnormal and hyperpermeable vasculature that hinders T cell access to tumours. Furthermore, tumour release of vascular endothelial growth factor (VEGF) inhibits T cell migration towards tumours from the vasculature [73]. Normalization of tumour vasculature by anti-VGEF therapy can significantly increase the effectiveness of tumour immunotherapy [102].

1.5 Indoleamine 2,3-dioxygenase

The immunoregulatory molecule IDO is a 45 kDa hemoprotein that is essential for oxidative catabolism of tryptophan in the kynurenine pathway [103]. IDO catalyzes this step by the oxidative cleavage of the 2,3-double bond in the indole moiety of L-tryptophan, resulting in the production of the first kynurenine pathway metabolite, N-

formyl kynurenine (Figure 1.1) [104]. IDO has broad substrate specificity because of its ability to degrade indoleamine derivatives, including L- and D-tryptophan, serotonin, melatonin, and tryptanine [105]. IDO degradation of tryptophan in the kynurenine pathway forms a series of biologically active metabolites such as quinolinic acid (QA), kynurenic acid (KA), and 3-hydroxykynurenine [106]. QA acts as an agonist of N-methyl-D-aspartate (NMDA) receptors, for glutamate. QA is also neurotoxic and induces death in neurons through apoptosis and necrosis [107]. KA is another metabolite of the kynurenine pathway and is an antagonist of NMDA and nicotinic acetylcholine receptors. Both QA and KA are assumed to be active at peripheral sites outside the nervous system because of the presence of NMDA receptors in the periphery [106]. In addition to the above, 3-hydroxykynurenine is another neurotoxic byproduct of the kynurenine pathway capable of generating free radicals [108]. QA produced from IDO catabolism of tryptophan can be converted to NAD^+ in monocytic cells including macrophages and microglia. Therefore, IDO can provide a source of NAD^+ to cells from tryptophan catabolism [109]. In mice, IDO protein can be naturally found in various organs including prostate, epididymis, uterus, colon, lung, spleen, and bladder [110]. In humans, IDO can also be found in different tissues including lung, placenta, and small intestine [111, 112]. However, IDO can be induced in most human cells, especially APCs by inflammatory cytokines such as interferon gamma (IFNγ), tumour necrosis factor (TNF)-α and infections [113, 114]. IDO expression in cells is tightly regulated at the transcriptional and post-translational levels. IDO mRNA transcription is promoted by factors such as interferon regulatory factor (IRF)-8 and the transcription factor Forkhead box O3 (FOXO3) [115, 116]. DNAX-activation protein 12 (DAP12), on the other hand, suppresses IDO mRNA transcription in cells [116]. The regulatory factor suppressor of cytokine signaling 3 (SOCS3) binds to IDO protein and marks it for ubiquitinylation and degradation [117]. The main function of IDO is to regulate the immune system and suppress the inflammatory response of the immune cells that will be discussed below.

1.5.1 IDO and the Immune System

IDO promotes innate immunity during host-pathogen interactions, while it inhibits adaptive immunity through suppressing pro-inflammatory responses [103]. Most

intracellular pathogens such as *Listeria monocytogens* depend on host tryptophan for replication [118]. As part of its role in innate immunity, IDO can directly suppress pathogen replication by limiting the availability of tryptophan. IDO therefore plays a vital antimicrobial role in suppressing the infection of *Toxoplasma gondii* [119], *Listeria monocytogens* [118], and many other intracellular pathogens. However, IDO's role in adaptive immunity is mainly to suppress lymphocytes [103]. It mainly modifies immune response by two means: first, by depleting tryptophan in the cellular environment that would otherwise trigger amino acid-sensing signal transduction pathways in immune cells. This depletion leads to an arrest of T cell proliferation [120]. Second, IDO produces kynurenine products that are toxic for T cells and this induces their death via apoptosis [103]. IDO's rapid consumption of tryptophan from the local microenvironment triggers a regulatory signal in T cells by inhibiting or activating molecular stress response pathway mediators, such as the mammalian target of rapamycin (mTOR) and general control non-repressed (GCN)-2 kinase, respectively [103]. The GCN2 molecule responds to elevated levels of uncharged tRNA induced by tryptophan insufficiency [120]. GCN2 phosphorylates eukaryotic initiation factor (eIF2α). Phosphorylation of eIF2α results in general inhibition of most mRNA translation in the cell, thus blocking protein synthesis and arresting cell growth [121]. GCN2 activation in $CD8^+$ T cells leads to cell cycle arrest and anergy [120], but its role in $CD4^+$ T cells is more complex. Activation of GCN2 in $CD4^+$ T cells blocks the differentiation of T helper (TH) 17 cells [122], but promotes differentiation and enhances the function of T_{regs}. IDO, therefore, also appears to suppress activated T cells by increasing the number and enhancing the function of T_{regs} (Figure 1.1) [123, 124].

On the other hand, IDO-mediated production of kynurenine metabolites can directly induce apoptosis in lymphocytes [125] and appears to suppress the activated T cells in three major ways. First, kynurenine metabolites promote the differentiation of T_{regs} by activating aryl hydrocarbon receptor (AHR), a central player in T cell differentiation [126]. Second, kynurenine-mediated AHR activation can directly suppress tumour-infiltrating $CD8^+$ T cells [127]. Third, kynurenine metabolites negatively impact the immunogenicity of DCs [128]. Moreover, IDO appears to have additional, non-enzymatic functions, including a signaling role in transforming growth factor (TGF) β-

induced tolerance in plasmacytoid DCs [129]. IDO was originally reported to prevent allogeneic fetal rejection in mice, which is consistent with its expression in the placenta [130]. It suppresses the alloresponse and attenuates allograft rejection [131, 132]. Furthermore, IDO expression by APCs prevents graft versus host disease (GVHD) [133].

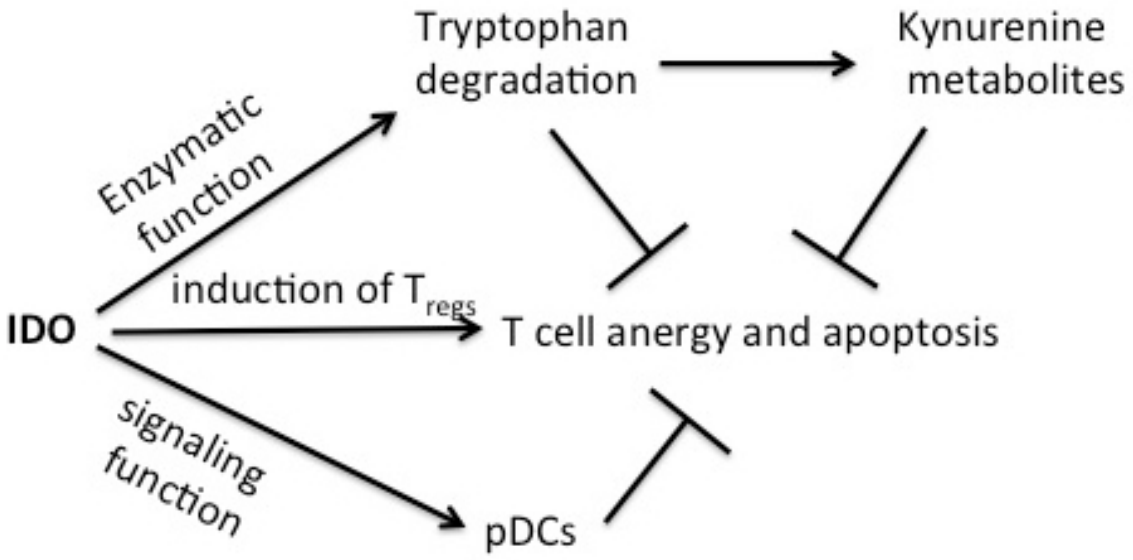
Tryptophan
degradation
Kynurenine
metabolites
Enzymatic
function
induction of T_{regs}
IDO
T cell anergy and apoptosis
signaling
function
pDCs

Figure 1. 1. IDO function. IDO is primarily involved in the breakdown of tryptophan in the body. IDO also suppresses immune cells through its enzymatic and signaling functions. Tryptophan depletion and production of kynurenine metabolites directly induces anergy and apoptosis in T cells and NK cells. IDO also causes $CD4^+$ T cells to reprogram to T_{regs} that further suppress $CD8^+$ T cells. IDO signaling also induces a stable regulatory phenotype in plasmacytoid DCs that further suppresses T cells (Figure modified from [108]).

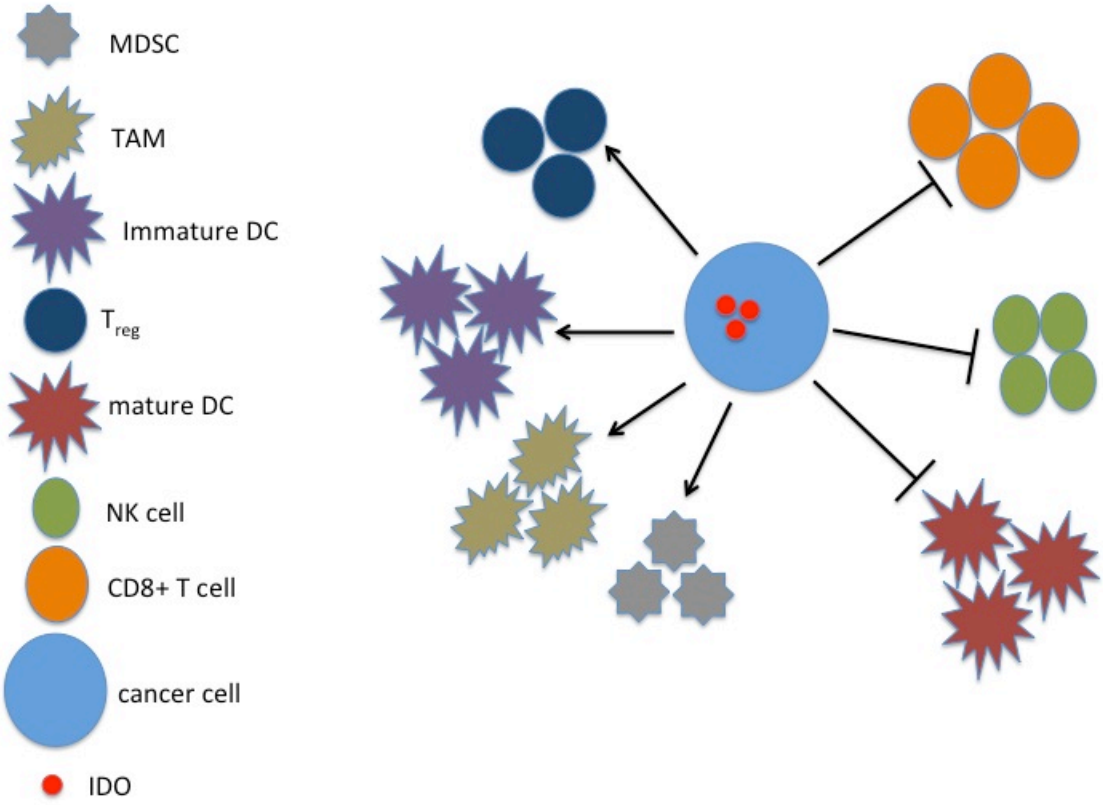
MDSC
TAM
Immature DC
T_{reg}
mature DC
NK cell
CD8+ T cell
cancer cell
IDO

Figure 1. 2. IDO suppression of immune cells. IDO decreases the activity of cytotoxic T cells, NK cells, and mature DCs via tryptophan depletion, toxic tryptophan catabolites, and induction of T_{regs}, MDSCs, immature DCs, and TAMs. T_{reg} = T regulatory cell; MDSC = myeloid-derived suppressor cell, TAM = tumour-associated macrophage, immature DC = immature dendritic cell, mature DC = mature dendritic cell, NK cell = natural killer cell, $CD8^+$ T cell = cytotoxic $CD8^+$ T cell, IDO = indoleamine 2,3-dioxygenase (Figure modified from [134]).

1.5.2 IDO and Cancer

Most human tumours express IDO [135], which contributes to tumour-induced tolerance and suppression of the immune system (Figure 1.2 and Table 1.1). The tumour suppressor BAR adapter-encoding gene *Bin 1* is commonly mutated in cancers [136]. *Bin 1* genetically controls IDO. Transient or stable downregulation of *Bin 1* enhances the basal and IFNγ-induced activity of the IDO promoter in cancer cells and macrophages. Conversely, ectopic expression of Bin 1 cDNA reverses IDO promoter activity in the same type of cells [136]. IDO induces a tolerogenic state in the tumour microenvironment and tumour-draining lymph nodes [134]. Tumour-draining lymph nodes are sites vital for T cell activation. Therefore, IDO expression by APCs at these sites effectively suppresses naïve T cells before they can become fully activated. Furthermore, IDO-expressing APCs induce T_{regs} at tumour-draining lymph nodes, thus enhancing the tolerogenic environment against effector T cells [134].

In the majority of patient studies, IDO expression has been correlated with decreased overall survival and decreased progression-free survival of the patients. For example, in one study, IDO expression was evaluated in samples from 138 patients with hepatocellular carcinoma. Lower IDO expression was correlated with high overall survival in the studied cancer patients [137]. Moreover, IDO has been linked to increased metastasis in various human cancers including NSCLC, breast cancer, and colorectal cancer [138-140]. Colorectal cancer patients with high tumour IDO levels have a higher rate of hepatic metastasis than patients with low IDO levels [140]. IDO was also associated with distant metastases in patients with hepatocellular tumours [137]. Interestingly, high IDO expression was found in advanced stages of disease in patients with ovarian cancer, nasopharyngeal carcinoma, and endometrial cancer [141-143].

IDO is also important in developing resistance to immunotherapy. The anti-CTLA-4 antibody ipilimumab, described earlier, is effective only in a subset of melanoma patients, suggesting that most melanoma cells are either intrinsically resistant or develop resistance to this novel immunotherapy drug. It has been suggested that IDO plays a major role in resistance to ipilimumab [144]. In fact, in two different mouse tumour models (B16 melanoma and 4T1 mammary carcinoma) the anti-tumour effects of ipilimumab were significantly greater in IDO knockout mice and wild type mice treated

with the IDO inhibitor 1-methyl tryptophan (1-MT) than controls [144]. Melanoma tumours overexpressing IDO were resistant to antibody blockage of CTLA-4. However, the IDO inhibitor 1-MT could effectively reverse this phenomenon *in vivo*. The protective role of IDO inhibition depended on the presence of both $CD8^+$ T cells and IFNγ in the same system [144].

Table 1. 1. Many human tumours express IDO. Human tumour samples were analyzed for IDO protein levels (table modified from [135]).

Tumour Type	IDO protein (IDO^+/total tumours assayed)
Prostatic carcinomas	11/11
Colorectal carcinomas	10/10
Pancreatic carcinomas	10/10
Cervical carcinomas	10/10
Endometrial carcinomas	5/5
Gastric carcinomas	9/10
Glioblastomas	9/10
NSCLC	9/11
Bladder carcinomas	8/10
Ovarian carcinomas	8/10
Head and Neck carcinomas	7/11
Esophageal carcinomas	7/10
Mesotheliomas	6/10
Renal cell carcinomas	5/10
Melanoma	11/25
Breast carcinomas	3/10
Thyroid carcinomas	2/10
Lymphomas	4/18
Small-cell lung carcinomas	2/10
Sarcomas	2/10
Hepatocarcinmas	2/5
Adrenal carcinomas	2/5
Choriocarcinomas	1/5
Cutaneous basocellular carcinomas	1/5
Testicular seminomas	0/5

1.5.3 IDO Inhibitors

There is compelling evidence that IDO plays a major role in suppressing the immune system during cancer progression [145]. Because IDO has been linked to higher rates of metastasis and poor patient outcome, it is an attractive target for cancer treatment [146]. Thus, the search for IDO inhibitors has become a very active area of research, particularly since the seminal work of the Van den Eynde group in 2003 that showed IDO could confer immunoresistance in tumours [135]. The best-known IDO inhibitor at that time was 1-MT, discovered in 1991, which is a tryptophan derivative with an affinity in the micromolar range (Ki ~ 34 μM) [147]. The first IDO inhibitor to enter a phase I clinical trial, in 2008, was the D-stereoisomer of 1-MT (D-1MT; NLG8189). Unfortunately, the L-stereoisomer of 1-MT (L-1MT) was shown later to be an IDO inhibitor while the D-1MT tested in the clinical trial is not [148, 149]. Regardless, D-1MT is currently undergoing phase II clinical trial for treatment of prostate cancer and metastatic breast cancer [150]. D-1MT can also bind and inhibit IDO_2, a putative paralogue of IDO1 (IDO), although the physiological relevance of IDO_2 in cancer in not well understood [150]. Another breakthrough in developing novel IDO inhibitors took place in 2006, when the 3-dimensional structure of IDO complexed with 4-phenylimidazole (PIM) and cyanide ion (CN^-) was elucidated [104]. PIM was discovered earlier as a modestly potent IDO inhibitor, which bound to the active site of IDO and inhibited its enzymatic activity in a non-competitive manner [151]. The discovery of three-dimensional structures of IDO, complexed with PIM and CN^-, provided vital information for the structure-based drug design of novel IDO inhibitors [104]. In fact, the discovery of most newer IDO inhibitors originated from detailed analysis of the structural interaction between IDO and PIM.

Three major companies have led in the discovery of IDO inhibitors in recent years: 1) Newlink Genetics, focused mainly on phenyl-imidazole-derived compounds. They produced a number of soluble IDO inhibitors with activities in the nanomolar range. None of these compounds has yet progressed to clinical trials, 2) The Ludwig Institute for Cancer Research (LICR) works mainly on PIM analogues such as phenyl-trizoles and a series of amino-hydroxyquinolines, which have also not yet progressed to clinical trials, and 3) Incyte Corp, which has discovered a number of active IDO inhibitors with activity

in the nanomolar range. Their main focus is on a series of hydroxyamidines including INCB24360 which is under phase II clinical testing [150]. INCB24360 effectiveness has been assessed in comparison to tamoxifen treatment in recurrent ovarian cancer patients [150]. Patients with myelodysplastic syndrome (MDS) were reported to have elevated tryptophan metabolites in their sera. Incyte Corp, therefore, is planning to assess whether INCB24360 is effective in MDS patients and whether it inhibits hematopoietic progenitor amplification in these patients [152].

There are certain challenges to discovering IDO inhibitors. First, IDO's active site topology is resistant to a high degree of inhibition. This is because of the relatively small size of IDO, which hinders the binding of large inhibitor molecules [153]. Second, IDO inhibition kinetics are not completely understood. Some IDO inhibitors were reported to bind IDO in a competitive manner and others in a non-competitive way [154]. Some inhibitors have been shown to bind IDO based on a redox activity [155, 156]. Therefore, designing better drug candidates requires a better understanding of IDO inhibition kinetics. The third and major challenge in developing a promising IDO inhibitor is the ability to translate the results of IDO inhibitors from preclinical studies into clinical settings, which requires compounds with appropriate bioavailability and low toxicity profile [157]. The encouraging aspect of blocking IDO is the mild nature of unfavorable side effects [157]. Importantly, there is no sign of development of spontaneous autoimmunity in IDO knockout mice [157]. Furthermore, the side effects of D-1MT during phase I clinical trials were generally mild, including reports of easily managed hypophysitis [150].

In addition to small molecule inhibitors, antisense targeting of IDO mRNA has been investigated in a number of preclinical settings using small interfering RNA (siRNA) and short hairpin RNA (shRNA). For example, siRNA knockdown of IDO mRNA in B16F10 mouse melanoma cells *in vitro* inhibited the enzymatic function of IDO and thus prevented tryptophan catabolism [158]. B16F10 cells cocultured with $CD4^+$ and $CD8^+$ T cells *in vitro* induced apoptosis in both T cell subsets. However, siRNA downregulation of IDO significantly reduced apoptosis in T cells [158]. IDO downregulation in B16F10 melanoma cells, before tumour inoculation into mice, slowed tumour growth *in vivo*. Interestingly, siRNA knockdown of IDO was more protective

than 1-MT in inhibiting IDO function in cancer cells [158]. Intratumoural administration of IDO siRNA in established tumours significantly delayed growth and decreased tumour size. These results were attributed to the effect of IDO inhibition in reinstalling an antitumour immune response against melanoma in mice [158]. Skin delivery of IDO siRNA in tumour-bearing mice inhibited IDO mRNA in DCs and effectively delayed bladder tumour growth in syngeneic mice [159]. Animals treated with IDO siRNA had a significant increase in their survival rate compared to the control group. Interestingly, local IDO siRNA treatment was more effective than systemic administration of L-1MT in IDO inhibition. The therapeutic effect of IDO siRNA in this model was attributed to $CD8^+$ T cells, since depletion of these cells abolished the protective effect of IDO siRNA [159]. In another study, IDO shRNA was shown to be effective in impeding tumour growth in three mouse models of liver cancer, including subcutaneous, orthotopic, and metastatic disease [160]. The cytotoxic function of $CD8^+$ T cells and NK cells was improved following IDO shRNA skin delivery [160]. In addition, IDO shRNA treatment of tumour-bearing animals increased the serum mRNA levels of proinflammatory cytokines IL-12 and IFNγ (both important in anti-tumour immunity) and decreased IL-10 mRNA levels that suppresses anti-tumour responses [160].

1.5.4 IDO Inhibition to Improve Chemotherapy and Radiation

In a mouse transgenic model of breast cancer in which tumours were induced by expression of the oncogene Neu under the control of the mouse mammary tumour virus (MMTV) promoter, IDO inhibition with 1-MT has been combined with paclitaxel, a chemotherapeutic agent commonly used to treat breast cancer [136]. The combination resulted in tumour regression in tumour-bearing animals [136]. This effect was greater than using 1-MT or paclitaxel alone. In addition, each agent was effective at a lower dose than its maximally tolerated dose. Analysis of tumour sections showed evidence of higher tumour cell death in the combination group. Strikingly, depletion of $CD4^+$ T cells or the use of T cell-deficient athymic mice instead of immunocompetent mice abolished the effect of combined treatment, indicating that an immune-mediated effect was involved in blocking IDO in the context of paclitaxel treatment [136]. In the same study, the effect of combining 1-MT with other chemotherapy agents with broad mechanisms of action that

are used to treat breast cancer was examined. 1-MT improved the therapeutic effect of cisplatin, cyclophosphamide, and doxorubicin (Table 1.2). The authors of the study concluded that combining IDO inhibition with a diverse group of chemotherapeutic agents could effectively increase their therapeutic activity in the treatment of breast cancer [136].

Several clinical studies have suggested that high IDO levels during treatment could be related to a poor response to chemotherapy and/or radiotherapy and perhaps contribute to resistance to therapy. In a single arm phase II study in patients with stage III NSCLC, serum kynurenine/tryptophan levels were measured as a surrogate marker for IDO activity during treatment [161]. Patients were treated with induction gemcitabine and carboplatin and then received concurrent carboplatin, paclitaxel, and 74 Gray (Gy) thoracic radiation. Cancer patients showed high IDO activity compared to healthy controls. This high IDO activity after chemotherapy was associated with poor patient outcome. However, the power of this study was limited by the relatively low number of patients and therefore low statistical power [161]. In another study, IDO was positively associated with chemoresistance in a gene expression profiling study that aimed to identify molecules associated with resistance to paclitaxel-based chemotherapy in ovarian cancer cell lines and refractory surgical ovarian cancer specimens [162]. IDO was highly expressed in both paclitaxel-resistant cell lines and refractory ovarian tumours but was absent in paclitaxel-sensitive cell lines and tumours [162]. In a clinical study that analyzed NSCLC patient response to platinum-based chemotherapy in a small cohort of patients, IDO expression in monocytes and granulocytes was analyzed pre- and post-treatment. The patient population that benefited from the treatment showed lower IDO expression in blood monocytes post-treatment [163]. All the aforementioned studies provide a rationale for IDO inhibition in order to sensitize tumour cells to chemotherapy and radiation.

Table 1. 2. IDO inhibition increases the effectiveness of certain chemotherapeutic drugs in the presence of the immune system in a mouse model of breast cancer. Tumour-bearing MMTV-*Neu* mice were treated with or without the IDO inhibitor 1-MT in combination with the indicated chemotherapy agents. IDO inhibition potentiated the effect of cisplatin, cyclophosphamide, doxorubicin, and paclitaxel. (* $p < 0.05$) (Table adapted from [136]).

Compound	Class	Mean Tumour Volume ± SEM (+ 1-MT)	Mean Tumour Volume ± SEM (- 1-MT)
Cisplatin	Alkylating agent	0.77 ± 0.18	1.7 ± 0.33
Cyclophosphamide	Alkylating agent	0.81 ± 0.12	1.4 ± 0.18
Doxorubicin	Antineoplastic antibiotic agent	0.79 ± 0.07	1.5 ± 0.25
5FU	Antimetabolite	1.2 ± 0.20	1.1 ± 0.25
Methotrexate	Antimetabolite	1.7 ± 0.28	1.7 ± 038
Paclitaxel	Mitotic inhibitor	0.68 ± 0.11	2.4 ± 0.43
Vinblastine	Mitotic inhibitor	1.3 ± 0.19	1.2 ± 0.18
FTI	Signal transduction inhibitor	0.67 ± 0.11	1.0 ± 0.16
Rapamycin	Signal transduction inhibitor	0.97 ± 0.07	0.99 ± 0.25
Tetrathiomolybdate	Antiangiogenic	1.9 ± 0.52	2.0 ± 0.42
Vehicle		1.7 ± 0.17	3.0 ± 0.44

1.6 DNA Repair

DNA is the source of all genetic information in cells and its integrity is vital to life [164]. DNA integrity, however, can be reduced by the action of damaging environmental agents (*e.g.*, ultraviolet [UV] light) and/or reduced cellular capacity for high fidelity DNA replication. The resulting DNA damage, whether it be caused directly or indirectly from faulty DNA repair, if not corrected, will result in mutation and possible development of genetically-based diseases such as cancer [164]. Cells have evolved various DNA repair mechanisms that are responsible for detection and repair of DNA damage, independent of the damage source but related to the type of lesion [164]. At a minimum, mammalian cells utilize five forms of DNA repair to cope with various types of DNA lesions: BER, mismatch repair (MMR), NER, and double-strand break repair, which includes both HRR and non-homologous end joining (NHEJ) [165]. This section contains a brief description of DNA repair mechanisms relevant to this thesis and specific molecules relevant to those mechanisms, including PARP, TS, and NAD^+.

1.7 Base Excision Repair

The BER pathway repairs base lesions and SSBs induced by deaminating, alkylating, and oxidative agents [166]. BER starts with identification of damaged bases by a DNA glycosylase. The glycosylase catalyzes the cleavage of an N-glycosidic bond to remove the damaged base to create an apurinic or apyrmidinic site (AP site) in the DNA strand [167]. A DNA AP endonuclease or DNA AP lyase then cleaves the DNA backbone resulting in a SSD nick 5' or 3', respectively, to the AP site. The processing activity of the AP endonuclease converts the newly-formed nick into a single-nucleotide gap. DNA polymerase β (PolB) uses the correct nucleotide to fill in the gap; polymerase activity is facilitated by the 3'-hydroxyl and a 5'-phosphate groups of bases flanking the gap. A DNA ligase completes the final repair process by sealing the nick (Figure 1.3) [167].

There are two forms of BER: short-patch and long-patch. The difference between them lies mainly in the enzymes that are involved in the repair process [167]. Cells choose to proceed with either repair process based on the relative ATP concentration adjacent to the AP site and the effectiveness of the AP lyase activity of PolB [168] . Short-patch BER occurs more frequently at high ATP concentrations, whereas long-patch BER is the preferred mechanism at low ATP levels [168]. The second determining factor for cells to choose between short and long patch repair is the presence or absence of the 5'-terminal deoxyribophosphate (dRP) intermediate that is produced by the AP endonuclease. Efficient removal of the dRP by PolB lyase activity leads to short-patch BER. However, failure to successfully remove the dRP results in long-patch BER, forming nicks that are refractory to DNA ligase action [168-170]. X-ray repair cross-complementing protein 1 (XRCC1) is among the first proteins to be recruited to the nick generated by the activity of either glycosylase and/or AP endonuclease. This scaffold protein modulates the ATP concentration near the nick and coordinates short-patch BER [171]. Moreover, it interacts with ligase III and PolB [171, 172]. Long-patch BER, on the other hand, requires proliferating cell nuclear antigen (PCNA). This abundant nuclear protein coordinates the long-patch BER process by interacting with DNA polymerases δ and ε (PolD and PloE) and flap structure-specific endonuclease 1 (FEN1). Resistance of dRP to cleavage by PolB results in a switch to PolD or PolE. These DNA polymerases add 2-8 extra nucleotides into the repair gap, which generates a flap structure. This structure is then removed by FEN1 in a PCNA-dependent manner. Eventually, DNA ligase I seals the nick and completes the repair process [170, 173].

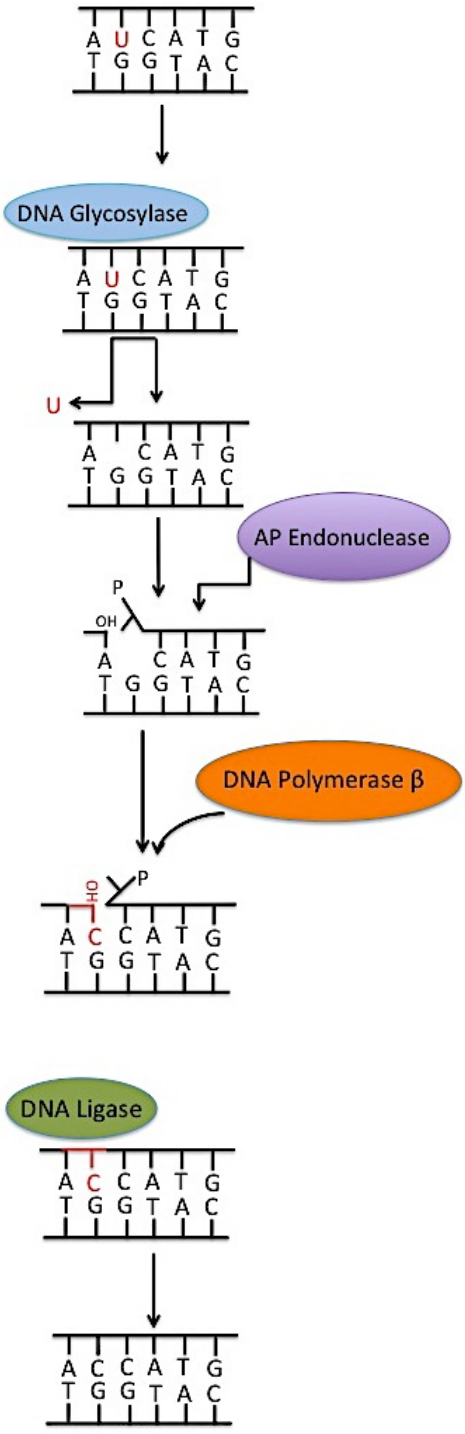
DNA Glycosylase
AP Endonuclease
DNA Polymerase β
DNA Ligase

Figure 1. 3. The BER pathway. DNA glycosylase identifies and removes damaged bases, leaving an AP site. The AP site is then cleaved by DNA AP endonuclease leaving a gap in the DNA backbone. PolB then fills the gap with the correct nucleotide, based on its complementarity with the bound DNA strand. Finally, DNA ligase seals the nick and completes the repair (Figure adapted from [167]).

1.7.1 Base Excision Repair and Cancer

Cancer cells are highly dependent on DNA repair for survival. Many alkylating agents create DNA adducts. Cancer cells need to excise and repair these adducts before DNA replication can occur [174]. BER executes this vital function in cancer cells. BER, therefore, plays a crucial role in mediating resistance to many DNA-damaging cytotoxic drugs in cancer cells [174]. In fact, many BER proteins are overexpressed in human cancers and increased resistance to therapy has been attributed to their action [175]. For example, AP endonuclease levels are elevated in ovarian cancer, prostate cancer, and osteosarcoma [175]. However, all enzymes involved in BER are also essential for normal cells, making therapeutic targeting of BER enzymes problematic. For example, AP1 knockout is an embryonic lethal event in mice and AP1 is essential for the viability of cultured cells [176]. On the other hand, knocking down PolB, the major DNA polymerase in BER, increases sensitivity to chemical mutagens and irradiation, but multiple DNA polymerases in human cells can compensate for the lack of BER PolB [175]. Therefore, targeting BER proteins efficiently and specifically could be challenging.

1.7.2 Base Excision Repair Inhibition in Cancer Treatment

BER can be effectively blocked by the alkoxyamine derivative MX, which specifically reacts with the aldehyde group in the sugar moiety formed in the DNA abasic site following the glycosylase removal of the damaged base. This forms a stable MX-bound AP site that is refractory to the AP endonuclease lyase activity and PolB function necessary for completion of repair [177]. MX has been shown to be active in sensitizing various forms of human tumours to chemotherapy and radiation. For example, MX combined with the alkylating agent TMZ induced more DNA damage in T98G glioblastoma cells than treatment with TMZ alone. MX also sensitized TMZ-resistant T98G cells to the TMZ [178]. Moreover, MX combination treatment with pemetrexed resensitized pemetrexed-resistance lung cancer cell lines to this drug [179]. The sensitizing effect of MX in this study was attributed to the dual inactivation of uracil DNA glycosylase (UDG) and topoisomerase IIα (topo IIα) in cancer cells. MX stably bound to the AP site effectively trapped UDG and topo IIα at the AP site. Since tumour cells express higher levels of these enzymes than normal bone marrow (BM) cells, it was

suggested that MX potentiated the pemetrexed effect with minimal hematopoietic toxicity [179]. In another study, combination treatment with MX and TMZ sensitized platinum-resistant ovarian cancer cells to TMZ cytotoxicity, increased DNA damage in tumour cells, and enhanced apoptosis [180]. A phase I study of combined MX and TMZ in patients with advanced solid tumours is currently under way [181]. In another phase I study that is currently recruiting patients, combined MX and fludarabine phosphate is being tested in patients with hematological malignancies [182]. A phase I study of combined MX and pemetrexed is already completed and several phase II studies in multiple indications including NSCLC are planned [179].

1.8 Homologous Recombination Repair

HRR is a DNA repair process conserved across all species [183]. It serves as a high fidelity template-dependent repair mechanism for double-strand breaks (DSBs), DNA gaps, and DNA interstrand crosslinks (ICLs)(Figure 1.4). HRR is essential to preserve genomic integrity and avoid tumour progression. The first step in HRR starts with Rad51, a protein with DNA binding and ATPase properties, which positions the invading 3' end on a DNA strand and forms a nucleoprotein filament. Rad51 recruitment to the DNA damage site is facilitated by BRCA1, which is also involved in processing DSBs. Another central protein to HRR is the tumour suppressor protein BRCA2 [179, 184]. BRCA1 and BRCA2 mutations predispose women to ovarian and breast cancers [185]. BRCA2 is also involved in recruiting Rad51 to DSBs through the eight BRC repeats of BRCA2 protein that bind to Rad51. Upon binding to RAD51, BRCA2 binds to single-stranded DNA (ssDNA) and double-stranded DNA (dsDNA) through its DNA-binding domain. Cells lacking BRCA2 are defective in HRR. In fact, BRCA2-deficient cells cannot recruit Rad51 to DSBs [186]. Therefore, targeting BRCA2 in cancer cells is of great interest as a therapeutic strategy [187]. SiRNA-mediated reduction of BRCA2 decreased the proliferation rate of A549 adenocarcinoma cells, even in the absence of drug treatment, likely because of increased DNA damage due to genomic instability mediated by decreased DNA repair [187]. Moreover, the cytotoxic effect of the alkylating agents cisplatin and melphalan was significantly enhanced after siRNA downregulation of BRCA2 in A549 and Hela cells [187].

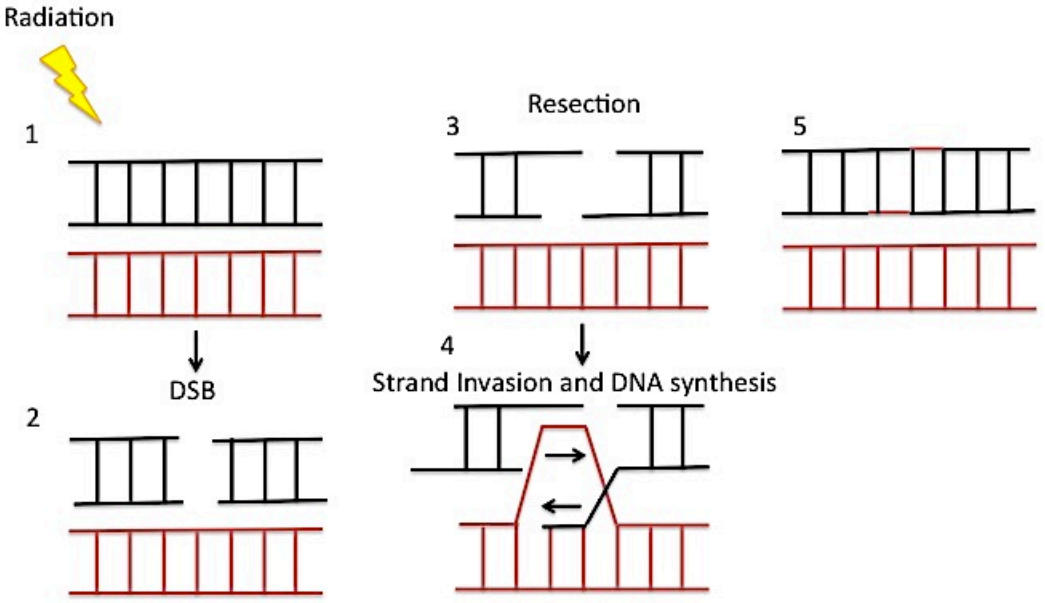
Radiation
1
2
DSB
3
Resection
4
Strand Invasion and DNA synthesis
5

Figure 1. 4. Homologous recombination repair of DSB. 1-2: Radiation induces DSBs. 3: Efficient 5' to 3' resection of DSB ends allows recruitment of the single-stranded DNA-binding complex and Rad51. The complex begins HRR by positioning the invading 3' end on a DNA strand and forming a nucleoprotein filament. BRCA1 facilitates RAD51 recruitment to the damaged site. BRCA1 association with histones near sites of DNA damage depends on histone γH2AX. 4: Strand invasion of 3' ssDNA overhangs into a homologous sequence allows the completion of DNA synthesis at the invading end. This is followed by the second DSB end capture and formation of an intermediate. 5: DNA synthesis to the gap and ligation to form a crossover. DSBs = double strand breaks. ssDNA = single strand DNA (Figure adapted from [188]).

1.9 PARPs and DNA Repair

PARP-1 is the most studied member of the PARP superfamily. PARP-1 is a molecular sensor of DNA breaks and plays a crucial role in organizing their repair (Figure 1.5). The catalytic activity of PARP-1 increases dramatically (over 500-fold) on binding to DNA breaks [189]. It catalyzes the covalent transfer of ADP-ribose units from the NAD^+ substrate to the γ-carboxyl group of glutamic acid residues on a variety of acceptor proteins, a process called heteromodification [189]. These acceptor proteins are normally associated with DNA regulation and modification. PARP-1 can also poly-ADP-ribosylate itself (automodification). Through poly-ADP-ribosylation of its partner proteins, PARP-1 regulates chromatin structure and DNA metabolism [189]. PARP-1 partner proteins include high mobility group (HMG) proteins, histones, DNA helicases, topoisomerases I and II, BER and single-strand break repair (SSBR) factors, and different transcription factors. PARP-1 is important in genomic integrity [190-192] and the induction of cell death in injured tissues [193]. PARP-2, the second member of the PARP family, is also activated by DNA breaks [194]. PARP-2 is required for efficient repair of SSBs in DNA and for genomic integrity [195, 196]. Although there are other PARP family members, they are less important in DNA repair. Both PARP-1 and PARP-2 regulate multiple DNA repair mechanisms in cells. Therefore, they are vital for the survival of cancer cells, particularly those affected by chemotherapy and radiation [197]. Some of the interactions between PARP molecules and DNA repair mechanisms that are relevant to this thesis are described next.

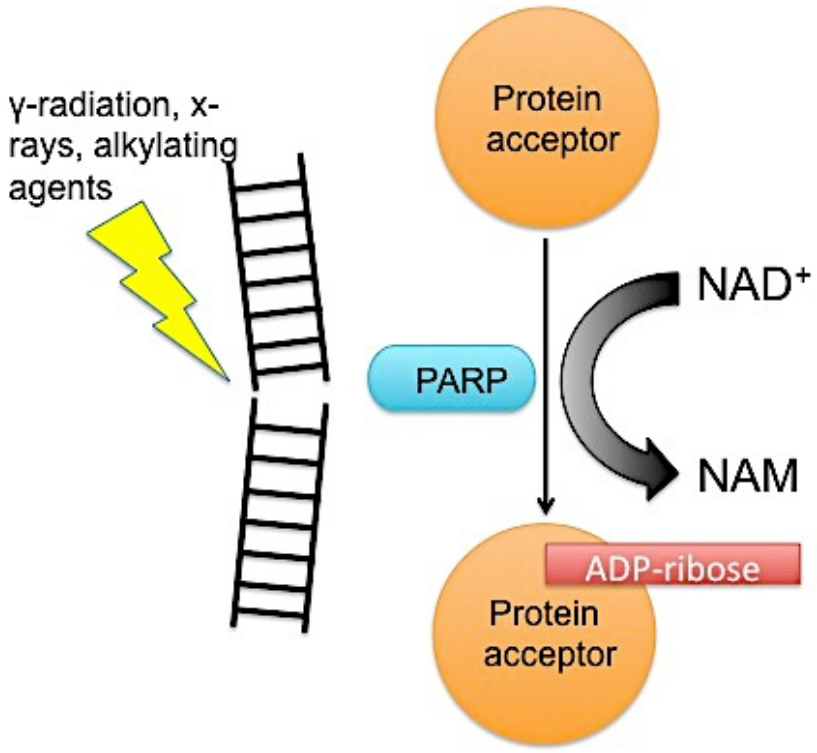
γ-radiation, x-rays, alkylating agents
Protein acceptor
NAD+
PARP
NAM
ADP-ribose
Protein acceptor

Figure 1. 5. PARP function during DNA damage and repair. PARP proteins use NAD^+ molecules as substrates for mono- and/or poly-ADP ribosylation of acceptor proteins such as XRCC1. PARP function is crucial for the recruitment of acceptor proteins to the site of DNA damage. PARP = poly(adenosine diphosphate-ribose) polymerase. NAD^+ = nicotinamide adenine dinucleotide. NAM = nicotinamide (Figure adapted from [198]).

1.9.1 PARP-1 and XRCC1

Poly-ADP-ribosylated PARP-1 preferentially interacts with XRCC1, the BER/SSBR scaffold protein [199]. *In vivo*, in the context of locally induced SSBs or DSBs, recruitment of XRCC1 to the damaged area of DNA is strictly dependent on poly-ADP-ribosylation [200]. Chemical inhibition of polymer of ADP-ribose (PAR) formation abolishes XRCC1 recruitment to the damaged site [200], consistent with observations made in irradiated PARP-$1^{-/-}$ cells [189]. Inhibition of XRCC1 recruitment to the damaged area of DNA subsequently affects DNA repair processes such as BER and SSBR, because XRCC1 mediates DNA repair by stimulating DNA repair enzymes [201]. In response to base damage, PARP-1 and XRCC1 also interact with the chromosome-organizing complex condensin I to allow efficient BER through modifying the local chromatin and organizing the structure of DNA [202].

1.9.2 PARP-2 and XRCC1

PARP-2 also interacts with XRCC1 and other BER/SSBR proteins including DNA ligase III and DNA polymerase β [196]. Cells lacking PARP-2 have enhanced sensitivity to genotoxic agents and have delayed SSB rejoining [190, 196]. However, unlike PARP-1, XRCC1 recruitment to the site of DNA damage and recognition of SSBs does not require PARP-2, suggesting that PARP-2 functions at later stages of DNA repair [189].

1.9.3 PARP-1 and Homologous Recombination Repair

A direct role for PARP-1 in DSB repair has not yet been demonstrated. PARP-1 appears not to be required for HRR-mediated DNA DSB repair [203]. Indeed, Rad51 foci are still generated in the absence of PARP-1. More importantly, DSB repair is functional in PARP-1 inhibited cells [203]. Furthermore, PARP-1 does not colocalize to RAD51 foci [204]. However, inhibition of PARP-1 results in increased HRR, suggesting an important role for PARP-1 in genomic instability [203]. This provides further rationale for blocking HRR in the context of PARP-1 inhibition in cancer cells, which could overwhelm the DNA repair machinery of cancer cells and induce apoptosis.

1.9.4 Inhibiting PARP in Cancer Treatment

PARP-1 is overexpressed in many human cancers and has been linked to poor prognosis [205]. Through the BER pathway, PARP plays a vital role in the repair of the SSBs, and blocking PARP leads to DSBs in DNA. Tumour cells with impaired or low level PARP activity depend heavily on HRR to survive. Thus, tumours with mutated BRCA1/2 genes (important in HRR) have elevated sensitivity to PARP inhibitors [206, 207]. A randomized, phase II clinical study in high grade serous ovarian cancer patients with HRR deficiency showed that blocking PARP increased progression-free survival compared to treatment with placebo [208]. Olaparib is a potent oral PARP inhibitor [209, 210]. Olaparib has antitumour activity at non-toxic doses in phase I/II monotherapy studies in ovarian cancer patients with BRCA1/2 mutations [211, 212]. PARP inhibition enhanced the effect of DNA-damaging cytotoxic drugs such as cisplatin and cyclophosphamide, presumably due to inhibition of BER [213]. This effect could also be observed in human tumour cells with PTEN deficiency: PTEN plays a role in the expression of Rad51 and, therefore, PTEN-deficient cells lack HRR [214].

1.10 Nicotinamide Adenine Dinucleotide

NAD^+ plays a vital role in many biological and biochemical functions in cells. NAD^+ biosynthesis proceeds through both *de novo* and salvage pathways. *De novo* biosynthesis of NAD^+ is linked to IDO [215]. NAD^+ is also important for DNA repair and contributes to cancer cell survival and drug resistance [215]. NAD^+ biosynthesis and function in DNA repair are described below.

1.10.1 *De Novo* NAD^+ Biosynthesis

Cells depend highly on NAD^+ for many biological processes [215]. In most eukaryotic cells, tryptophan is the NAD^+ precursor in the *de novo* pathway, where tryptophan is converted to QA *via* kynurenine (Figure 1.6). The tryptophan-catabolizing enzymes IDO and tryptophan 2,3-dioxygenase (TDO) catalyze the first step in NAD^+ production in all eukaryotic cells. IDO is expressed in most tissues, whereas TDO is primarily a liver enzyme [215]. The first step in the kynurenine pathway is oxidation of tryptophan to N-formylkynurenine by IDO or TDO (Figure 1.6.) [216]. Kynurenine

formidase (KFase) then removes the formyl group by catalyzing N-formylkynurenine hydrolysis to produce kynurenine [217]. The hydroxylase enzyme 3-monooxygenase (KMO) then hydroxylases kynurenine to generte 3-hydroxykynurenine [218]. In the next step, kynureninase cleaves the amino acid side chain of 3-hydroxyhynurenine to form 3-hydroxyanthranilate. In the last step of kynurenine pathway, QA is generated by complex oxidative rearrangement of 3-hydroxyanthranilate by 3-hydroxyanthranilate-3,4-dioxygenase (HAD) [219-221]. QA is the NAD^+ building block through the *de novo* pathway. QA phosphoribosyltransferase (QAPRT) uses QA to produce nicotinic acid mononucleotide (NAMN), which is subsequently converted to NA adenine dinucleotide (NAAD). Finally, NAD synthase (NADS) converts NAAD to NAD^+ (Figure 1.6) [222].

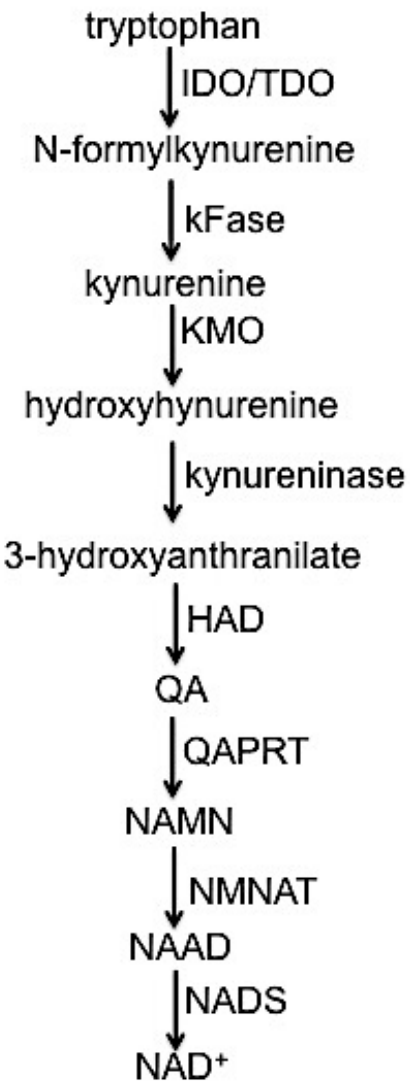
tryptophan
IDO/TDO
N-formylkynurenine
kFase
kynurenine
KMO
hydroxyhynurenine
kynureninase
3-hydroxyanthranilate
HAD
QA
QAPRT
NAMN
NMNAT
NAAD
NADS
NAD+

Figure 1. 6. *De novo* NAD$^+$ production. In the first step of the kynurenine pathway, IDO or TDO catabolize tryptophan to generate N-formylkynurenine. Kynurenine formidase (KFase) then produces kynurenine from N-formylkynurenine. In the next step, hydroxylase enzyme 3-monooxygenase (KMO) hydroxylyses kynurenine to make 3-hydroxykynurenine. Kynureninase then forms 3-hydroxyanthranilate from 3-hydroxykynurenine. In the last step of the kynurenine pathway, oxidative rearrangement of 3-hydroxyanthranilate by 3-hydroxyanthranilate-3,4-dioxygenase (HAD) yields quinolinic acid (QA), which is then converted into nicotinic acid mononucleotide (NAMN) by QA phosphoribosyltransferase (QAPRT). Next, NAM mononucleotide adenylyltransferase (NMNAT) produces NAAD from NAMN. Finally, NAD synthase uses NAAD to produce NAD$^+$ as the final product of this pathway (Figure adapted from [198]).

1.10.2 Salvage Pathway of NAD^+ Biosynthesis

The building blocks of NAD^+ in the salvage pathway are nicotinamide (NAM), nicotinic acid (NA), and nicotinamide riboside (NR) [223, 224]. NAM and NA are used by two different phosphoribosyltransferases for production of NAM mononucleotides (NMN) and NA mononucleotides (NAMN), respectively. These molecules are used in two distinct salvage pathways to produce NAD^+ [215]. NMN adenylyltransferase subsequently converts NMN into NAD^+. NAMN, on the other hand, is converted to NAAD by NMN adenylyltransferase (NMNAT) and finally NAD^+ is produced from NAAD by NAD synthase [222]. Finally, in a third salvage pathway, NR can be used as a NAD^+ precursor. NR kinase (NRK) phosphorylates NR to make NMN, which can be then directly converted to NAD^+ [215].

1.11 NAD^+ and DNA Repair

NAD^+ is the substrate for mono- and poly-ADP-ribosylation in cells [189]. In this reaction, breakage of the glycosidic bond between NAM and ribose consumes parent NAD^+ and donates ADP-ribose to an acceptor molecule. As described above, poly-ADP ribosylation is essential for DNA repair and genomic stability in cells [215]. This phenomenon was first reported by Chambon *et al.*, who described how liver nuclear extracts synthesized poly-ADP-ribose upon addition of NAD^+ [225]. This finding led to the understanding of how ADP-ribose is linked to an amino acid acceptor and not transferred to an acetyl group, which takes place with most sirtuins [226]. In cells, PARP enzymes are responsible for building ADP-ribosyl groups into polymers from NAD^+ [189]. The PARP family of proteins may have as many as 17 members and is the most abundant of the ADP-ribosyl transferases. All these enzymes share a similar active site in their structures [227]. PARP-1 is the most studied member of PARP family and is responsible for most PARP activity in cells [198]. As previously described, PARP-1 is a ubiquitous nuclear protein that responds to DNA damage. Moreover, DNA damage stimulates NAD^+ biosynthesis because of the need to cleave more NAD^+ for poly-ADP-ribosylation by PARPs [228]. In fact, NAD^+ availability has been shown to affect the length of poly-ADP-ribosyl polymer synthesis by PARP-1 [228]. In addition, DNA repair occurs faster in the presence of higher NAD^+ levels or in cells with active NAD^+

biosynthesis [228]. Some studies suggest that PARP activation might not depend on NAD^+, due to the low K_m of PARP-NAD^+ association (20-80 μM) [198]. Furthermore, PARP binding to DNA breaks via its DNA-binding domain seems to regulate PARP catalytic activity [229]. However, despite possible limitations on the role of NAD^+ on PARP activity, PARP function has an important impact on NAD^+ metabolism. PARP activity is the main mediator of NAD^+ catabolism in cells, and high PARP activity reduces intracellular NAD^+ [230, 231]. Since cells depend highly on NAD^+ for survival, PARP activity induces cells to produce NAD^+ through *de novo* and/or salvage pathways [198, 232]. Treatment of cells with genotoxic agents that damage DNA leads to sustained PARP activity in a short period of time and decreases NAD^+ by 10-20%. This can be detrimental to cells since NAD^+ depletion decreases ATP production [230, 231, 233]. It is conceivable that cancer cells possess increased NAD^+ production to overcome constant depletion of NAD^+ consumed in the course of PARP-mediated DNA repair necessitated by genomic instability and concomitant accumulation of DNA damage [234, 235]. Interestingly, NMPRTase, a key enzyme in the NAD^+ salvage pathway, is upregulated in human colorectal cancers. This suggests that human tumours increase their production of NAD^+ as a survival mechanism [236, 237].

1.12 NAD^+ Inhibition as a Strategy for Cancer Treatment

As mentioned above, tumours depend highly on NAD^+ and possess high NAD^+ turnover due to high PARP activity [189, 227, 235, 238, 239]. Therefore, blocking NAD^+ production is an attractive approach to sensitize cancer cells to PARP-mediated depletion of NAD^+ and induction of apoptosis [240]. The NAD^+ precursors NM and NA in most human tissues are obtained from the diet. Tryptophan, on the other hand, is not a major source of tissue NAD^+ in humans [241]. These data provide a rationale for targeting the NAD^+ salvage pathway in cancer cells. FK866 is an effective small-molecule inhibitor of that pathway. It non-competitively blocks NMPRTase and consequently decreases cellular levels of NAD^+, and induces apoptosis in cancer cells with little side effects on healthy cells because of their lower rate of catabolic depletion of NAD^+ by PARP [242]. FK866 administered *in vitro* begins to reduce intracellular NAD^+ by ~50% in HepG2 liver carcinoma cells as early as 8 hours after addition [242]. As mentioned above, NAD^+

is a necessary coenzyme for ATP production and blocking NAD^+ production by FK866 treatment drops ATP production in HepG2 cells after 3 days of drug treatment [242]. This is important, since ATP enables cells to undergo apoptosis which requires sufficient energy for nuclear condensation and subsequent DNA degradation and phosphatidylserine transfer to the cell surface to facilitate phagocytic removal of dead cell particles [242, 243]. FK866 selectively blocks NAD^+ synthesis by blocking the NAM pathway of NAD production. However, a high concentration of NAM (10 mM) is able to reverse the inhibitory effect of FK866 in HepG2 cells. Moreover, 1mM NA also antagonizes the antiproliferative activity of FK866. Thus, increased amounts of NAD^+ precursors could antagonize FK866 function [242].

1.13 Thymidylate Synthase

BER induces resistance to pemetrexed, a thymidylate synthase (TS)-targeting drug [179]. TS is a key rate-limiting enzyme in DNA synthesis and is responsible for *de novo* synthesis of deoxythymidine-5'-monophosphate (dTMP) through methylation of dUMP by a methyl donor [244]. Since DNA replication and repair is largely dependent on the dTMP pool, cell proliferation depends on TS [245]. Intriguingly, most human tumours have elevated levels of TS mRNA and protein. Ectopic expression of TS in normal cells can lead to a variety of malignant phenotypes in cells including: anchorage independent growth, hyperplasia, foci formation, and tumour formation in immunodeficient mice [246, 247].

1.13.1 TS Inhibition in Cancer

TS has been a target in cancer treatment since the late 1950s [248]. The TS inhibitor 5FU remains the drug of choice for colorectal cancer patients in both adjuvant and palliative care since its initial application in the 1950s [249]. In recent years a combination of 5FU with other chemotherapeutic anticancer drugs and biological agents, including bevacizumab and cetuximab, have successfully increased the response of patients with metastatic colorectal cancer to treatment [249]. TS-targeting drugs have anti-tumour activity against other types of cancers including NSCLC, and the TS-targeting drug pemetrexed, in combination with cisplatin, is now administered in the first

line to treat advanced non-squamous NSCLC [250]. A common mechanism of resistance to TS-targeting drugs is through increased TS mRNA translation after binding of TS inhibitors to TS protein both *in vitro* and in patients [251, 252]. The underlying mechanism of this phenomenon is the ability of TS protein to bind to its own mRNA at two different sequences to repress translation [253]. However, binding of TS-targeting drugs to TS protein reduces TS interaction with TS mRNA. This leads to decreased TS protein-mediated translational repression, increased TS mRNA translation, increased amounts of TS protein and, ultimately, resistance to TS protein-targeting drugs due to target overproduction [245]. To overcome this common problem, antisense targeting of TS mRNA in conjunction with TS-inhibitors has been shown to sensitize a variety of human tumour cell lines to TS-targeting drugs including raltitrexed, 5FU, and 5FUdR [254]. Moreover, concurrent targeting of TS mRNA and BRCA2 or TK mRNA with antisense oligodeoxynucleotides (ODNs) or siRNA sensitizes cancer cells to a number of chemotherapy drugs *in vitr*o [187, 255].

1.14 Targeting mRNA with RNA Interference

Silencing RNA through RNA interference (RNAi) is a post-transcriptional process that results in sequence-specific gene silencing. Double-stranded RNA (dsRNA) molecules are first introduced into target cells. Dicer, an RNase III family member, then cleaves the dsRNA molecules into 19-23 nucleotide fragments (siRNAs) that contain a 5' phosphorylated end and an unphosphorylated 3' end with two unpaired nucleotide overhangs. The unwindase activity of Argonaute (Ago)-2 unwinds the siRNA duplex into two single strands: the guide and passenger strands. The guide strand is incorporated into the RNA-induced silencing complex (RISC) and the passenger strand is degraded. The RISC complex then finds endogenous RNA complementary to the guide strand and cleaves the target RNA through the separate endonuclease activity of Ago-2 [256].

RNAi is a powerful tool to regulate gene expression. Hence, it is emerging as a form of treatment for many human diseases including cancer [257]. Antisense molecules combined with conventional treatments can be used to induce synthetic or complementary lethality in human cancers [187]. Preclinical studies have revealed the effectiveness of RNAi in silencing cancer-related genes [258]. RNAi targeting of many

RNAs regulating critical characteristics of tumour cells *in vivo* (including tumour growth, metastasis, chemoresistance, and angiogenesis) has resulted in favorable outcomes [258].

Chapter 2

2 Thesis Hypotheses:

1- IDO confers resistance to the chemotherapeutic anticancer drugs cisplatin, 5FUdR, pemetrexed, gemcitabine, olaparib, methoxyamine, and FK866 and γ radiation in cancer cells.

2- IDO downregulation sensitizes cancer cells to the chemotherapeutic anticancer drugs cisplatin, 5FUdR, pemetrexed, gemcitabine, olaparib, methoxyamine, and FK866 and γ radiation.

2.1 Thesis Objectives

A) To reduce IDO mRNA levels using an antisense shRNA expression vector in human lung adenocarcinoma A549 cells, human cervical adenocarcinoma HeLa cells, and human lung adenocarcinoma H441 cells, in order to generate clonal human tumour cell populations with: a) cytokine-inducible IDO (A549 and HeLa), b) cytokine-inducible IDO downregulated by antisense IDO shRNA (A549 and HeLa), and c) basal IDO expression downregulated by antisense IDO shRNA (H441).

B) To assess the effect of IDO downregulation on human tumour cell sensitivity to the chemotherapeutic drugs cisplatin, olaparib, 5FUdR, pemetrexed, gemcitabine, methoxyamine, and FK866; or ionizing radiation; in the clonal human tumour cell populations.

C) To assess the effect of combined downregulation of IDO and TS on human tumour cell sensitivity to chemotherapeutic drugs 5FUdR and pemetrexed.

D) To assess the effect of combined downregulation of IDO and BRCA2 on human tumour cell sensitivity to chemotherapeutic drugs olaparib and cisplatin.

E) To assess the effect of IDO downregulation on human tumour cell sensitivity to combined treatments of pemetrexed and methoxyamine.

F) To assess the effect of IDO downregulation on human tumour cell sensitivity to combined treatments of γ radiation and olaparib.

2.2 Thesis Overview

The immune regulatory molecule IDO plays an important and still largely unexplored immune-independent role in the tumour cell response to some common forms of cancer treatment including chemotherapy (cisplatin, olaparib, 5FUdR, pemetrexed, gemcitabine, methoxyamine, and FK866) and therapeutic ionizing γ radiation. The importance of IDO in immune evasion and metastasis of cancer cells is well established [135]. Moreover, targeting IDO with 1-MT improves the effectiveness of some chemotherapy drugs in the context of an intact immune system in mouse models [136]. Here, for the first time, I show the importance of targeting IDO in human cancer cell resistance to the chemotherapy drugs cisplatin, olaparib, pemetrexed, gemcitabine, methoxyamine, and FK866 and γ radiation *in vitro* and in the absence of immune cells.

Conventional IDO inhibitors target IDO's enzymatic function and not its signaling function. The approach I have employed to target IDO has been to use RNAi: a strategy to block IDO expression prior to protein synthesis (*i.e.*, by reducing IDO mRNA levels) that has certain advantages over conventional inhibition of the enzymatic function of IDO protein. For example, targeting IDO mRNA will, by reducing the amount of IDO protein, reduce both its well-described enzymatic function (tryptophan degradation) and putative, but poorly explored signaling and other function(s).

To assay these, the first step was to stably transfect human adenocarcinoma A549 and HeLa cells with vectors directing expression of anti-IDO shRNA (capable of mediating degradation of IDO mRNA) or scrambled shRNA (scr shRNA, incapable of downregulating any known human RNA sequences). Next, and because A549 and HeLa cells express IDO *in vitro* only after cytokine induction [259, 260], 44 and 6 stably transfected A549 and HeLa clones, respectively, were treated with IFNγ to determine whether anti-IDO shRNA incorporation altered IDO mRNA and/or protein levels compared to control, non-targeting, scrambled shRNA (scr-shRNA) incorporation. Because IDO expression is causally associated with reduced proliferation [145], the

functionality of IFNγ-induced IDO was determined by assessing the proliferation rate of cells after IFNγ induction of IDO in cells harbouring: a) anti-IDO shRNA or, b) scr shRNA). The prediction was that IFNγ treatment would reduce proliferation more effectively in cells with scr shRNA (and unimpeded induction of IDO) than in cells with anti-IDO shRNA (and specific reduction in capacity to synthesize IDO). Moreover, differences in proliferation associated with changes in IDO level (and not IFNγ treatment) would be evidence that the critical factor was IDO and not other effects of IFNγ treatment. We also determined whether IDO expression affected cell cycle progression in A549 cells. We found that IDO induced cell cycle arrest at G_1, and that anti-IDO shRNA abolished this effect in A549 cells.

Since IDO is responsible for *de novo* synthesis of NAD^+ as a product of enzymatic degradation of tryptophan in mammalian cells, the level of NAD^+ levels in A549 cells expressing high levels of IDO after IFNγ induction (scr shRNA-transfected cells) and those with reduced IDO expression (anti-IDO shRNA-transfected cells) was assessed. On the basis of evidence presented in the *Results* section, we concluded that anti-IDO shRNA reduced NAD^+ levels in A549 cells.

Because NAD^+ is required for PARP activity, we assessed the effect of antisense-mediated knockdown of IDO on the sensitivity of A549 and HeLa cells to the PARP inhibitor olaparib. IDO-producing A549 human tumour cells exhibited elevated resistance to olaparib while anti-IDO shRNA ablated that resistance in that cell line. However, IDO-producing HeLa cells did not show the same phenomenon.

PARP activity is essential for some DNA repair pathways including BER. In light of results revealing the involvement of IDO in mediating resistance to olaparib in A549 cells, we assessed the effect of IDO upregulation and antisense-mediated IDO reduction on the capacity of the BER inhibitor FK866 to reduce A549 cell proliferation. IDO conferred resistance to FK866, an effect that was abolished by anti-IDO shRNA in A549 cells. Overall, IDO expression mediated resistance to PARP inhibition by olaparib and BER inhibition by FK866, both important processes in repair of DNA damage to tumour cells induced by chemotherapy or radiation.

To expand observations beyond chemotherapy, the effect of IDO upregulation and downregulation on A549 and HeLa cell sensitivity to γ radiation was assessed. IDO

conferred resistance to γ radiation in IDO-expressing cells and anti-IDO shRNA reversed that resistance. Since γ radiation induces double strand breaks in DNA, we examined the effect of IDO on sensitivity to cisplatin (an alkylating agent that causes DNA DSBs). IDO downregulation sensitized cancer cells to cisplatin. Moreover, IDO conferred resistance to cisplatin similar to γ radiation. Because olaparib has been reported to sensitize human tumour cells to ionizing radiation [261], the capacity of IDO upregulation or downregulation to alter sensitivity to combined treatment with γ radiation and olaparib was examined. As described below (*Results*), IDO induced resistance to the combined treatment in A549 cells and IDO downregulation decreased this phenomenon.

Since BER is involved in resistance to the TS-targeting drug pemetrexed, and IDO conferred resistance to BER inhibition in cancer cells, we assessed whether upregulation or downregulation of IDO prior to monotherapy or combined treatment with pemetrexed and the BER inhibitor methoxyamine affected cancer cells sensitivity to these drugs. IDO increased cell resistance to both monotherapy and combined treatment with the two drugs. IDO downregulation reduced this phenomenon.

IDO downregulation sensitized cancer cells to monotherapy with the TS-targeting drug pemetrexed or gemcitabine, but not to another TS-targeting drug 5FUdR. On the other hand, concurrent reduction of IDO and TS using antisense shRNA and siRNA, respectively, sensitized A549 cells to both drugs. These data implicate IDO as a mediator of resistance to TS-targeting drugs in general, and particularly in the context of antisense-reduced TS.

Lastly, we examined the effect of concurrent antisense-mediated reduction of IDO and BRCA2 on A549 cell sensitivity to either olaparib or cisplatin. Concurrent BRCA2 and IDO downregulation sensitized cancer cells to each of these drugs to a greater degree than expected based on the sensitizing effect of knockdown of either target alone (*i.e.*, more than additive).

In an additional series of experiments, human H441 epithelial adenocarcinoma-derived cells, which naturally express IDO without the need for cytokine induction [262], were assessed for sensitivity to cisplatin. They were stably transfected with anti-IDO shRNA or control scr-shRNA. IDO mRNA levels were measured in clonal populations and cells with low IDO levels were compared to populations with high IDO levels with

respect to cisplatin sensitivity, and compared with data obtained after IFNγ-induced IDO expression in human A549 lung tumour-derived and human HeLa cervical tumour-derived cells with respect to drug sensitivity. Similar to A549 and HeLa cells, IDO downregulation sensitized H441 cells to cisplatin.

Chapter 3

3 Materials and Methods

3.1 Cell Culture

Human lung adenocarcinoma A549 cells, human cervical adenocarcinoma HeLa cells, and human lung papillary adenocarcinoma H441 cells were obtained from the American Type Culture Collection (ATCC), and maintained in Minimal Essential Medium α (MEMα), Dulbecco's Modified Eagle Medium (DMEM), and Roswell Park Memorial Institute medium (RPMI)-1640, respectively. Cultured media were supplemented with 10% fetal bovine serum (FBS)(Gibco, Life Technologies, Carlsbad, California, USA, catalogue # 325-043-EL), 100 units/ml penicillin and 100 µg streptomycin (pen/strep)(Gibco, Life Technologies, Carlsbad, California, USA, catalogue # 15140-122) in 70 cm^2 flasks (Sigma-Aldrich, St. Louis, Missouri, USA). Cells were maintained in an incubator and kept at 37°C in 5% CO_2. For most experiments, cells were allowed to proliferate to no more than 70-80% of maximum occupancy on tissue culture plastic (*i.e.*, 70-80% confluent). Trypsin/EDTA (Wisent, Inc., Quebec, Canada) was used to detach cells from flasks. To detach cells, they were first rinsed with sterile Dulbecco's phosphate buffered saline (PBS)(Wisent, Inc., Quebec, Canada) to remove residual FBS. PBS was then aspirated and 1 ml of trypsin/EDTA was added to the cells. Cells were returned to the incubator for 2-3 minutes then 9 ml of growth medium was added to the cells to neutralize the trypsin/EDTA. Harvested cells were then analyzed as described below.

3.2 Cytotoxic Drugs

Olaparib (AZD2281) was purchased from Selleckchem (Houston, Texas, USA). 5FUdR was purchased from Sigma Chemical Co. (St. Louis, Missouri, USA). Pemetrexed (Alimta, manufactured by Eli Lilly and Co., Toronto, Ontario, Canada) and cisplatin (Platinol, manufactured by Bristol-Myers Squibb, Montreal, Quebec, Canada) were obtained from the pharmacy at London Health Sciences Centre (London, Ontario,

Canada). Methoxyamine and FK866 were purchased from Sigma-Aldrich (St. Louis, Missouri, USA).

3.3 Stable IDO Downregulation

3.3.1 Bacterial Strain, Growth, and Preparation of Competent Cells

The *Escherichia coli* (*E.coli*) strain DH5α was used for plasmid amplification. Bacteria were grown in Luria-Bertani (LB) broth, Miller (Bioshop Canada Inc, Burlington, ON) overnight in a shaking incubator at 37°C. To transform bacterial cells with foreign DNA (plasmid), they were first rendered competent as follows: An overnight bacterial culture (4 ml) was transferred into fresh LB broth (70 ml) in a 250 ml Erlenmeyer flask and incubated in a shaking incubator at 37°C for 2 hours. The optical density (OD) of the bacterial culture at 600 nm was measured relative to sterile LB medium (blank control). When $OD_{600\ nm}$ reached 0.354 the bacteria were transformed with plasmid as follows. The bacterial culture was centrifuged at 4000 g for 10 minutes at 4°C. The supernatant was discarded and the cell pellet gently suspended (vortexing was avoided) in 25 ml of sterile, ice-cold transformation solution (10 mM morpholinopropane sulfonic acid (MOPS), pH 7.0; 10 mM rubidium chloride (RbCl). The bacteria were then centrifuged (4000 X g, 10 min, 4°C). The supernatant was discarded and the cell pellet was resuspended in 25 ml of filtered sterile, cold transformation solution II (MOPS, pH 6.5; 50 mM $CaCl_2$; 10 mM RbCl). The bacterial suspension was left on ice for 1 h and cells were then recovered by centrifugation (4000 X g, 10 min, 4°C). The supernatant was aspirated without disturbing the bacterial pellet. Transformation solution II (5 ml) was then added to the pellet, resulting in competent cells ready for transformation. Competent bacteria were used immediately, after up to 2 weeks after storage at 4^{o} C, or after storage at -20^{o} C in 10% glycerol.

3.3.1.1 Bacterial Transformation with Plasmids

Anti-IDO shRNA (1 μg) and non-targeting scrambled control shRNA [Qiagen KH01328P SureSilencing™ Puromycin vector (human IDO1, catalogue # 336314)] were added to separate tubes of competent bacteria (150 μl) and mixed gently. The puromycin

vector pGeneClip™ (Figure 3.1) contains a beta-lactamase (ampicillin resistance) region that allows transformed bacteria to become resistant to ampicillin. This vector also contains a puromycin-N-acetyltransferase coding region that confers puromycin resistance to successfully-transfected mammalian cells, to allow clonal selection. There were four different anti-IDO shRNA sequences and one non-targeting scrambled control shRNA (Table 3.1). Each shRNA sequence was individually inserted into the plasmid vector as part of an insert sequence. The loop structure of the shRNA consists of the sequence CTTCCTGTCA. The insert sequence containing each shRNA was inserted between positions 438 and 439 in the plasmid vector. Each shRNA inserted into the plasmid vector targets a different exon on the IDO1 gene. The plasmid vectors were used to transform *E.coli* strain DH5α before plasmid purification. The plasmid- DH5α mixture was kept on ice for 25 min, then heat-shocked (2.5 min, 42°C) followed by incubation at 4^{o} C for 2 min. LB broth (1 ml) was then added to the bacteria, followed by incubation at 37°C for 1 hour in a shaking incubator. Bacteria were centrifuged at 6000 X g for 2 min and the majority of the supernatant was removed leaving 50-100 µl. The bacterial pellet was resuspended in the remaining supernatant and spread on LB agar plates (containing 50 µg/ml ampicillin to select for transformed cells). Transformed cells were grown overnight at 37° C. Non-transformed bacteria were cultured on agar plates with and without ampicillin as a control experiment to confirm the activity of ampicillin.

Table 3. 1. SureSilencing shRNA plasmid sequences. Each anti-IDO shRNA sequence targets a specific exon on the IDO gene. Each shRNA sequence was inserted into a plasmid vector. Those vectors were propagated in bacteria then purified and used to stably transfect cancer cells.

shRNA ID	Insert Sequence
1	AGACTGCAGTAAAGGATTCTT
2	GTGACTAAGTACATCCTGATT
3	CAGTGTTCTTCGCATATATTT
4	TCCTCCAGGACATGAGAAGAT
NC (control)	GGAATCTCATTCGATGCATAC

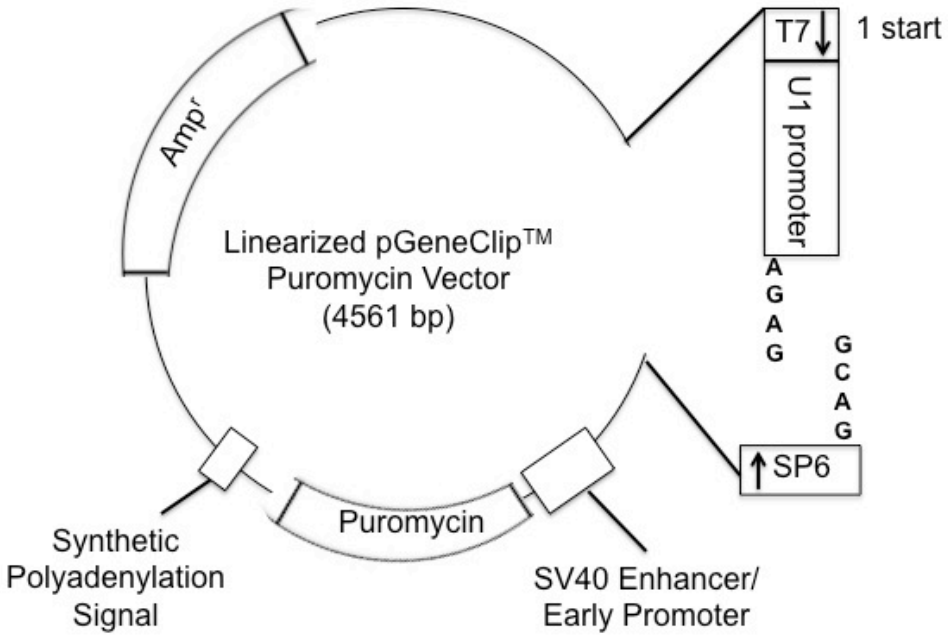
T7
1 start
U1 promoter
A
G
A
G
G
C
A
G
SP6
Amp^r
Linearized pGeneClip™
Puromycin Vector
(4561 bp)
Puromycin
Synthetic
Polyadenylation
Signal
SV40 Enhancer/
Early Promoter

Figure 3. 1. The puromycin-resistant vector pGeneClip™. Anti-IDO shRNA sequences or non-targeting scrambled shRNA control sequence were separately inserted into this vector prior to stable transfection of mammalian cells. The vector contains an ampicillin resistance region to allow the transformed bacteria to grow in the presence of ampicillin in order to propagate the plasmid, and a puromycin-N-acetyltransferase coding region that allows stably transfected cells to grow in the presence of puromycin.

3.3.1.2 Plasmid Purification

After growing bacteria on plates overnight, single colonies were inoculated by sterile pipette into 2.5 ml of LB medium containing 50 μg/ml ampicillin. The bacterial culture was incubated in a shaking incubator at 37° C for 5 hours, inoculated into 250 ml of LB medium containing 50 μg/ml ampicillin, and then grown overnight at 37° C with shaking. Plasmids were purified from these bacterial cultures using Qiagen HiSpeed plasmid maxi kits (Qiagen, catalog # 12662) according to the following protocol that was described by the manufacturer:

Bacterial cells were harvested by centrifugation at 6000 X g for 15 minutes at 4° C. The supernatant was discarded and the bacterial pellet suspended in 10 ml of buffer P1 containing RNase A (100 μg/ml), Tris base (50 mM, pH 8.0), and EDTA (10 mM) that was provided in the kit (added immediately prior to use) to lyse bacteria. Buffer P2 (10 ml) containing NaOH (200 mM) and 1% SDS (w/v) was then added (without vortexing, to avoid shearing genomic DNA), mixed, and incubated for 5 min at 25^{o} C. After incubation, 10 ml of chilled buffer P3 containing potassium acetate (3.0 mM, pH 5.5) was added to the lysate and mixed immediately by inverting 4-6 times. The lysate was then poured into the barrel of QIAfilter Maxi cartridges, incubated for 10 minutes, and then allowed to empty by gravity flow after adding 10 ml of QBT buffer [750 mM NaCl, 50 mM MOPS (pH 7.0), 15% isopropanol (v/v), and 0.15% Triton X-100 (v/v)]. Non-plasmid DNA material remaining in the cartridge was eluted using the supplied syringe plunger, the cartridge contents were washed with 60 ml of QC buffer [1.0 M NaCl, 50 mM MOPS (pH 7.0), and 15% isopropanol (v/v)] by gravity flow, and plasmid DNA was eluted in 15 ml of QF buffer [1.25 M NaCl, 50 mM Tris-base (pH 8.5), and 15% isopropanol v/v]. The eluted DNA was precipitated by adding 10.5 ml room temperature isopropanol followed by incubation for 5 min. The elute/isopropanol mixture was then filtered to immobilize plasmid DNA on a QIA filter membrane, washed with 2 ml of 70% ethanol, air dried, and dissolved in 0.5 ml of Tris-EDTA (TE) buffer (pH 8.0).

3.3.2 Plasmid Quality Control and Diagnostic Restriction Digest

To verify that purified plasmids contained the desired shRNA inserts, a plasmid quality control by Pst I restriction enzyme digestion was carried out. Plasmids containing shRNA inserts were expected to generate two diagnostic bands 3209 bp and 1402 bp upon digestion. All 5 plasmid samples described in section 3.4.2 were used for this experiment (anti-IDO shRNA plasmids 1-4 and scrambled control shRNA plasmid). Each reaction contained 1.2 μg plasmid DNA, 2 μl of the 10x reaction mix, 0.5 μl Pst I enzyme, and sufficient sterile water to achieve a final volume of 20 μl. Restriction digestion proceeded at 37° C for one hour before separating the digestion products on the basis of electrophoretic mobility through a 1% agarose gel. As a negative control for each sample, 1 μg of each supercoiled plasmid (uncleaved) was assessed by gel electrophoresis.

3.3.2.1 Ethanol Precipitation of DNA

To maximize plasmid concentrations before transfection of cancer cells, plasmids were precipitated in ethanol and resuspended in 100-200 μl of TE buffer to obtain a final concentration of a 1 μg/μl for each plasmid.

3.3.2.2 Linearization of shRNA Plasmids for A549 Stable Transfection

To increase the efficiency of plasmid integration into the genomic DNA, plasmid linearization was performed as described below:

Anti-IDO shRNA 2 and scrambled shRNA plasmids (40 μg) were linearized using Sca I restriction enzyme (Fermentas, 10 U/μl, Hanover, MD) using the protocol and buffers supplied by the manufacturer. The reaction mix was: 5 μl Buffer (10x concentration), 40 μl DNA, 6 μl Sca I enzyme, 4 μl dH_2O. Restriction cleavage proceeded at 37°C for 3 h, followed by ethanol precipitation. Precipitated plasmids were dissolved in dH_2O to a final concentration of 1 μg/μl.

3.3.2.3 Stable Transfection of A549, HeLa, and H441 Cells with anti-IDO shRNA or Scrambled shRNA Plasmids

Human A549, HeLa, and H441 cells were stably transfected with a vector expressing short hairpin RNA (shRNA) antisense to human IDO1, or a scrambled, non-targeting control shRNA (SuperArray, Mississauga, ON), using Lipofectamine 2000 (LFA2K)(Invitrogen, Burlington, ON, Canada) according to the manufacturer's instructions. Anti-IDO shRNA 2 exerts the most robust IDO downregulation in human SW480 colorectal adenocarcinoma cells (Dr. M.D. Andersen, Center for Cancer Immunotherapy, Herlev University hospital, Denmark, *personal communication*). Therefore, we used plasmid shRNA 2 and scrambled control shRNA to stably transfect A549 and HeLa cells. We stably tranfected H441 cells with each plasmid shRNAs (1, 2, 3 and 4) and scrambled control shRNA. H441 (1×10^6) were cultured overnight in 25 cm^2 flasks in 2 ml of AMEM supplemented with 10% FBS. On the day of transfection with shRNA, cells were approximately 70% confluent. For transfection, 10 μg of anti-IDO gene-specific plasmid expressing shRNA or scrambled control shRNA was mixed with 10 μl LFA2K and 125 μl serum-free MEMα. The mixture was then incubated for 20 minutes in room temperature to allow shRNA:LFA2K complex formation. After incubation, 250 μl of the mixture was added to each flask of cells. At 4 h after transfection, culture medium was exchanged for fresh MEMα containing 10% fetal bovine serum. Cells were washed with PBS (1x) and trypsinized 24 h later, and seeded into a 14 cm mammalian tissue culture dish in 30 ml MEMα supplemented with 10% FBS. Cells were allowed to proliferate in culture for 72 h, followed by replacement with fresh medium containing 2 μg/ml puromycin (Bioshop, Burlington, ON). Medium was replaced every 3 days with fresh medium containing 2 μg/ml puromycin. Stably-transfected cells formed colonies, and single colonies (approximately 30 transfected with each of the shRNA-expressing plasmids) were selected and grown in 48-well plates in 0.8 ml MEMα supplemented with 10% FBS and 2 μg/ml puromycin. When confluent, cells were transferred to 6-well plates and were cultured in triplicate. A549 and HeLa cells were then treated with IFNγ (25 ng/ml) and IDO mRNA and protein levels were

measured by qPCR and immunoblotting, respectively. Since H441 cells express IDO endogenously, IDO mRNA was directly measured in the selected clones by qPCR.

3.4 Transient Transfection of A549 Cells with anti-IDO shRNA or Scrambled shRNA Plasmids

To test the capability of each shRNA to transiently downregulate IDO, A549 cells were transfected with 8 μg of each plasmid using a modification of established protocols (Plasmid DNA transfection Lipofectamine^{TM} 2000 transfection guideline, Invitrogen, Burlington, ON, Canada). A549 cells (7 x 10^5) were cultured in 25 cm^2 flasks in 2 ml of MEMα supplemented with 10% FBS. Each plasmid (8 μg) was added to 20 μl of LFA2K for 20 min at 25^o C to allow shRNA: LFA2K complex formation. Cells were transfected by adding a mixture of plasmids and LFA2K (250 μl total volume) and incubating for 4 h at 37° C. Fresh medium containing IFNγ (16 ng/ml, R&D Systems, Minneapolis, MN)(4 ml) was added to each flask. Total RNA was isolated 24 h after transfection and cDNA generated from those isolated RNAs. Semi-quantitative PCR analysis of IDO and GAPDH cDNAs in each sample was performed to assess IDO downregulation by each plasmid.

3.5 RNA Isolation

A549 and HeLa cells were cultured overnight and then the growth medium was replaced with medium containing IFNγ (25, 50 or 100 ng/ml). RNA was isolated from A549 and HeLa cells 20 h after IFNγ treatment. Cells were washed with PBS twice. Trizol reagent (1 ml, Invitrogen) was added to each flask to lyse cells directly. The cell lysate was pipetted up and down several times and then transferred to 1.5 ml microcentrifuge tubes. Chloroform (200 μl) was added to each cell lysate and vortexed for 10 sec, followed by incubation for 5 min at 25^o C. Samples were centrifuged at 20000 X g at 4° C. The top aqueous phase (450-500 μl, containing RNA) was transferred into a new microcentrifuge tube. Isopropyl alcohol (600 μl) was added to precipitate the RNA. Samples were vortexed and incubated at room temperature for 10 min, centrifuged at 20000 X g for 20 min at 4°C. The supernatant was discarded and the RNA pellet was

washed twice with 1 ml of 70% ethanol, air dried, and dissolved in 20 μl of DEPC-treated water measurement of RNA concentration by NanoDrop® analysis.

3.6 IDO mRNA Detection via Conventional PCR

Isolated mRNA (1 μg) was used to synthesize cDNA by reverse transcription using MMLV-RT (Invitrogen). PCR amplification of IDO cDNA proceeded as follows: 95°C, 5 min; 95°C, 30 s; 57°C, 30 s; 72°C, 30 s; 95°C, 30 (39 times); 72°C, 10 min; 4°C GAPDH cDNA was similarly amplified except for 24 rather than 39 amplifications at step 5. The reverse and forward primer sequences for IDO and GAPDH are shown in Table 3.2. To visualize PCR amplification products, 25 μl of PCR product was added to 6 μl of Orange-G loading dye in glycerol, mixed, and separated by electrophoresis through a 1.5% non-denaturing agarose gel. A sample (1 μg) of the RNA used to generate cDNA was similarly separated by gel electrophoresis to visually determine RNA integrity.

3.7 IDO mRNA Quantitation by Real-Time PCR

A549 and HeLa clonally-selected populations stably-transfected with anti-IDO shRNA or non-targeting scrambled control shRNA were collected 24 h after treatment with IFNγ (25 ng/ml, R&D Systems, Minneapolis, MN). H441 clonal populations, stably transfected with anti-IDO shRNA or non-targeting scrambled control shRNA were collected 24-36 h post cell culture without IFNγ treatment. Cells were lysed (Trizol reagent, Invitrogen) and total RNA isolated according to the manufacturer's instructions. cDNA was synthesized by reverse transcription (MMLV-RT) using 1 μg of purified RNA. IDO and 18S rRNA or GAPDH (control housekeeping genes) levels were measured simultaneously by multiplex real-time PCR amplification using a TaqMan IDO1 gene expression assay kit (Applied Biosystems, Carlsbad, CA).

Table 3. 2. IDO and GAPDH PCR primer sequences.

IDO Forward primer	5'-TAATGGCACACGCTATGGAA-3'
IDO Reverse primer	3'-GGAAGGACAAACTCACGGACT-5'
GAPDH Forward primer	5'-TATTGGGCGCCTGGTCACCA-3'
GAPDH Reverse primer	3'-CCACCTTCTTGATGTCATCA-5'

3.8 IDO, BRCA2 and TS Protein Detection and Measurement

A549 and HeLa cells were cultured in 75 cm^2 flasks and treated with IFNγ (25 ng/ml). Cells were incubated for 48 h, washed twice with ice-cold PBS, harvested, and sonicated. Lysed cells were centrifuged at 20,000 X g for 15 min at 4° C and the supernatant collected and stored at -80° C for future use. Protein extracts (20 μg) were quantified by BioRad protein assay, separated by electrophoresis through a 12% polyacrylamide gel, and then electro-transferred to a nitrocellulose membrane. Primary monoclonal antibodies against IDO (Abcam, Cambridge, UK) and actin (Sigma, St. Louis, MO) were used to detect and quantify these proteins. Secondary anti-mouse and anti-rabbit IgG (peroxidase-linked whole antibodies; GE Healthcare Life Sciences), were bound to primary IDO and actin antibodies, respectively. The antibody-protein complexes were visualized using a Storm scanner (GE Healthcare Life Sciences).

BRCA2 protein was assessed in A549 cells similar to the method to detect IDO protein except that BRCA2 monoclonal rabbit antibody (Cell Signaling Technology # 90125, Danvers, MA, USA) was used to detect and quantify BRCA2 protein. A Ready Gel® Tris-HCL gradient gel 4-15% (Cat # 161-1158, BioRad) was used to separate the proteins. Trans-blot Turbo transfer pack (Mini format) 0.2 μM PVDF (cat # 170-4150, BioRad) was used for the transfer of proteins from the gel to the PVDF membrane.

TS protein was assessed in A549 cells similar to the method to detect IDO and BRCA2 protein except that TS monoclonal antibody (Taiho Pharmaceutical, Hanno-City, Japan) was kindly provided by Dr. Masakazu Fukushima (Taiho Pharmaceuticals, Hanno Research Center, Hanno-City, Japan). Protein samples were isolated at 96 h post-siRNA transfection of A549 cells.

3.9 NAD^+ Quantification

NAD^+ levels were measured in A549 clonal populations stably transfected with plasmids directing expression of anti-IDO shRNA or scrambled shRNA, using a NAD^+/NADH quantification Kit (BioVision, Milpitas, CA; Catalog#K337- 100). Briefly, 2 x 10^5 cells were seeded into 25 cm^2 flasks and grown overnight. Medium was replaced

16-24 h later with 3 ml of fresh growth medium containing IFNγ (25 ng/ml). Cells were washed 48 h later with ice-cold PBS, pelleted by centrifugation, and extracted using 2 freeze/thaw cycles and NADH/NAD extraction buffer (400 µl). NADt (total NAD including NADH and NAD) was detected in 50 µl of extracted samples after addition of NAD cycling buffer and NAD cycling enzyme mix to a total volume of 100 µl. NADH levels were measured in a similar fashion in aliquots where NAD^+ was degraded beforehand by heating the samples to 60° C for 30 min. NAD^+ levels were calculated by subtracting NADH levels from NADt levels. Samples were read at OD 450 nm using a Wallac Victor2 plate reader (Perkin Elmer Life Sciences, Waltham, MA).

3.10 Cell Cycle Analysis

A549 cells ($2x10^5$) were cultured overnight and then IFNγ (25 ng/ml) was added (vehicle only was added to control cells). After 48 h, cells were washed with PBS, trypsinized, and fixed in 70% ice-cold ethanol. Cells were washed with PBS 24 h after fixation and resuspended in 1 ml of propidium iodide (20 µg/ml) (Sigma Aldrich, St. Louis, MO) and 0.1% Triton X-100 (BDH Chemicals, Poole, UK) staining solution with RNAse A (Bioshop, Burlington, ON, Canada) for 15 minutes at 37° C. The stage of cell cycle was analyzed using a BD FACSCalibur flow cytometer (BD Biosciences, Franklin Lakes, NJ) and FlowJo software (Tree Star, Inc., Ashland, OR, USA).

3.11 Olaparib Treatment

A549 and HeLa cells ($5x10^4$) were seeded into 25 cm^2 flasks in 2 ml of MEMα and DMEM supplemented with 10% FBS plus pen/strep, respectively. Medium was replaced with fresh growth medium with or without IFNγ (25 ng/ml) 16-24 h after seeding. Twenty-four or 48 h after addition of IFNγ, medium was replaced with fresh medium containing olaparib (1, 1.5 or 5 µM). Three days after addition of olaparib, cells were washed to remove the dead cells and particles and adherent cells were trypsinized and enumerated using a Coulter counter (Beckman, Mississauga, ON). Viability of the counted cells was confirmed by trypan blue exclusion.

3.12 γ Radiation Treatment

A549 and HeLa cells ($5x10^4$) were seeded into 25 cm^2 flasks in 2 ml of growth medium. Culture media was replaced with medium with or without IFNγ (25 ng/ml) 16-24 h later. Cells were exposed to γ radiation (4 Gy) using a ^{60}Co irradiator (London, Ontario, Canada) or a Varian Clinical 21EX Linear accelerator (Varian Medical System, Palo Alto, CA) using a 6 MV X ray beam (40 x 40 cm with 1.5 cm water equivalent buildup material) 48 h after addition of IFNγ. After irradiation, medium was replaced with fresh growth medium without IFNγ and cells were allowed to proliferate for 72 h. Cells were then trypsinized and live cells were enumerated using a Coulter counter.

3.13 Combined Treatment with Radiation and Olaparib

A549 and HeLa cells ($5x10^4$) were grown and irradiated as described above. Immediately after irradiation, medium was replaced with fresh medium containing olaparib (5 μM) and cells were allowed to proliferate in culture for 72 h. Cells were then trypsinized and live cells were enumerated using a Coulter counter.

3.14 Cisplatin, Gemcitabine, Pemetrexed, and 5FUdR Treatment

A549 cells ($5x10^4$) were seeded into 25 cm^2 flasks in 2 ml of MEMα supplemented with 10% FBS containing pen/strep. Medium was replaced with fresh growth medium with or without IFNγ (25 ng/ml) 16-24 h after seeding. Twenty-four or 48 h after addition of IFNγ, medium was replaced with fresh medium containing either cisplatin (4 or 8 μM), gemcitabine (10 nM), pemetrexed (200 nM), or 5FUdR (40 nM). Three days after addition of drugs, cells were washed to remove the dead cells and particles. Adherent cells were trypsinized and enumerated using a Coulter counter (Beckman, Mississauga, ON). Viability of the counted cells was confirmed by trypan blue exclusion. H441 cells ($5x10^4$) were seeded into 6-well plates in 3 ml of RPMI-1640 supplemented with 20% FBS plus pen/strep and grown overnight. Medium was replaced the next day with 4 ml of fresh growth medium containing cisplatin (5 or 10 μM). Cells were allowed to proliferate for 8 days. On day 5 after initial culture, 2 ml fresh medium was added to each well. At the end of the experiment cells were washed to remove the dead cells and particles.

Adherent cells were trypsinized and enumerated using a Coulter counter (Beckman, Mississauga, ON).

3.15 Blocking NAD^+ Synthesis by FK866 Treatment

A549 cells ($5x10^4$) were seeded into 25 cm^2 flasks in 2 ml of MEMα supplemented with 10% FBS plus pen/strep. Medium was replaced with fresh growth medium with or without IFNγ (25 ng/ml) 16-24 h after seeding. Forty-eight h after addition of IFNγ, medium was replaced with fresh medium containing FK866 (5 nM). Three days after addition of FK866, cells were washed to remove the dead cells and particles and adherent cells were trypsinized and enumerated using a Coulter counter (Beckman, Mississauga, ON). Viability of the counted cells was confirmed by trypan blue exclusion.

3.16 Blocking BER by Methoxyamine Treatment

A549 cells ($5x10^4$) were seeded into 25 cm^2 flasks in 2 ml of MEMα supplemented with 10% FBS plus pen/strep. Medium was replaced with fresh growth medium with or without IFNγ (25 ng/ml) 16-24 h after seeding. Forty-eight h after addition of IFNγ, medium was replaced with fresh medium containing methoxyamine (MX)(3 mM). Three days after addition of MX, cells were washed to remove the dead cells and particles and adherent cells were trypsinized and enumerated using a Coulter counter (Beckman, Mississauga, ON). Viability of the counted cells was confirmed by trypan blue exclusion.

3.17 Combined Treatment with Pemetrexed and MX

A549 cells ($5x10^4$) were grown and co-treated with pemetrexed (30 nM) and MX (3 mM) as described above. Cells were allowed to proliferate in culture for 72 h. Cells were then trypsinized and live cells were enumerated using a Coulter counter.

3.18 IDO siRNA Transfection

Human IDO siRNA [OnTarget Plus SMARTPool IDO (Dharmacon RNAi Technologies)] was used to transfect A549 and H441 cells (Table 3.3). IDO siRNA (10 nM) and control non-targeting siRNA (2.5 nM) in serum-free MEMα and LFA2K (2.5 μg/ml) were incubated together for 20 min. The siRNA:LFA2K mix was then added to

A549 and H441 cells that had been seeded, in triplicate, at 2 x10^5 cells per 25 cm^2 flask 24 h beforehand. In case of A549 cells, at 4 h after addition of siRNA:LFA2K, media were exchanged for fresh growth medium containing IFNγ (16 ng/ml). In another method, A549 cells were treated with IFNγ (50 ng/ml) 6 h before siRNA transfection. Transfection was conducted as above. At 4 h post transfection fresh medium containing IFNγ (50 ng/ml) was added to the A549 cells. H441 cells that endogenously express IDO, without induction with added cytokines, were similarly transfected with IDO siRNA as above, without IFNγ induction. RNA was isolated from the cells 24 h post-siRNA transfection. cDNA was synthesized and IDO and GAPDH cDNAs amplified by PCR.

Table 3. 3. ON-Target Plus® IDO1, TS and BRCA2 siRNA target mRNA sequences.

siRNA ID	Targeted RNA	Target mRNA Sequence	Target Position in mRNA Transcript
IDO A	IDO1 mRNA	5'-UCACCAAAUCCACGAUCAU-3'	1281-1299
IDO B	IDO1 mRNA	5'-UUUCAGUGUUCUUCGCAUA-3'	422-440
IDO C	IDO1 mRNA	5'-GUAUGAAGGGUUCUGGGAA-3'	1383-1401
IDO D	IDO1 mRNA	5'- GAACGGGACACUUUGCUAA-3'	1213-1231
TS #3	TS mRNA	5′-ACAGAGAUAUGGAAUCAGA-3′	576-594
TS #4	TS mRNA	5′-GGACUUGGGCCCAGUUUAU-3′	526-544
BRCA2	BRCA2 mRNA	5′-GAAACGGACUUGCUAUUUA-3′	4285-4303
BRCA2	BRCA2 mRNA	5′-GGUAUCAGAUGCUUCAUUA-3′	558-576
BRCA2	BRCA2 mRNA	5′-GAAGAAUGCAGGUUUAAUA-3′	1949-1967
BRCA2	BRCA2 mRNA	5′-UAAGGAACGUCAAGAGAUA-3′	7242-7260
Control	No Target	5'-UGGUUUACAUGUUGUGUGA-3'	

3.19 BRCA2 siRNA Transfection and Drug Treatment

Concentrations of siRNAs targeting human BRCA2 [OnTarget Plus SMARTPool BRCA2 (Dharmacon RNAi Technologies)] (Table 3.3) that reduced target mRNAs by approximately 70% by 24 h after transfection were determined (10 nM). BRCA2 siRNA (10 nM) and control non-targeting siRNA (2.5 nM) in serum-free MEMα and LFA2K (2.5 μg/ml) were incubated together for 20 min. The siRNA:LFA2K mix was then added to A549 cells that had been seeded, in triplicate, at 2 $x10^5$ cells per 25 cm^2 flask 24 h beforehand. At 4 h after addition of siRNA:LFA2K, medium was exchanged for fresh growth medium containing IFNγ (25 ng/ml). Medium was replaced with fresh medium containing olaparib or cisplatin 16-24 h later. Tumour cell proliferation was enumerated 72 h later using a Coulter counter.

3.20 TS siRNA Transfection and Drug Treatment

TS siRNA number 3 or TS siRNA number 4 (Table 3.3) (targeting different regions of human TS mRNA)[OnTarget Plus (Dharmacon RNAi Technologies, Lafayette, CO, USA)] that reduced target mRNAs by approximately 70% by 24 h after transfection, were used to downregulate TS mRNA in A549 cancer cells. TS siRNA (5 nM) and control non-targeting siRNA (5 nM) in serum-free MEMα and LFA2K (2.5 μg/ml) were incubated together for 20 min. The siRNA:LFA2K mix was then added to A549 cells that had been seeded, in triplicate, at 2 $x10^5$ cells per 25 cm^2 flask 24 h beforehand. At 4 h after addition of siRNA:LFA2K, media was exchanged for fresh growth medium containing IFNγ (25 ng/ml). Medium was replaced with fresh medium containing pemetrexed, 5FUdR, or gemcitabine 48 h later. Tumour cell proliferation was enumerated 72 h later using a Coulter counter.

A549 cells were transiently transfected with either control siRNA or TS siRNA for 4 h. Cultured medium was then replaced with growth medium containing IFNγ (16 ng/ml). RNA was isolated from cells 24 h post-transfection and IDO and TS mRNA were measured by PCR.

3.21 Puromycin Treatment of A549 Cells

A549, HeLa, and H441 cells (5 x 10^5) were seeded in a 10 cm^2 plastic tissue culture dish in 5 ml of growth medium overnight. Puromycin (0, 1, 2, 4, 6, or 8 μg/ml) was added to the cells. Cell growth was monitored by visual microscopy daily. The lowest concentration that killed all cells was chosen to maintain the stably-transfected A549, HeLa and H441 cells.

3.22 Colony Forming Assay after Irradiation

A549 clonal populations were seeded in 25 cm^2 flasks in 2 ml of growth medium overnight. Cultured medium was replaced by fresh medium with or without IFNγ (25 ng/ml) and maintained for 48 h. Cells were then irradiated (4 Gy) or not (control cells). All cells were trypsinized and 300 cells were seeded in 6 well plates in 4 ml of growth medium. Medium was replaced with fresh medium 72 h later. Cells were allowed to proliferate for a total 7 days. Medium was aspirated and cells were washed with PBS and stained with 0.5% crystal violet for 45 min at 20° C. Cells were washed twice with dH_2O and colonies were counted. The number of colonies in each treatment group was divided by the number of colonies in the control and multiplied by 100 to estimate % colony formation.

3.23 Statistical Analysis

Student's *t* test (2-tailed) was used to determine differences between two means. One-way ANOVA was used to assess differences among multiple means. A *p* value of 0.05 was selected *a priori* to indicate significant differences. In some analyses, data were pooled from A549 and HeLa clonal populations that expressed anti-IDO shRNA and compared to the pooled measurements of multiple clones expressing scrambled control shRNA. Tumours are heterogenous populations and each clonal population, although relatively similar to other clones because of their derivation from a common parent, potentially has differences due to variation induced by ongoing genomic instability. Combining tumour clones allows examinination of the role of IDO in drug sensitivity and resistance in a heterogenous cancer population originating from the same parental cell line. Observing meaningful statistical differences in radiation and drug sensitivity in

examined clones provides clear evidence for the importance of IDO downregulation in cancer cells despite other differences among cells.

Chapter 4

4 Results

4.1 IDO Induction in A549 and HeLa Cells

IDO plays a major role in suppressing the immune response during tumour progression. Most human tumours express IDO *in vivo* [135], but IDO protein is undetectable in A549 and HeLa cells *in vitro* until induced by IFNγ. Therefore, IFNγ was used to induce IDO in A549 and HeLa cells in these studies as described in chapter 3, section 3.5. RNA quality was tested from representative samples (Figure 4.1), cDNA was synthesized, and IDO and GAPDH mRNA levels determined using the synthesized cDNA (Table 3.2 shows primer sequences). IFNγ strongly induced IDO mRNA in both A549 and HeLa adenocarcinoma cells (Figures 4.2 and 4.3). Since all IFNγ concentrations induced IDO mRNA in cancer cells, and to limit non-IDO related effects of IFNγ, 25 ng/ml IFNγ was used to induce IDO in subsequent experiments unless otherwise noted. This strongly induced IDO mRNA and protein in both A549 and HeLa cells. In the next step, we measured A549 IDO protein levels after IFNγ treatment as described (Chapter 3, section 3.8). IFNγ (25 ng/ml) induced IDO protein in A549 cells (Figure 4.4).

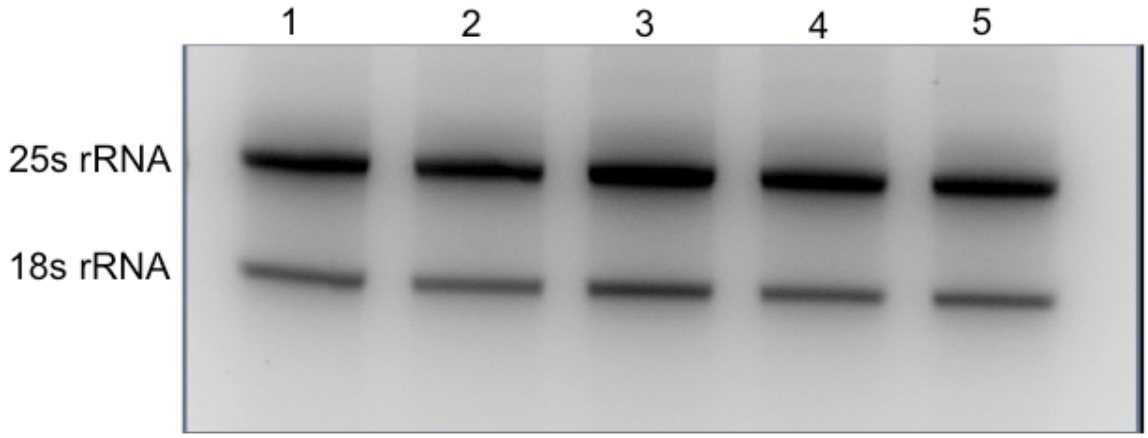
1
2
3
4
5
25s rRNA
18s rRNA

Figure 4. 1. Quality of RNA isolated from A549 cells ± IFNγ (50 ng/ml). A549 cells were cultured overnight then treated with or without IFNγ (50 ng/ml). RNA was isolated 20 h post-IFNγ treatment. RNA samples were separated on a 1.5% agarose gel to confirm RNA integrity. Top bands are 25S rRNA and the lower bands are 18s rRNA. Lanes 1-2: A549 cells without IFNγ treatment. Lanes 3-5, A549 cells with IFNγ treatment.

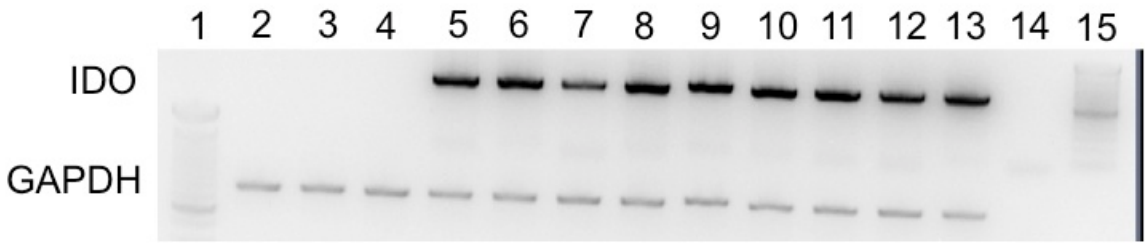
1 2 3 4 5 6 7 8 9 10 11 12 13 14 15
IDO
GAPDH

Figure 4. 2. IDO mRNA levels in A549 cells ± IFNγ (25, 50 or 100 ng/ml). A549 cells were treated with or without IFNγ (25, 50 or 100 ng/ml) and RNA was isolated 20 h later. cDNA was synthesized from the isolated RNA (1 μg) and then used as the template for IDO and GAPDH cDNA amplification by PCR. Top bands represent IDO and the lower bands represent the housekeeping gene GAPDH. PCR amplification products were separated by electrophoresis through a 1.5% non-denaturing agarose gel. Lane 1: Molecular weight ladder for GAPDH. Lane 2-4: A549 cells without IFNγ treatment. Lane 5-7: A549 cells with IFNγ treatment (25 ng/ml). Lane 8-10: A549 cells with IFNγ treatment (50 ng/ml). Lane 11-13: A549 cells with IFNγ treatment (100 ng/ml). Lane 14: non-template control. Lane 15: Molecular weight ladder for IDO. The GAPDH PCR product is 750 bp and IDO PCR product is 800 bp.

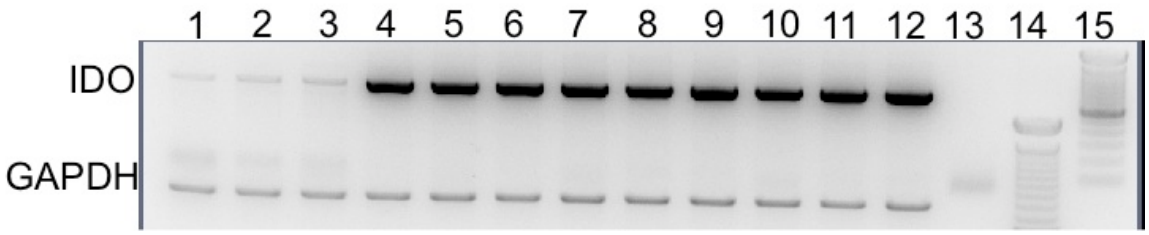
1 2 3 4 5 6 7 8 9 10 11 12 13 14 15
IDO
GAPDH

Figure 4. 3. IDO mRNA levels in HeLa cells ± IFNγ (25, 50 or 100 ng/ml). HeLa cells were treated with or without IFNγ (25, 50 or 100 ng/ml) and RNA was isolated 20 h later. cDNA was synthesized from the isolated RNA (1 μg) and then used as the template for IDO and GAPDH cDNA amplification by PCR. Top bands represent IDO and the lower bands represent the housekeeping gene GAPDH. PCR amplification products were separated by electrophoresis through a 1.5% non-denaturing agarose gel. Lane 1-3: HeLa cells without IFNγ treatment. Lane 4-6: HeLa cells with IFNγ treatment (25 ng/ml). Lane 7-9: HeLa cells with IFNγ treatment (50 ng/ml). Lane 10-12: HeLa cells with IFNγ treatment (100 ng/ml). Lane 13: non-template control. Lane 14: Molecular weight ladder for GAPDH. Lane 15: Molecular weight ladder for IDO. The GAPDH PCR product is 750 bp and IDO PCR product is 800 bp.

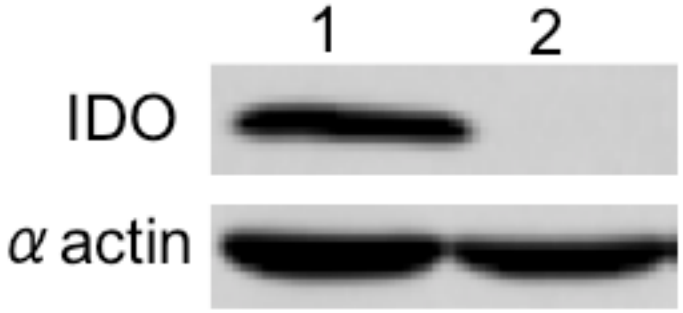
1
2
IDO
α actin

Figure 4. 4. IDO protein levels in A549 cells ± IFNγ (25 ng/ml). A549 cells were treated with or without IFNγ (25 ng/ml) and lysed 48 h later. Immunoblots were probed for IDO and α actin. The top bands represent IDO and the lower bands represent α actin. Lane 1: A549 cells with IFNγ treatment. Lane 2: A549 cells without IFNγ treatment.

4.2 IDO mRNA Levels in H441 Cells

H441 human lung adenocarcinoma cells endogenously express IDO [262][*personal communication,* Dr. Vios Karanikas (Cancer Immunology unit, department of Immunology, University of Thessaly, Greece)]. IDO mRNA levels were measured in H441 cells 24 h after culture (without IFNγ treatment). H441 cells endogenously express IDO mRNA and do not require IFNγ induction (Figure 4.5).

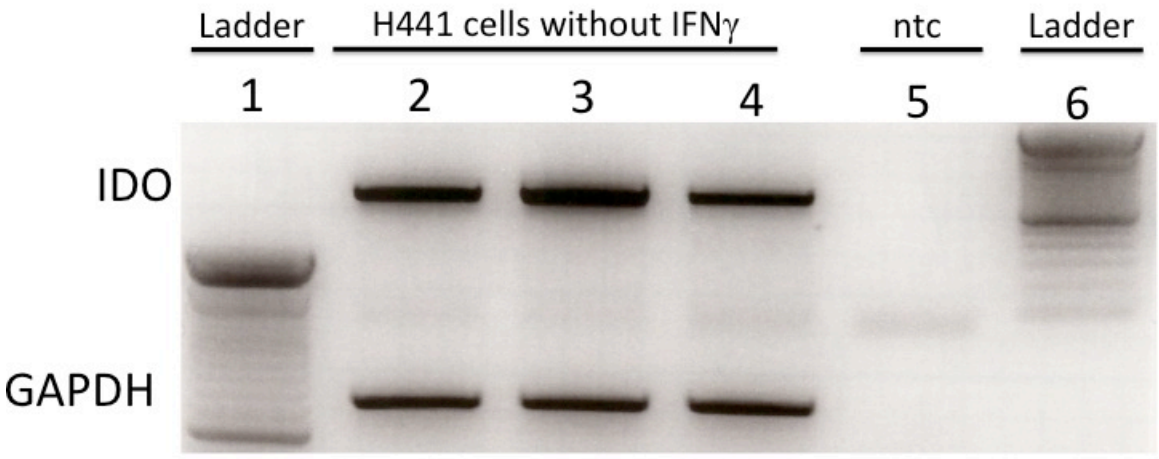
Ladder
H441 cells without IFNγ
ntc
Ladder
1
2
3
4
5
6
IDO
GAPDH

Figure 4. 5. IDO mRNA levels in H441 cells. H441 cells were cultured for 24 h (without IFNγ treatment) and RNA isolated. cDNA was synthesized from the isolated RNA (1 μg) and then used as the template for IDO and GAPDH cDNA amplification by PCR. Top bands represent IDO and the lower bands represent the housekeeping gene GAPDH. PCR amplification products were separated by electrophoresis through a 1.5% non-denaturing agarose gel. Lane 1: Molecular weight ladder for GAPDH. Lane 2-4: H441 cells without IFNγ treatment (three replicates). Lane 5: non-template control. Lane 6: Molecular weight ladder for IDO. GAPDH PCR product is 750 bp and IDO PCR product is 800 bp.

4.3 IDO siRNA Downregulation in A549 and H441 Cells

In order to study the effect of IDO on tumour cell response to chemotherapy and radiation, we reduced IDO mRNA in A549 cells by siRNA transfection. We transfected A549 cells with 4 different IDO siRNAs (siRNAs A, B, C, and D) using two different methods (described in Chapter 3, Section 3.18). IDO-expressing H441 cells were similarly transfected with 4 different IDO siRNAs but without IFNγ induction. As shown, siRNA did not appreciably reduce IDO mRNA in tumour cells (Figures 4.6 A-B, 4.7, 4.8). The numerical reductions in IDO mRNA observed after siRNA transfection (PCR-generated bands quantified using GelEval 1.37 software), were:

A549 cells: IDO siRNA A: 20% reduction, IDO siRNA B: 4% reduction, IDO siRNA C: 14% reduction, IDO siRNA D: 30% reduction.
H441 cells: IDO siRNA A: no reduction, IDO siRNA B 0%, IDO siRNA C 50%, IDO siRNA D 10% downregulation.

Note that these did not achieve statistical significance.

The minimal capacity of IDO siRNA to reduce IDO mRNA was confirmed by qPCR (Figure 4.8 and Figure 4.9).

4.4 Plasmid Quality Control and Diagnostic Restriction Digest (anti-IDO shRNA Stable Transfection)

To analyze the purified plasmids isolated from bacteria, we digested plasmid DNA with Pst I (described in Chapter 3, Section 3.3.2). The undigested plasmid was used as negative control. Plasmids containing the desired shRNA generated 2 diagnostic bands (3200 bp and 1400 bp) when separated by gel electrophoresis (Figure 4.10).

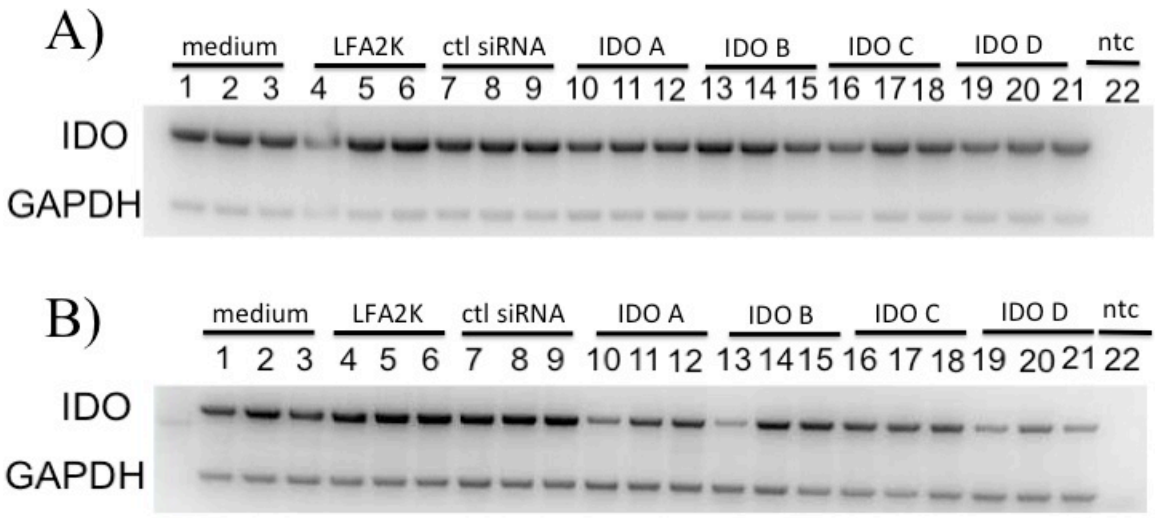
A)
medium
LFA2K
ctl siRNA
IDO A
IDO B
IDO C
IDO D
ntc
1 2 3 4 5 6 7 8 9 10 11 12 13 14 15 16 17 18 19 20 21 22
IDO
GAPDH
B)
medium
LFA2K
ctl siRNA
IDO A
IDO B
IDO C
IDO D
ntc
1 2 3 4 5 6 7 8 9 10 11 12 13 14 15 16 17 18 19 20 21 22
IDO
GAPDH

Figure 4. 6. IDO mRNA levels in A549 cells after transfection with IDO siRNA. A, A549 cells were treated with IFNγ (50 ng/ml) 6 h before transfection. A549 cells were transfected with IDO siRNA. Growth medium containing IFNγ (25 ng/ml) was added to the cells 4 h after transfection. RNA was isolated from cells 24 h post transfection and cDNA was synthesized. Generated cDNA was used for PCR amplification of IDO and GAPDH cDNA. **B,** A549 cells were transfected with IDO siRNA. Growth medium containing IFNγ (25 ng/ml) was added to the cells 4 h after transfection. RNA was isolated from cells 24 h post-transfection and cDNA was synthesized using that RNA as template. Generated cDNA was used for PCR amplification of IDO and GAPDH cDNA to quantitate relative IDO mRNA. Lanes 1-3: A549 cells treated with medium (no transfection). Lanes 4-6: A549 cells transfected with LFA2K only. Lanes 7-9: A549 cells transfected with control (ctl) 2 siRNA. Lanes 10-12: A549 cells transfected with IDO siRNA A. Lanes 13-15: A549 cells transfected with siRNA B. Lanes 16-18: A549 cells transfected with siRNA C. Lanes 19-21: A549 cells transfected with siRNA D. Lane 22: non-template control (ntc) for PCR. The top bands represent IDO and lower bands represent GAPDH.

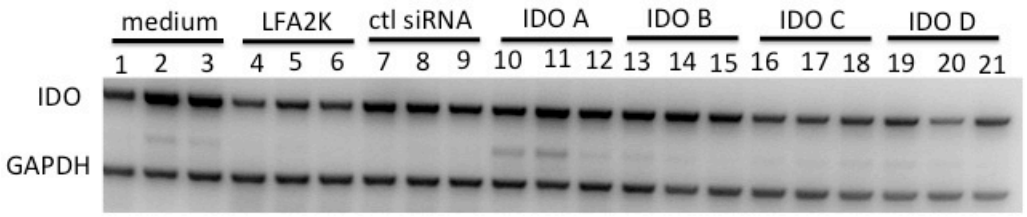
medium
LFA2K
ctl siRNA
IDO A
IDO B
IDO C
IDO D
1 2 3 4 5 6 7 8 9 10 11 12 13 14 15 16 17 18 19 20 21
IDO
GAPDH

Figure 4. 7. IDO mRNA levels in H441 cells after transfection with IDO siRNA. H441 cells were transfected with IDO siRNA. Growth medium was added to the cells 4 h after transfection. RNA was isolated from cells 24 h post transfection and cDNA was synthesized. Generated cDNA was used for PCR amplification of IDO and GAPDH cDNA. Lanes 1-3: H441 cells treated with medium (no transfection). Lanes 4-6: H441 cells transfected with LFA2K only. Lanes 7-9: H441 cells transfected with control (ctl) 2 siRNA. Lanes 10-12: H441 cells transfected with IDO siRNA A. Lanes 13-15: H441 cells transfected with siRNA B. Lanes 16-18: H441 cells transfected with siRNA C. Lanes 19-21: H441 cells transfected with siRNA D. The top bands represent IDO and lower bands represent GAPDH.

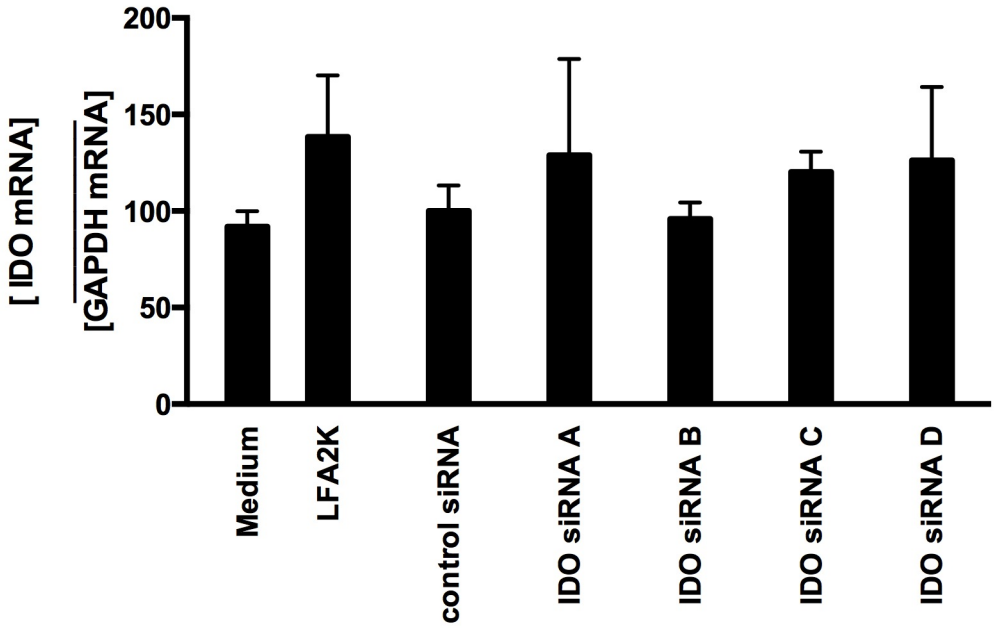
[IDO mRNA]
[GAPDH mRNA]
200
150
100
50
0
Medium
LFA2K
control siRNA
IDO siRNA A
IDO siRNA B
IDO siRNA C
IDO siRNA D

Figure 4. 8. qPCR analysis of IDO mRNA in A549 cells following siRNA transfection. A549 cells were transfected with IDO siRNA. Growth medium containing IFNγ (25 ng/ml) was added to the cells 4 h after transfection. RNA was isolated from cells 24 h post transfection and cDNA was synthesized. Generated cDNA was used for qPCR analysis of IDO and GAPDH mRNA. Results from all groups were normalized to control siRNA. Medium, treated with cultured medium only. LFA2K, treated with Lipofectamine 2000 only. Control siRNA, transfected with control siRNA. IDO siRNA A, transfected with IDO siRNA A. IDO siRNA B, transfected with IDO siRNA B. IDO siRNA C, transfected with IDO siRNA C. IDO siRNA D, transfected with IDO siRNA D. Each bar represents the mean of 3 values (*n*=3 for determination of each value from 3 independent experiments) ± SEM.

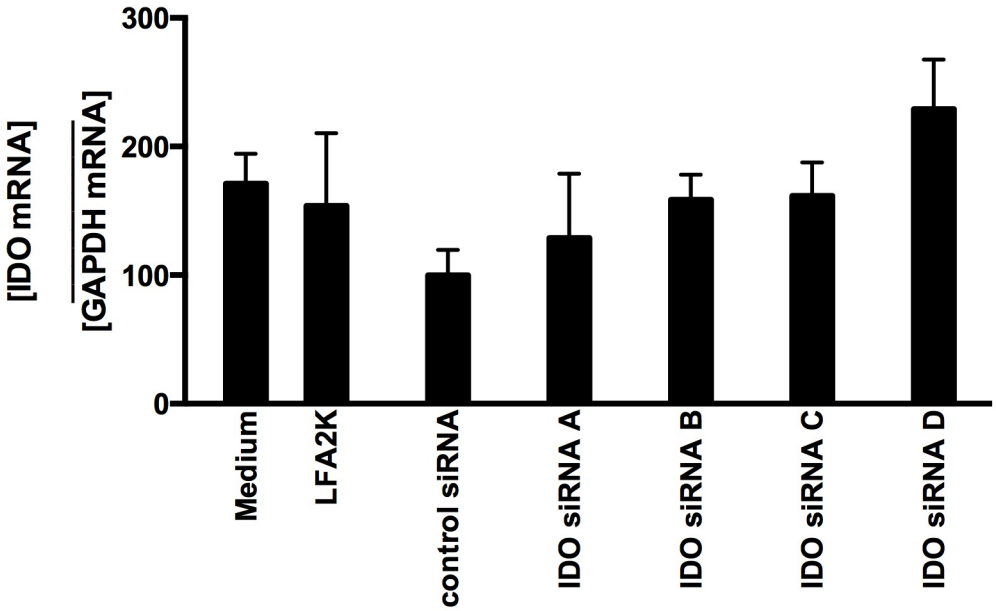
[IDO mRNA]
[GAPDH mRNA]
300
200
100
0
Medium
LFA2K
control siRNA
IDO siRNA A
IDO siRNA B
IDO siRNA C
IDO siRNA D

Figure 4. 9. qPCR analysis of IDO mRNA in H441 cells following siRNA transfection. H441 cells were transfected with IDO siRNA. Growth medium containing was added to the cells 4 h after transfection. RNA was isolated from cells 24 h post transfection and cDNA was synthesized. Generated cDNA was used for qPCR analysis of IDO and GAPDH mRNA. Results from all groups were normalized to control siRNA. **Medium**, cells were treated with cultured medium only. LFA2K, treated with Lipofectamine 2000 only. Control siRNA, transfected with control siRNA. IDO siRNA A, transfected with IDO siRNA A. IDO siRNA B, transfected with IDO siRNA B. IDO siRNA C, transfected with IDO siRNA C. IDO siRNA D, transfected with IDO siRNA D. Each bar represents the mean of 3 values (n=3 for determination of each value from 3 independent experiments) ± SEM.

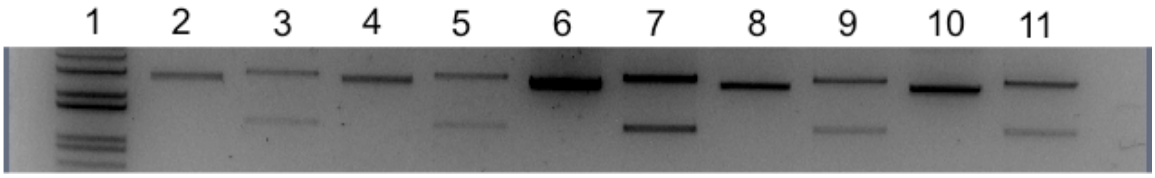
1
2
3
4
5
6
7
8
9
10
11

Figure 4. 10. Pst 1 digestion to confirm the presence of IDO shRNA in the expression vector. Pst I cleavage generates two DNA bands diagnostic for IDO shRNA (3200 bp and 1400 bp). Purified plasmids were digested with the restriction enzyme Pst I for one hour at 37° C to confirm the presence of desired shRNA. The final products of digestion along with undigested supercoiled plasmids were separated on a 1% agarose gel. **Lane 1:** Molecular weight ladder. **Lane 2,** Pst I-digested plasmid containing shRNA 1. **Lane 3:** undigested supercoiled plasmid containing shRNA 1. **Lane 4:** Pst I-digested plasmid containing shRNA 2. **Lane 5:** undigested supercoiled plasmid containing shRNA 2. **Lane 6:** Pst I-digested plasmid containing shRNA 3. **Lane 7:** undigested supercoiled plasmid containing shRNA 3. **Lane 8:** Pst I-digested plasmid containing shRNA 4. **Lane 9:** undigested supercoiled plasmid containing shRNA 4. **Lane 10:** Pst I-digested plasmid containing scrambled shRNA. **Lane 11:** undigested supercoiled plasmid containing scrambled shRNA.

4.5 IDO mRNA Quantification in A549 and H441 Clonal Population

To measure IDO mRNA levels in the stable cell lines, RNA was isolated from stably-transfected A549 and H441 clonally-selected populations as described (Chapter 3, Section 3.5). IDO mRNA and 18S rRNA levels were measured simultaneously by multiplex real-time PCR amplification (Figure 4.11) as described (Chapter 3, Section 3.7). Several A549 clonal cell lines, which are NC-3, NC-10, NC-30, 2-4, 2-6, and 2-18 were selected for further analysis based on the degree of shRNA-associated reduction in IDO mRNA levels after IFNγ induction (Figure 4.12). Similarly, several H441 clonal populations were selected for analysis based on IDO mRNA reduction in these naturally-IDO expressing clones (Figure 4.13).

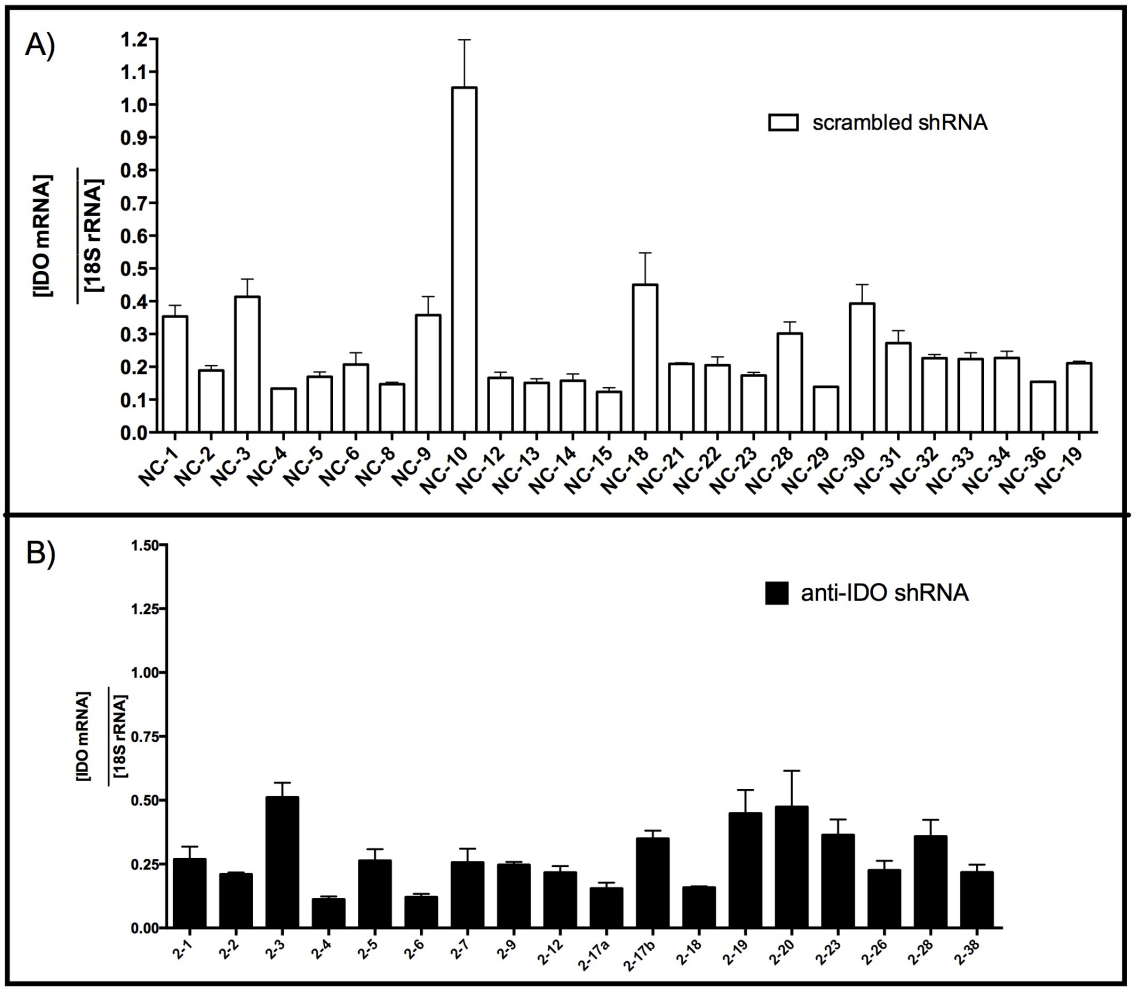
A)
[IDO mRNA] / [18S rRNA]
scrambled shRNA
1.2
1.1
1.0
0.9
0.8
0.7
0.6
0.5
0.4
0.3
0.2
0.1
0.0
NC-1
NC-2
NC-3
NC-4
NC-5
NC-6
NC-8
NC-9
NC-10
NC-12
NC-13
NC-14
NC-15
NC-18
NC-21
NC-22
NC-23
NC-28
NC-29
NC-30
NC-31
NC-32
NC-33
NC-34
NC-36
NC-19
B)
[IDO mRNA] / [18S rRNA]
anti-IDO shRNA
1.50
1.25
1.00
0.75
0.50
0.25
0.00
2-1
2-2
2-3
2-4
2-5
2-6
2-7
2-9
2-12
2-17a
2-17b
2-18
2-19
2-20
2-23
2-26
2-28
2-38

Figure 4. 11. IDO mRNA quantification in A549 clonal populations. A549 clonal populations were treated with IFNγ (25 ng/ml) for 24 h. RNA was isolated and used to generate cDNA. IDO mRNA and 18S rRNA levels were assessed simultaneously by multiplex qPCR amplification. **A**, white bars, A549 clonal cells transfected with scrambled control shRNA and **B**, black bars A549 clonal cells transfected with anti-IDO shRNA. Each bar represents the mean of 3 values (*n*=3 for determination of each value) ± SEM.

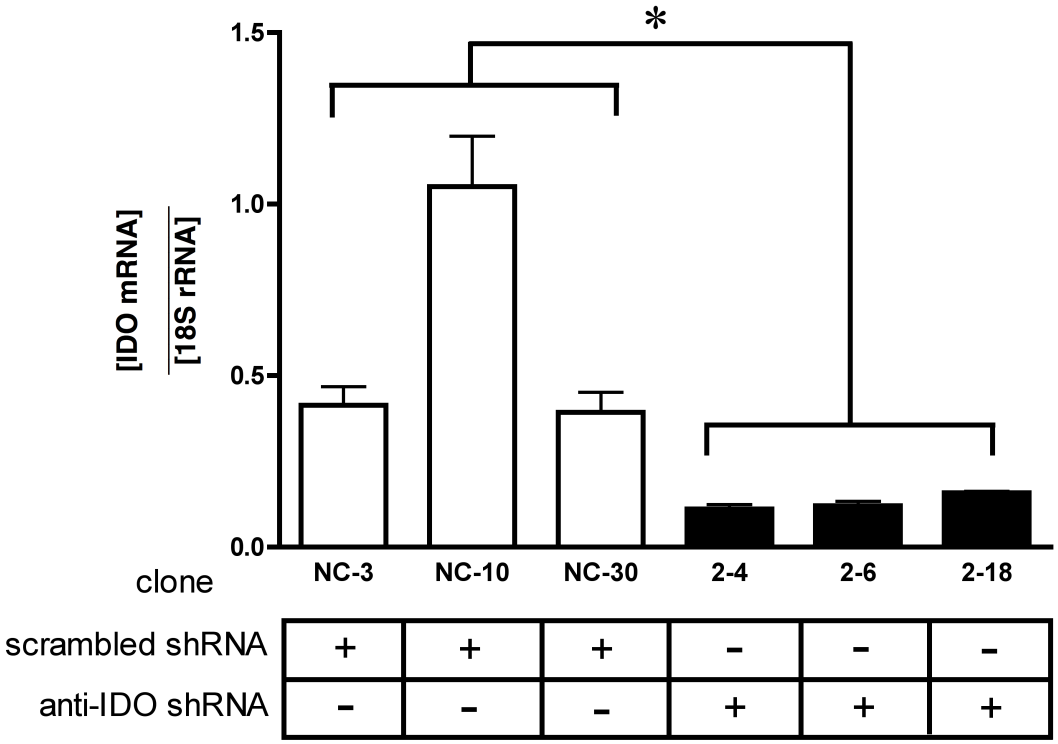
*
1.5
1.0
0.5
0.0
[IDO mRNA]
[18S rRNA]
clone
NC-3
NC-10
NC-30
2-4
2-6
2-18
scrambled shRNA
anti-IDO shRNA
+ + + - - -
- - - + + +

Figure 4. 12. IDO mRNA levels in selected A549 clonal cell lines. A549 cell lines stably-transfected with anti-IDO shRNA (2-4, 2-6, and 2-18) or scrambled shRNA (NC-3, NC-10, and NC-30) were treated with IFNγ (25 ng/ml) for 24 h. IDO mRNA and 18S rRNA were quantified 24 h post-IFNγ treatment by qPCR. **White bars:** A549 clonal cells transfected with scrambled control shRNA. **Black bars:** A549 clonal cells transfected with anti-IDO shRNA. The selected clones were used for future experiments. Each bar represents the mean of 3 values (n=3 for determination of each value) ± SEM (*$P < 0.05$).

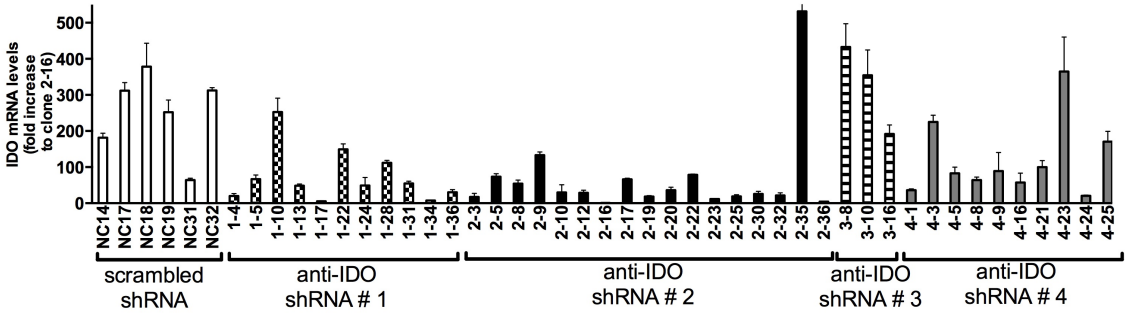
IDO mRNA levels
(fold increase
to clone 2-16)
500
400
300
200
100
0
NC14
NC17
NC18
NC19
NC31
NC32
1-4
1-5
1-10
1-13
1-17
1-22
1-24
1-28
1-31
1-34
1-36
2-3
2-5
2-8
2-9
2-10
2-12
2-16
2-17
2-19
2-20
2-22
2-23
2-25
2-30
2-32
2-35
2-36
3-8
3-10
3-16
4-1
4-3
4-5
4-8
4-9
4-16
4-21
4-23
4-24
4-25
scrambled
shRNA
anti-IDO
shRNA # 1
anti-IDO
shRNA # 2
anti-IDO
shRNA # 3
anti-IDO
shRNA # 4

Figure 4. 13. IDO mRNA quantification in H441 clonal populations. H441 clonal populations stably transfected with scrambled shRNA or anti-IDO shRNA were cultured for 24 h without IFNγ treatmen). RNA was isolated from cells and used to generate cDNA. IDO mRNA and 18S rRNA levels were measured simultaneously by multiplex qPCR amplification. From left to right: **Scrambled shRNA**, H441 cells transfected with scrambled shRNA. **Anti-IDO shRNA #1**, H441 cells transfected with anti-IDO shRNA#1. **Anti-IDO shRNA #2**, H441 cells transfected with anti-IDO shRNA #2. **Anti-IDO shRNA #3**, H441 cells transfected with anti-IDO shRNA #3. **Anti-IDO shRNA #4**, H441 cells transfected with anti-IDO shRNA #4. All clones are normalized to clone 2-16, which exhibited the lowest IDO mRNA level. Each bar represents the mean of 3 values (*n*=3 for determination of each value) ± SEM.

4.6 IDO Protein Levels in A549 and HeLa Clonal Populations

IDO protein levels were measured in A549 and HeLa selected clonal populations as described (Chapter 3, Section 3.8). Anti-IDO shRNA decreased IDO protein levels in A549 and HeLa clonal populations compared to non-targeting control shRNA, respectively (Figures 4.14 and 4.15).

4.7 IDO Levels are Inversely Correlated with Tumour Cell Proliferation

IDO expression is correlated with decreased proliferation [135]. Therefore, the effect of anti-IDO shRNA on IDO-mediated slow growth was examined. A549 and HeLa cell clonal populations were treated with IFNγ (25 ng/ml) and allowed to proliferate for 72 h. High IDO levels were associated with reduced proliferation of A549 and HeLa clonal cells, and the presence of anti-IDO shRNA attenuated IFNγ-induced reduction in proliferation (Figures 4.16 and 4.17). These data suggest that IFNγ-induced IDO protein is functional in these cells and that anti-IDO shRNA reduces IDO function.

4.8 IDO Effect on A549 Cell Cycle

IDO-mediated depletion of tryptophan induces cell cycle arrest in T cells at the G_1 phase of the cell cycle [263]. We therefore determined whether IDO-induced reduction in growth of cancer cells was associated with altered cell cycle. A549 cells were cultured with and without IFNγ for 48 h. The cell cycle was then measured as described in section 3.12. IFNγ induction of IDO increased the number of cells in G_1 by 10% and decreased the numbers in G_2/M in cells expressing scrambled control shRNA by the same amount. The presence of anti-IDO shRNA in cells treated with IFNγ abolished the increase in the number of cells in G_1 and the decrease in the number of cells in G_2/M (Figure 4.18).

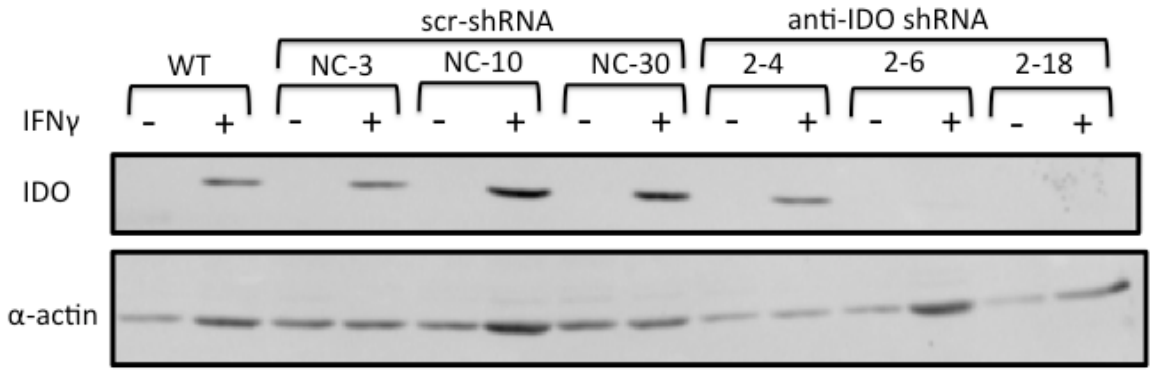
scr-shRNA
anti-IDO shRNA
WT
NC-3
NC-10
NC-30
2-4
2-6
2-18
IFNγ
- + - + - + - + - + - + - +
IDO
α-actin

Figure 4. 14. IDO protein levels in A549 clonal cell populations with and without IFNγ (25 ng/ml) treatment. IDO was induced in A549 clonal populations by IFNγ treatment (25 ng/ml) for 48 h. Non-treated A549 clonal cells were used to determine the basal level of IDO without IFNγ induction by immunoblot. A549 cells untransfected with plasmids harbouring shRNA were used as controls (WT).

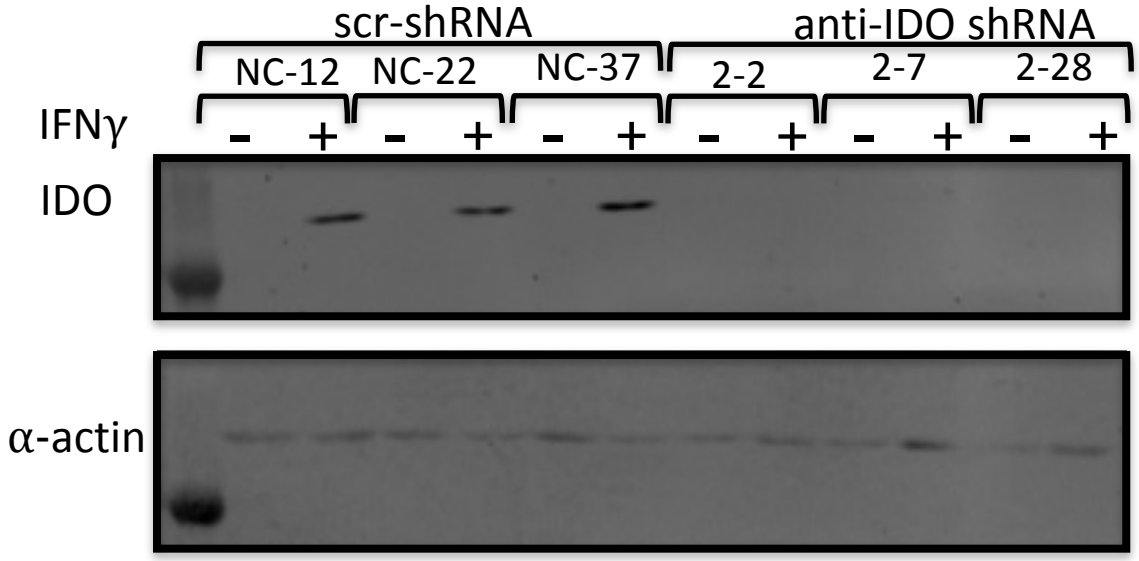
scr-shRNA
anti-IDO shRNA
NC-12
NC-22
NC-37
2-2
2-7
2-28
IFNγ
- + - + - + - + - + - +
IDO
α-actin

Figure 4. 15. IDO protein levels in HeLa clonal cells with and without IFNγ (25 ng/ml) treatment. IDO was induced in HeLa clonal populations by IFNγ treatment (25 ng/ml) for 48 h and assessed by immunoblot. Untreated HeLa clonal cell populations were used to determine the basal level of IDO without IFNγ induction.

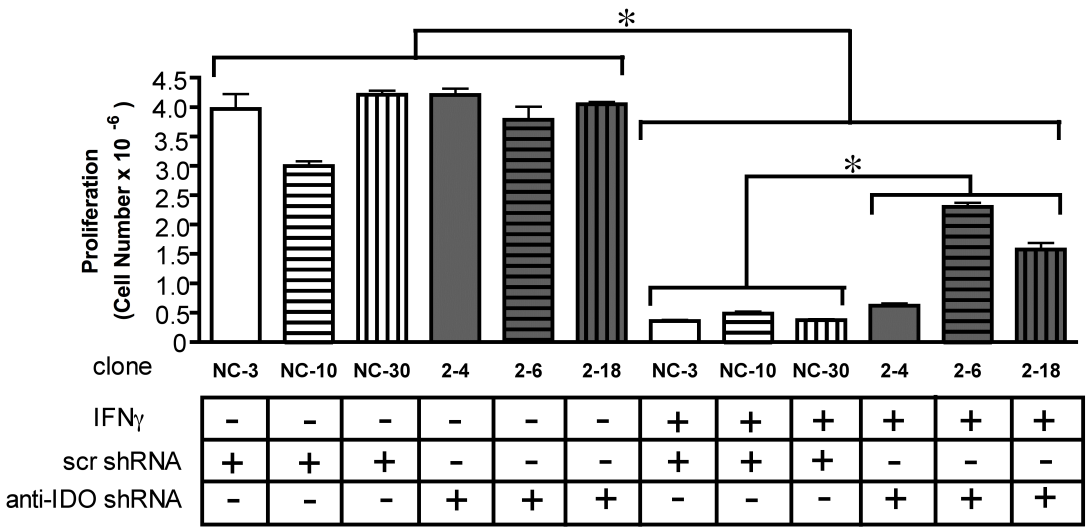
*
*
Proliferation (Cell Number x 10 -6)
4.5
4.0
3.5
3.0
2.5
2.0
1.5
1.0
0.5
0
clone
NC-3
NC-10
NC-30
2-4
2-6
2-18
NC-3
NC-10
NC-30
2-4
2-6
2-18
IFNγ
scr shRNA
anti-IDO shRNA

Figure 4. 16. IDO slows proliferation of A549 cells and anti-IDO shRNA attenuates the IDO-mediated reduction in proliferation. A549 clonal populations were cultured with and without IFNγ (25 ng/ml) for 72 h. Tumour cells were washed with PBS and trypsinized. Tumour cell proliferation was enumerated by cell counting. Each bar represents the mean of 3 independent experiments (n=3 for determination of each value) ± SEM (*$P < 0.05$).

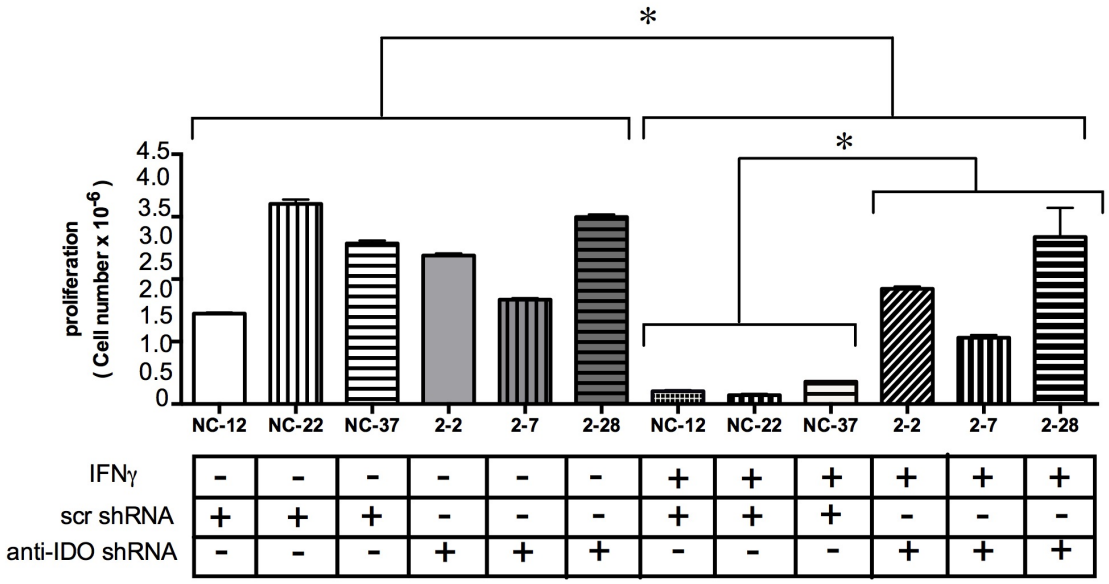
*
*
proliferation
(Cell number x 10^-6)
4.5
4.0
3.5
3.0
2.5
2.0
1.5
1.0
0.5
0
NC-12
NC-22
NC-37
2-2
2-7
2-28
NC-12
NC-22
NC-37
2-2
2-7
2-28
IFNγ
scr shRNA
anti-IDO shRNA

Figure 4. 17. IDO slows proliferation of HeLa cells and anti-IDO shRNA attenuates IDO-mediated reduction in proliferation. HeLa clonal cell populations were cultured with and without IFNγ (25 ng/ml) for 72 h. Tumour cells were washed with PBS and trypsinized. Tumour cell proliferation was enumerated by cell counting. Each bar represents the mean of 3 independent experiments (n=3 for determination of each value) ± SEM (*$P < 0.05$).

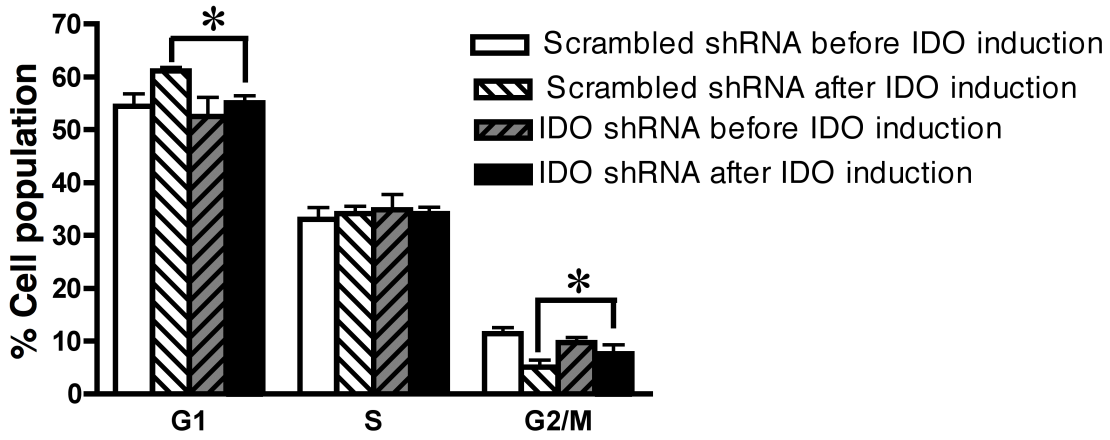
% Cell population
70
60
50
40
30
20
10
0
*
*
G1
S
G2/M
Scrambled shRNA before IDO induction
Scrambled shRNA after IDO induction
IDO shRNA before IDO induction
IDO shRNA after IDO induction

Figure 4. 18. IDO mediated the increased accumulation of cells in G_1 and decreased accumulation in G_2/M in A549 cells. Tumour cells were cultured overnight, treated with or without IFNγ (25 ng/ml) for 48 h, and analyzed for cell cycle compartmentalization as described in *Materials and Methods*. Each bar represents pooled data to generate mean values from 3 independent clonal populations harbouring scrambled control shRNA or anti-IDO shRNA, and each bar represents the mean of those 3 values (n=3 for determination of each value) ± SEM (*$P < 0.05$).

4.9 IDO Downregulation Decreases Intracellular NAD^+

IDO is responsible for *de novo* synthesis of NAD^+ from tryptophan. Whether or not anti-IDO shRNA decreased NAD^+ levels in A549 cells (as described in Chapter 3, Section 3.9) was examined. Anti-IDO shRNA decreased NAD^+ levels in A549 clonal populations by 60% (Figure 4.19).

4.10 IDO Mediates Resistance to the NAD^+ Inhibitor FK866

FK866 is a pharmacological inhibitor of NAD^+ synthesis from the salvage pathway and is being evaluated for clinical anticancer efficacy [264]. IDO inhibition decreased NAD^+ levels in A549 cells by approximately 60% (Figure 4.19), similar to the degree of reduction of NAD^+ induced in human tumour cells by FK866 [242]. I hypothesized that the IDO-mediated increase in NAD^+ had the potential to counter the therapeutic effect of FK866. To test this hypothesis, I induced IDO in A549 clonal populations with IFNγ (25 ng/ml) for 48 h and then treated the cells with FK866 as described (Chapter 3, Section 3.15). IDO increased the resistance of A549 clonal cells to FK866 and anti-IDO shRNA partially decreased this effect (Figure 4.20). Clone 2-4 (containing anti-IDO shRNA) has a greater amount of IDO than clones 2-6 and 2-18 (Figures 4.14 and 4.20) and was also more resistant than those clones to the effect of FK866 (Figure 4.20). There was a relatively modest positive linear correlation (R^2=0.54) between IDO protein levels and resistance to FK866 (Figure 4.20, Panel C).

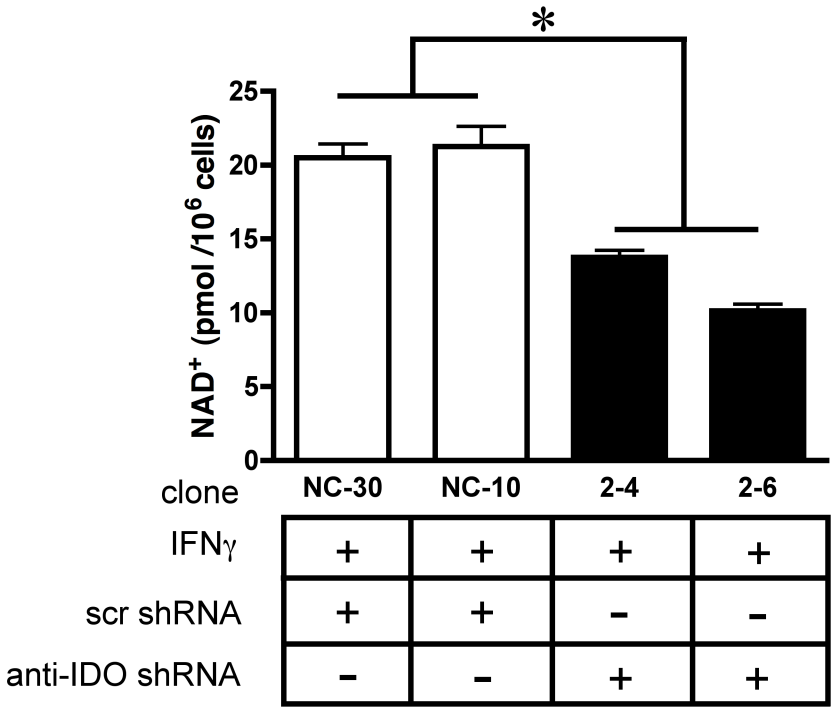
*
25
20
15
10
5
0
NAD+ (pmol /10^6 cells)
clone
NC-30
NC-10
2-4
2-6
IFNγ
+
+
+
+
scr shRNA
+
+
-
-
anti-IDO shRNA
-
-
+
+

Figure 4. 19. IDO downregulation decreased NAD^+ in A549 cells. A549 clonal cell populations were treated with IFNγ (25 ng/ml) for 48 h. Lysates were prepared from treated cells and total NAD (NADt) and NADH were measured. NAD^+ levels were calculated by subtracting NADH from NADt. Each bar represents the mean of 3 values (n=3 for determination of each value) ± SEM (*$P < 0.05$).

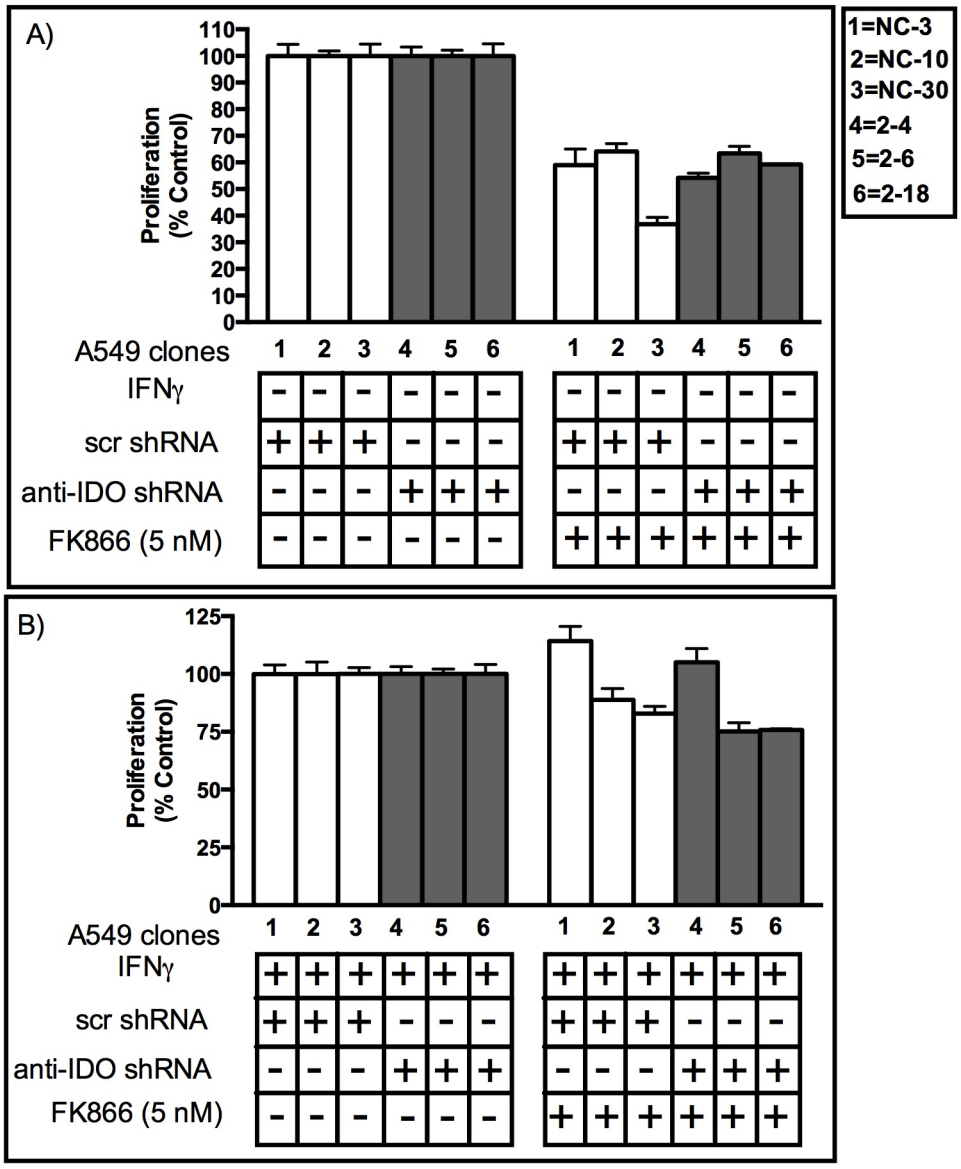
A)
Proliferation (% Control)
110
100
90
80
70
60
50
40
30
20
10
0
A549 clones
1 2 3 4 5 6 1 2 3 4 5 6
IFNγ
scr shRNA
anti-IDO shRNA
FK866 (5 nM)
1=NC-3
2=NC-10
3=NC-30
4=2-4
5=2-6
6=2-18
B)
Proliferation (% Control)
125
100
75
50
25
0
A549 clones
1 2 3 4 5 6 1 2 3 4 5 6
IFNγ
scr shRNA
anti-IDO shRNA
FK866 (5 nM)

C)

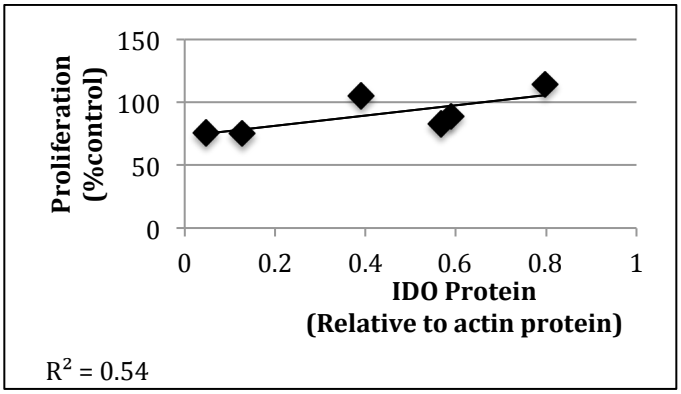
Proliferation (%control)
150
100
50
0
0
0.2
0.4
0.6
0.8
1
IDO Protein
(Relative to actin protein)
R² = 0.54

Figure 4. 20. A549 clonal cell population sensitivity to FK866 (5 nM) before and after IDO induction. Panels A-B present data for each of 6 individual clonal populations before and after IDO induction. A549 clonal cell populations were cultured with or without IFNγ (25 ng/ml) for 48 h. Medium was then replaced with fresh growth medium containing FK866 (5 nM) and cells were allowed to proliferate for 72 h. Cells were then trypsinized and live cells were enumerated. White bars: A549 clones transfected with scrambled shRNA. **Gray bars:** A549 cells transfected with anti-IDO shRNA. Each bar represents the mean of 3 values (*n*=3 for determination of each value) ± SD. **Panel C:** Correlation analysis of the relationship between IDO protein content (relative to actin) and clonal population resistance to FK866 (proliferation relative to untreated control cells).

4.11 IDO in Tumour Cells Mediates Resistance to Olaparib

NAD^+ is necessary for PARP activity [215] and anti-IDO shRNA decreased NAD^+ levels in A549 cells. Therefore, the capacity of IDO to increase tumour cell resistance to olaparib, and the capacity of anti-IDO shRNA to reverse this effect, was assessed. A549 and HeLa clonal cell populations were treated with olaparib as described (Chapter 3, Section 3.11). IDO downregulation sensitized A549 cells to low dose olaparib by 16% (p= 4 x 10^{-4})(Figures 4.21 and 4.22). Similarly, IDO downregulation sensitized A549 cells to high doses of olaparib by 18% (p= 1 x 10^{-3})(Figures 4.23 and 4.24). Cells with unimpeded IDO expression after IFNγ induction had increased resistance to olaparib (*i.e.*, increased IDO was associated with reduced drug effectiveness), while antisense-downregulation of IDO during and after IFNγ induction resulted in sensitivity to olaparib equal to that of cells untreated with IFNγ (Figure 4.25). Some HeLa clonal cells showed a similar pattern of sensitivity to olaparib in the absence of IDO. However, their sensitivity was less potent compared to A549 cells (Figure 4.26 and 4.27). These results show that IDO expression in tumour cells confers resistance to olaparib and, since all clonal populations were treated identically with IFNγ, the observed resistance to olaparib was due solely to the presence of shRNA (and, by extension, IDO knockdown) and not effects of IFNγ unrelated to IDO.

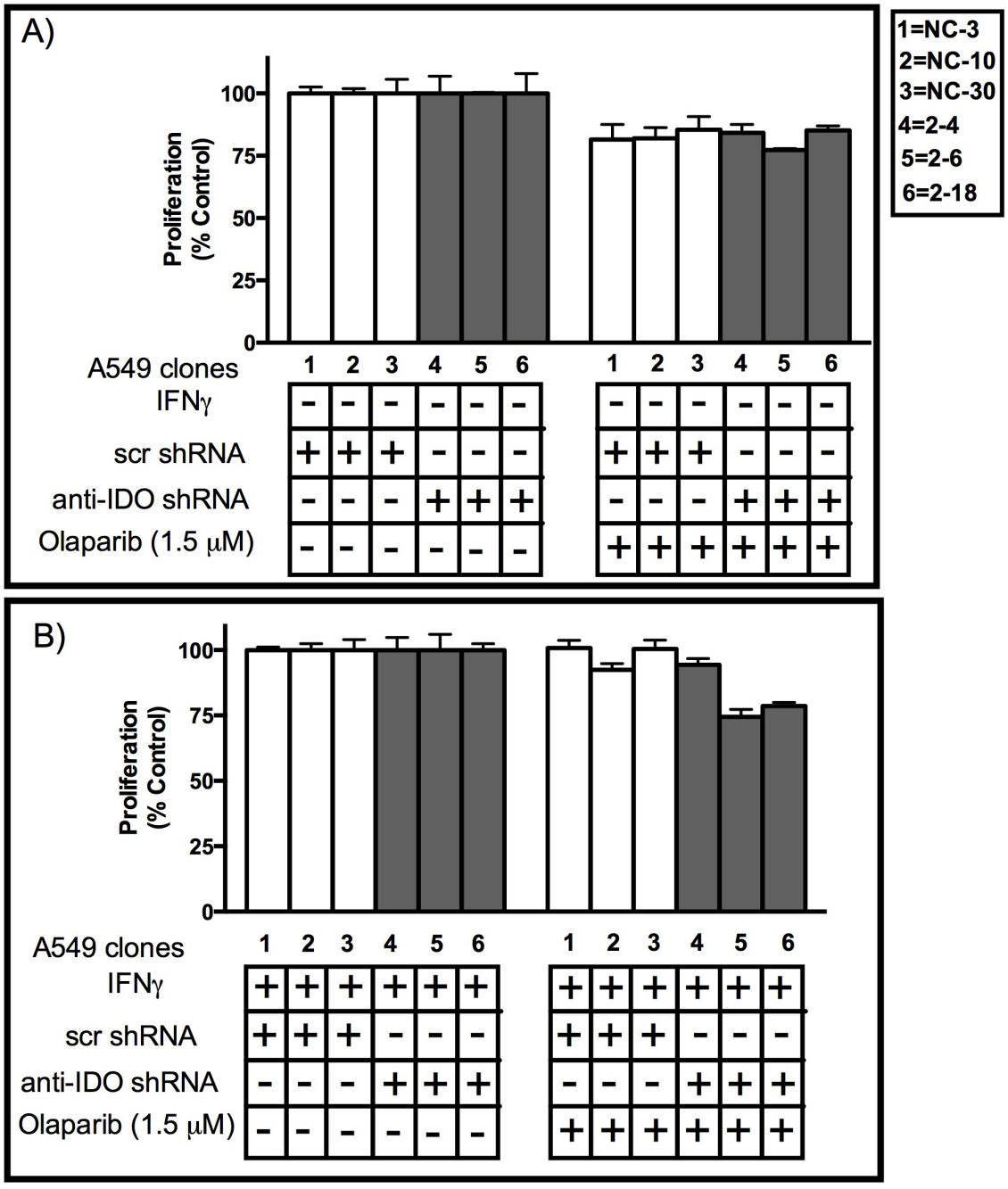
A)
1=NC-3
2=NC-10
3=NC-30
4=2-4
5=2-6
6=2-18
Proliferation (% Control)
100
75
50
25
0
A549 clones
1 2 3 4 5 6
1 2 3 4 5 6
IFNγ
scr shRNA
anti-IDO shRNA
Olaparib (1.5 μM)
B)
Proliferation (% Control)
100
75
50
25
0
A549 clones
1 2 3 4 5 6
1 2 3 4 5 6
IFNγ
scr shRNA
anti-IDO shRNA
Olaparib (1.5 μM)

Figure 4. 21. A549 clonal cell population sensitivity to low dose olaparib (1.5 μM) before and after IDO induction. **Panels A-B** present data for each of 6 individual clonal populations before and after IDO induction. A549 clonal populations were cultured with or without IFNγ (25 ng/ml) for 48 h. Cultured medium was then replaced with fresh growth medium containing olaparib (1.5 μM) and cells were allowed to proliferate for 72 h. Cells were then trypsinized and live cells were enumerated using a Coulter counter. White bars represent A549 clones transfected with scrambled shRNA and gray bars represent A549 cells transfected with anti-IDO shRNA. Each bar represents the mean of 3 values (*n*=3 for determination of each value) ± SD. Significant changes are shown in pooled results (Figure 4.22).

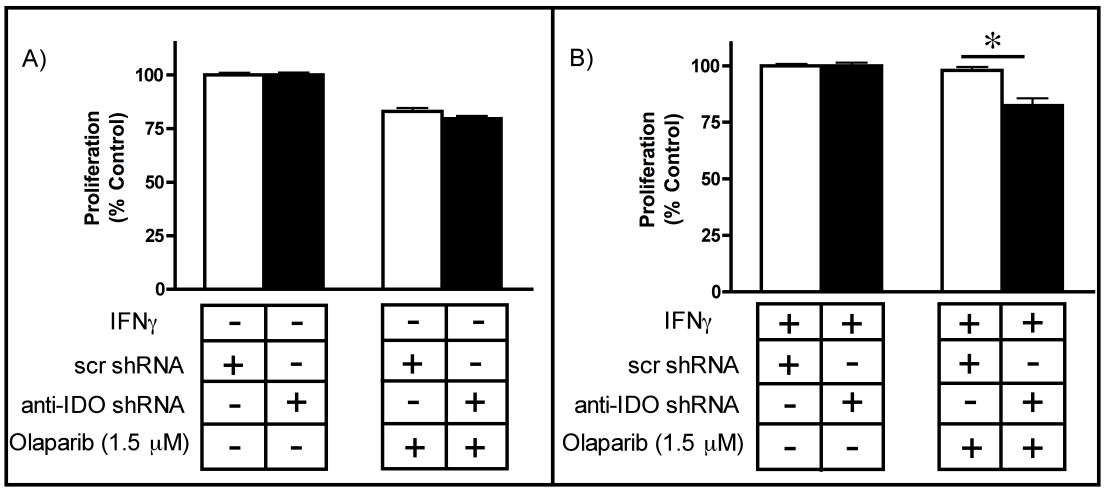
A)
Proliferation (% Control)
100
75
50
25
0
IFNγ
scr shRNA
anti-IDO shRNA
Olaparib (1.5 μM)
B)
*
Proliferation (% Control)
100
75
50
25
0
IFNγ
scr shRNA
anti-IDO shRNA
Olaparib (1.5 μM)

Figure 4. 22. Sensitivity of clonal A549 populations to low dose olaparib (1.5 μM) before (A) and after (B) IDO induction. Data shown in Figure 4.21 were pooled to generate mean values from 3 independent clonal populations harbouring scrambled control shRNA or anti-IDO shRNA, and each bar represents the mean of those 3 values (n=3 for determination of each value) ± SEM (*$P < 0.05$).

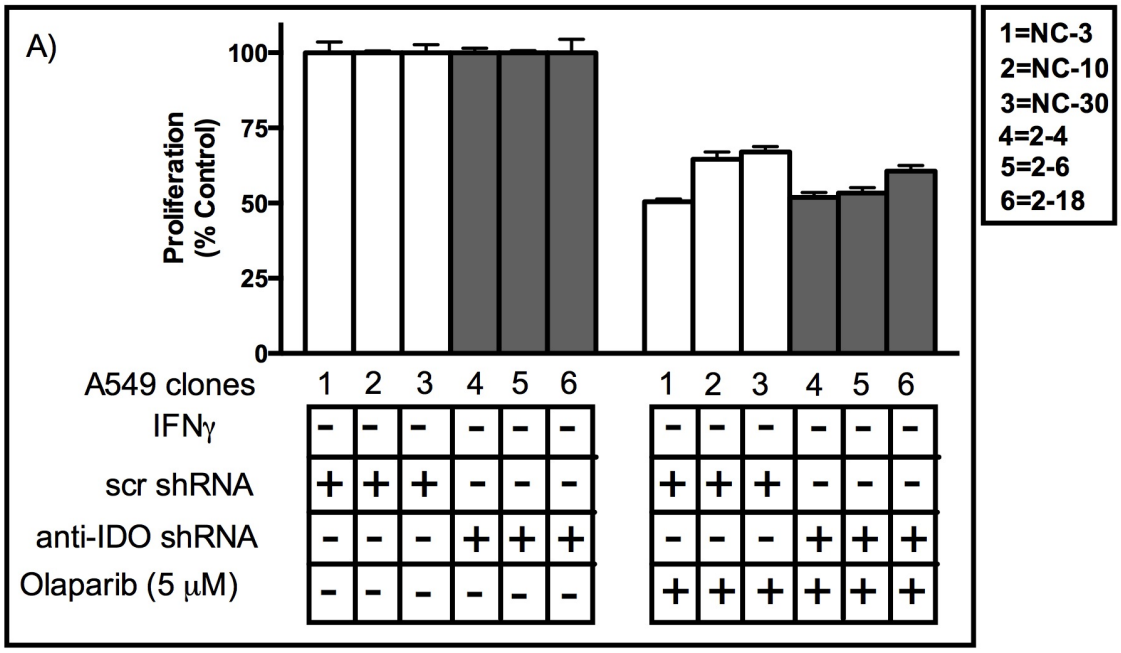
A)
Proliferation (% Control)
100
75
50
25
0
1=NC-3
2=NC-10
3=NC-30
4=2-4
5=2-6
6=2-18
A549 clones
1 2 3 4 5 6
1 2 3 4 5 6
IFNγ
scr shRNA
anti-IDO shRNA
Olaparib (5 μM)

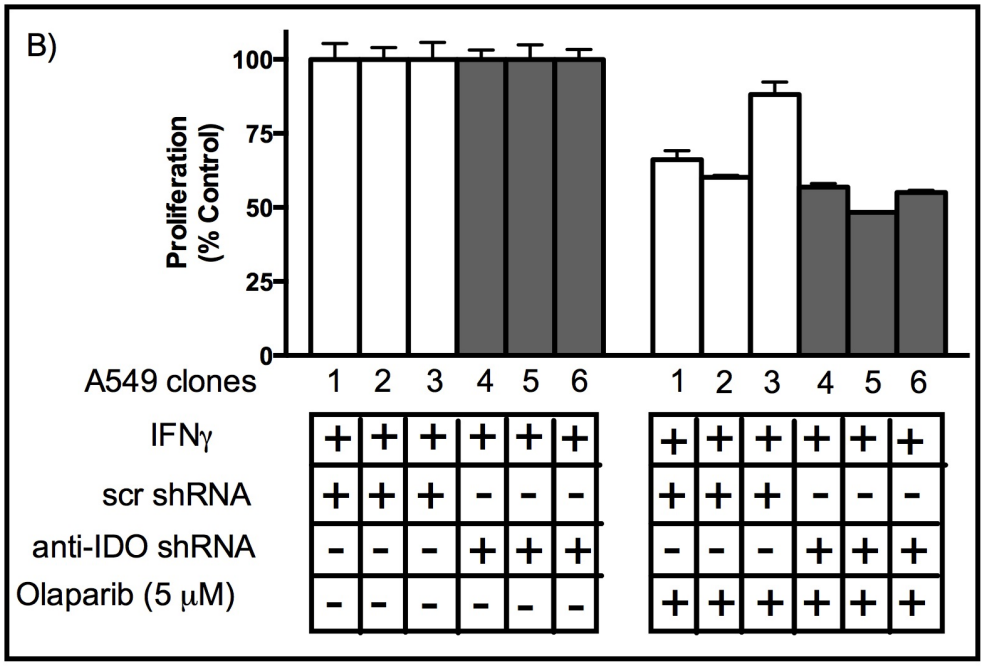
B)
Proliferation (% Control)
100
75
50
25
0
A549 clones
1 2 3 4 5 6
1 2 3 4 5 6
IFNγ
scr shRNA
anti-IDO shRNA
Olaparib (5 μM)

Figure 4. 23. A549 clone sensitivity to high dose olaparib (5 μM) before and after IDO induction. Panels A-B present data for each of 6 individual clonal populations before and after IDO induction. A549 clonal populations were cultured with or without IFNγ (25 ng/ml) for 48 h. Cultured medium was then replaced with fresh growth medium containing olaparib (5 μM) and cells were allowed to proliferate for 72 h. Cells were then trypsinized and live cells were enumerated using a Coulter counter. White bars represent A549 clones transfected with scrambled shRNA and gray bars represent A549 cells transfected with anti-IDO shRNA. Each bar represents the mean of 3 values (*n*=3 for determination of each value) ± SD. Significant changes are shown in pooled results (Figure 4.24).

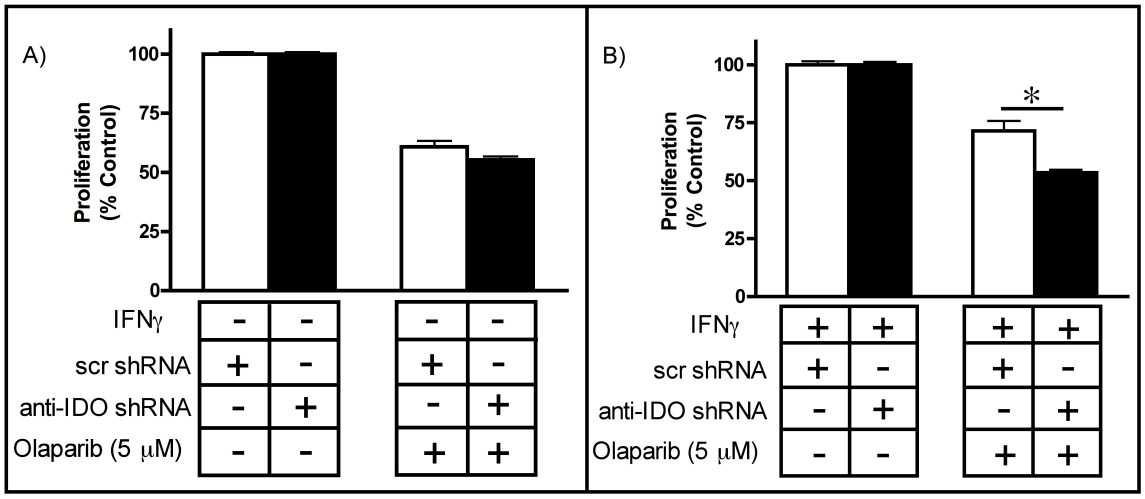
A)
Proliferation (% Control)
100
75
50
25
0
IFNγ
scr shRNA
anti-IDO shRNA
Olaparib (5 μM)
B)
Proliferation (% Control)
100
75
50
25
0
*
IFNγ
scr shRNA
anti-IDO shRNA
Olaparib (5 μM)

Figure 4. 24. Sensitivity of clonal A549 populations to high dose olaparib (5 μM) before (A) and after (B) IDO induction. Data shown in Figure 4.23 were pooled to generate mean values from 3 independent clonal populations harbouring scrambled control shRNA or anti-IDO shRNA, and each bar represents the mean of the 3 values (n=3 for determination of each value) ± SEM (*$P < 0.05$).

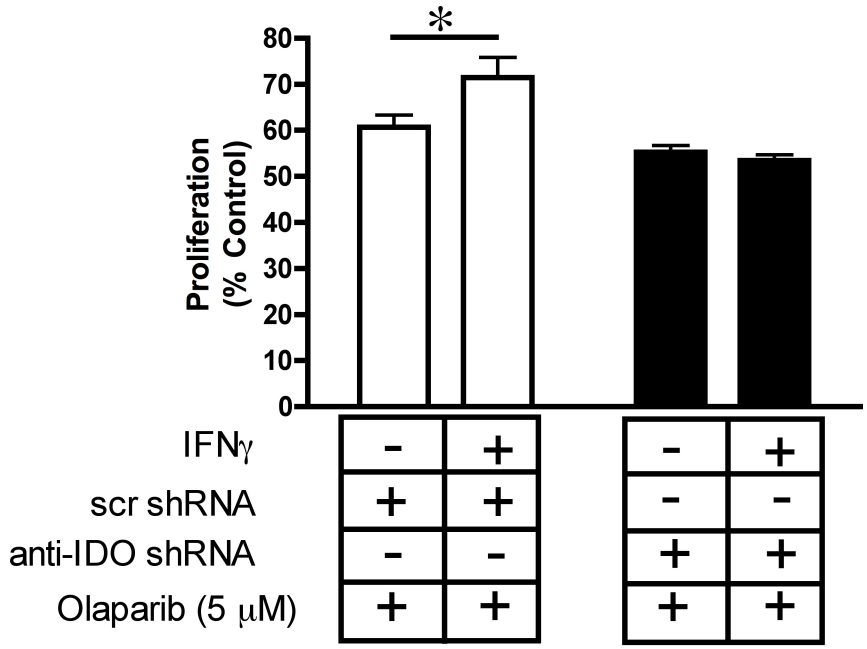
*
80
70
60
50
40
30
20
10
0
Proliferation (% Control)
IFNγ
scr shRNA
anti-IDO shRNA
Olaparib (5 μM)
- + - +
+ + - -
- - + +
+ + + +

Figure 4. 25. Induction of IDO in A549 clonal cell populations decreases the effectiveness of olaparib. Results were obtained from 3 independent clonal cell populations with scrambled control shRNA or anti-IDO shRNA, and each bar represents the mean of the 3 values (n=3 for determination of each value) ± SEM (*$p < 0.05$).

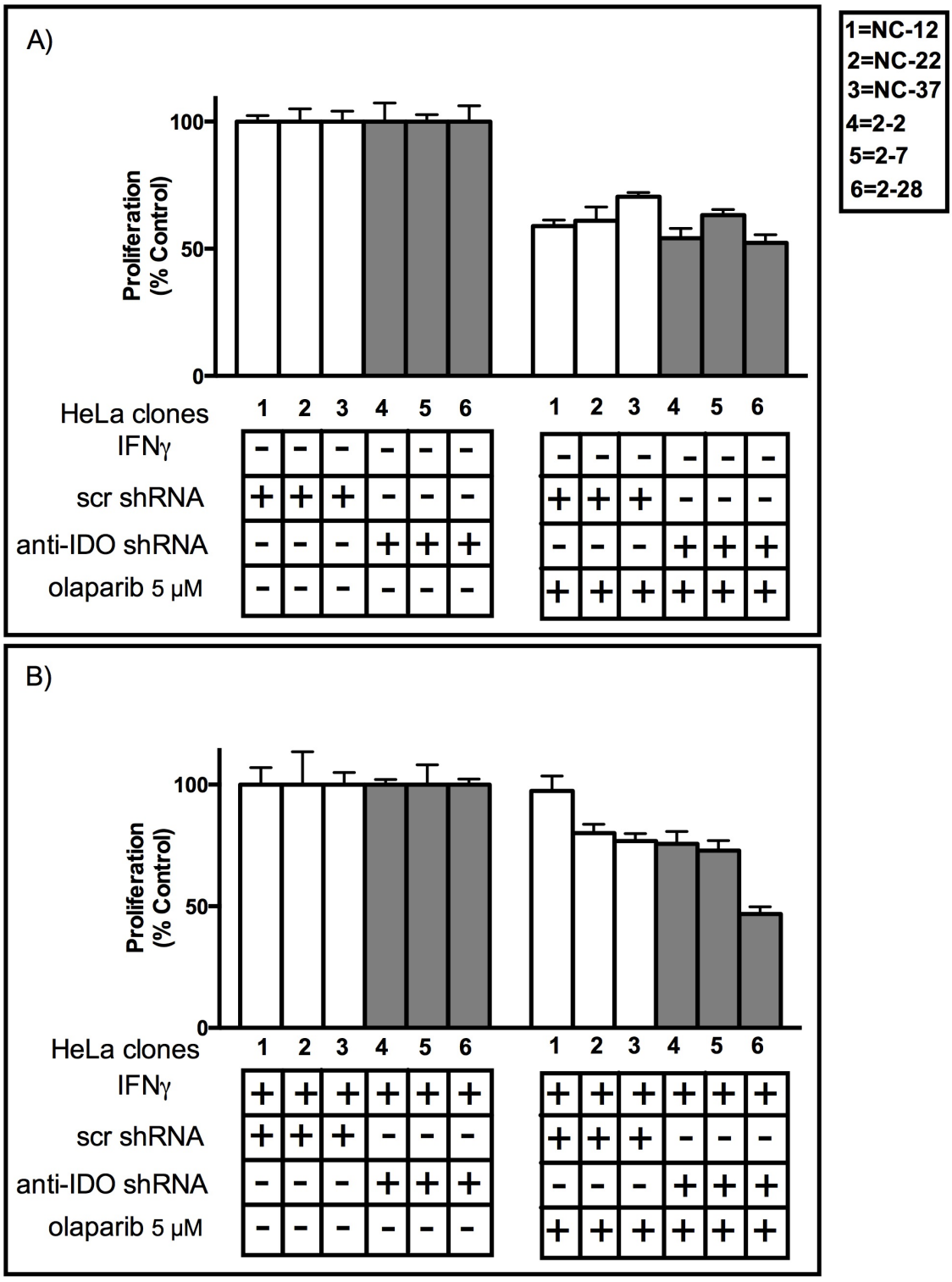
A)
1=NC-12
2=NC-22
3=NC-37
4=2-2
5=2-7
6=2-28
Proliferation (% Control)
100
50
0
HeLa clones
1 2 3 4 5 6 1 2 3 4 5 6
IFNγ
scr shRNA
anti-IDO shRNA
olaparib 5 μM
B)
Proliferation (% Control)
100
50
0
HeLa clones
1 2 3 4 5 6 1 2 3 4 5 6
IFNγ
scr shRNA
anti-IDO shRNA
olaparib 5 μM

Figure 4. 26. HeLa clone sensitivity to high dose olaparib (5 μM) before and after IDO induction. **Panels A-B** present data for each of 6 individual clonal populations before and after IDO induction. HeLa clonal populations were cultured with or without IFNγ (25 ng/ml) for 48 h. Cultured medium was then replaced with fresh growth medium containing olaparib (5 μM) and cells were allowed to proliferate for 72 h. Cells were then trypsinized and live cells were enumerated using a Coulter counter. White bars represent HeLa clones transfected with scrambled shRNA and gray bars represent HeLa cells transfected with anti-IDO shRNA. Each bar represents the mean of 3 values (*n*=3 for determination of each value) ± SD. Significant changes are shown in pooled results (Figure 4.27).

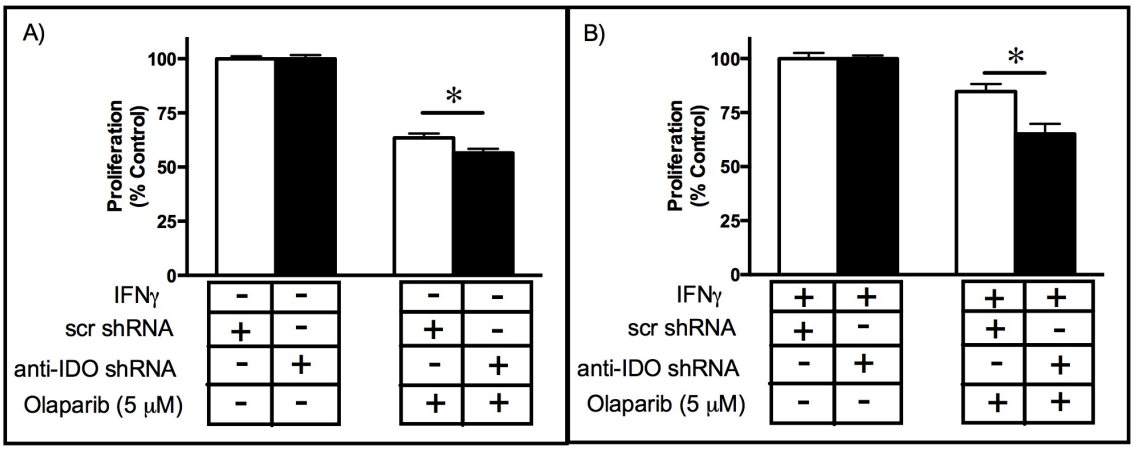
A)
Proliferation (% Control)
100
75
50
25
0
*
IFNγ
scr shRNA
anti-IDO shRNA
Olaparib (5 μM)
B)
Proliferation (% Control)
100
75
50
25
0
*
IFNγ
scr shRNA
anti-IDO shRNA
Olaparib (5 μM)

Figure 4. 27. Sensitivity of clonal HeLa populations to high dose olaparib (5 μM) before (A) and after (B) IDO induction. Data shown in Figure 4.26 were pooled to generate mean values from 3 independent clonal populations harbouring scrambled control shRNA or anti-IDO shRNA, and each bar represents the mean of the 3 values (n=3 for determination of each value) ± SEM (*$P < 0.05$).

4.12 IDO Mediates Resistance to γ Radiation in Cancer Cells

In view of the potential for IDO to modulate PARP activity, it was hypothesized that human tumour cell IDO mediates resistance to ionizing γ radiation. We irradiated A549 and HeLa clonal cell lines as described (Chapter 3, Section 3.12). IDO downregulation sensitized A549 and HeLa cells to radiation by approximately 20% (P=2.6 x 10^{-7}) and 10% (P=0.021), respectively (Figures 4.28, 4.29, 4.31, 4.32, and 4.33). A549 and HeLa clones untreated with IFNγ (*i.e.*, lacking IDO) were equally sensitive to radiation regardless of whether or not they harboured anti-IDO shRNA. In addition, IDO induced by IFNγ treatment of A549 clones lacking anti-IDO shRNA (*i.e.*, stably expressing only control scrambled shRNA) increased resistance to γ radiation by approximately 15%, compared with no change in clones harbouring anti-IDO shRNA (Figures 4.30). A trend toward a similar response was observed in HeLa cells, but did not achieve statistical significance (Figure 4.34).

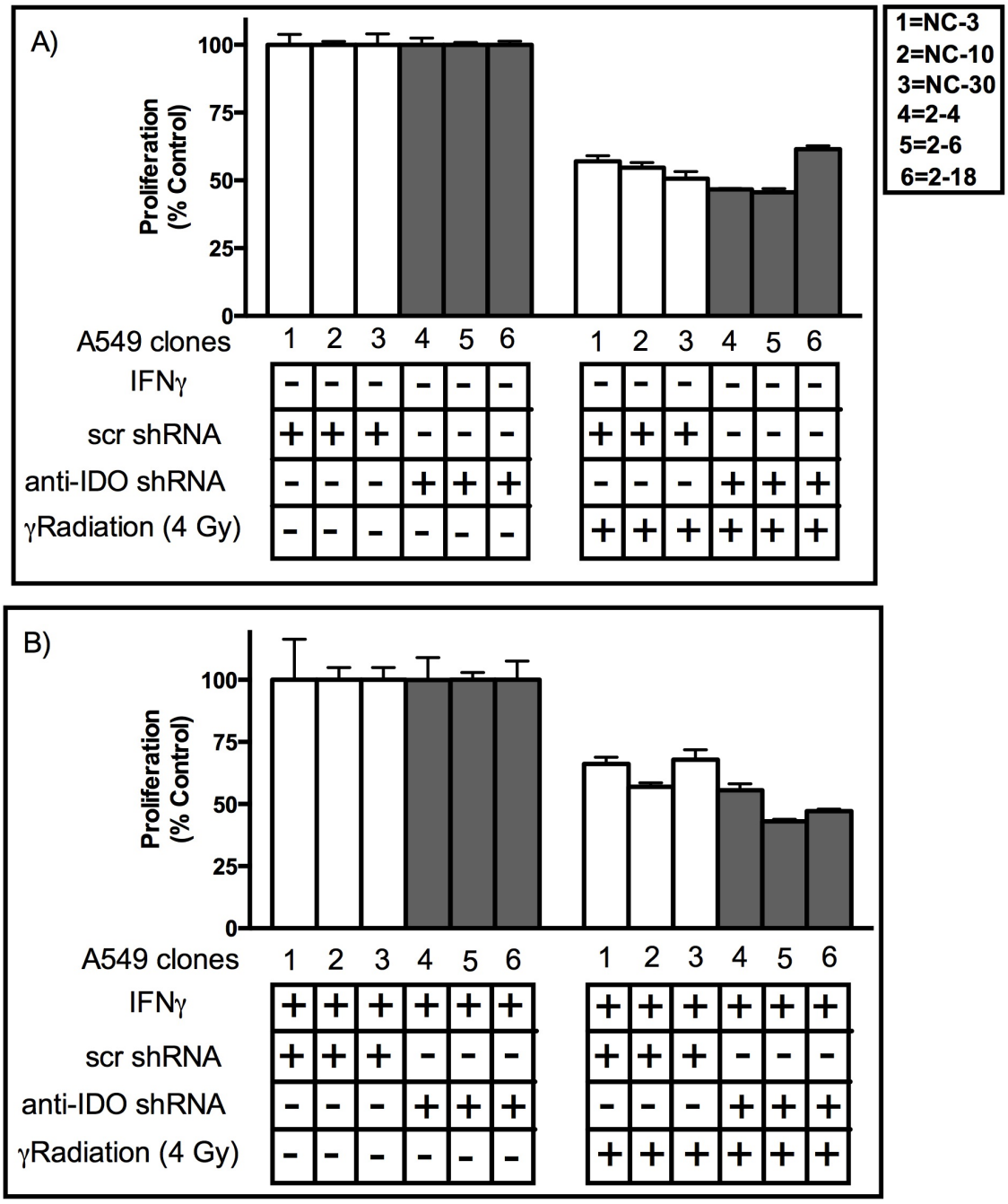
A)
Proliferation (% Control)
100
75
50
25
0
A549 clones
1 2 3 4 5 6
1 2 3 4 5 6
IFNγ
scr shRNA
anti-IDO shRNA
γRadiation (4 Gy)
1=NC-3
2=NC-10
3=NC-30
4=2-4
5=2-6
6=2-18
B)
Proliferation (% Control)
100
75
50
25
0
A549 clones
1 2 3 4 5 6
1 2 3 4 5 6
IFNγ
scr shRNA
anti-IDO shRNA
γRadiation (4 Gy)

Figure 4. 28. A549 clone sensitivity to γ radiation (4 Gy) before and after IDO induction. **Panels A-B** present data for each of 6 individual clonal populations before and after IDO induction. A549 clonal populations were cultured with or without IFNγ (25 ng/ml) for 48 h. Cultured cells were then irradiated (4 Gy) then the medium was then replaced with fresh growth medium and cells were allowed to proliferate for 72 h. Cells were then trypsinized and live cells were enumerated using a Coulter counter. White bars represent A549 clones transfected with scrambled shRNA and gray bars represent A549 cells transfected with anti-IDO shRNA. Each bar represents the mean of the 3 values (*n*=3 for determination of each value) ± SD. Significant changes are shown in pooled results (Figure 4.29).

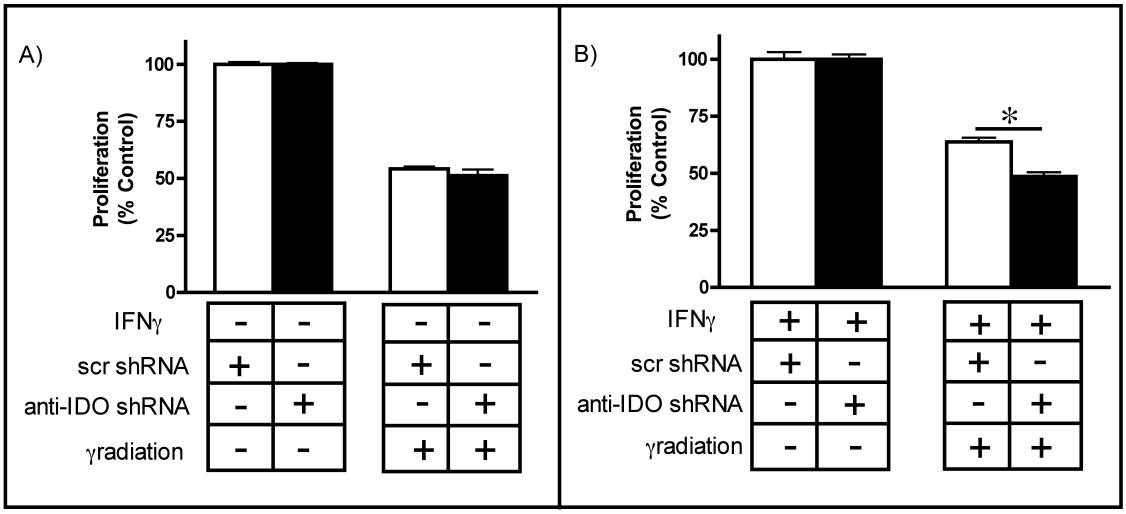
A)
Proliferation (% Control)
100
75
50
25
0
IFNγ
scr shRNA
anti-IDO shRNA
γradiation
B)
Proliferation (% Control)
100
75
50
25
0
*
IFNγ
scr shRNA
anti-IDO shRNA
γradiation

Figure 4. 29. Sensitivity of clonal A549 populations to γ radiation (4 Gy) before (A) and after (B) IDO induction. Data shown in Figure 4.28 were pooled to generate mean values from 3 independent clonal populations harbouring scrambled control shRNA or anti-IDO shRNA, and each bar represents the mean of the 3 values (n=3 for determination of each value) ± SEM (*$P < 0.05$).

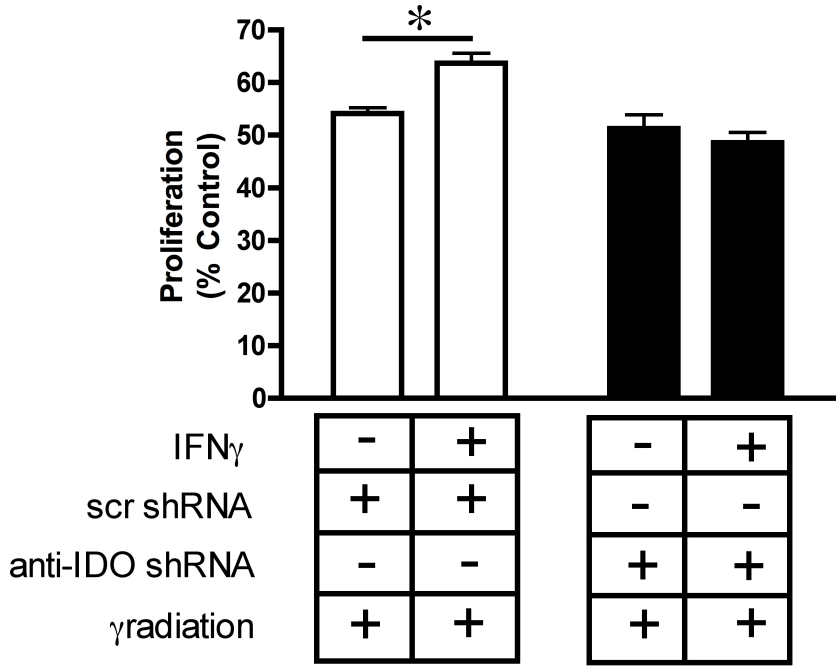
*
70
60
50
40
30
20
10
0
Proliferation (% Control)
IFNγ
scr shRNA
anti-IDO shRNA
γradiation
- + - +
+ + - -
- - + +
+ + + +

Figure 4. 30. Induction of IDO in A549 clonal cell induces resistance to γ radiation. Results were obtained from 3 independent clonal cell populations with scrambled control shRNA or anti-IDO shRNA, and each bar represents the mean of those 3 values (n=3 for determination of each value) ± SEM (*P<0.05).

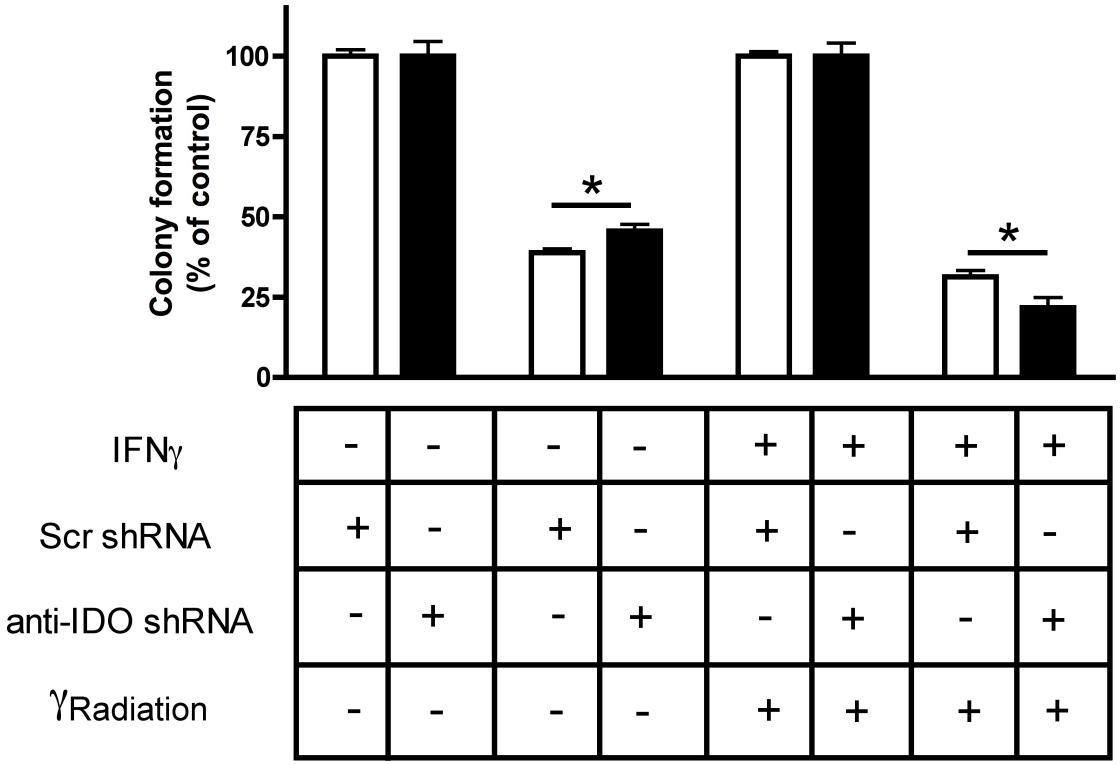
Colony formation
(% of control)
100
75
50
25
0
*
*
IFNγ
Scr shRNA
anti-IDO shRNA
γRadiation
- - - - + + + +
+ - + - + - + -
- + - + - + - +
- - - - + + + +

Figure 4. 31. Induction of IDO in A549 clonal cell induces resistance to γ radiation. A549 cells were induced with IFNγ (25 ng/ml) for 48 h. Cells were then γ irradiated (4 Gy), trypsinized and 300 cells were seeded in 6-well plates. Colonies were stained with 0.5% crystal violet 7 days later. Each bar represents the mean of 3 values (*n*=3 for determination of each value) ± SEM (* $P < 0.05$).

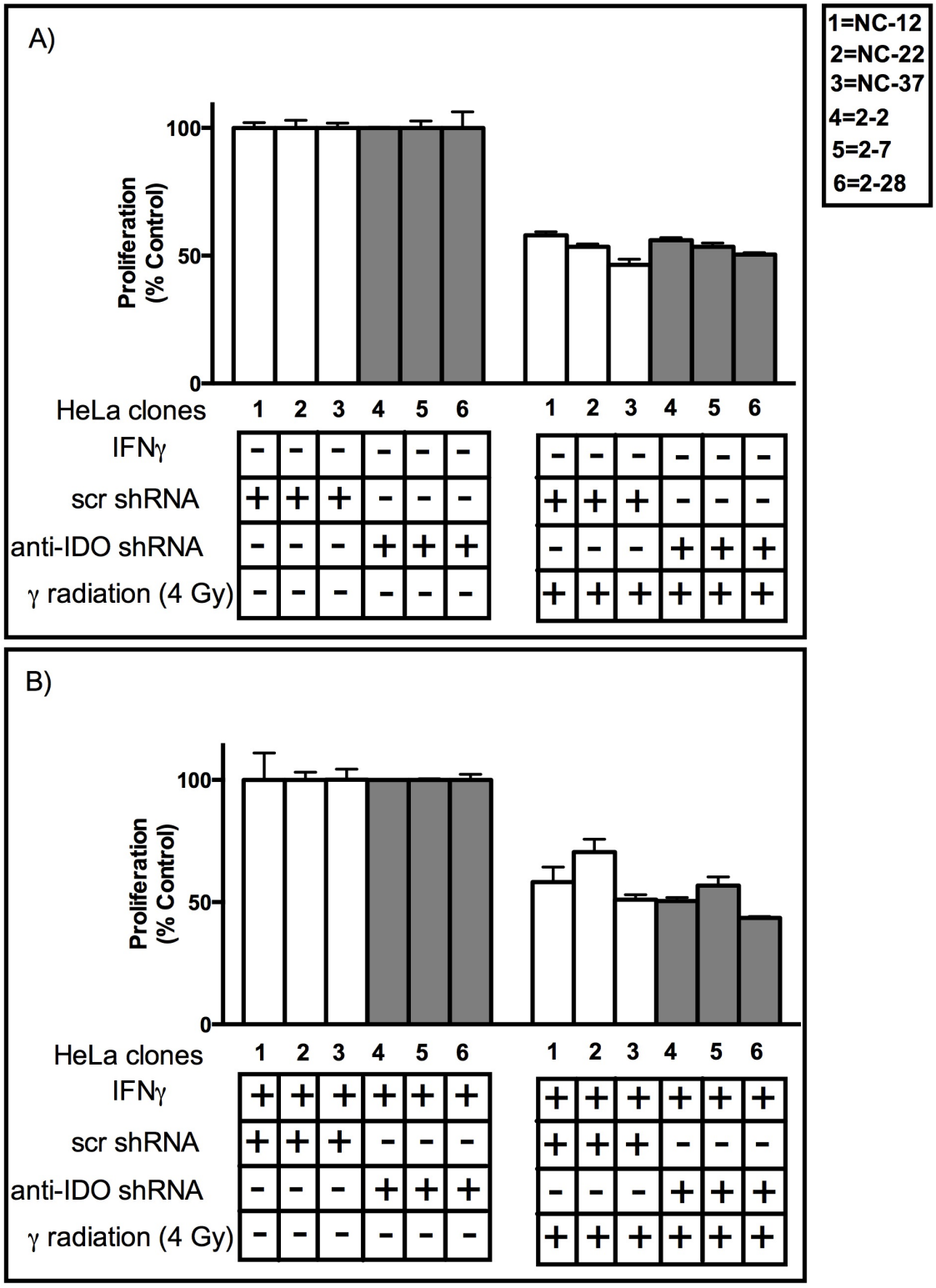
A)
1=NC-12
2=NC-22
3=NC-37
4=2-2
5=2-7
6=2-28
Proliferation (% Control)
100
50
0
HeLa clones
1 2 3 4 5 6
1 2 3 4 5 6
IFNγ
scr shRNA
anti-IDO shRNA
γ radiation (4 Gy)
B)
Proliferation (% Control)
100
50
0
HeLa clones
1 2 3 4 5 6
1 2 3 4 5 6
IFNγ
scr shRNA
anti-IDO shRNA
γ radiation (4 Gy)

Figure 4. 32. HeLa clone sensitivity to γ radiation (4 Gy) before and after IDO induction. Panels A-B present data for each of 6 individual clonal populations before and after IDO induction. HeLa clonal populations were cultured with or without IFNγ (25 ng/ml) for 48 h. Cultured cells were then irradiated (4 Gy) then the medium was then replaced with fresh growth medium and cells were allowed to proliferate for 72 h. Cells were then trypsinized and live cells were enumerated using a Coulter counter. White bars represent HeLa clones transfected with scrambled shRNA and gray bars represent HeLa cells transfected with anti-IDO shRNA. Each bar represents the mean of the 3 values (*n*=3 for determination of each value) ± SD. Significant changes are shown in pooled results (Figure 4.33).

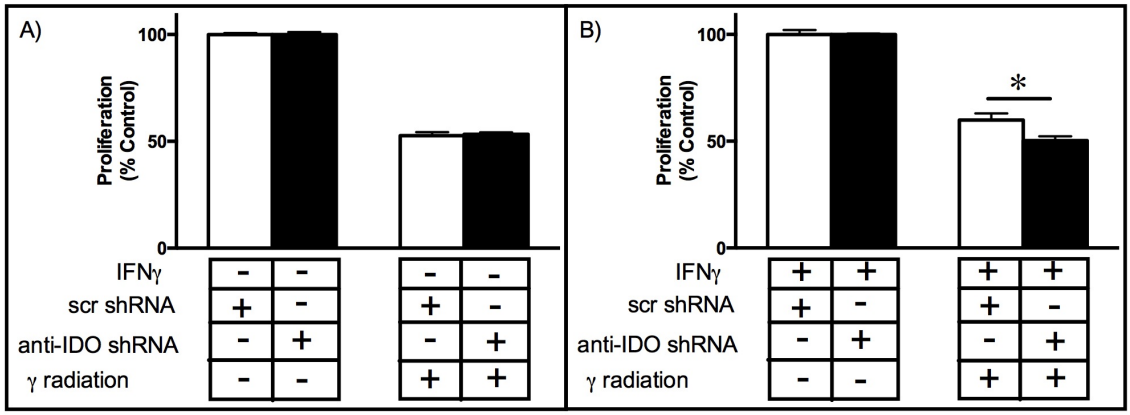
A)
Proliferation (% Control)
100
50
0
IFNγ
scr shRNA
anti-IDO shRNA
γ radiation
B)
Proliferation (% Control)
100
50
0
*
IFNγ
scr shRNA
anti-IDO shRNA
γ radiation

Figure 4. 33. Sensitivity of clonal HeLa populations to γ radiation (4 Gy) before (A) and after (B) IDO induction. Data shown in Figure 4.32 were pooled to generate mean values from 3 independent clonal populations harbouring scrambled control shRNA or anti-IDO shRNA, and each bar represents the mean of the 3 values (n=3 for determination of each value) ± SEM (*$P < 0.05$).

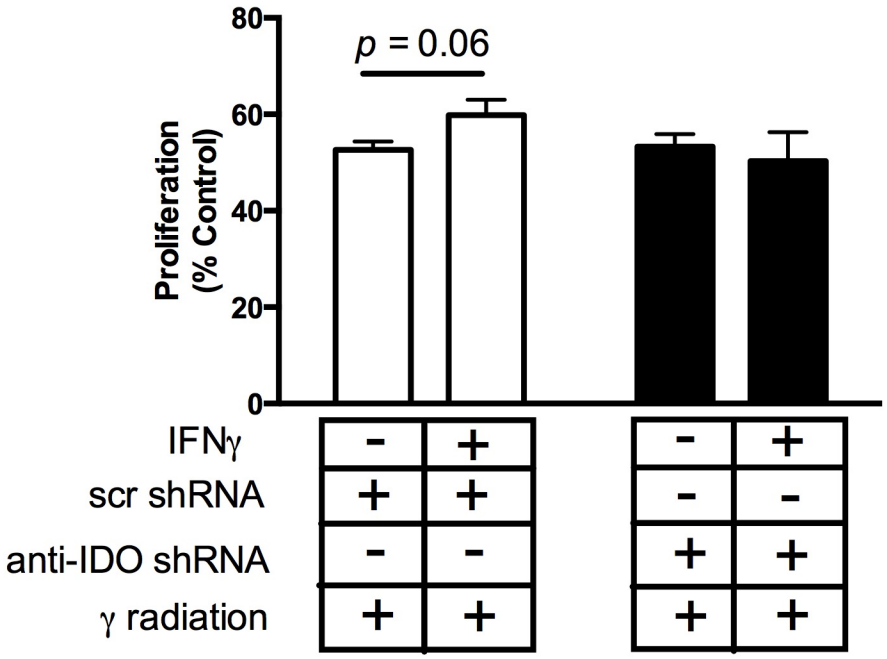
p = 0.06
Proliferation (% Control)
80
60
40
20
0
IFNγ
scr shRNA
anti-IDO shRNA
γ radiation
- + - +
+ + - -
- - + +
+ + + +

Figure 4. 34. Induction of IDO in HeLa clonal cell populations and association with resistance to γ radiation. Results were obtained from 3 independent clonal cell populations with scrambled control shRNA or anti-IDO shRNA, and each bar represents the mean of those 3 values (n=3 for determination of each value) ± SEM (p = 0.06). A trend toward increased resistance to γ radiation with increased IDO was observed but did not achieve statistical significance.

4.13 IDO in Human Tumour Cells Mediates Resistance to Combined γ Radiation and PARP Inhibition

In light of the common clinical use of combination therapies and the common goal of causing DNA damage and subsequently inhibiting DNA repair through the use of γ radiation and PARP inhibitors, respectively, it was of interest to determine the effect of IDO on cancer cell sensitivity to the combination of these treatments. We tested this questions by inducing IDO in A549 and HeLa clones as described (Chapter 3, Section 3.13). Prior to treatment with IFNγ, all clonal A549 populations harbouring either anti-IDO shRNA or control scrambled shRNA were equally sensitive to combined treatment (Figures 4.35 and 4.36). In the case of HeLa clonal cell populations, those harbouring scrambled shRNA were more sensitive to combination treatment than clonal cells with anti-IDO shRNA (Figures 4.38 and 4.39). After IDO induction by IFNγ, A549 and HeLa clones harbouring anti-IDO shRNA were approximately 30% and 20% more sensitive to combined treatment with γ radiation and olaparib, respectively, than similarly-treated clones harbouring control scrambled shRNA ($p<0.05$)(Figures 4.35 and 4.38). In addition, in A549 clonal cell populations, IFNγ induced IDO-mediated resistance to the antiproliferative effects of combined olaparib and γ radiation, but anti-IDO shRNA abolished that resistance (Figure 4.37). HeLa clonal populations showed a similar trend but that trend did not achieve statistical significance (Figure 4.40).

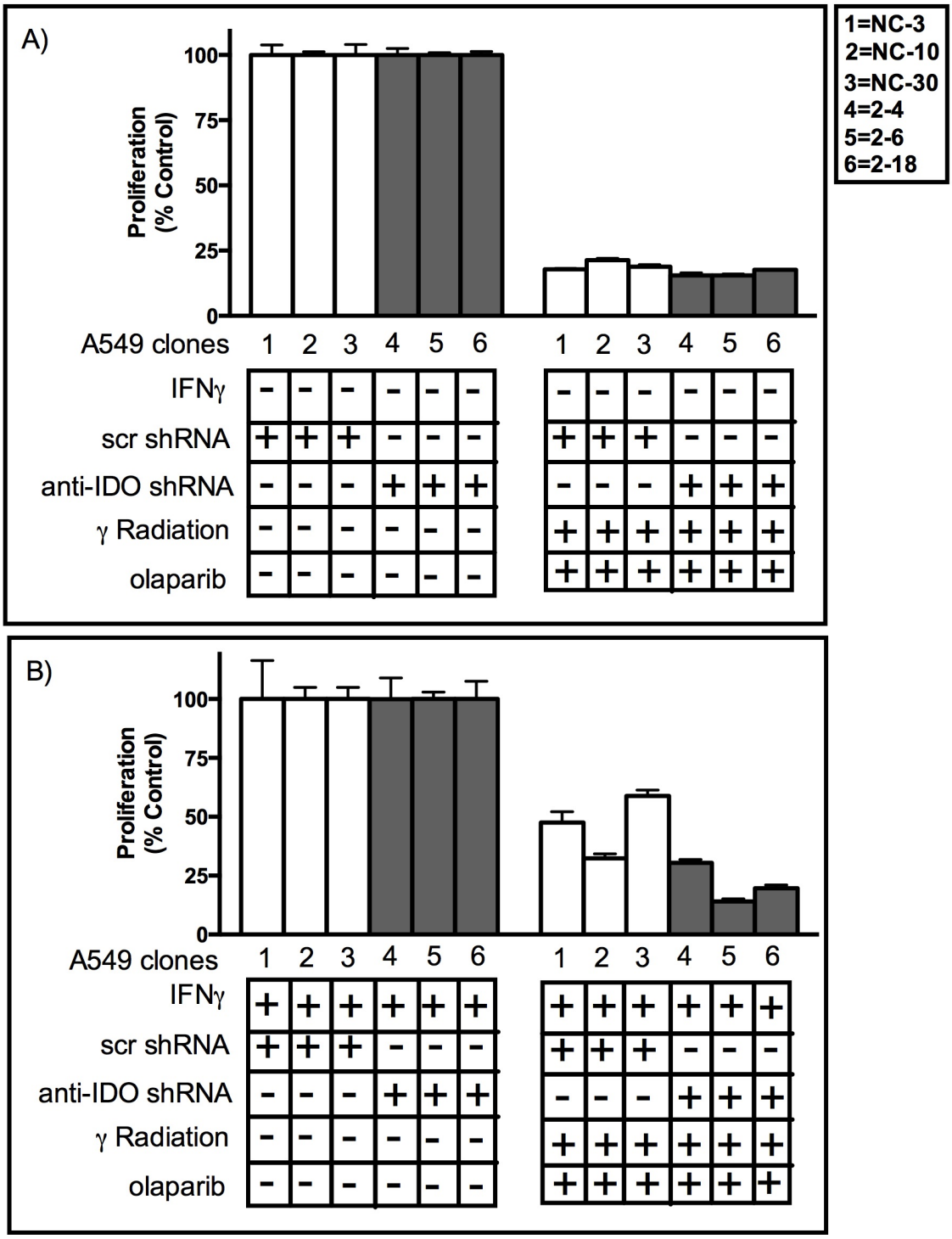
A)
Proliferation (% Control)
100
75
50
25
0
A549 clones 1 2 3 4 5 6 1 2 3 4 5 6
IFNγ
scr shRNA
anti-IDO shRNA
γ Radiation
olaparib
1=NC-3
2=NC-10
3=NC-30
4=2-4
5=2-6
6=2-18
B)
Proliferation (% Control)
100
75
50
25
0
A549 clones 1 2 3 4 5 6 1 2 3 4 5 6
IFNγ
scr shRNA
anti-IDO shRNA
γ Radiation
olaparib

Figure 4. 35. A549 sensitivity to combined γ irradiation (4 Gy) and olaparib (5 μM) treatment before (A) and after (B) IDO induction. A549 cells were induced with with or without IFNγ (25 ng/ml) for 48 h. Cells were then treated with γ radiation (4 Gy) and the medium was immediately replaced with fresh growth medium with olaparib (5 μM). Cells were allowed to proliferate for 72 h. Results were obtained from independent measurements of proliferation of three A549 clonal populations (2 independent experiments for each population) with control scrambled shRNA and 3 with anti-IDO shRNA. Bars represent the means of those 3 independent measurements (*n*=3 for each measurement) ± SEM (*p<0.05). White bars represent A549 clones transfected with scrambled shRNA and gray bars represent A549 cells transfected with anti-IDO shRNA. Each bar represents the mean of the 3 values (*n*=3 for determination of each value) ± SD. Significant changes are shown in pooled results (Figure 4.36).

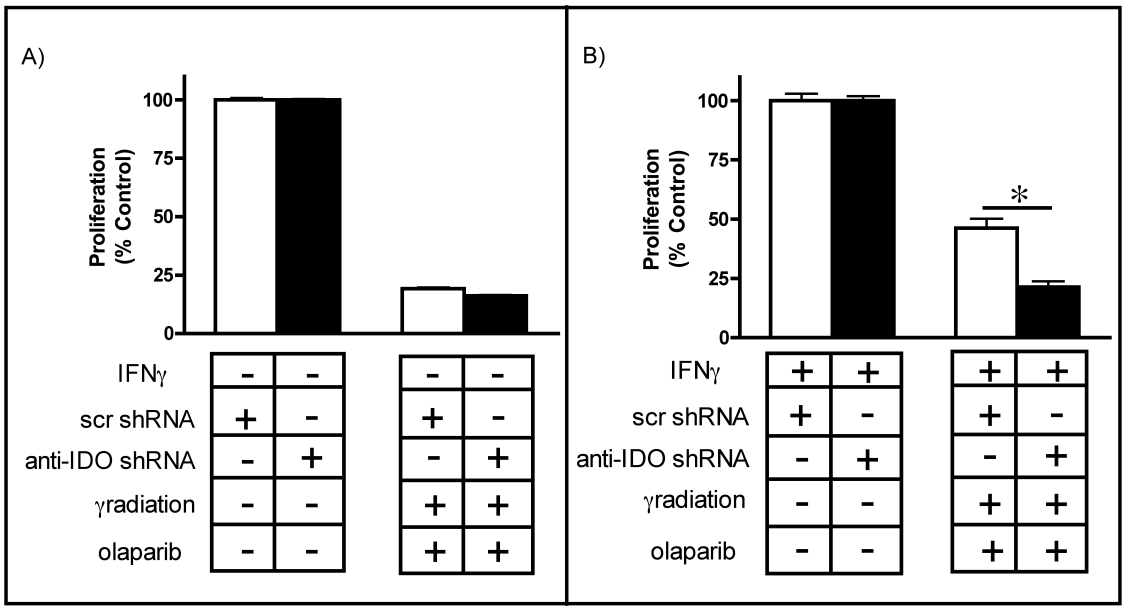
A)
Proliferation (% Control)
100
75
50
25
0
IFNγ
scr shRNA
anti-IDO shRNA
γradiation
olaparib
B)
Proliferation (% Control)
100
75
50
25
0
*
IFNγ
scr shRNA
anti-IDO shRNA
γradiation
olaparib

Figure 4. 36. Sensitivity of clonal A549 populations to combined γ radiation (4 Gy) and olaparib (5 μM) treatment before (A) and after (B) IDO induction. Data shown in Figure 4.35 were pooled to generate mean values from 3 independent clonal populations harbouring scrambled control shRNA or anti-IDO shRNA, and each bar represents the mean of those 3 values (n=3 for determination of each value) ± SEM (*P < 0.05).

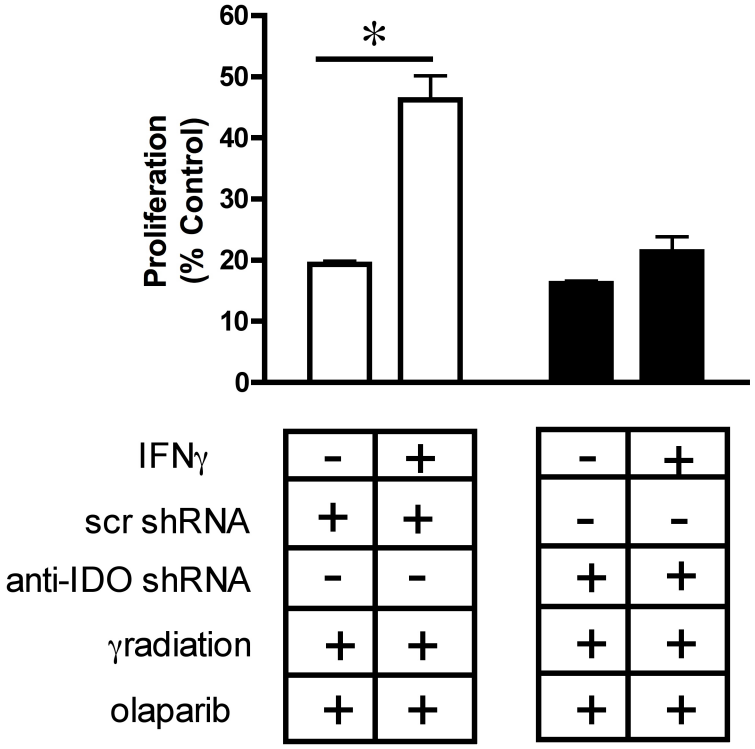
60
50
40
30
20
10
0
*
Proliferation (% Control)
IFNγ
scr shRNA
anti-IDO shRNA
γradiation
olaparib
- + - +
+ + - -
- - + +
+ + + +
+ + + +

Figure 4. 37. Induction of IDO in A549 clonal cell induces resistance to combined γ radiation and olaparib treatment. Results were obtained from 3 independent clonal cell populations with scrambled control shRNA or anti-IDO shRNA, and each bar represents the mean of those 3 values (n=3 for determination of each value) ± SEM (*p<0.05).

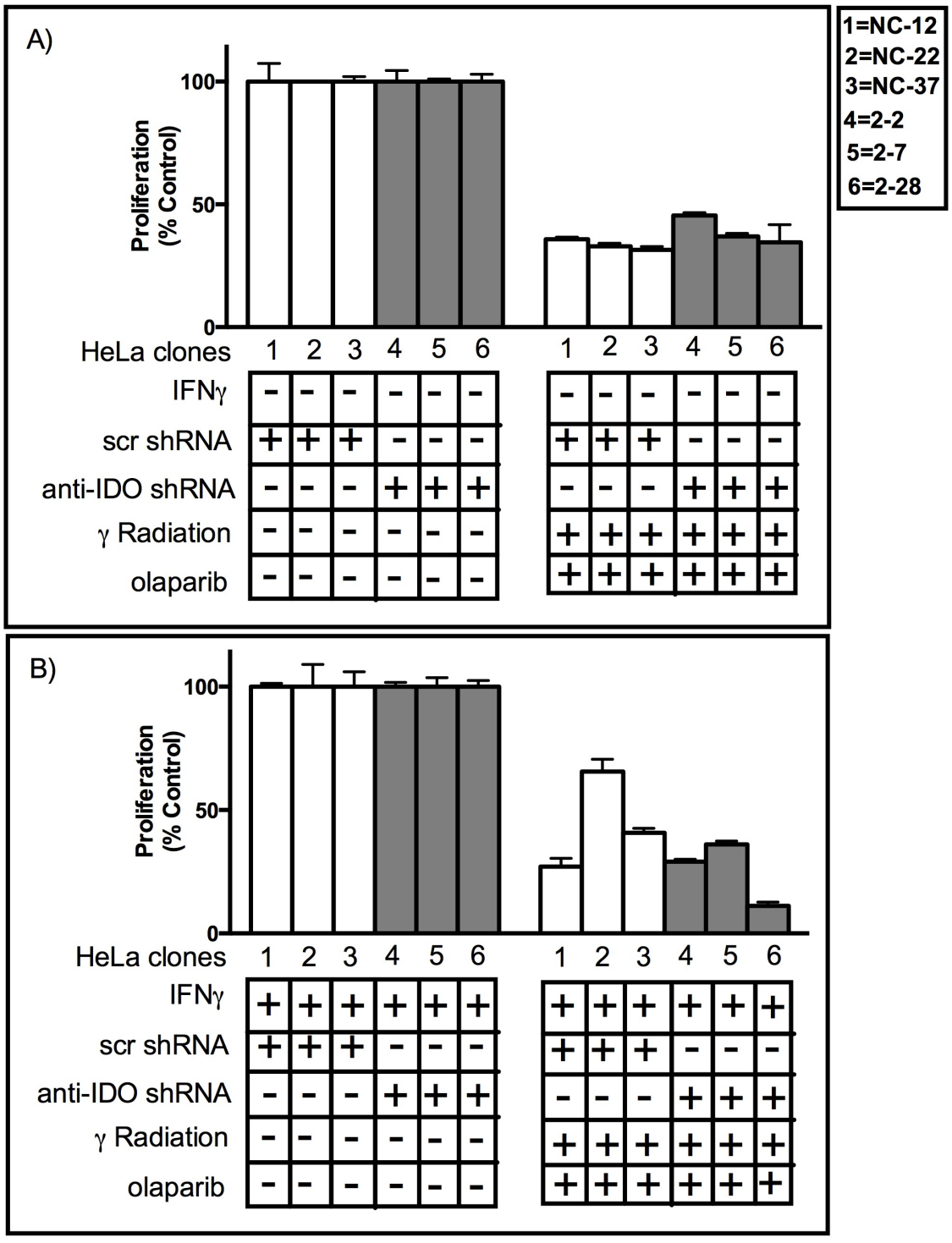
A)
Proliferation (% Control)
100
50
0
HeLa clones 1 2 3 4 5 6 1 2 3 4 5 6
IFNγ
scr shRNA
anti-IDO shRNA
γ Radiation
olaparib
1=NC-12
2=NC-22
3=NC-37
4=2-2
5=2-7
6=2-28
B)
Proliferation (% Control)
100
50
0
HeLa clones 1 2 3 4 5 6 1 2 3 4 5 6
IFNγ
scr shRNA
anti-IDO shRNA
γ Radiation
olaparib

Figure 4. 38. HeLa sensitivity to combined γ irradiation (4 Gy) and olaparib (5 μM) treatment before (A) and after (B) IDO induction. HeLa cells were induced with with or without IFNγ (25 ng/ml) for 48 h. Then the cells were treated with γ radiation (4 Gy) and the medium was immediately replaced with fresh growth medium harbouring olaparib (5 μM). Cells were allowed to proliferate for 72 h. Results were obtained from independent measurements of proliferation of 3 HeLa clonal populations (2 independent experiments for each population) with control scrambled shRNA and 3 with anti-IDO shRNA. Bars represent the means of those 3 independent measurements (*n*=3 for each measurement) ± SEM (*p<0.05). White bars represent HeLa clones transfected with scrambled shRNA and gray bars represent HeLa cells transfected with anti-IDO shRNA. Each bar represents the mean of the 3 values (*n*=3 for determination of each value) ± SD. Significant changes are shown in pooled results (Figure 4.39).

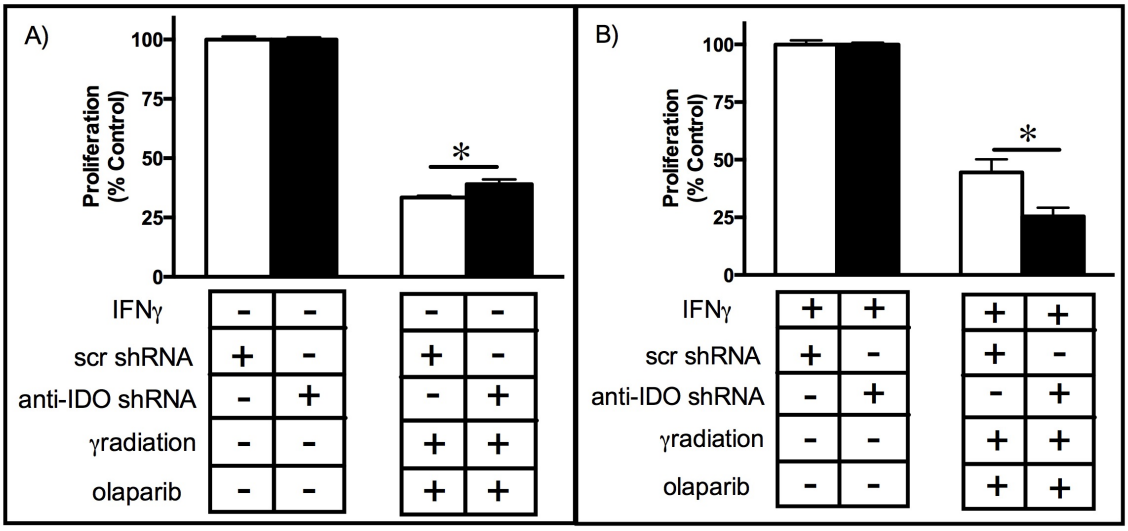
A)
Proliferation (% Control)
100
75
50
25
0
*
IFNγ
scr shRNA
anti-IDO shRNA
γradiation
olaparib
B)
Proliferation (% Control)
100
75
50
25
0
*
IFNγ
scr shRNA
anti-IDO shRNA
γradiation
olaparib

Figure 4. 39. Sensitivity of clonal HeLa populations to combined γ radiation (4 Gy) and olaparib (5 μM) treatment before (A) and after (B) IDO induction. Data shown in Figure 4.38 were pooled to generate mean values from 3 independent clonal populations harbouring scrambled control shRNA or anti-IDO shRNA, and each bar represents the mean of those 3 values (n=3 for determination of each value) ± SEM (*P < 0.05).

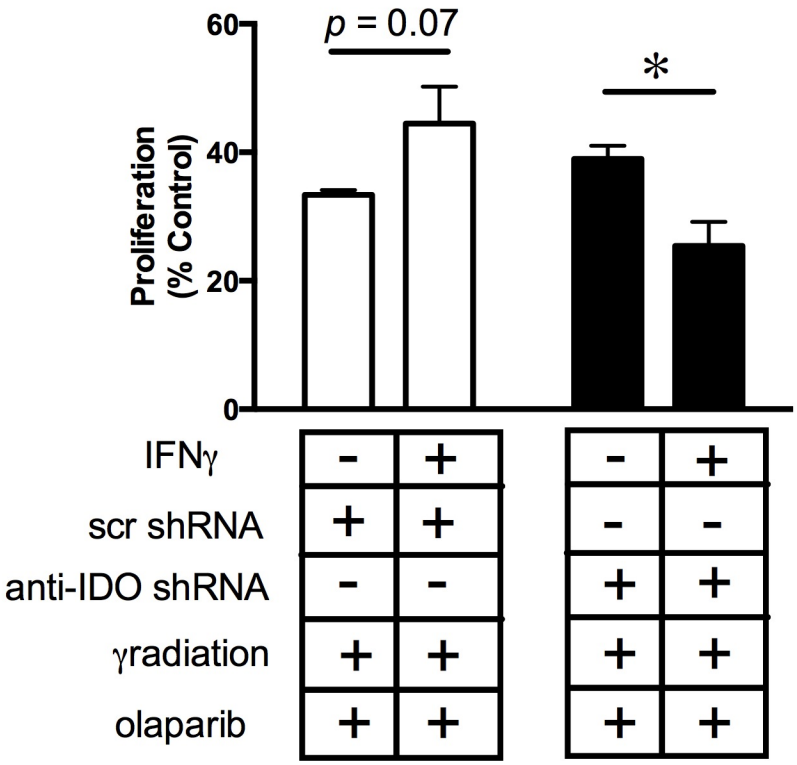
p = 0.07
*
60
40
20
0
Proliferation (% Control)
IFNγ
scr shRNA
anti-IDO shRNA
γradiation
olaparib
- + - +
+ + - -
- - + +
+ + + +
+ + + +

Figure 4. 40. Antisense reduction of IDO in A549 clonal cell reduces resistance to combined γ radiation and olaparib treatment. Results were obtained from 3 independent clonal cell populations with scrambled control shRNA or anti-IDO shRNA, and each bar represents the mean of those 3 values (n=3 for determination of each value) ± SEM (*p<0.05). Increased IDO in these cells induced a trend toward increased cell survival in the presence of olaparib but that trend did not achieve statistical significance (p=0.07).

4.14 IDO in Human Tumour Cells Mediates Resistance to the Base Excision Repair Inhibitor Methoxyamine

NAD^+ is required for PARP function and PARP is essential for recruitment of the BER scaffold protein XRCC1 to damaged DNA [200]. In light of our observation that IDO plays a role in mediating resistance to the PARP inhibitor olaparib, the capacity of IDO to mediate resistance to the BER inhibitor methoxyamine was examined. A549 cells were treated with or without IFNγ (25 ng/ml) for 48 h to induce IDO. Tumour cells were then treated with methoxyamine as described (Chapter 3, Section 3.16). IDO downregulation sensitized cancer cells to methoxyamine (Figures 4.41 and 4.42). Of particular note, A549 clone 2-4, although it is stably transfected with anti-IDO shRNA, had a higher level of IDO than anti-IDO shRNA-containing clones 2-6 and 2-18 (Figure 4.12) and showed a higher degree of methoxyamine resistance than shRNA-transfected clones with lower levels of IDO (Figure 4.41, Panel C, showing a moderate correlation between IDO level and methoxyamine resistance [$R^2 = 0.83$]). In addition, IFNγ induced IDO-mediated resistance to the antiproliferative effects of methoxyamine, and anti-IDO shRNA abolished that resistance (Figure 4.43).

4.15 IDO in Human Tumour Cells Mediates Resistance to the TS-targeting Drug Pemetrexed

Thymidylate synthase (TS) is important in DNA repair and DNA synthesis and is overexpressed in most human cancers [245]. The TS-targeting drug pemetrexed is commonly used to treat multiple types of human cancer including NSCLC and colorectal cancer [179]. BER is reported to be important in cancer cell resistance to this drug. The sensitivity of A549 clonal populations to pemetrexed in the presence of IDO was therefore tested. Clonal A549 cell populations were treated with pemetrexed as described in chapter 3, section 3.14. IDO downregulation sensitized cancer cells to pemetrexed (Figures 4.44 and 4.45). Furthermore, IFNγ-induced IDO decreased the effectiveness of pemetrexed in IDO-expressing cancer cells but the IDO-mediated decrease in pemetrexed effectiveness was reduced in A549 clonal cell populations harbouring anti-IDO shRNA (Figure 4.46).

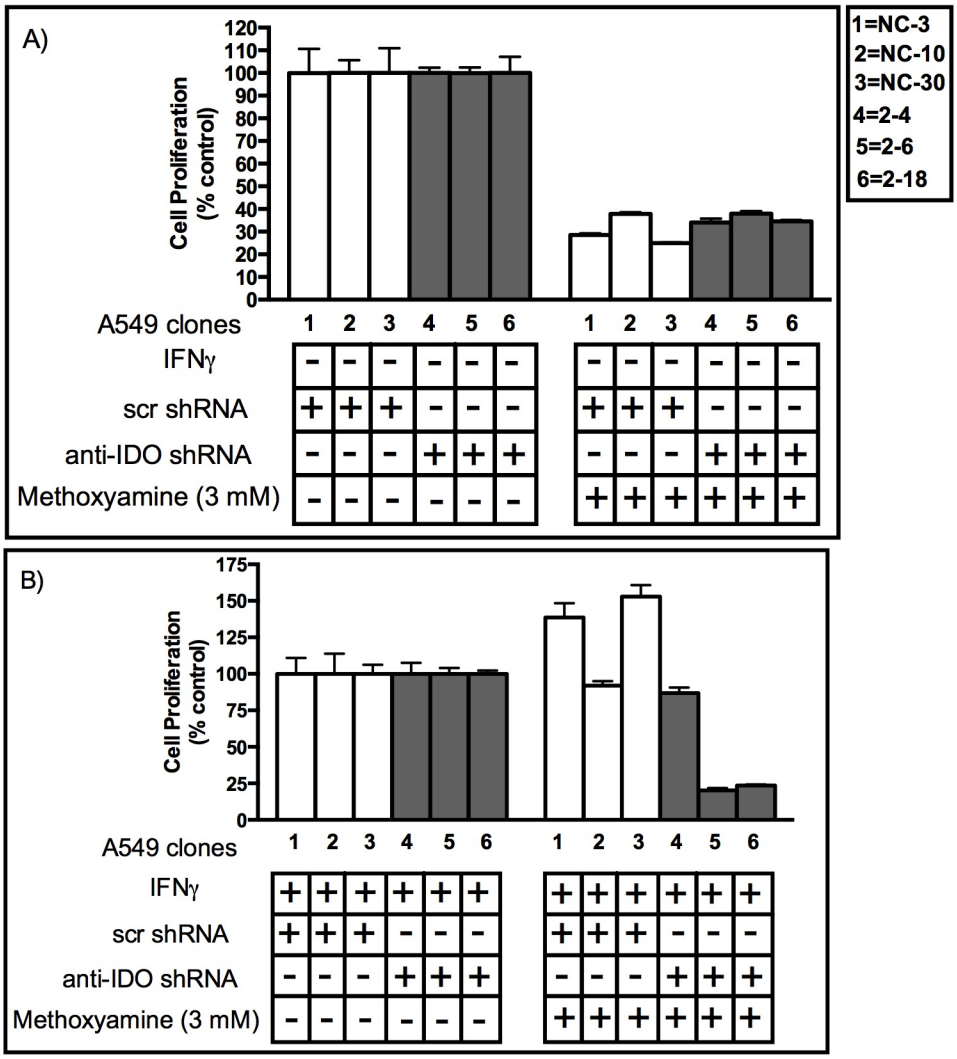
A)
Cell Proliferation (% control)
120
110
100
90
80
70
60
50
40
30
20
10
0
A549 clones
1 2 3 4 5 6 1 2 3 4 5 6
IFNγ
scr shRNA
anti-IDO shRNA
Methoxyamine (3 mM)
1=NC-3
2=NC-10
3=NC-30
4=2-4
5=2-6
6=2-18
B)
Cell Proliferation (% control)
175
150
125
100
75
50
25
0
A549 clones
1 2 3 4 5 6 1 2 3 4 5 6
IFNγ
scr shRNA
anti-IDO shRNA
Methoxyamine (3 mM)

C)

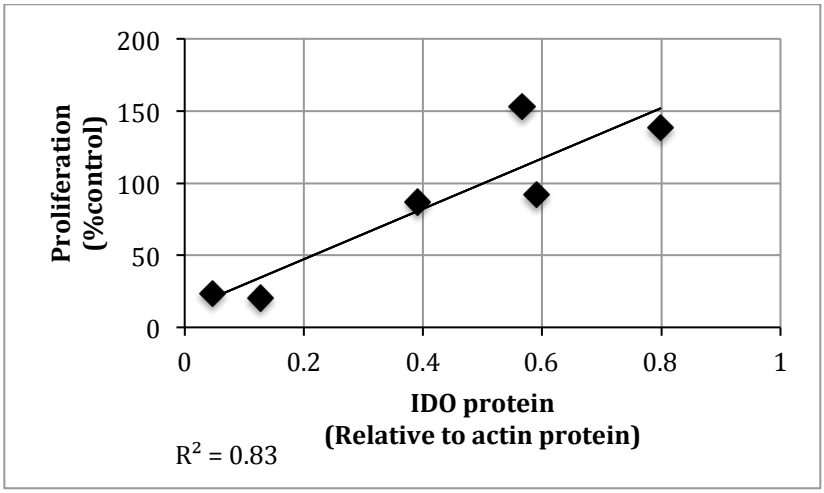
Proliferation (%control)
200
150
100
50
0
0
0.2
0.4
0.6
0.8
1
IDO protein
(Relative to actin protein)
R² = 0.83

Figure 4. 41. A549 clone sensitivity to methoxyamine (3 mM) before and after IDO induction. Panels A-B present data for each of 6 individual clonal populations before and after IDO induction. A549 clonal populations were cultured with or without IFNγ (25 ng/ml) for 48 h. Cultured medium was then replaced with fresh growth medium containing methoxyamine (3 mM) and cells were allowed to proliferate for 72 h. Cells were then trypsinized and live cells were enumerated. White bars represent A549 clones transfected with scrambled shRNA and gray bars represent A549 cells transfected with anti-IDO shRNA. Each bar represents the mean of 3 values (*n*=3 for determination of each value) ± SD. Significant changes are shown in pooled results (Figure 4.42). **Panel C**: relationship between IDO protein level (relative to actin) and resistance to methpxyamine (MX) (proliferation relative to untreated control cells). The R^2 value of 0.83 represents a moderate positive relationship.

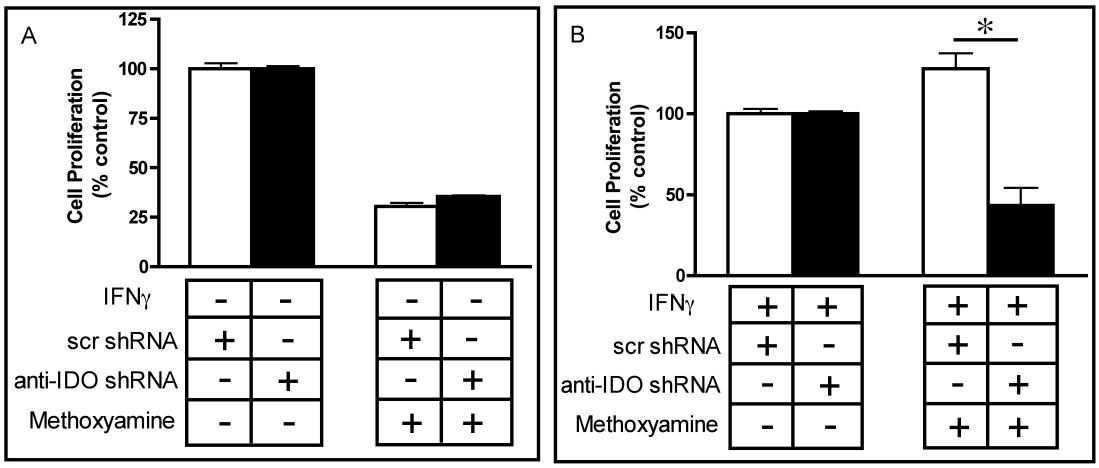
A
Cell Proliferation (% control)
125
100
75
50
25
0
IFNγ
scr shRNA
anti-IDO shRNA
Methoxyamine
B
Cell Proliferation (% control)
150
100
50
0
*
IFNγ
scr shRNA
anti-IDO shRNA
Methoxyamine

Figure 4. 42. Sensitivity of clonal A549 populations to methoxyamine (3 mM) before (A) and after (B) IDO induction. Data shown in Figure 4.41 were pooled to generate mean values from 3 independent clonal populations harbouring scrambled control shRNA or anti-IDO shRNA, and each bar represents the mean of those 3 values (n=3 for determination of each value) ± SEM (*$P < 0.05$).

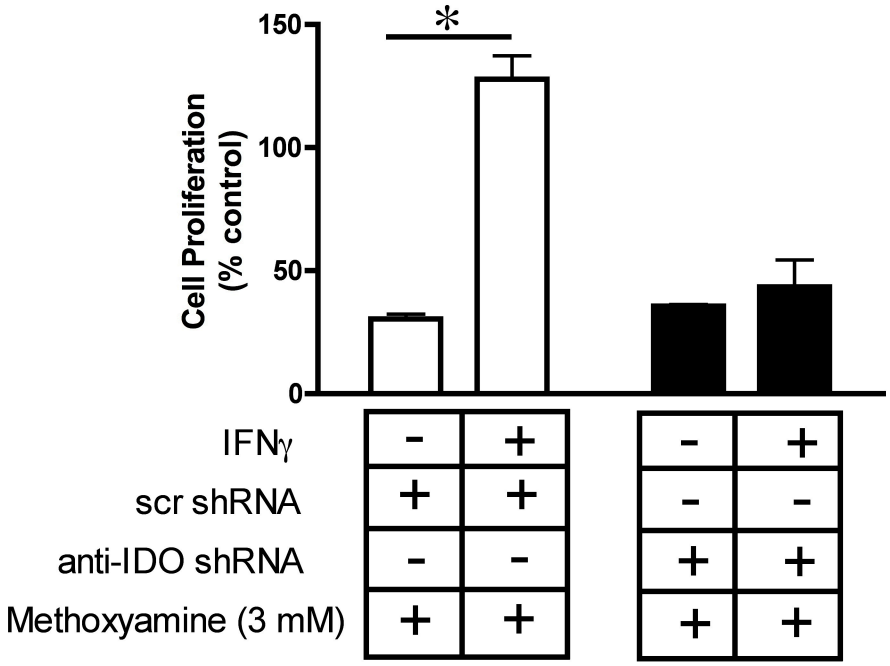
*
150
100
50
0
Cell Proliferation
(% control)
IFNγ
scr shRNA
anti-IDO shRNA
Methoxyamine (3 mM)
- + - +
+ + - -
- - + +
+ + + +

Figure 4. 43. Induction of IDO in A549 clonal cell induces resistance to methoxyamine (3 mM). Results were obtained from 3 independent clonal cell populations with scrambled control shRNA or anti-IDO shRNA, and each bar represents the mean of those 3 values (n=3 for determination of each value) ± SEM (*$p < 0.05$).

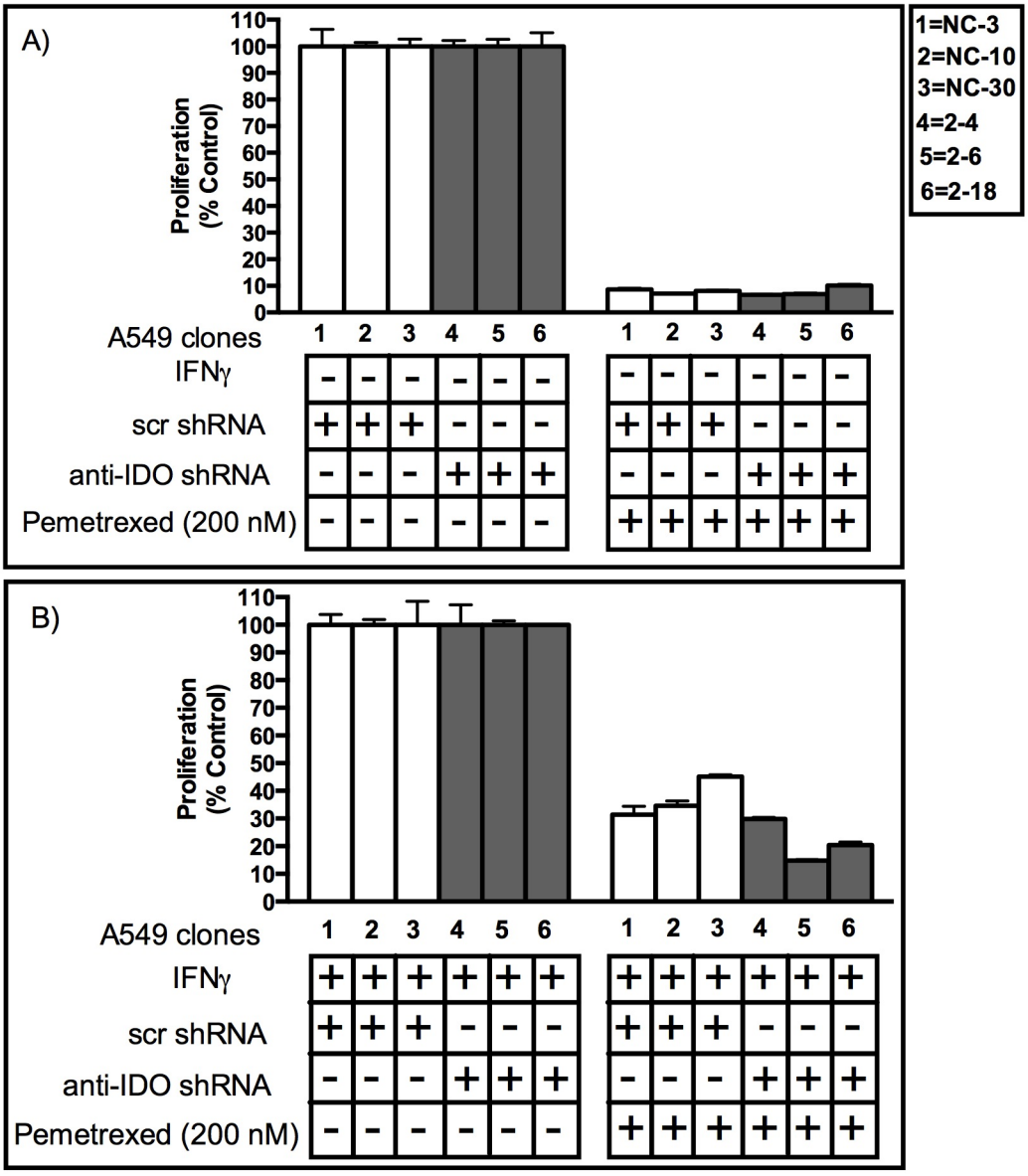
A)
Proliferation (% Control)
110
100
90
80
70
60
50
40
30
20
10
0
A549 clones
1 2 3 4 5 6 1 2 3 4 5 6
IFNγ
scr shRNA
anti-IDO shRNA
Pemetrexed (200 nM)
1=NC-3
2=NC-10
3=NC-30
4=2-4
5=2-6
6=2-18
B)
Proliferation (% Control)
110
100
90
80
70
60
50
40
30
20
10
0
A549 clones
1 2 3 4 5 6 1 2 3 4 5 6
IFNγ
scr shRNA
anti-IDO shRNA
Pemetrexed (200 nM)

Figure 4. 44. A549 clone sensitivity to pemetrexed (200 nM) before and after IDO induction. Panels A-B present data for each of 6 individual clonal populations before and after IDO induction. A549 clonal populations were cultured with or without IFNγ (25 ng/ml) for 48 h, then with pemetrexed (200 nM), and enumerated 72 h later. White bars represent A549 clones transfected with scrambled shRNA and gray bars represent A549 cells transfected with anti-IDO shRNA. Each bar represents the mean of 3 values (*n*=3 for determination of each value) ± SD. Significant changes are shown in pooled results (Figure 4.45).

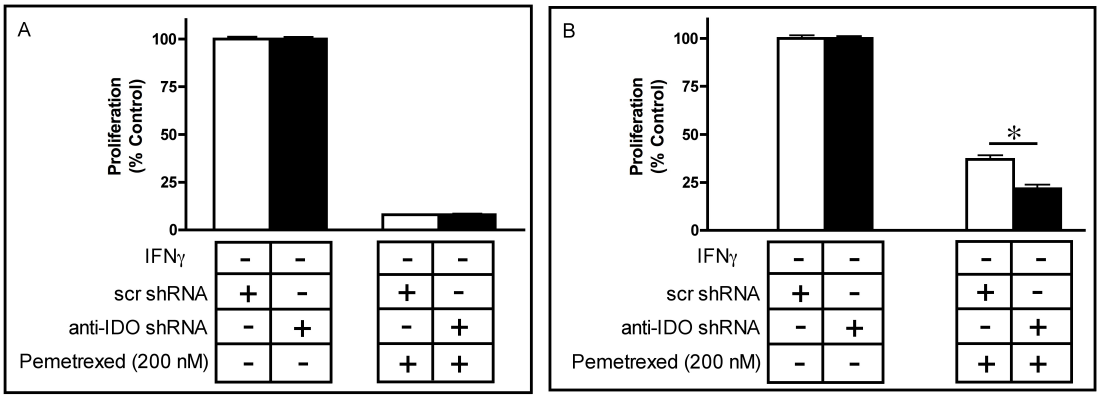
A
Proliferation (% Control)
100
75
50
25
0
IFNγ
scr shRNA
anti-IDO shRNA
Pemetrexed (200 nM)
B
Proliferation (% Control)
100
75
50
25
0
*
IFNγ
scr shRNA
anti-IDO shRNA
Pemetrexed (200 nM)

Figure 4. 45. Sensitivity of clonal A549 populations to pemetrexed (200 nM) before (A) and after (B) IDO induction. Data shown in Figure 4.44 were pooled to generate mean values from 3 independent clonal populations harbouring scrambled control shRNA or anti-IDO shRNA, and each bar represents the mean of those 3 values (n=3 for determination of each value) ± SEM (*$P < 0.05$).

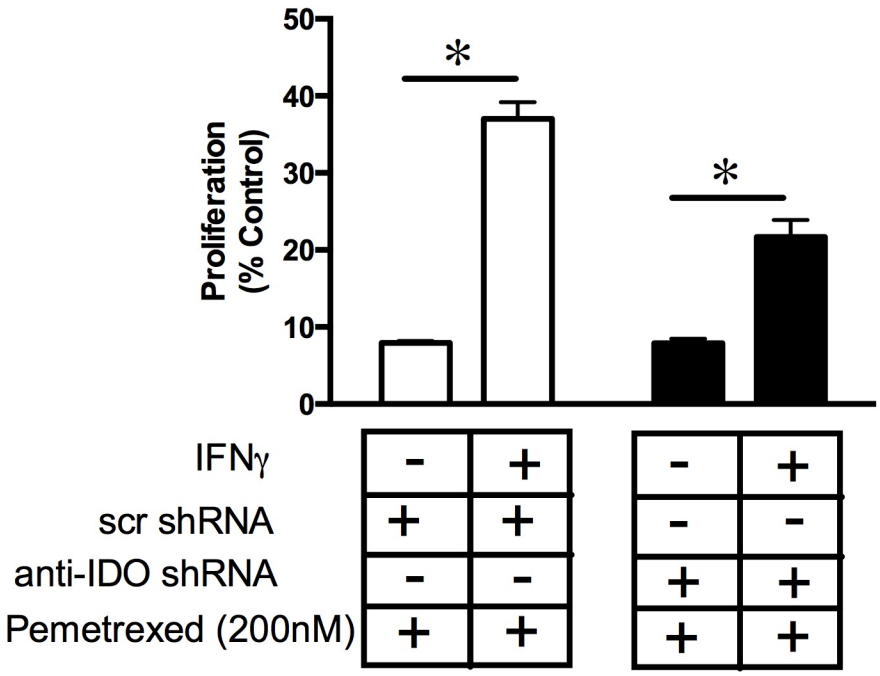
Proliferation (% Control)
50
40
30
20
10
0
*
*
IFNγ
scr shRNA
anti-IDO shRNA
Pemetrexed (200nM)
- + - +
+ + - -
- - + +
+ + + +

Figure 4. 46. Induction of IDO in A549 clonal cell induces resistance to pemetrexed (200 nM). Results were obtained from 3 independent clonal cell populations with scrambled control shRNA or anti-IDO shRNA, and each bar represents the mean of those 3 values (n=3 for determination of each value) ± SEM (*$p < 0.05$).

4.16 IDO in Human Tumour Cells Mediates Resistance to Combined Treatment of Pemetrexed and Methoxyamine

A phase I clinical trial of combined methoxyamine and pemetrexed has been completed and phase II clinical trials of that drug combination in multiple indications including NSCLC are planned [179]. In view of our observation of IDO-mediated resistance to both pemetrexed and methoxyamine, it was hypothesized that IDO could induce resistance to combined methoxyamine and pemetrexed treatment. To test this hypothesis, IDO was induced in A549 clonal cell populations and then those populations were treated with a combination of pemetrexed (30 nM) and methoxyamine (3 mM) as described in chapter 3, section 3.17. IDO downregulation sensitized cancer cells to combined treatment (Figures 4.47 and 4.48). Moreover, IFNγ-induced IDO mediated resistance to the combined pemetrexed and methoxyamine treatment and resistance was reduced in the presence of anti-IDO shRNA (Figure 4.49). It should be noted that, although it is stably transfected with anti-IDO shRNA, clone 2-4 has a higher level of IDO than other clonal A549 populations containing anti-IDO shRNA (clones 2-6 and 2-18)(Figure 4. 12). Clone 2-4 was more resistant to combined pemetrexed and methoxyamine treatment than clones 2-6 and 2-18, consistent with the existence of a relationship between the amount of IDO in tumour cells and their resistance to combined treatment with these two drugs (Figure 4.47, Panel C, R^2=0.70).

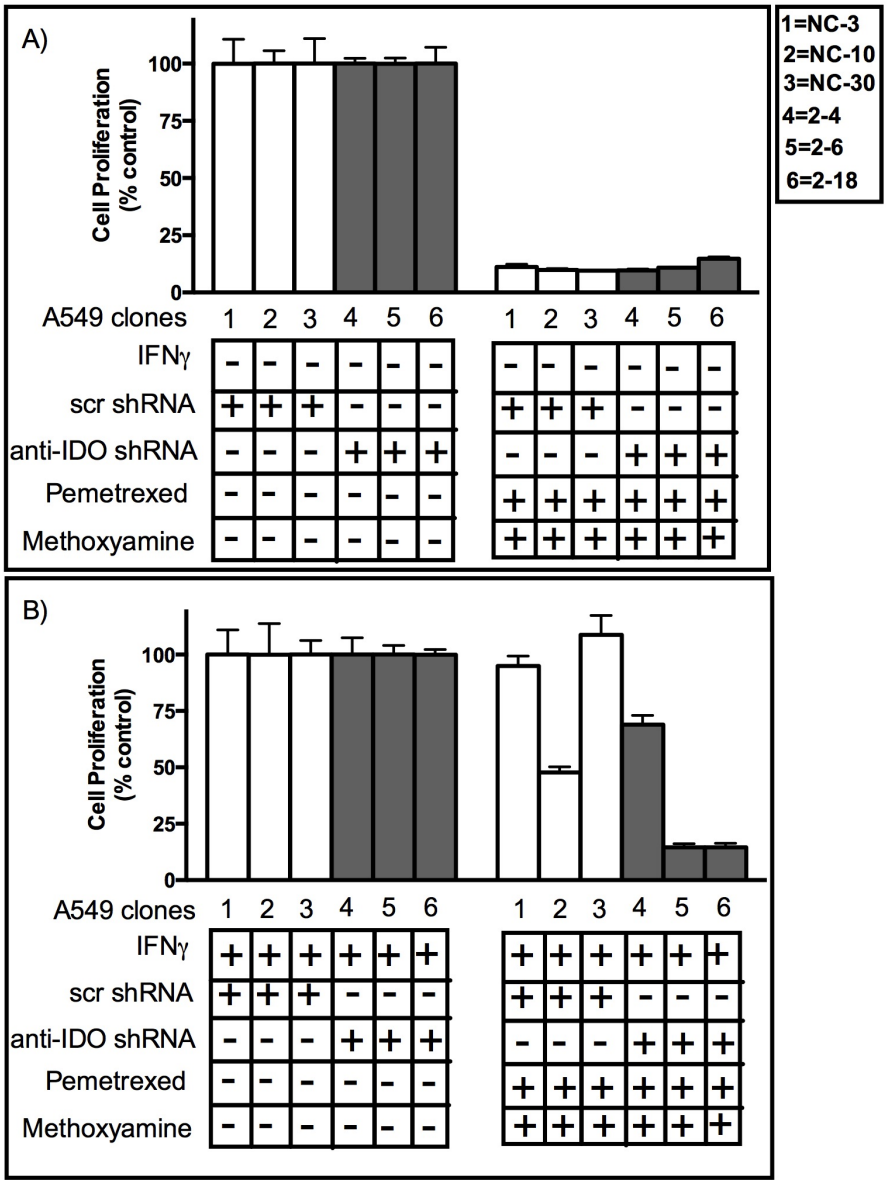
A)
Cell Proliferation (% control)
100
75
50
25
0
A549 clones 1 2 3 4 5 6 1 2 3 4 5 6
IFNγ
scr shRNA
anti-IDO shRNA
Pemetrexed
Methoxyamine
1=NC-3
2=NC-10
3=NC-30
4=2-4
5=2-6
6=2-18
B)
Cell Proliferation (% control)
100
75
50
25
0
A549 clones 1 2 3 4 5 6 1 2 3 4 5 6
IFNγ
scr shRNA
anti-IDO shRNA
Pemetrexed
Methoxyamine

C)

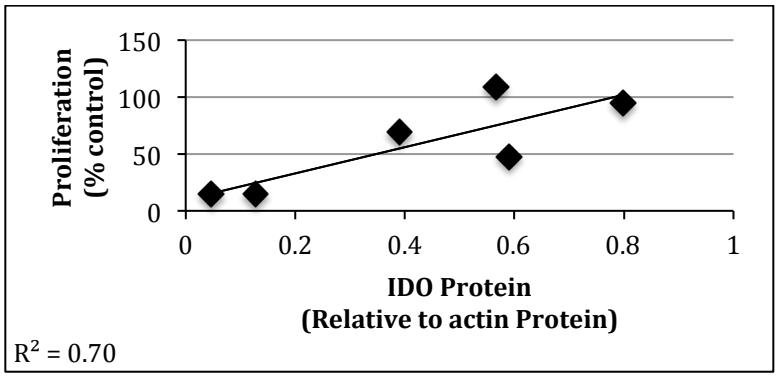
Proliferation (% control)
150
100
50
0
0
0.2
0.4
0.6
0.8
1
IDO Protein
(Relative to actin Protein)
R² = 0.70

Figure 4. 47. A549 clone sensitivity to combined pemetrexed (30 nM) and methoxyamine (3 mM) treatment before and after IDO induction. Panels A-B present data for each of 6 individual clonal populations before and after IDO induction. A549 clonal populations were cultured with or without IFNγ (25 ng/ml) for 48 h. Cultured medium was then replaced with fresh growth medium containing pemetrexed (30 nM) and methoxyamine. Tumour cells were then allowed to proliferate for 72 h. Finally, cells were trypsinized and live cells were enumerated using a Coulter counter. White bars represent A549 clones transfected with scrambled shRNA and gray bars represent A549 cells transfected with anti-IDO shRNA. Each bar represents the mean of 3 values (*n*=3 for determination of each value) ± SD. Significant changes are shown in pooled results (Figure 4.48). **Panel C**: relationship between IDO protein (relative to actin) and clonal population resistance to combined pemetrexed and methoxyamine (MX) treatment proliferation relative to untreated control cells). The R^2 value of 0.7 represents a moderate positive relationship.

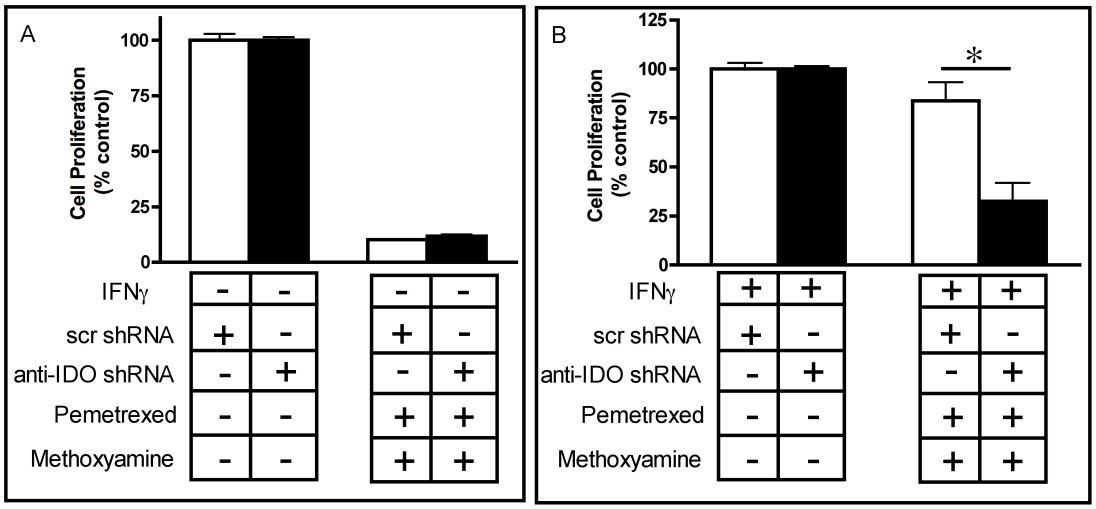
A
Cell Proliferation (% control)
100
75
50
25
0
IFNγ
scr shRNA
anti-IDO shRNA
Pemetrexed
Methoxyamine
B
Cell Proliferation (% control)
125
100
75
50
25
0
*
IFNγ
scr shRNA
anti-IDO shRNA
Pemetrexed
Methoxyamine

Figure 4. 48. Sensitivity of clonal A549 populations to combined pemetrexed (30 nM) and methoxyamine (3 mM) treatment before (A) and after (B) IDO induction. Data shown in Figure 4.47 were pooled to generate mean values from 3 independent clonal populations harbouring scrambled control shRNA or anti-IDO shRNA, and each bar represents the mean of those 3 values (n=3 for determination of each value) ± SEM (*P< 0.05).

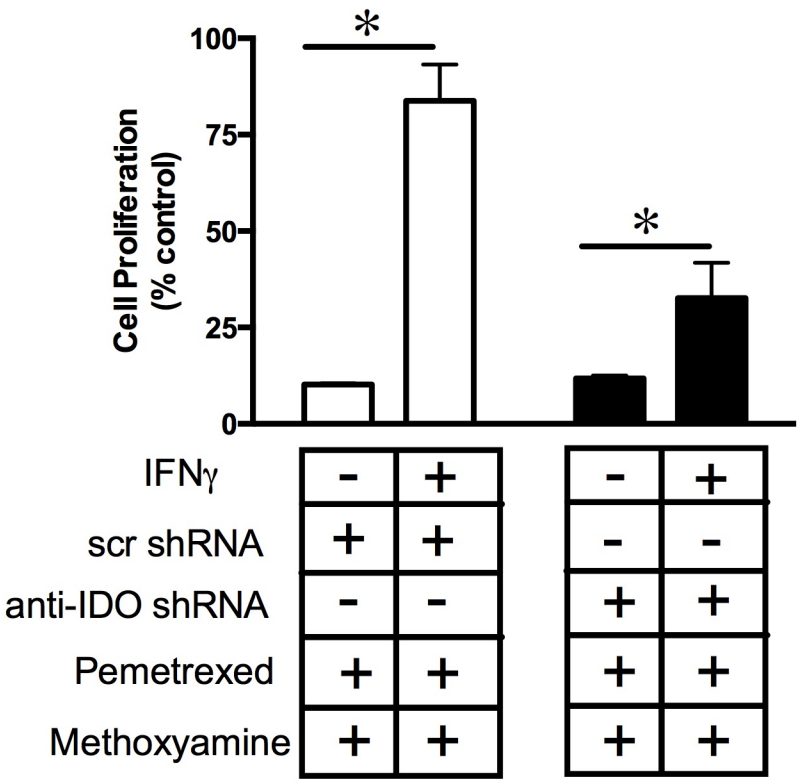
Cell Proliferation (% control)
100
75
50
25
0
*
*
IFNγ
scr shRNA
anti-IDO shRNA
Pemetrexed
Methoxyamine
- + - +
+ + - -
- - + +
+ + + +
+ + + +

Figure 4. 49. Induction of IDO in A549 clonal cell induces resistance to combined pemetrexed (30 nM) and methoxyamine (3 mM) treatment. Results were obtained from 3 independent clonal cell populations with scrambled control shRNA or anti-IDO shRNA, and each bar represents the mean of those 3 values (n=3 for determination of each value) ± SEM (*p<0.05).

4.17 The Effect of IDO Downregulation in Human Tumour Cells Sensitivity to other TS-targeting Drugs (5FUdR and Gemcitabine)

Because IDO downregulation sensitized cancer cells to the TS-targeting drug pemetrexed (Figure 4.44 and 4.45), we hypothesized that IDO downregulation could sensitize cancer cells to other TS-targeting drugs commonly used in clinic, including 5FUdR and gemcitabine. Cancer cells were treated with IFNγ (25 ng/ml) for 48 h and then 5FUdR or gemcitabine as described in chapter 3, section 3.14. IDO downregulation did not sensitize cancer cells to 5FUdR (Figures 4.50 and 4.51), but did increase sensitivity to gemcitabine (Figure 4.52 and 4.53). I should note that 5FUdR treatment equally reduced proliferation in both scrambled control shRNA and anti-IDO shRNA harbouring clonal populations before and after IFNγ treatment (Figures 4.50 and 4.51).

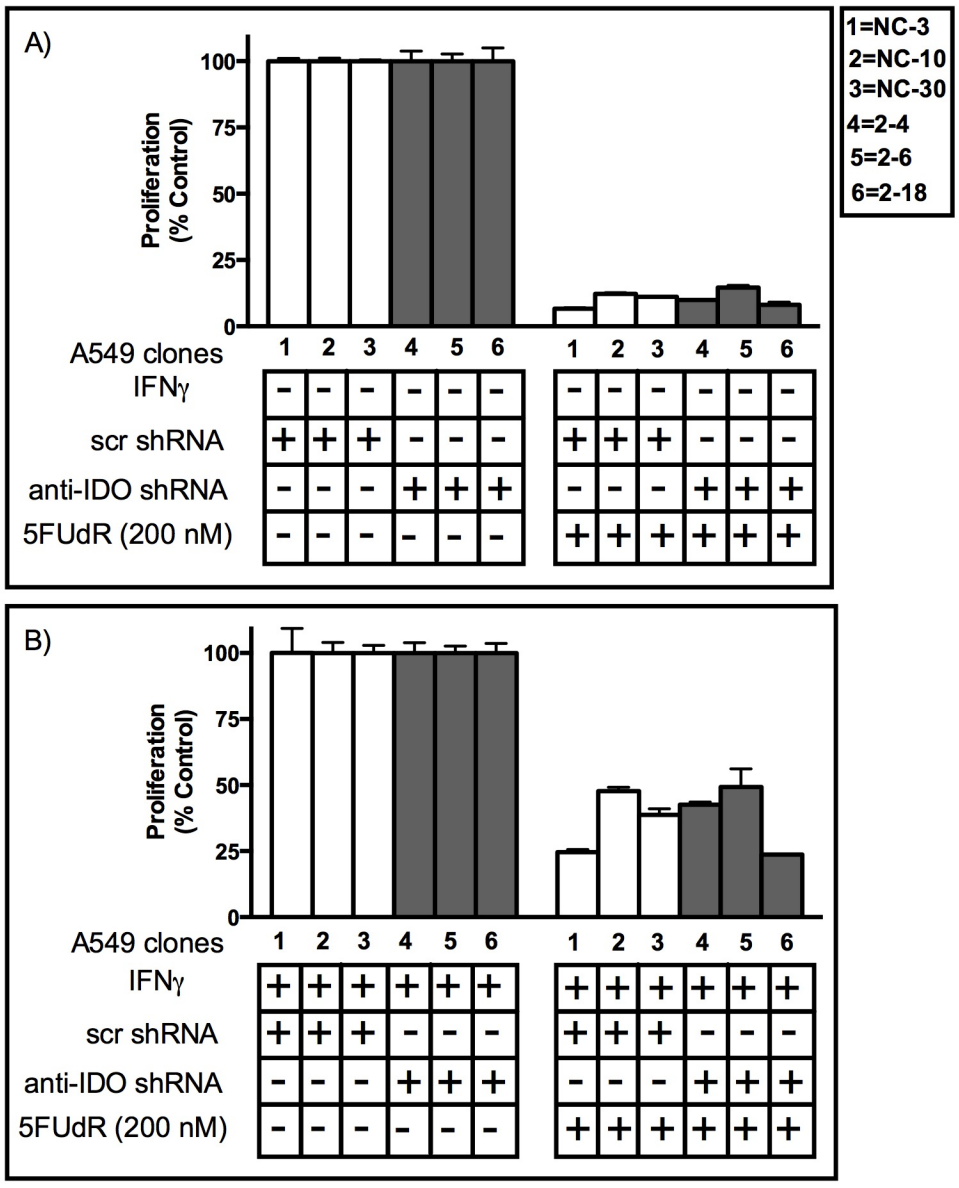
A)
Proliferation (% Control)
100
75
50
25
0
1=NC-3
2=NC-10
3=NC-30
4=2-4
5=2-6
6=2-18
A549 clones
1 2 3 4 5 6 1 2 3 4 5 6
IFNγ
scr shRNA
anti-IDO shRNA
5FUdR (200 nM)
B)
Proliferation (% Control)
100
75
50
25
0
A549 clones
1 2 3 4 5 6 1 2 3 4 5 6
IFNγ
scr shRNA
anti-IDO shRNA
5FUdR (200 nM)

Figure 4. 50. A549 clone sensitivity to 5FUdR (200 nM) before and after IDO induction. Panels A-B present data for each of 6 individual clonal populations before and after IDO induction. A549 clonal populations were cultured with or without IFNγ (25 ng/ml) for 48 h and then 5FUdR (200 nM) for 72 h at which time live cells were enumerated by Coulter counting. White bars represent A549 clones transfected with scrambled shRNA and gray bars represent A549 cells transfected with anti-IDO shRNA. Each bar represents the mean of 3 values (*n*=3 for determination of each value) ± SD. Significant changes are shown in pooled results (Figure 4.51).

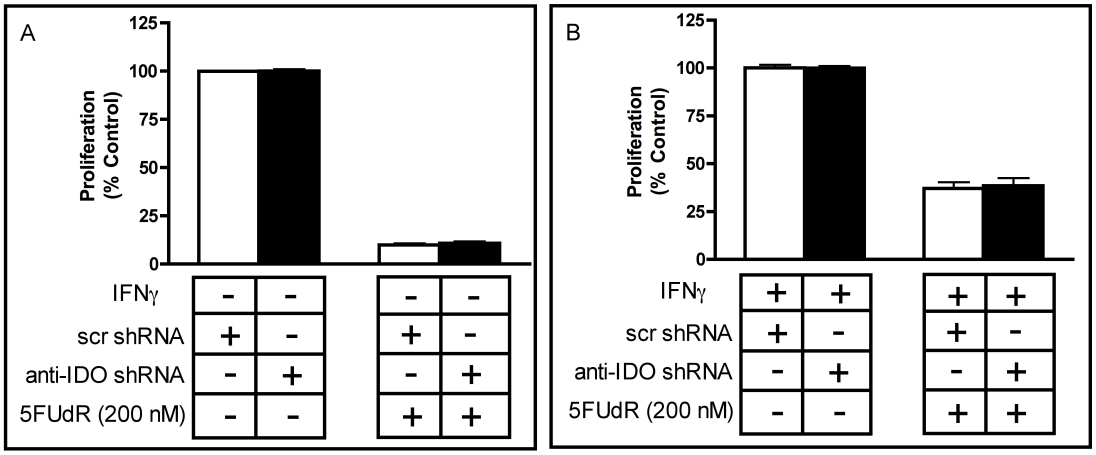
A
Proliferation (% Control)
125
100
75
50
25
0
IFNγ
scr shRNA
anti-IDO shRNA
5FUdR (200 nM)
B
Proliferation (% Control)
125
100
75
50
25
0
IFNγ
scr shRNA
anti-IDO shRNA
5FUdR (200 nM)

Figure 4. 51. Sensitivity of clonal A549 populations to 5FUdR (200 nM) before (A) and after (B) IDO induction. Data shown in Figure 4.50 were pooled to generate mean values from 3 independent clonal populations harbouring scrambled control shRNA or anti-IDO shRNA, and each bar represents the mean of the 3 values (n=3 for determination of each value) ± SEM (*$P < 0.05$).

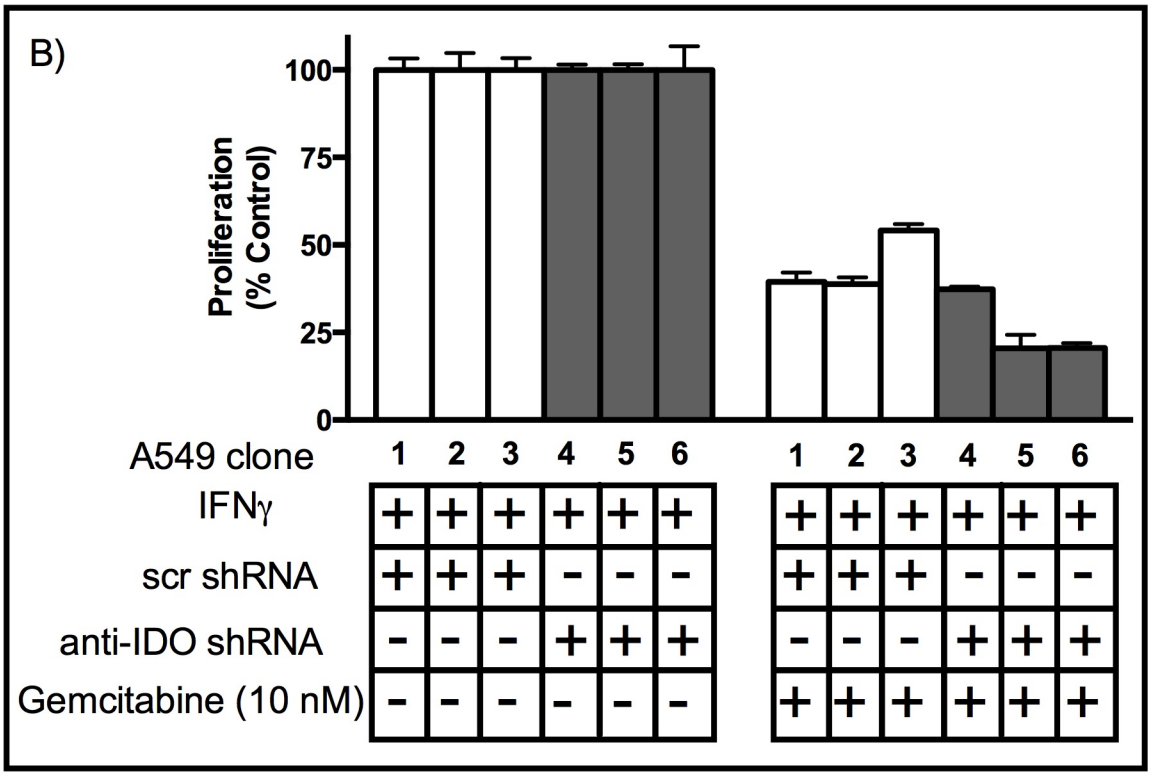
B)
Proliferation (% Control)
100
75
50
25
0
A549 clone
1 2 3 4 5 6
1 2 3 4 5 6
IFNγ
scr shRNA
anti-IDO shRNA
Gemcitabine (10 nM)

Figure 4. 52**. A549 clone sensitivity to gemcitabine (10 nM) before and after IDO induction. Panels A-B** present data for each of 6 individual clonal populations before and after IDO induction. A549 clonal populations were cultured with or without IFNγ (25 ng/ml) for 48 h, then treated with gemcitabine (10 nM) for 72 h, at which time live cells were enumerated by Coulter counting. White bars represent A549 clones transfected with scrambled shRNA and gray bars represent A549 cells transfected with anti-IDO shRNA. Each bar represents the mean of 3 values (*n*=3 for determination of each value) ± SD. Significant changes are shown in pooled results (Figure 4.53).

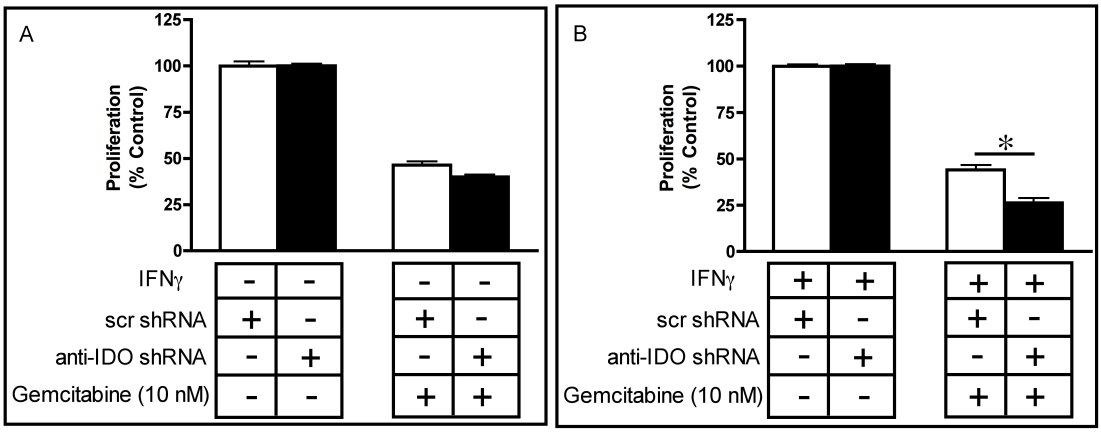
A
Proliferation (% Control)
125
100
75
50
25
0
IFNγ
scr shRNA
anti-IDO shRNA
Gemcitabine (10 nM)
B
Proliferation (% Control)
125
100
75
50
25
0
*
IFNγ
scr shRNA
anti-IDO shRNA
Gemcitabine (10 nM)

Figure 4. 53. Sensitivity of clonal A549 populations to gemcitabine (10 nM) before (A) and after (B) IDO induction. Data shown in Figure 4.52 were pooled to generate mean values from 3 independent clonal populations harbouring scrambled control shRNA or anti-IDO shRNA, and each bar represents the mean of those 3 values (n=3 for determination of each value) ± SEM (*$P < 0.05$).

4.18 The Effect of IDO Downregulation in Human Tumour Cells' Sensitivity to Cisplatin

Since IDO downregulation sensitized cancer cells to γ radiation, it was also determined whether IDO knockdown sensitized A549, HeLa and H441 cells to the DNA cross-linking agent cisplatin. We induced IDO in A549 and HeLa cells by treatment with IFNγ and then exposed cells to cisplatin for 72 h to determine the effect on proliferation. We treated H441 cells with cisplatin as described (Chapter 3, Section 3.14). IDO downregulation sensitized both A549 and HeLa cells to cisplatin treatment by 18% compared to cells without IDO reduction ($p<0.05$)(Figures 4.54, 4.55, 4.57, and 4.58). IFNγ-induced IDO mediated cancer cell resistance to cisplatin. In addition, the effect of IFNγ-induced IDO was reduced by anti-IDO shRNA in A549 and HeLa cells by 25% and 18% ($p<0.05$), respectively (Figure 4.56 and Figure 4.59). IDO downregulation also sensitized natural IDO expressers (H441 cells) to cisplatin in the absence of IFNγ treatment (Figure 4.60).

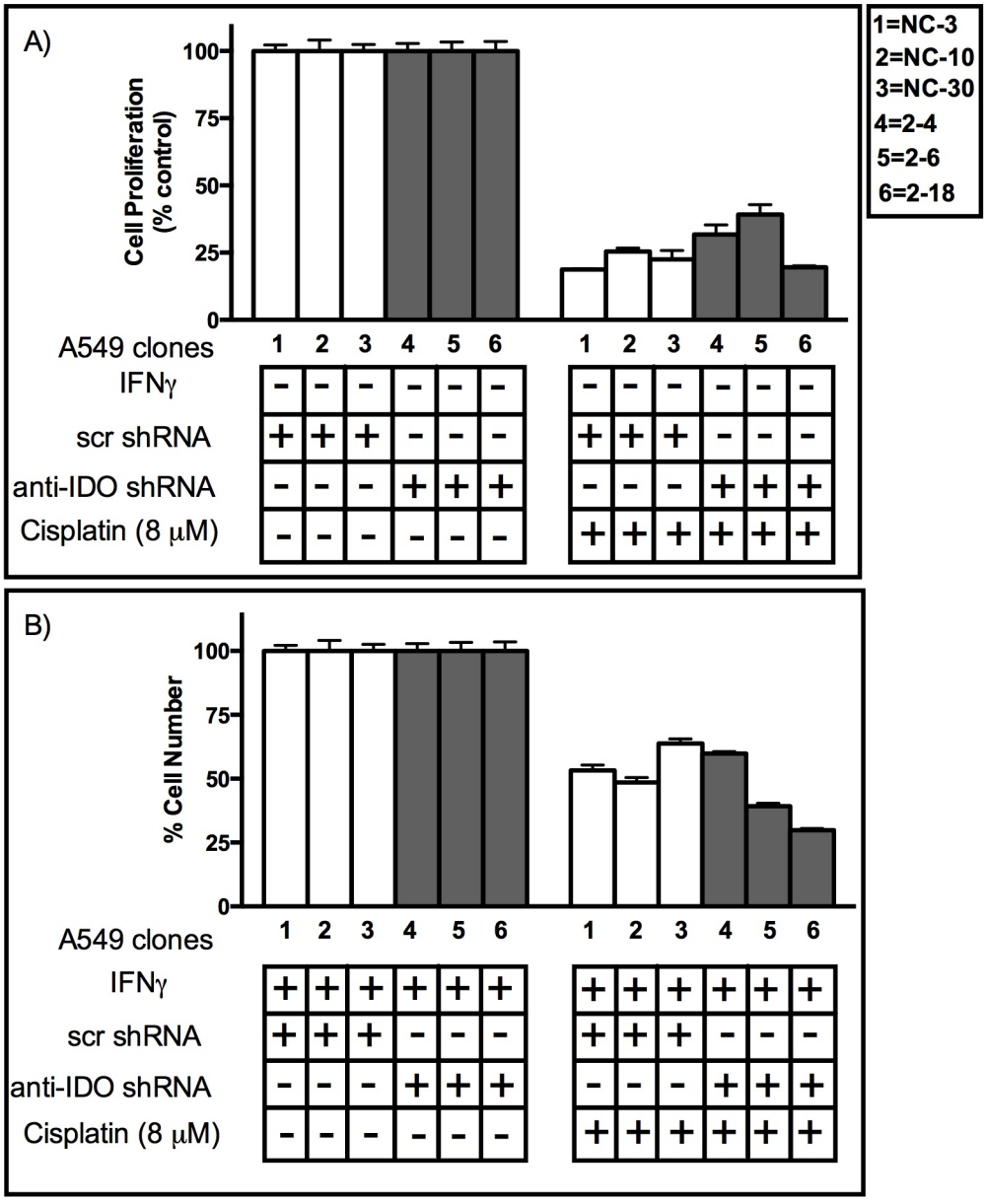
A)
Cell Proliferation (% control)
100
75
50
25
0
1=NC-3
2=NC-10
3=NC-30
4=2-4
5=2-6
6=2-18
A549 clones
1 2 3 4 5 6 1 2 3 4 5 6
IFNγ
scr shRNA
anti-IDO shRNA
Cisplatin (8 μM)
B)
% Cell Number
100
75
50
25
0
A549 clones
1 2 3 4 5 6 1 2 3 4 5 6
IFNγ
scr shRNA
anti-IDO shRNA
Cisplatin (8 μM)

Figure 4. 54. A549 clone sensitivity to cisplatin (8 μM) before and after IDO induction. Panels A-B present data for each of 6 individual clonal populations before and after IDO induction. A549 clonal populations were cultured with or without IFNγ (25 ng/ml) for 48 h, then cisplatin (8 μM) for 72 h, at which time live cells were enumerated. White bars represent A549 clones transfected with scrambled shRNA and gray bars represent A549 cells transfected with anti-IDO shRNA. Each bar represents the mean of 3 values (*n*=3 for determination of each value) ± SD. Significant changes are shown in pooled results (Figure 4.55).

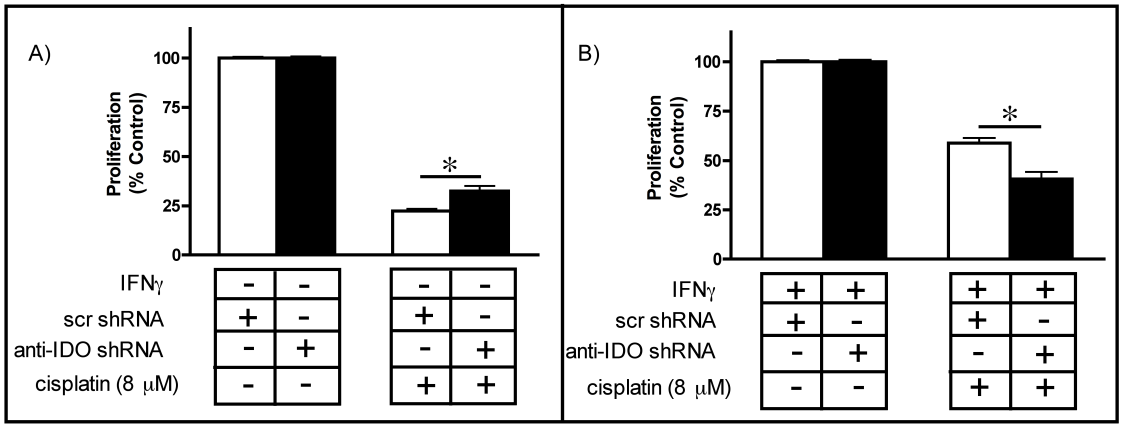
A)
Proliferation (% Control)
100
75
50
25
0
*
IFNγ
scr shRNA
anti-IDO shRNA
cisplatin (8 μM)
B)
Proliferation (% Control)
100
75
50
25
0
*
IFNγ
scr shRNA
anti-IDO shRNA
cisplatin (8 μM)

Figure 4. 55. Sensitivity of clonal A549 populations to cisplatin (8 μM) before (A) and after (B) IDO induction. Data shown in Figure 4.54 were pooled to generate mean values from 3 independent clonal populations harbouring scrambled control shRNA or anti-IDO shRNA, and each bar represents the mean of those 3 values (*n*=3 for determination of each value) ± SEM (**P* < 0.05).

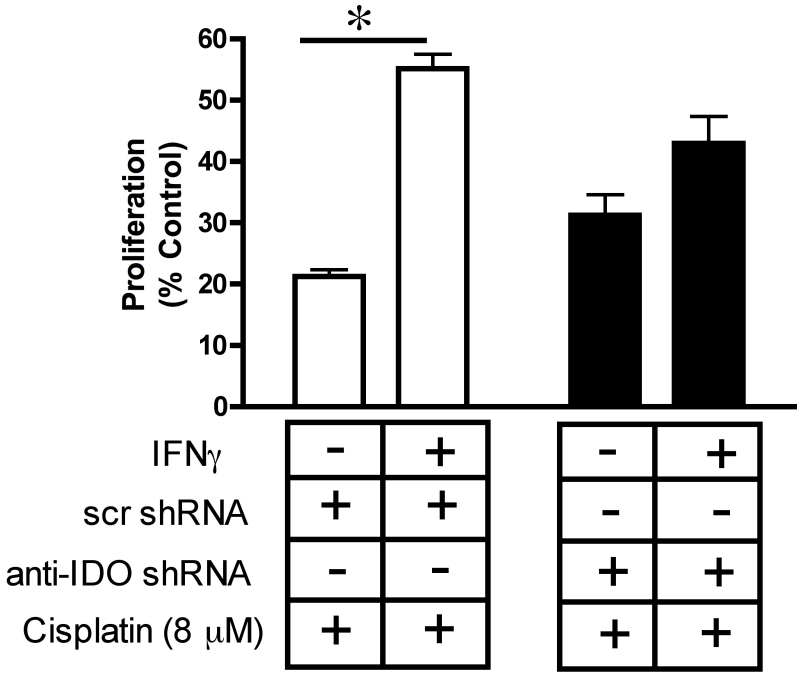
*
60
50
40
30
20
10
0
Proliferation (% Control)
IFNγ
scr shRNA
anti-IDO shRNA
Cisplatin (8 μM)
- + - +
+ + - -
- - + +
+ + + +

Figure 4. 56. Induction of IDO in A549 clonal cell induces resistance to cisplatin (8 μM). Results were obtained from 3 independent clonal cell populations with scrambled control shRNA or anti-IDO shRNA, and each bar represents the mean of those 3 values (n=3 for determination of each value) ± SEM (*p<0.05).

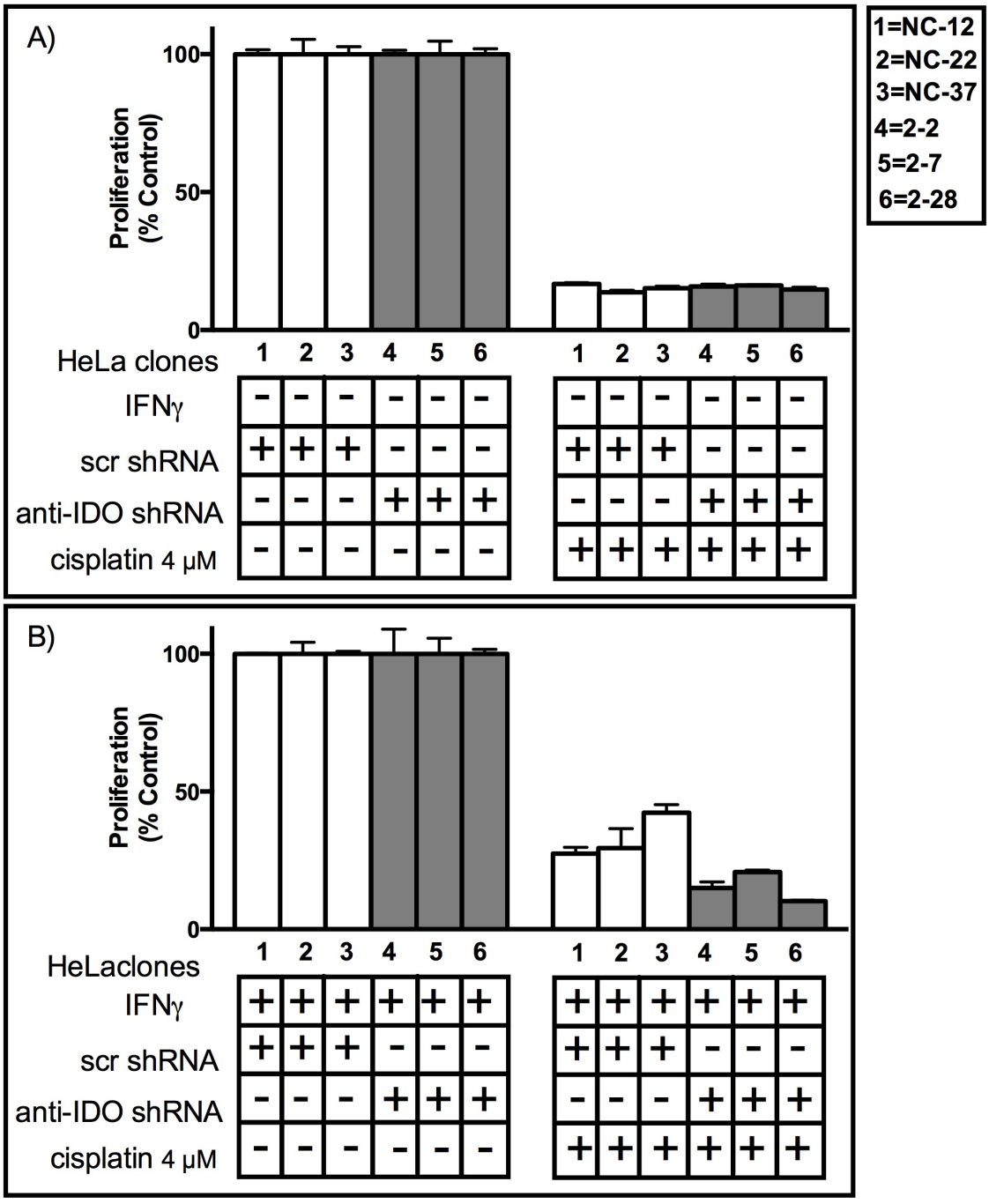
A)
Proliferation (% Control)
100
50
0
1=NC-12
2=NC-22
3=NC-37
4=2-2
5=2-7
6=2-28
HeLa clones
1 2 3 4 5 6
1 2 3 4 5 6
IFNγ
scr shRNA
anti-IDO shRNA
cisplatin 4 μM
B)
Proliferation (% Control)
100
50
0
HeLaclones
1 2 3 4 5 6
1 2 3 4 5 6
IFNγ
scr shRNA
anti-IDO shRNA
cisplatin 4 μM

Figure 4. 57. HeLa clone sensitivity to cisplatin (4 μM) before and after IDO induction. Panels A-B present data for each of 6 individual clonal populations before and after IDO induction. HeLa clonal populations were cultured with or without IFNγ (25 ng/ml) for 48 h, then treated with cisplatin (8 μM) for 72 h, at which time live cells were enumerated. White bars represent HeLa clones transfected with scrambled shRNA and gray bars represent HeLa cells transfected with anti-IDO shRNA. Each bar represents the mean of 3 values (*n*=3 for determination of each value) ± SD. Significant changes are shown in pooled results (Figure 4.58).

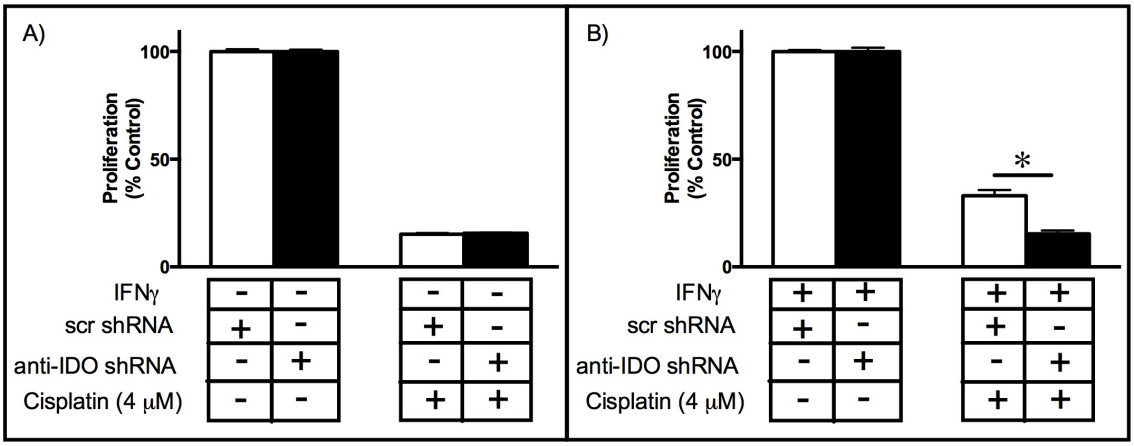
A)
Proliferation (% Control)
100
50
0
IFNγ
scr shRNA
anti-IDO shRNA
Cisplatin (4 μM)
B)
Proliferation (% Control)
100
50
0
*
IFNγ
scr shRNA
anti-IDO shRNA
Cisplatin (4 μM)

Figure 4. 58. Sensitivity of clonal HeLa populations to cisplatin (4 μM) before (A) and after (B) IDO induction. Data shown in Figure 4.57 were pooled to generate mean values from 3 independent clonal populations harbouring scrambled control shRNA or anti-IDO shRNA, and each bar represents the mean of those 3 values (n=3 for determination of each value) ± SEM (*$P < 0.05$).

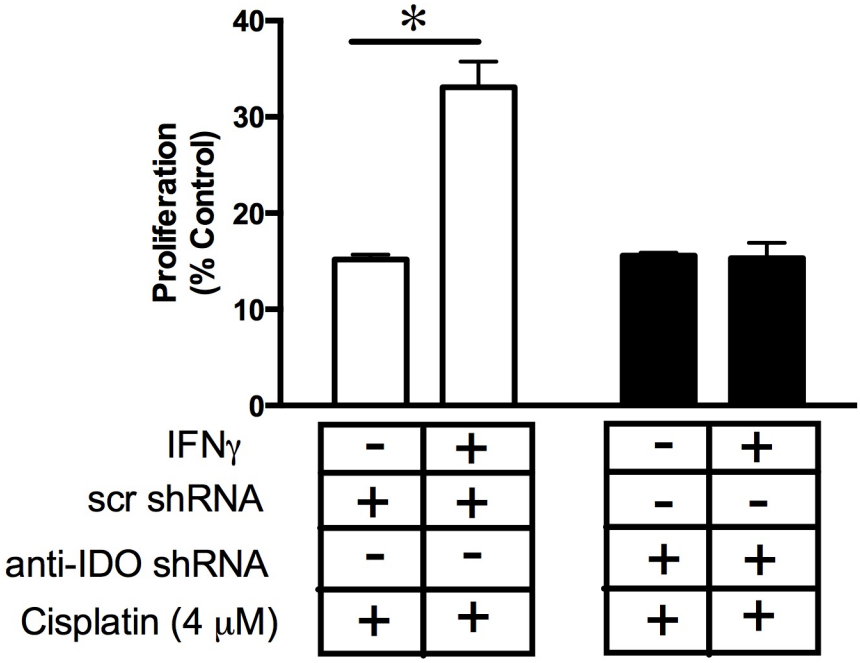
*
40
30
20
10
0
Proliferation (% Control)
IFNγ
scr shRNA
anti-IDO shRNA
Cisplatin (4 μM)
- + - +
+ + - -
- - + +
+ + + +

Figure 4. 59. Induction of IDO in HeLa clonal cell induces resistance to cisplatin (4 μM). Results were obtained from 3 independent clonal cell populations with scrambled control shRNA or anti-IDO shRNA, and each bar represents the mean of those 3 values (n=3 for determination of each value) ± SEM (*$p < 0.05$).

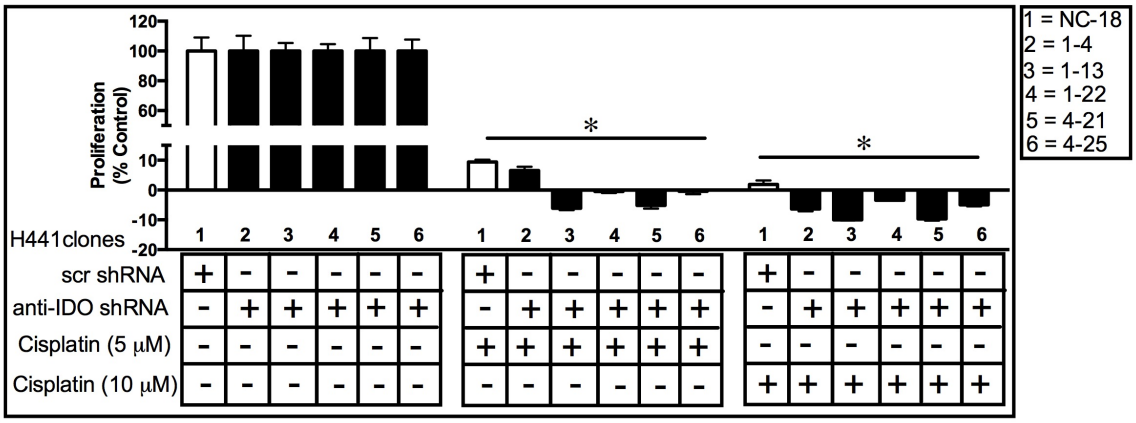
Proliferation (% Control)
120
100
80
60
10
0
-10
-20
*
*
H441clones
1 2 3 4 5 6 1 2 3 4 5 6 1 2 3 4 5 6
scr shRNA
anti-IDO shRNA
Cisplatin (5 μM)
Cisplatin (10 μM)
1 = NC-18
2 = 1-4
3 = 1-13
4 = 1-22
5 = 4-21
6 = 4-25

Figure 4. 60. H441 clone sensitivity to cisplatin (5 and 10 μM). Data represents one H441 clone with scrambled shRNA (**white bar**) and 5 H441 clones cells with anti-IDO shRNA (**black bars**). H441 clonal populations were cultured overnight, then treated with cisplatin (5 and 10 μM) for 8 days, at which time live cells were enumerated. Each bar represents the mean of 3 values (n=3 for determination of each value) ± SD (*P<0.05). Each bar represents the mean of 3 values (n=3 for determination of each value) ± SD.

4.19 Thymidylate Synthase siRNA Downregulation in A549 Clonal Populations

TS-targeting drugs have anti-tumour activity against multiple types of cancers. However, increased TS mRNA levels upon treatment with TS-targeting drugs is a common mechanism of resistance to these agents [254] and knockdown of TS mRNA using anti-TS siRNA or antisense oligonucleotides sensitizes tumour cells to TS-targeting drugs [187, 254, 255, 265]. In view of the observation that IDO can at least partially mediate resistance to some TS-targeting drugs, it was hypothesized that concurrent downregulation of IDO and TS in cancer cells will sensitize cancer cells to these drugs to a greater degree than knockdown of TS alone. To test the hypothesis, A549 tumour cells were transfected with TS siRNA to confirm TS mRNA downregulation using this strategy, as described (Chapter 3, Section 3.20). TS mRNA was downregulated in A549 cells upon TS siRNA transfection (Figure 4.61).

4.20 Thymidylate Synthase siRNA Downregulation in A549 Clonal Populations after IFNγ Induction

Since we ultimately wished to simultaneously downregulate TS and IDO in A549 cells, it was necessary to determine whether siRNA transfection of A549 clones affected IFNγ induction of IDO and/or whether IFNγ treatment altered siRNA-mediated knockdown of TS. To test this, A549 cells were transiently transfected with either control siRNA or TS siRNA and then treated with IFNγ as described in chapter 3, section 3.20. IFNγ treatment did not interfere with siRNA transfection, and siRNA transfection did not alter IFNγ induction of IDO induction in A549 cells (Figure 4.62).

A)

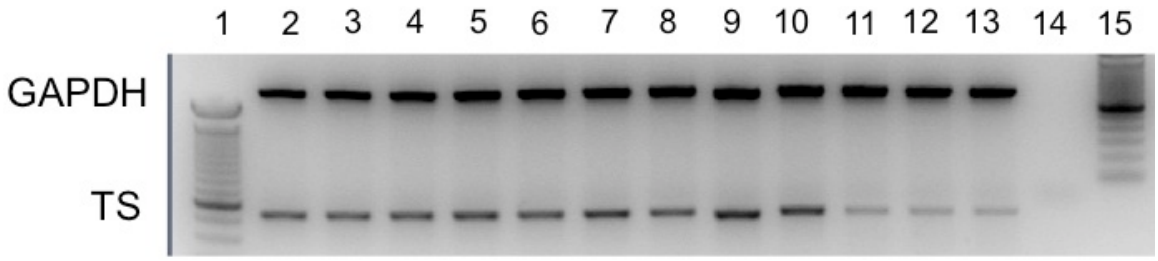
1 2 3 4 5 6 7 8 9 10 11 12 13 14 15
GAPDH
TS

B)

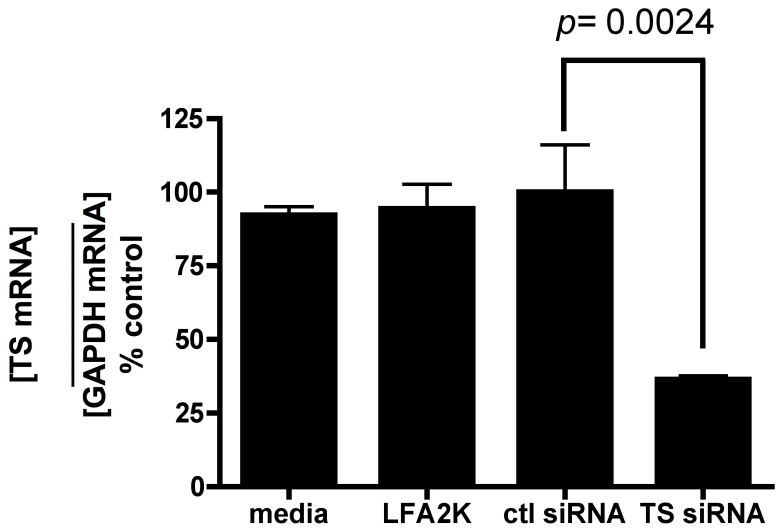
p= 0.0024
[TS mRNA]
[GAPDH mRNA]
% control
125
100
75
50
25
0
media
LFA2K
ctl siRNA
TS siRNA

Figure 4. 61. TS siRNA transfection of A549 cells. A549 cells (untransfected with anti-IDO shRNA plasmid) were transfected with control or TS siRNA. After 24 h, RNA was isolated and used to generate cDNA. TS and GAPDH cDNA were amplified by PCR from the cDNA. **A:** PCR products were separated by electrophoresis through a 1.5% agarose gel. **B:** PCR-generated bands were quantified using Alpha Ease FC software. **Lanes 1 and 15:** MW ladder. **Lanes 2-4:** control cells treated with medium alone. **Lanes 5-7:** cells treated with liposomal transfection reagent (LFA2K). **Lanes 8-10:** cells transfected with control siRNA (all groups were normalized to this group). **Lanes 11-13:** cells transfected with TS siRNA. **Lane 14:** PCR products from reaction without template cDNA. Each bar represents the mean of 3 values (n=3 for determination of each value) ± SEM.

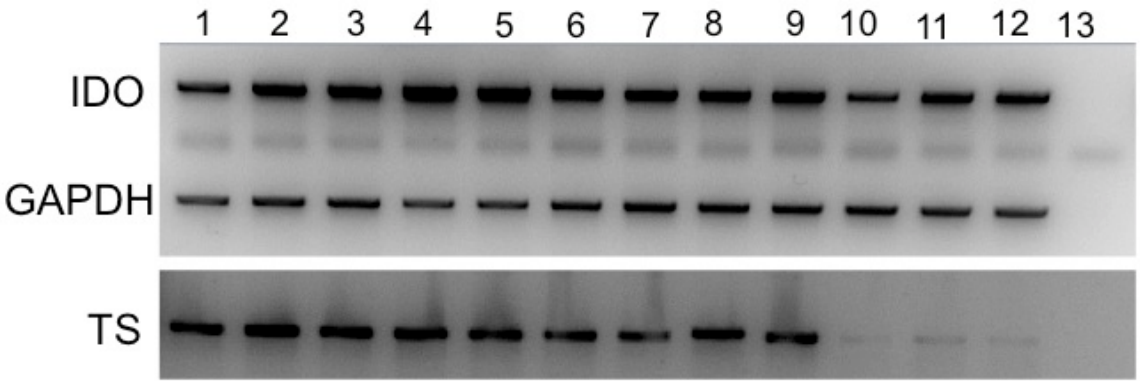
1 2 3 4 5 6 7 8 9 10 11 12 13
IDO
GAPDH
TS

Figure 4. 62. TS siRNA downregulation in A549 cells after IFNγ (16 ng/ml) treatment. A549 cells were treated with IFNγ (16 ng/ml) and then transfected with either control or TS siRNA for 4 h. Cultured medium was then replaced with growth medium containing IFNγ (16 ng/ml). RNA was isolated 24 h post transfection and used to synthesize cDNA. IDO, TS and GAPDH cDNAs were amplified by PCR. **Lanes 1-3:** cells treated with medium alone (control). **Lanes 4-6:** cells treated with liposomal transfection reagent (LFA2K). **Lanes 7-9:** cells transfected with control siRNA. **Lanes 10-12:** cells transfected with TS siRNA. **Lane 13:** PCR products from reaction without template cDNA.

4.21 TS siRNA Downregulation in A549 Clonal Populations

TS siRNA downregulation in A549 clonal populations was assessed after transfection of two different TS siRNAs targeting different regions of TS mRNA (TS siRNA # 3 and TS siRNA #4). All A549 clonal populations were transfected as described (Chapter 3, Section 3.20). TS siRNA downregulated TS protein in A549 clonal populations harbouring either control, non-targeting shRNA or anti-IDO shRNA at 96 h post-transfection (Figure 4.63).

4.22 TS Downregulation Enhances the Capacity of IDO Downregulation to Sensitize A549 Cells to Pemetrexed

TS mRNA downregulation sensitizes A549 cells to the TS-targeting drug 5FUdR [266]. IDO downregulation sensitized A549 cells to the TS-targeting drugs pemetrexed and gemcitabine (Figures 4.44 and 4.52) but not 5FUdR (Figure 4.50). To test whether concurrent knockdown of both TS and IDO sensitized A549 cells to anti-TS drugs more effectively than knockdown of IDO alone, A549 clonal populations (stably transfected with anti-IDO shRNA or control shRNA) were transiently transfected with TS siRNAs numbers 3 or 4 as described (Chapter 3, Section 3.20). Concurrent IDO and TS downregulation sensitized cancer cells to pemetrexed more effectively than knockdown of IDO alone (Figure 4.64, A-C).

A)

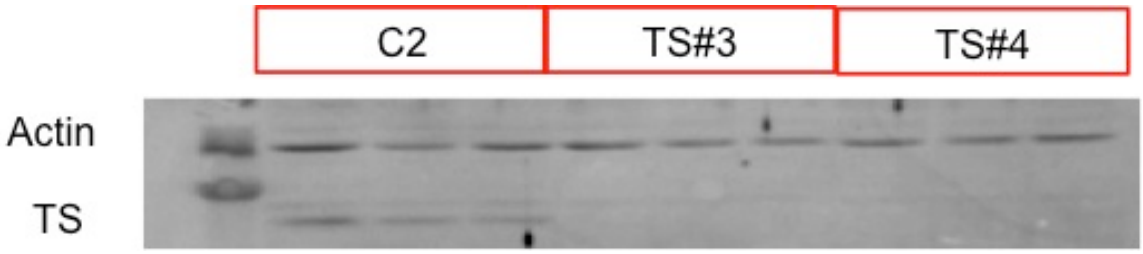
C2
TS#3
TS#4
Actin
TS

B)

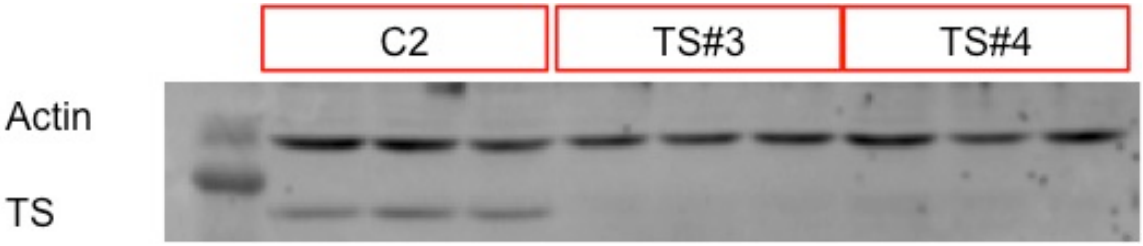
C2
TS#3
TS#4
Actin
TS

C)

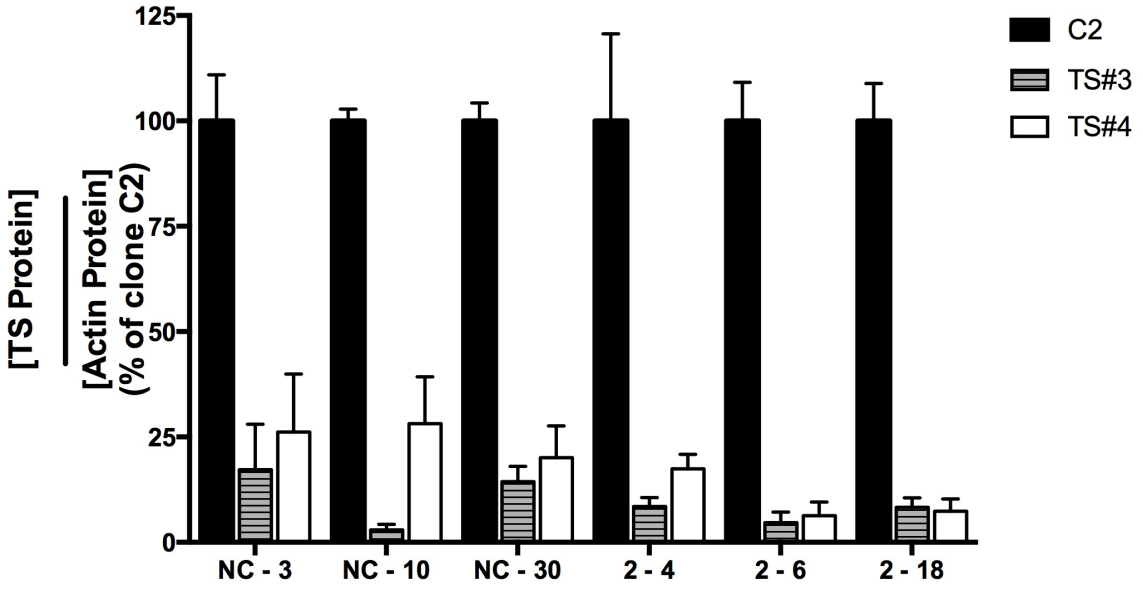
125
100
75
50
25
0
[TS Protein]
[Actin Protein]
(% of clone C2)
C2
TS#3
TS#4
NC - 3
NC - 10
NC - 30
2 - 4
2 - 6
2 - 18

Figure 4. 63. TS siRNA downregulation in A549 clonal populations. A549 clonal cells were seeded and grown overnight. TS siRNA number 3 or 4 or control siRNA was then used to transfect all clonal cells. Cells were lysed and protein was harvested 96 h later. TS protein levels were determined using antibodies against TS and actin. Results were quantified for each clone separately. **A)** TS siRNA transfection in A549 clone NC-3 (with control, non-targeting shRNA). (**B)** TS siRNA transfection of clone 2-4 (with anti-IDO shRNA). **C)** TS protein quantification results for all clonal populations. Each bar represents the mean of 3 values (*n*=3 for determination of each value) ± SEM.

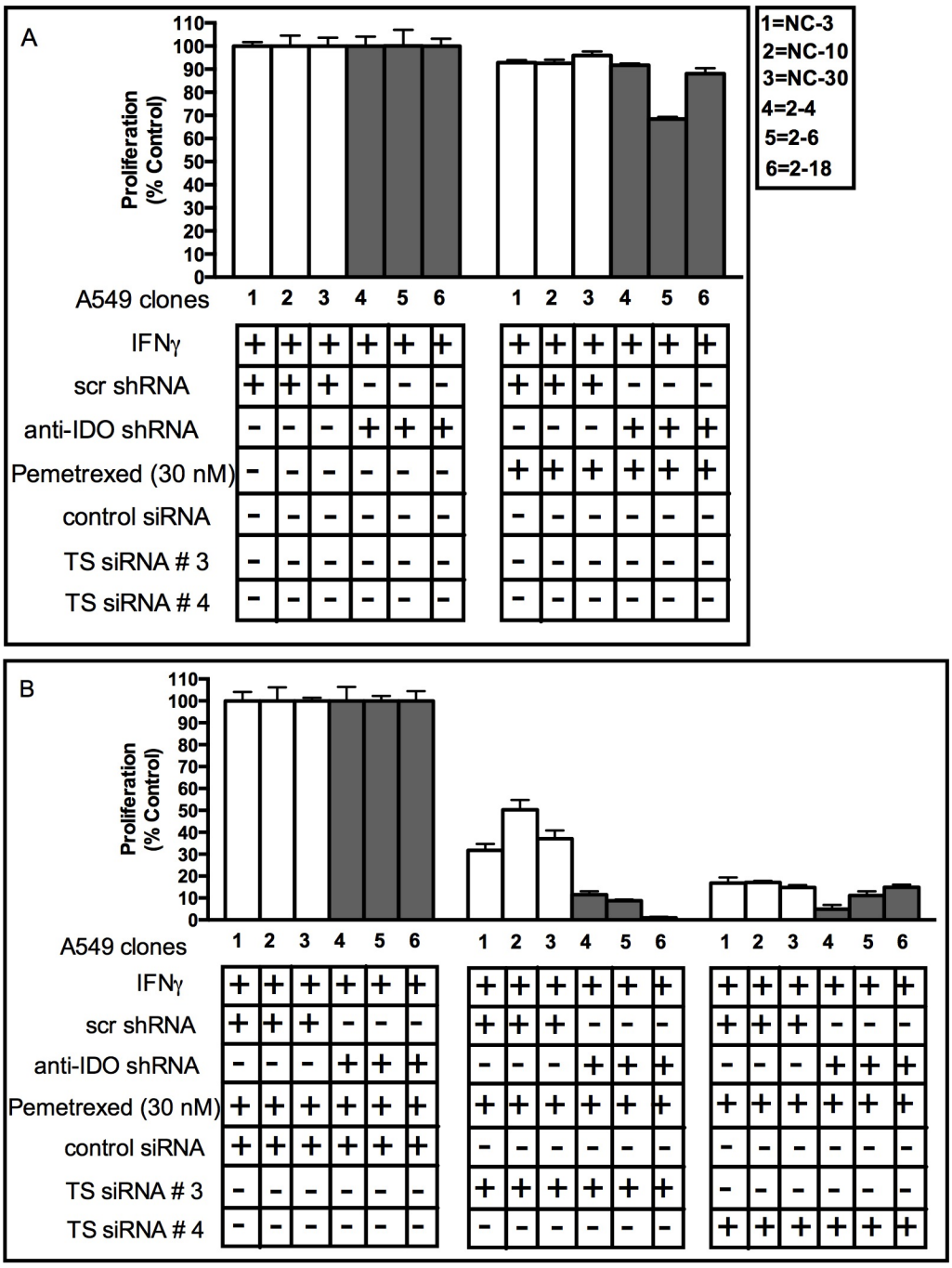
A
Proliferation (% Control)
110
100
90
80
70
60
50
40
30
20
10
0
1=NC-3
2=NC-10
3=NC-30
4=2-4
5=2-6
6=2-18
A549 clones
1 2 3 4 5 6 1 2 3 4 5 6
IFNγ
scr shRNA
anti-IDO shRNA
Pemetrexed (30 nM)
control siRNA
TS siRNA # 3
TS siRNA # 4
B
Proliferation (% Control)
A549 clones
1 2 3 4 5 6 1 2 3 4 5 6 1 2 3 4 5 6
IFNγ
scr shRNA
anti-IDO shRNA
Pemetrexed (30 nM)
control siRNA
TS siRNA # 3
TS siRNA # 4

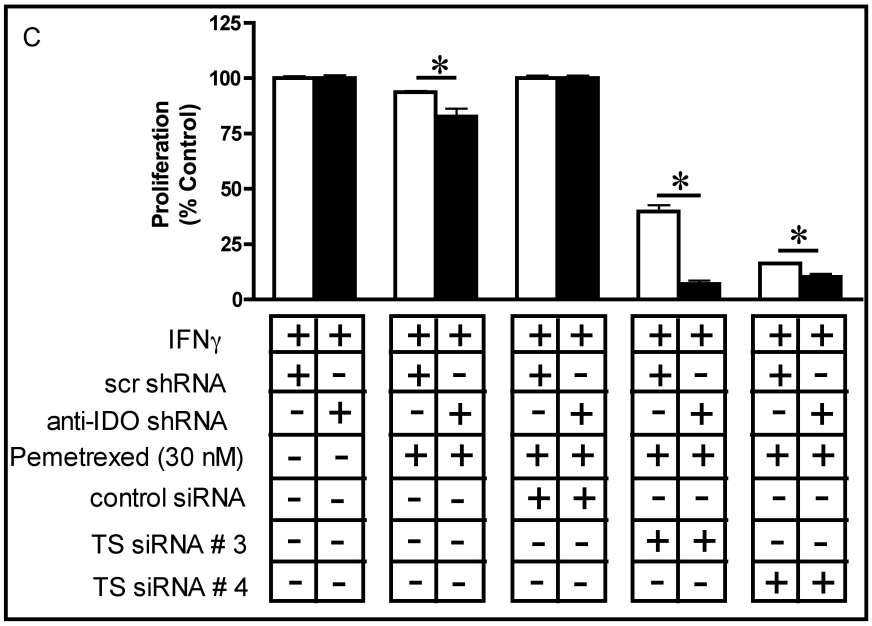
C
Proliferation (% Control)
125
100
75
50
25
0
*
*
*
IFNγ
scr shRNA
anti-IDO shRNA
Pemetrexed (30 nM)
control siRNA
TS siRNA # 3
TS siRNA # 4

Figure 4. 64. Concurrent IDO and TS downregulation sensitizes A549 cells to pemetrexed more effectively than knockdown of IDO alone. A549 cells were transfected with control or TS siRNA, then treated with IFNγ (25 ng/ml) for 48 h. Pemetrexed (30 nM) was then added and cell number enumerated after 72 h drug treatment. Bars indicate the mean relative number of cells (n=3 ± SD).

A) Proliferation of clonal A549 cell populations induced with IFNγ and then treated with pemetrexed, but untransfected with siRNA of any kind. **Gray bars** indicate clones containing anti-IDO shRNA and **white bars** indicate clones containing non-targeting control shRNA.

B) Proliferation of the same clonal A549 cell populations transfected with control non-targeting siRNA, TS siRNA #3, or TS siRNA #4, induced with IFNγ, and then treated with pemetrexed. The bars represent values normalized to values obtained from clones treated with IFNγ but untreated with pemetrexed or siRNA; those cells were each considered to have a proliferation value of 100% after IFNγ treatment. **Gray bars** indicate clones containing anti-IDO shRNA and white bars indicate clones containing non-targeting control shRNA.

C) Data for 3 individual A549 clones with anti-IDO shRNA and 3 clones with control, non-targeting shRNA (from panels A and B) were pooled and mean values (n=3) are show ± SEM (*p<0.05). **Black bars** indicate clones containing anti-IDO shRNA and **white bars** indicate clones containing non-targeting control shRNA.

4.23 IDO Downregulation Enhances the Capacity of TS Downregulation to Sensitize A549 Cells to 5FUdR

Combined antisense downregulation of IDO and TS sensitized A549 cells to the TS-targeting drug pemetrexed to a greater degree than antisense downregulation of TS alone (Figure 4.64). In addition, IDO downregulation alone did not alter A549 cell sensitivity to 5FUdR (Figure 4.50). Therefore, the capacity of combined, concurrent downregulation of both IDO and TS downregulation to sensitize human tumour cells to 5FUdR to a greater degree than TS downregulation alone was assessed. Concurrent IDO and TS downregulation using TS siRNAs numbers 3 or 4, combined with shRNA-mediated reduction of IDO in response to induction with IFNγ, sensitized cancer cells to 5FUdR to a greater degree than TS downregulation alone (30% for TS siRNA number 3 and 15% for TS siRNA number 4 (Figure 4.65, A-C).

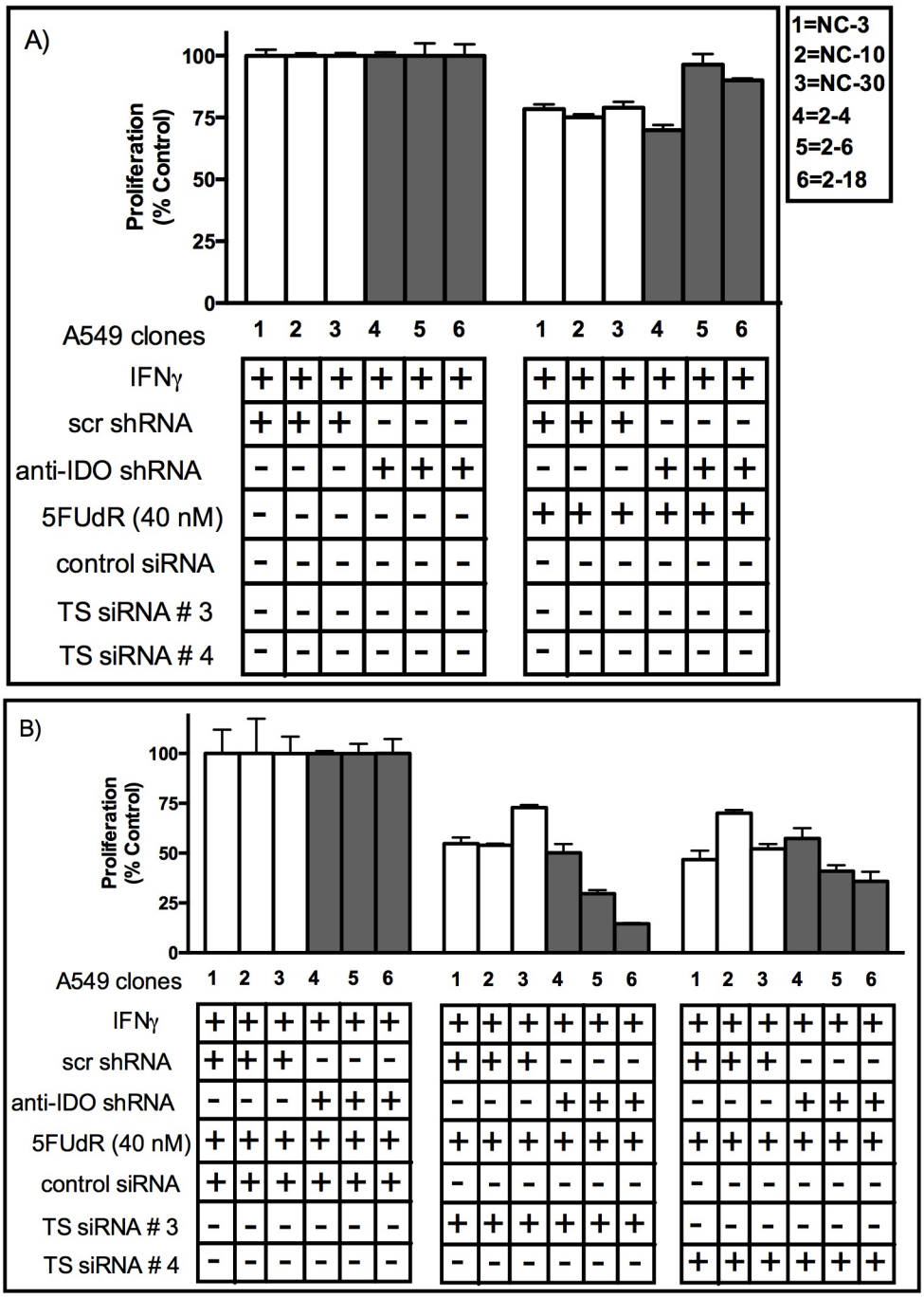
A)
Proliferation (% Control)
100
75
50
25
0
1=NC-3
2=NC-10
3=NC-30
4=2-4
5=2-6
6=2-18
A549 clones
1 2 3 4 5 6 1 2 3 4 5 6
IFNγ
scr shRNA
anti-IDO shRNA
5FUdR (40 nM)
control siRNA
TS siRNA # 3
TS siRNA # 4
B)
Proliferation (% Control)
100
75
50
25
0
A549 clones
1 2 3 4 5 6 1 2 3 4 5 6 1 2 3 4 5 6
IFNγ
scr shRNA
anti-IDO shRNA
5FUdR (40 nM)
control siRNA
TS siRNA # 3
TS siRNA # 4

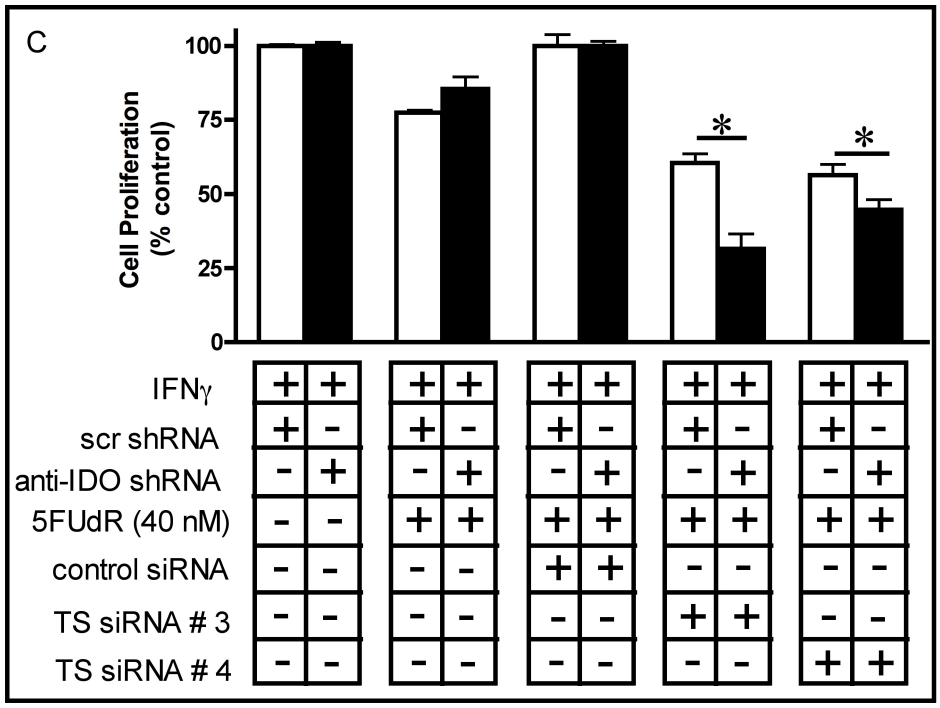
C
Cell Proliferation (% control)
100
75
50
25
0
*
*
IFNγ
scr shRNA
anti-IDO shRNA
5FUdR (40 nM)
control siRNA
TS siRNA # 3
TS siRNA # 4

Figure 4. 65. Concurrent IDO and TS downregulation sensitizes A549 cells to 5FUdR more effectively than knockdown of TS alone. A549 cells were transfected with control or TS siRNA, treated with IFNγ (25 ng/ml) for 48 h, and then with 5FUdR (40 nM) for 72 h, at which time the number of live cells was assessed as a measure of proliferation. Bars indicate mean proliferation relative to appropriate controls ± SD (n=3).

A) Proliferation of clonal A549 cell populations induced with IFNγ and then treated with 5FUdR, but untransfected with siRNA of any kind. **Gray bars** indicate clones containing anti-IDO shRNA and **white bars** indicate clones containing non-targeting control shRNA.

B) Proliferation of the same clonal A549 cell populations transfected with control non-targeting siRNA, TS siRNA #3, or TS siRNA #4, induced with IFNγ, and then treated with 5FUdR. Bars represent values normalized to values obtained from clones treated with IFNγ but untreated with pemetrexed or siRNA; those cells were considered to have a proliferation value of 100% after IFNγ treatment. **Gray bars** indicate clones containing anti-IDO shRNA and **white bars** indicate clones containing non-targeting control shRNA.

C) Data for 3 individual A549 clones with anti-IDO shRNA and 3 clones with control, non-targeting shRNA (from panels A and B) were pooled and mean values (n=3) are show ± SEM (*$p < 0.05$). **Black bars** indicate clones containing anti-IDO shRNA and **white bars** indicate clones containing non-targeting control shRNA.

4.24 BRCA2 Downregulation in A549 Clonal Populations

BRCA2 is important in homologous recombination repair. Cancer cells lacking BRCA2 are more sensitive to olaparib and alkylating agents [208]. IDO downregulation sensitized cancer cells to olaparib (Figures 4.24 and 4.27) and cisplatin (Figures 4.54, 4.57, and 4.60). It therefore hypothesized that concurrent IDO and BRCA2 downregulation in cancer cells would further sensitize A549 tumour cells to the PARP inhibitor olaparib and the DNA cross-linking agent cisplatin. To test this hypothesis, A549 clonal cell populations were first transiently transfected with BRCA2 siRNA to assess the capacity to reduce BRCA2 protein. BRCA2 siRNA downregulated BRCA2 protein in A549 cells by approximately 50% at 48 h post-transfection (Figure 4.66).

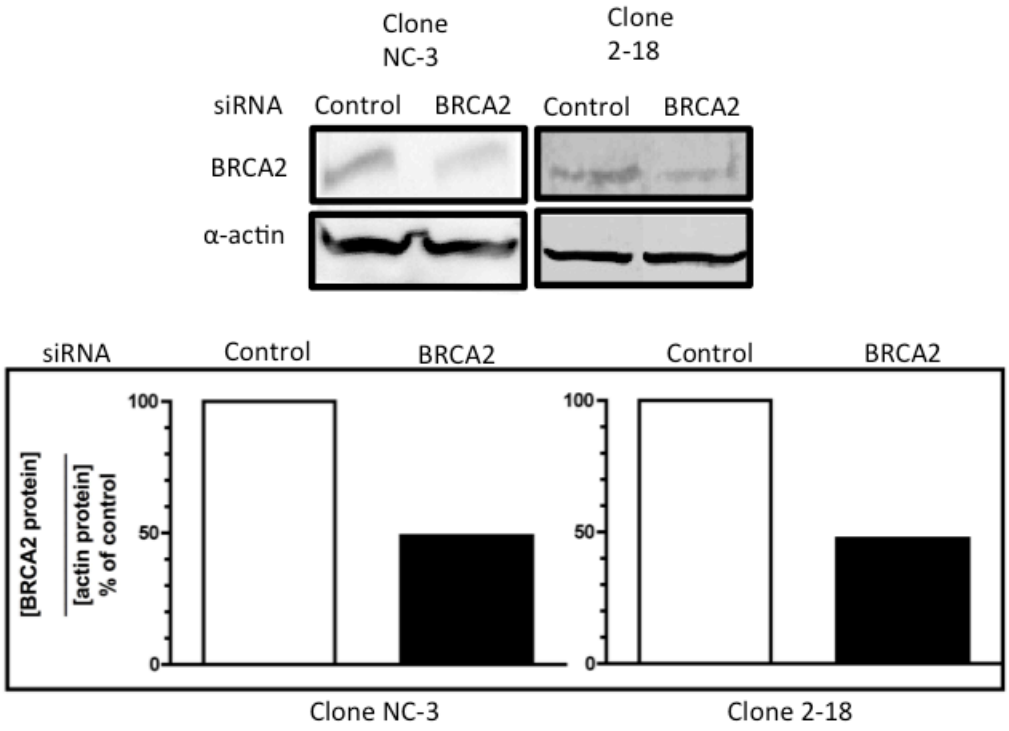
Clone
NC-3
Clone
2-18
siRNA
Control
BRCA2
Control
BRCA2
BRCA2
α-actin
siRNA
Control
BRCA2
Control
BRCA2
[BRCA2 protein]
[actin protein]
% of control
100
50
0
100
50
0
Clone NC-3
Clone 2-18

Figure 4. 66. siRNA downregulation of BRCA2 in A549 clones NC-3 and 2-18. A549 cells were transiently transfected with either control siRNA or BRCA2 siRNA smart pool. Cell lysates were prepared and protein extracts were prepared at 48 h post-transfection. BRCA2 and actin antibodies were used to probe membranes. BRCA2 protein content relative to actin protein was reduced by 50% in clone NC-3 (control, non-targeting shRNA) and by 50% in clone 2-18 (anti-IDO shRNA).

4.25 Concurrent IDO and BRCA2 Downregulation Sensitizes A549 Cells to the PARP Inhibitor Olaparib More than Knockdown of Either Gene Alone

Cancer cells harbouring BRCA2 mutations have increased sensitivity to the PARP inhibitor olaparib [208]. As IDO downregulation sensitized A549 adenocarcinoma cells to olaparib (Figure 4.24), we therefore determined whether simultaneous knockdown of IDO and BRCA2 would sensitize A549 cells to olaparib with a greater degree than the knockdown of either gene alone. Concurrent downregulation of IDO and BRCA2 sensitized A549 cells to olaparib (75%) to a greater degree than either IDO downregulation (35%) or BRCA2 downregulation (30%)(Figure 4.67). These results suggest that combining IDO downregulation with the knockdown of the DNA repair molecule BRCA2 had a greater than additive effect on A549 cells.

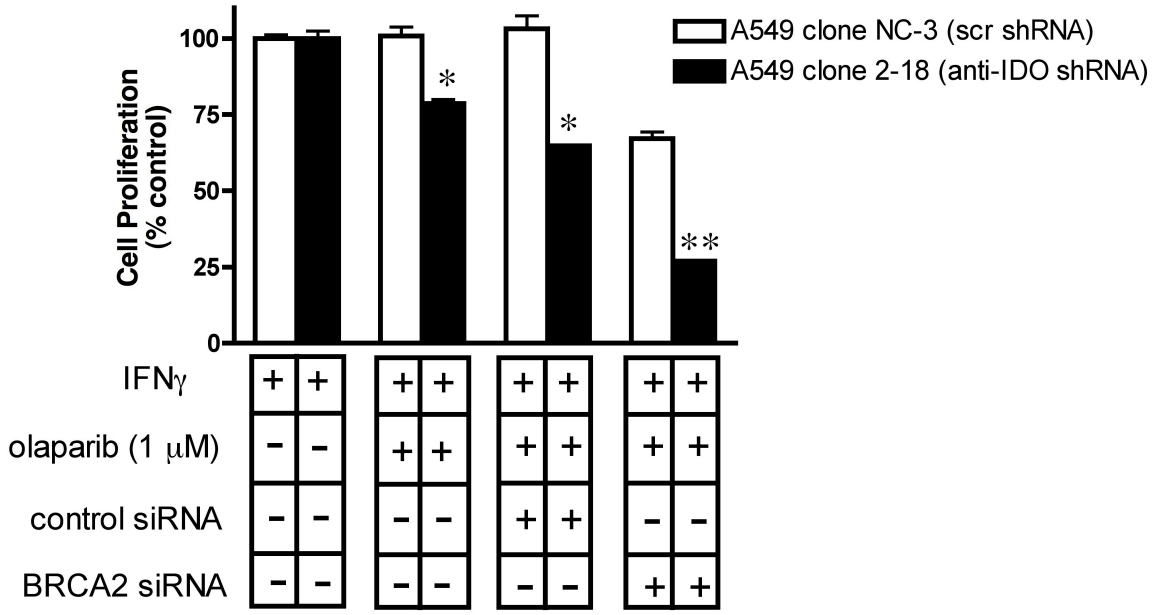
A549 clone NC-3 (scr shRNA)
A549 clone 2-18 (anti-IDO shRNA)
Cell Proliferation (% control)
100
75
50
25
0
*
*
**
IFNγ
olaparib (1 μM)
control siRNA
BRCA2 siRNA

Figure 4. 67. Concurrent IDO and BRCA2 downregulation sensitized cancer cells to olaparib to a greater degree than the knockdown of either gene alone. A549 clonal cells transfected with either scrambled shRNA (NC-3) or anti-IDO shRNA (2-18) were transiently transfected with BRCA2 siRNA, induced with IFNγ (25 ng/ml) and 24 h later, treated with low dose olaparib (1 μM) for 72 h. Live cells enumerated at the end of that time. Bars indicate the mean proliferation of cells from a representative experiment (n=3) ± SD, relative to appropriate controls. Values were normalized to those obtained from clones treated with IFNγ but untreated with olaparib or siRNA; those cells were considered to proliferate at a 100% level after IFNγ treatment. **Different from treatment with either siRNA alone (* $p \leq 0.05$).

4.26 Concurrent IDO and BRCA2 Downregulation Sensitizes A549 Cells to the DNA Cross-linking Agent Cisplatin More than Knockdown of Either Gene Alone

BRCA2 is vital for repair of DNA double stranded breaks (DDSBs) [187]. As cisplatin cytotoxicity results in DDSBs in cancer cells [267] and IDO downregulation sensitized A549 cells to cisplatin (Figure 4.54), we hypothesized that concurrent downregulation of IDO and BRCA2 would enhance cisplatin toxicity in A549 cells compared to knockdown of either IDO or BRCA2 alone. A549 clonal populations (with and without anti-IDO shRNA) were transfected with BRCA2 siRNA to inhibit DNA repair, treated with IFNγ to induce IDO, and then exposed to cisplatin for 72 h to assess the effect on proliferation. Simultaneous knockdown of both IDO and BRCA2 sensitized A549 cells to cisplatin to a greater degree (70%) than either IDO knockdown alone (47%) or BRCA2 knockdown alone (20%) (Figure 4.68).

4.27 Concurrent IDO and BRCA2 Downregulation does not Sensitize A549 Cells to 5FUdR

In view of the observation that antisense knockdown of IDO enhanced the capacity of antisense knockdown of TS to sensitize human tumour cells to 5FUdR (Figure 4.65), the capacity of antisense knockdown of IDO combined with BRCA2 knockdown to sensitize human tumour cells to 5FUdR was evaluated. Antisense reduction of IDO alone did not sensitize A549 cells to 5FUdR (Figure 4.69, lane 3 vs. lane 4), but antisense downregulation of BRCA2 sensitized A549 cells to 5FUdR (Figure 4.69, lane 3 vs. lane 5). Concurrent downregulation of IDO and BRCA2 did not sensitize cancer cells to 5FUdR to any greater degree than knockdown of BRCA2 alone (Figure 4.69, lane 5 vs. lane 6). These results suggest that knockdown of IDO does not contribute to sensitization to the TS-targeting drug 5FUdR, either alone or in combination with knockdown of BRCA2.

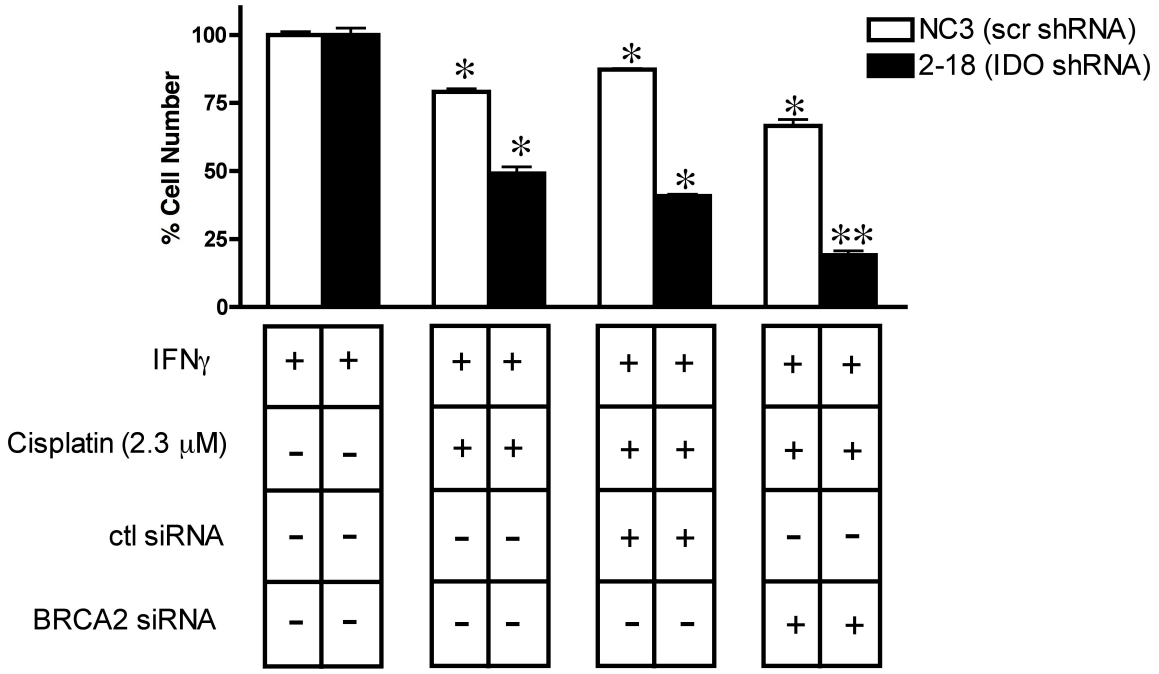
NC3 (scr shRNA)
2-18 (IDO shRNA)
% Cell Number
100
75
50
25
0
*
*
*
*
*
**
IFNγ
Cisplatin (2.3 μM)
ctl siRNA
BRCA2 siRNA
+ + + + + + + +
- - + + + + + +
- - - - + + - -
- - - - - - + +

Figure 4. 68. Concurrent downregulation of IDO and BRCA2 sensitizes A549 to cisplatin in an additive fashion. A549 clonal cells transfected with either scrambled shRNA (NC-3) or anti-IDO shRNA (2-18) were transiently transfected with BRCA2 siRNA, induced with IFNγ (25 ng/ml), treated with low dose cisplatin (2.3 μM), and live cells enumerated after 72 of drug treatment. Bars represent the means of 3 independent measurements of cells (with or without downregulation of IDO) after BRCA2 siRNA transfection + cisplatin treatment (*n*=3 for each measurement) ± SEM. Bars were normalized to values obtained from clones treated with IFNγ but untreated with cisplatin or siRNA; those cells were considered to proliferate at a 100% level after IFNγ treatment. **Different from treatment with either siRNA in combination with cisplatin (* $p \leq 0.05$).

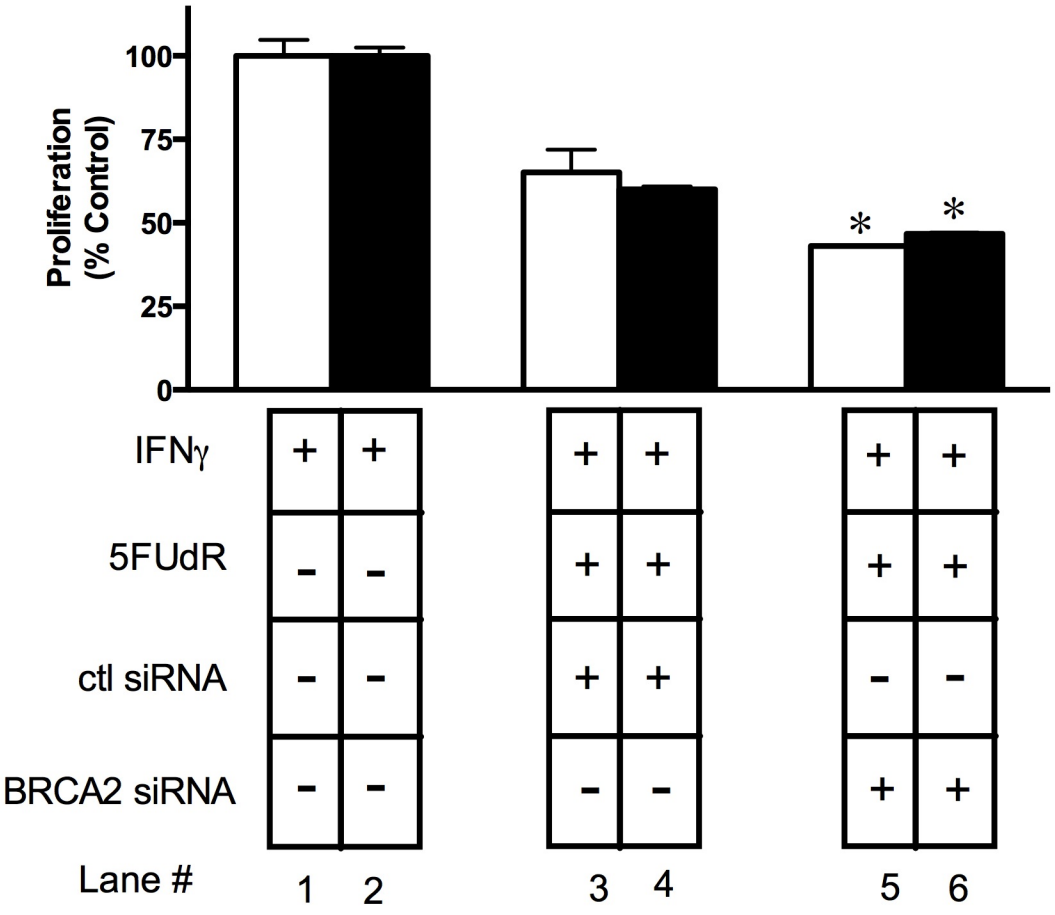
Proliferation (% Control)
100
75
50
25
0
*
*
IFNγ
5FUdR
ctl siRNA
BRCA2 siRNA
Lane #
1 2 3 4 5 6

Figure 4. 69. Concurrent downregulation of IDO and BRCA2 did not sensitize A549 to the TS-targeting drug 5FUdR to a greater degree than the knockdown of either gene alone. A549 clonal cells transfected with either scrambled shRNA (NC-3) or anti-IDO shRNA (2-18) were transiently transfected with BRCA2 siRNA, induced with IFNγ (25 ng/ml) for 24 h, and then treated with 5FUdR (40 nM) for 72 h, at which time live cells were enumerated. Bars represent the means of 3 independent measurements of cells (with or without downregulation of IDO) after BRCA2 siRNA transfection + 5FUdR treatment (*n*=3 for each measurement) ± SD. Bars were normalized to values obtained from clones treated with IFNγ but untreated with 5FUdR or siRNA; those cells were considered to proliferate at a 100% level after IFNγ treatment (*$p \leq 0.05$).

5 Chapter 5

Discussion

5.1 IDO Induction in A549 and HeLa Cells

Most human tumours express IDO *in vivo* [135]. Various situations including inflammation and infection can also induce IDO in the body [268, 269]. The pro-inflammatory cytokine IFNγ is a potent inducer of IDO in a variety of human cells including cancer cells [270]. A549 and HeLa cells were therefore treated *in vitro* with IFNγ and IDO mRNA and protein levels were examined. IDO is normally expressed in human lung [108,109] and is expressed in human lung adenocarcinomas and cervical cancer [68,71]. We therefore chose human cancer cell lines arising from the same organs and induced IDO in them with IFNγ. IFNγ-mediated IDO mRNA induction was measured at various times (12, 24, 48 and 72 h). IFNγ treatment induced IDO mRNA, 24 h (Figure 4.2 and Figure 4.3) and protein, 48 h (Figure 4.4) post-treatment in both A549 and HeLa adenocarcinoma cells (Figure 4.4 and Figure 4.15). IFNγ-mediated IDO mRNA is at its highest level at 24 h and begins to reduce at later time points.

H441 adenocarcinoma cells were also examined for IDO mRNA expression without IFNγ treatment. H441 cells expressed IDO mRNA in the absence of IFNγ (Figure 4.5). These results show that IDO mRNA and protein can be induced in A549 and HeLa cells, and that H441 cells are available as endogenous constitutive IDO expressers. We have have also tested other human cancer cell lines for IDO induction including SW480 and Caco-2 colorectal cancer cell line. However, IFNγ treatment did not induce IDO in these cell lines.

Induction of IDO with IFNγ, followed by IDO downregulation in cancer cells, provides a more physiologically relevant model to study IDO in cancer thanoverexpression of IDO mediated by stable cDNA transfection. Moreover, IFNγ provides the necessary post-translational modification of IDO protein that makes a fully functional protein [114]. We therefore chose IFNγ to induce IDO in A549 and HeLa cells.

5.2 IDO siRNA Downregulation in A549 and H441 Cells

To examine IDO's effect on drug sensitivity independent of the immune system, antisense siRNA was used in an attempt to first knockdown IDO in human cancer cells and then expose them to chemotherapy drugs. Successful transient siRNA knockdown of IDO mRNA has been previously demonstrated in multiple murine cancer models. In those models, IDO was downregulated in murine DCs and not in tumour cells [158, 159]. On the other hand, Mobergslien and Sioud have reported successful knockdown of IDO in human monocytes and DCs with an electroporation method [271], suggesting that siRNA could be effective in human tumour cells. I transiently transfected A549 and H441 cells with a human IDO siRNA SMARTpool® (a commercially-available combination of 4 different siRNAs that target different regions of human IDO mRNA)(Table 3.3). IDO siRNA was not capable of inhibiting IFNγ-induced IDO in A549 cells or naturally-occurring elevated IDO mRNA in H441 cells (Figure 4.6-4.9). SiRNA downregulation of human IDO has been, for the most part, reported in APCs and not tumour cells. Lack of effectiveness in human tumour cells could be attributed to multiple factors, including inefficiency of transient downregulation of IDO due to a high rate of IDO gene transcription capable of constantly replenishing the IDO mRNA pool, induction of RNAi repressors, or unknown factors suppressing Argonaute endonuclease effectiveness [56]. A high rate of IDO gene transcription would be expected to increase IDO mRNA levels and reduce the effectiveness of transiently-transfected anti-IDO siRNA. Constant production of antisense molecules (as would be produced by stably-incorporated shRNA) was next considered as an approach to effectively reduce IDO in human tumour cells. Regardless, it was apparent that the siRNA approaches tested here were insufficiently effective at reducing IDO mRNA to be useful in assessing the role of IDO in mediating treatment sensitivity in human tumour cells. However, using only siRNA is a limitation to our antisense approach for transient IDO downregulation in cancer cells since we have not tested ribonuclease (RNase) H-dependent ODNs to downregulate IDO.Antisense ODNs, because they invoke a different RNAse pathway and are more stable both *in vivo* and *in vitro*, may be more effective agents to reduce IDO than siRNAs.

5.3 Stable Transfection of A549, HeLa and H441 Cells with anti-IDO shRNA

A number of studies have successfully used shRNA to create stable knockdown of IDO and IDO_2 in human cancer cells [272-274]. Since siRNA downregulation of IDO was ineffective, I used anti-IDO shRNA to stably knock down IDO in A549, HeLa and H441 cells. I transfected all three tumour cell lines with either anti-IDO shRNA or scrambled control shRNA and picked multiple clones with reduced IDO mRNA (Figure 4.11-4.13) and protein (Figure 4.14 and Figure 4.15) for investigation. Measuring kynurenine/tryptophan levels in culture medium before and after IDO induction [144] or measuring cancer cell proliferation can assess IDO functionality in cancer cells. Since IDO decreases cancer cell proliferation [145], and this can be examined as a one step process, I tested the functionality of anti-IDO shRNA in clonal populations by assessing its ability to counteract IDO-mediated decreases in tumour cell proliferation. A549 and HeLa clonal populations with scrambled control shRNA showed decreased proliferation compared to clonal cells with anti-IDO shRNA (Figure 4.16 and Figure 4.17). Interestingly, A549 clone 2-4 with anti-IDO shRNA that was still capable of producing some IDO protein (Figure 4.14) showed decreased proliferation compared to other A549 clonal populations with anti-IDO shRNA (Figure 4.16). It should be noted that IFNγ has some anti-proliferative effects on all cells that are independent of IDO. However, since all clonal populations were similarly treated with IFNγ, the observed difference in proliferation is solely due to IDO expression in cancer cells and not IFNγ. These results confirm that anti-IDO shRNA is functional in inhibiting both IDO levels and effects on cancer cells.

5.4 The Effects of IDO on the A549 Cell Cycle

Published investigation of the characteristics of IDO is primarily in the context of the immune system because of the clear immune regulatory roles described for IDO. IDO-mediated tryptophan depletion induces cell cycle arrest in T cells in G_1 [275]. I determined whether IDO-induced reduction in growth of cancer cells was associated with altered cell cycle. IFNγ induction of IDO increased the number of cells in G_1 and decreased the numbers in G_2/M when cells were stably transfected with scrambled control shRNA. The presence of anti-IDO shRNA in cells treated with IFNγ abolished

the increase and decrease, respectively (Figure 4.18). To confirm these observations one could serum-starve the A549 tumour cells to synchronize them before IFNγ treatment.

The increased time in G_1 is important to increase the ability of tumour cells to undergo complete, error-free DNA repair capable of removing basal and therapy-induced DNA damage [276]. The increase in the number of cells in G_1 seen exclusively in IDO-expressing cell lines suggests a possible broader role for this protein in cell cycle checkpoint control, allowing for repair of DNA damage during G_1 phase of the cell cycle [276, 277]. I therefore decided to examine the role of IDO in DNA repair and and sensitivity to drugs that induce DNA damage in cancer cells independent of the immune system.

5.5 IDO Downregulation Decreases Intracellular NAD^+

NAD^+ is vital for PARP activity and DNA repair [215]. Since IDO is responsible for the *de novo* synthesis of NAD^+ from tryptophan, I examined whether anti-IDO shRNA could decrease NAD^+ levels in A549 clonal populations. After IFNγ stimulation, two independently-derived A549 clones expressing anti-IDO shRNA had lower amounts of NAD^+ than two similarly-generated clones expressing scrambled control shRNA (Figure 4.19). These data indicate that shRNA-mediated suppression of IFNγ-induced IDO decreases intracellular NAD^+ levels and has the potential to modulate PARP function. DNA damage-mediated PARP-1 activation can deplete the NAD^+ pool in cells, which is associated with inducing cellular apoptosis [278]. Therefore, IDO-mediated generation of NAD^+ might play a protective role in cancer cells during DNA damage inducing treatments that normally result in hyperactivation of PARP and depletion of NAD^+ sources in cells. This provides a rationale to examine the possible protective role of IDO in response to genotoxic chemotherapy and radiation in cancer cells. In addition, NAD^+ inhibitors are under consideration and evaluation for cancer treatment. In particular, FK866, a pharmacological inhibitor of the NAD^+ salvage pathway, is undergoing clinical testing as a cancer therapy [279]. FK866 efficiently blocks NAD^+ production in human cancer cells [279]. However, a high concentration of NAD^+ precursors (NAM and NA) from the salvage pathway is able to reverse the inhibitory effect of FK866. IDO increases *de novo* NAD^+ production [220]. However, the possible inhibitory role of IDO on the

efficiency of this drug has never been tested. Therefore, I examined the capacity of IDO to decrease human tumour cell sensitivity to this candidate anticancer drug.

5.6 IDO in Tumour Cells Mediates Resistance to the NAD^+ Inhibitor FK866

IDO inhibition decreased NAD^+ levels in A549 cells by approximately 60% (Figure 4.19), similar to the level to which FK866 inhibits NAD^+ in other cell types [242]. IDO was therefore induced in A549 clonal populations before treatment with FK866. IDO in A549 cells conferred resistance to FK866 (Figure 4.20). A549 clones express anti-IDO shRNA, with the exception of clone 2-4 that expressed IDO at a slightly higher level than the other anti-IDO shRNA-containing clones, retained sensitivity to FK866 (Figure 4.20). Higher IDO levels were also correlated with increased resistance to FK866 (Figure 4.20 C). This is a significant observation with respect to the capacity of FK866 to block NAD^+ in the presence of IDO because FK866 is a potent NAD^+ inhibitor that blocks NAD^+ production through the salvage pathway [262]. However, IDO-mediated NAD^+ production from the *de novo* pathway can clearly undermine FK866 efficiency (Figure 4.20). In addition, tumour-infiltrating cytotoxic T cells and NK cells are major sources of IFNγ in the tumour microenvironment [280, 281]. As shown in Figure 4.20, IFNγ-mediated increases in IDO induced resistance to FK866. Therefore, blocking IDO in conjunction with FK866 treatment may have therapeutic value and further studies are required.

5.7 IDO in Tumour Cells Mediates Resistance to Olaparib

IDO downregulation decreased NAD^+ in A549 cells (Figure 4.19). Since NAD^+ is critical for PARP activity [214], I examined whether IDO could increase tumour cell resistance to olaparib (a PARP inhibitor) and whether anti-IDO shRNA could reverse this effect. Anti-IDO shRNA sensitized A549 and HeLa cells to olaparib (Figure 4.21-4.24 and Figure 4.26-4.27). Moreover, A549 and HeLa cells transfected with scrambled shRNA had increased resistance to olaparib after IFNγ induction; the effectiveness of the administered dose of the drug was reduced, while antisense-downregulation of IDO during and after IFNγ induction resulted in sensitivity to olaparib equal to that of cells untreated with IFNγ (Figure 4.25 and Figure 4.27). These findings show, for the first time,

that IDO in tumour cells confers resistance to a PARP inhibitor, olaparib. Tumour cells with BRCA mutations showed high sensitivity to olaparib monotherapy [207]. However, secondary mutations that restored full-length BRCA2 protein in cancer patients conferred resistance to olaparib [282]. These data identify a new resistance mechanism to olaparib that is exerted by IDO and is independent of BRCA2 since A549 and HeLa cells have intact BRCA2. Therefore combining IDO inhibition with PARP inhibitors could offer an advantage over PARP inhibition monotherapy.

5.8 IDO Mediates Resistance to γ Radiation in Cancer Cells

Since PARP-mediated DNA repair is important in resistance to γ radiation [95], I assessed whether IDO could increase A549 and HeLa cell resistance to γ radiation. A549 and HeLa clonal populations were equally sensitive to γ radiation prior to IDO induction regardless of the presence of anti-IDO shRNA or scrambled shRNA (Figure 4.28-4.29 and Figure 4.32 and 4.33). However, IFNγ-induced IDO conferred resistance to γ radiation in both A549 and HeLa cells. This effect was abolished by anti-IDO shRNA (Figure 4.30 and Figure 4.34). Tumour cell resistance to γ radiation is generally attributed to DNA repair mediated by PARP activity and BER [88-89]. These data show, for the first time, that IDO plays a role in tumour cell resistance to γ radiation. This phenomenon may be due to IDO-mediated increase in available NAD^+ in cancer cells that supports the capacity of PARP to mediate DNA repair. Furthermore, increased NAD^+ has been attributed to improved BER in cancer cells [283]. It can be speculated that the IDO-mediated increase in NAD^+ levels might increase the effectiveness of BER in cancer cells, thereby increasing resistance towards radiation. Future studies are required to confirm or modify this possibility. For example, examining the level of key BER proteins such as XRCC1 after γ radiation of cancer cells in the presence or absence of IDO could provide valuable information regarding the direct impact of IDO on BER-mediated resistance to γ radiation.

5.9 IDO in Human Tumour Cells Mediates Resistance to Combined γ Radiation and PARP Inhibition

Inducing DNA damage and subsequently inhibiting DNA repair in cancer cells is an attractive approach to maximize radiation-induced cell death in tumour cells [93]. I therefore induced IDO in A549 and HeLa cells for 48 h and then treated them with γ radiation to induce DNA damage, followed by culture in the presence of olaparib to inhibit DNA repair for 72 h. A549 and HeLa cells harboring anti-IDO shRNA were sensitized to combination therapy to a greater degree than cells harbouring scrambled shRNA (Figure 4.35-4.36 and Figure 4.38-4.39). Clonal populations with scrambled shRNA and capable of producing IDO showed increased resistance to combined radiation and PARP inhibition (Figure 4.37 and Figure 4.40). In a combination treatment study, the PARP inhibitor rucaparib significantly increased radiosensitivity and enhanced DNA damage in BRCA-proficient prostate cancer cell lines [93]. The capacity of tumour cells to develop resistance to combination therapy is not unexpected; these data identify IDO as a possible underlying molecule for this phenomenon in combination treatment with γ radiation and PARP inhibition.

5.10 The Effect of IDO Downregulation on Human Tumour Cell Sensitivity to Cisplatin

Since IDO downregulation sensitized cancer cells to γ radiation, I determined whether IDO knockdown sensitizes A549, HeLa and H441 cells to the DNA cross-linking agent cisplatin. IDO downregulation sensitized cancer cells to cisplatin (Figure 4.54-4.55, Figure 4.57-4.58 and Figure 4.60). Furthermore, IDO in cancer cells decreased the effectiveness of the drug, and that increased effectiveness was reduced by anti-IDO shRNA in both A549 and HeLa cells (Figure 4.56 and Figure 4.59). Blocking IDO activity by the small molecule IDO inhibitor 1-MT has been previously attributed to increased sensitivity of mouse breast cancer cells to cisplatin in the presence of an active immune system [136]. This is in agreement with our results, but these data establish that this effect can occur in the absence of any involvement of immune cells and, perhaps more importantly, in human rather than rodent cancer cells.

5.11 IDO in Human Tumour Cells Mediates Resistance to the Base Excision Repair Inhibitor Methoxyamine

IDO induced resistance to olaparib (Figure 4.25 and Figure 4.27). In addition, PARP is essential for the recruitment of the BER scaffold protein XRCC1 to the damaged area of the DNA [199]. I therefore assessed whether IDO could induce resistance to the BER inhibitor methoxyamine. Knocking down IDO sensitized A549 cells to methoxyamine (Figure 4.41 and Figure 4.42). Moreover, IDO induced high levels of resistance to methoxyamine in A549 cells and that resistance was abolished by anti-IDO shRNA (Figure 4.43). Higher IDO levels were also positively correlated to methoxyamine resistance in cancer cells (Figure 4.41 C). Several phase I clinical trials of combined methoxyamine with chemotherapy drugs are currently underway [284]. One clinical trial in particular has studied the combination effect of methoxyamine and the TS-targeting drug pemetrexed in patients with advanced refractory cancers [284]. Therefore, IDO-mediated potent induction of resistance to methoxyamine could provide critical information in designing pre-clinical and clinical studies in future.

5.12 IDO in Human Tumour Cells Mediates Resistance to the TS-targeting Drug Pemetrexed

Since BER is reported to be involved in resistance to pemetrexed [179] and IDO inhibited the effectiveness of the BER inhibitor methoxyamine (Figure 4.43), I decided to assess whether IDO downregulation sensitized cancer cells to the TS-targeting drug pemetrexed. Antisense knockdown of IDO sensitized A549 cells to pemetrexed (Figure 4.44 and Figure 4.45). In addition, IDO-mediated resistance to pemetrexed was decreased by anti-IDO shRNA after IFNγ induction of IDO in A549 cells (Figure 4.46).

Pemetrexed inhibition of TS results in the misincorporation of uracil into DNA. The BER enzyme uracil-DNA glycosylase (UNG) removes the misincorporated uracil and, by mediating that process, confers resistance to pemetrexed (which exerts part of its toxicity to tumour cells by uracil incorporation into DNA)[285]. All A549 clonal populations were similarly sensitive to pemetrexed before IDO induction (Figure 4.44). However, IDO induced resistance to pemetrexed (Figure 4.45). Therefore, further studies

are required to examine whether or not UNG function is affected by IDO. Examining UNG kinetic and substrate binding assay [60] in the presence or absence of IDO can shed light on the possible effect of IDO on UNG function.

5.13 IDO in Human Tumour Cells Mediates Resistance to Combined Treatment of Pemetrexed and Methoxyamine

Pemetrexed-resistant sublines of H1299 adenocarcinoma cells have elevated levels of UNG and combined treatment of these H1299 sublines with methoxyamine and pemetrexed increased their sensitivity to pemetrexed [285]. However, despite their *in vivo* IDO expression, many human cancer cell lines do not express IDO *in vitro*. I therefore decided to test whether IDO in tumour cells can mediate resistance to combined pemetrexed and methoxyamine treatment. IFNγ-induced IDO undermined the therapeutic potential of the combined treatment of pemetrexed and methoxyamine (Figure 4.47 and 4.48). This effect was significantly reduced by anti-IDO shRNA in A549 cells (Figure 4.47 and 4.48). Moreover, IDO levels were positively correlated with resistance to combined pemetrexed and methoxyamine treatment in A549 clonal cells (Figure 4.47, Panel C). These results provide compelling evidence for a previously unidentified role for IDO in induced resistance to a combination of the TS-targeting drug pemetrexed and a BER inhibitor methoxyamine.

5.14 The Effect of IDO Human Tumour Cell Sensitivity to Other TS-targeting Drugs (5FUdR and Gemcitabine)

Since IDO downregulation sensitized cancer cells to the TS-targeting drug pemetrexed, I decided to examine whether IDO downregulation could sensitize A549 cells to other TS-targeting drugs, including 5FUdR and gemcitabine. IDO downregulation did not sensitize cancer cells to 5FUdR, but did sensitize them to gemcitabine (Figure 4.50-4.53). BER is considered to play a major role in resistance to gemcitabine [286]. IDO may be involved in BER-mediated gemcitabine resistance in these cells. Interestingly, BER has been invoked as a contributor to 5FUdR cytotoxicity in cancer cells due to its participation in a futile repair cycle that potentiates 5FUdR toxicity [287]. In futile repair, the DNA mismatch repair enzyme MutL removes some

parts of the newly synthesized DNA strand. However, the removed part does not contain the incorporated 5FUdR, FdUTP. Using the template strand that contains FdUTP for resynthesizing DNA results in cycles of futile mismatches and eventually cell death [61]. IDO-mediated enhancement of BER could, potentially, increase the cytotoxicity of 5FUdR due to the enhancing effect of BER on futile repair. This hypothesis might provide a rationale for the observed lack of sensitization to 5FUdR in A549 cells with antisense-downregulated IDO, as observed in experiments reported in this thesis (Figure 4.50 and Figure 4.451). On the other hand, IDO downregulation sensitized tumour cells to pemetrexed and gemcitabine (Figure 4.45 and 4.53). Pemetrexed and gemcitabine do not exert their toxicity by inducing BER futile repair [288, 289], so the hypothesis proposed above is consistent with the observation of sensitization to pemetrexed or gemcitabine by IDO reduction, but not sensitization to 5FUdR. These results suggest that combining IDO downregulation with chemotherapy agents does not universally sensitize cells to all DNA-damaging agents, but instead requires sufficient understanding of the mechanism of action of the chemotherapy drugs in question and the mechanism(s) by which IDO mediates resistance.

5.15 Concurrent IDO and TS Downregulation Sensitized A549 Cells to Pemetrexed More than Knocking Down Either Gene Alone

Knocking down TS can sensitize cancer cells to the TS-targeting drug 5FUdR [266]. Antisense-mediated reduction in IDO also sensitized cancer cells to some TS-targeting drugs, including pemetrexed (Figure 4.44 and Figure 4.45). To examine whether combining IDO and TS downregulation sensitizes cancer cells to pemetrexed to a greater degree than reduction of either target alone, A549 cells were transiently transfected with TS siRNA, and then IDO was induced with IFNγ in all A549 clonal populations before exposing them to pemetrexed. As shown in Figure 4.63 and Figure 4.64, simultaneous downregulation of IDO and TS increased the sensitivity of cancer cells to pemetrexed to a greater degree than reduction of either target alone. TS siRNA downregulation has been shown to sensitize A549 cells to pemetrexed [186]. I show here that combining TS and IDO downregulation further sensitized A549 cells to this drug (Figure 4.63 and Figure 4.64). The additive effect of TS and IDO downregulation in

A549 cells sensitivity to pemetrexed might result from the effect of TS downregulation on the available thymidylate to the cells [290] along with the IDO-mediated impact on BER (Figure 4.41 and Figure 4.42). These observations could provide the basis for a strategy to improve the effectiveness of the already-approved chemotherapeutic drug pemetrexed.

5.16 Concurrent IDO and TS Downregulation Sensitizes A549 Cells to 5FUdR to a Greater Degree than Reduction of Either Target Alone

Since IDO downregulation did not sensitize A549 cells to 5FUdR (Figure 4.50 and Figure 4.51), I determined whether combined IDO and TS downregulation could sensitize cancer cells to 5FUdR. As show in Figure 4.65 and Figure 4.66, concurrent IDO and TS downregulation did, in fact, sensitize A549 cells to 5FUdR more effectively than knockdown of IDO alone. This effect was less potent than observed with pemetrexed, but provides evidence that combining IDO and TS downregulation has potential as a therapeutic strategy to sensitize tumour cells to a range of TS-targeting drugs including pemetrexed and 5FUdR.

5.17 Concurrent IDO and BRCA2 Downregulation did Not Sensitize A549 Cells to 5FUdR

To further examine whether concurrent IDO and TS downregulation have value in sensitizing human tumour cells to the TS-targeting drug 5FUdR, I simultaneously downregulated IDO and BRCA2 (a DNA repair molecule not involved in enzymatic reactions mediated by TS), in A549 cells followed by treatment with 5FUdR. BRCA2 does not mediate BER [291], therefore, it is unlikely that, by targeting BRCA2 (which involves other, non-BER DNA repair pathways), cancer cells would be sensitized to a drug that requires BER for its toxicity. As shown in Figure 4.69, combining IDO and BRCA2 downregulation did not sensitize cancer cells to 5FUdR. These data emphasize the importance of simultaneous knockdown of IDO and a DNA repair molecule, to sensitize cancer cells to a drug that requires that specific DNA repair molecule for survival. In other words, reduction of IDO and BRCA2 does not appear to sensitize cancer cells to a drug such as 5FUdR that targets TS.

5.18 Concurrent IDO and BRCA2 Downregulation Sensitizes A549 Cells to the PARP Inhibitor Olaparib More than Knockdown of Either Gene Alone

Cancer cells with BRCA2 mutations are sensitive to olaparib monotherapy, most likely because of induced-synthetic lethality [207]. IDO could modulate PARP function by providing more NAD^+ (Figure 4.19). IDO downregulation also sensitized cancer cells to olaparib (Figure 4.21 and Figure 4.26). I used BRCA2 siRNA to downregulate BRCA2 and transiently induce BRCAness in A549 cells to determine whether simultaneous knockdown of IDO and BRCA2 would sensitize A549 cells to olaparib to a greater degree than the knockdown of either gene alone. Combining IDO and BRCA2 downregulation increased cancer cell sensitivity to olaparib more than targeting either gene product alone (Figure 4.67). These data support the hypothesis that sensitization of tumour cells to PARP inhibitors by reduction of IDO does not eliminate the capacity for reduction of other targets (including BRCA2) to contribute, in the context of IDO reduction, to enhanced sensitization of cancer cells to those PARP inhibitors. IDO reduction sensitizes tumour cells to PARP inhibitors independent of BRCA2 status (BRCA2 mutant or wild type) (Figure 4.21-4.24 and Figure 4.26-4.27); this supports the potential value of combining BRCA2 reduction with IDO reduction to sensitize human tumours to PARP inhibition, at least in tumour cells with functional BRCA2. Phase III trials of olaparib in ovarian cancer were terminated due to lack of increased overall survival in spite of evidence of olaparib-induced increase in progression-free survival [292]. These data support the concept of therapeutic targeting of IDO to decrease tumour cell resistance to PARP-inhibiting drugs such as olaparib, whether they are BRCA2 intact or deficient cells.

5.19 Concurrent IDO and BRCA2 Downregulation Sensitizes A549 Cells to Cisplatin to Greater Degree than Knockdown of Either Target Alone

Cisplatin induces DSBs in DNA in cancer cells [186] and BRCA2 is critical for repair of those breaks [186]. BRCA2 downregulation has been shown to sensitize cancer cells to cisplatin [186]. IDO mediates resistance to cisplatin in A549, HeLa and H441 cells (Figure 4.56, 4.59 and Figure 4.60). I therefore determined whether simultaneous downregulation of IDO and BRCA2 could increase cancer cell sensitivity to cisplatin

more than targeting either gene product alone. As shown in Figure 4.68, simultaneous knockdown of IDO and BRCA2 in A549 cells enhanced cisplatin toxicity in A549 cells compared to knockdown of either IDO or BRCA2 alone. These data provide clear evidence of the capacity of targeting IDO in conjunction with targeting other molecules involved in DNA repair to sensitize cancer cells to chemotherapy drugs that induce DNA damage and increase the requirement for, and dependence on, DNA repair on cancer cells.

5.20 A new function for IDO

Most human tumours express IDO [68] and IDO is linked to immune evasion, immunosuppression, metastasis, and poor patient outcome [69,70]. Here we have identified a previously unidentified role for IDO in human cancer that was independent of direct involvement of immune cells. We showed that, in an *in vitro* model and in the absence of immune cells, IDO increased intracellular NAD^+ levels and decreased the sensitivity of the tumour cells to the PARP inhibitor olaparib, a DNA cross-linking agent cisplatin, a folate antimetabolite pemetrexed, a nucleoside analogue gemcitabine, a base excision repair inhibitor methoxyamine, an NAD^+ inhibitor FK866, and combined treatments with olaparib and radiation, and methoxyamine and pemetrexed, in the absence of immune cells.

Combining 1-MT to paclitaxel has been shown to increase the effectiveness of this chemotherapy drug in the presence of an active immune system [76]. However, depletion of $CD4^+$ T cells completely abolished that synergistic effect [76]. In our model, however, the lack of immune cells in the entire process verifies a tumour cell-autonomous effect for IDO that is not dependent on the presence of immune cells. Chemotherapy drugs and radiation that we used in this study actively induce DNA damage or block DNA repair in cancer cells. We therefore identify, in this thesis, IDO involvement in DNA repair as a major IDO function.

5.21 Limitations:

Our findings are somewhat limited due to the use of only an *in vitro* model. These results therefore do not completely reflect what takes place in a tumour

microenvironment in the body. However, they are valuable as proof-of-principle for a new, and previously unidentified, function of IDO in cancer, independent of its immunosuppressive activity. We have also focused mainly on tumour cell proliferation as our final readout. Even though proliferation is of outmost importance in studying the impact of an anti-cancer treatment it does not provide detailed insight of what takes place as a consequence of treatment in cancer cells (for example, if reduced proliferation as a consequence of treatment is only because of cell cycle arrest or increased apoptosis, necrosis, or induced senescence in tumour cells). Reduced proliferation can also take place as a result of a combination of the aforementioned events. Further studies are therefore required to clarify the underlying mechanism of reduced proliferation in cancer cells in the presence of chemotherapy and radiation when combined with IDO downregulation in tumour cells. Finaly, we propose that IDO modulates DNA repair mechanisms in cancer cells by increasing intracellular NAD^+. We have used multiple chemotherapy drugs with different mechanisms of action to induce DNA damage in cancer cells and consequently activate DNA repair mechanisms in the presence or absence of IDO. However, our findings are limited to indirect examination of DNA repair mechanisms. A more direct approach of studying other enzymes involved in DNA repair pathways (BER in IDO-downregulated or IDO-sufficient cells, for example) would have significantly substantiated our findings at a molecular level. However, there are currently limitations to such studies. For example, the only available kit to measure PARP activity (HT universal colorimetric PARP assay kit, cat# 4677-096-k, Trevigen, Gaithersburg, MD) requires lack of NAD^+ in the cell lysate. Since IDO increases intracellular NAD^+ the experimental approach on which this kit depends would not be useful to our study. To examine whether IDO increases the expression of DNA repair enzymes, we could quantify them in cancer cells in the presence or absence of IDO to show a connection between IDO and DNA repair. However, although this approach would assess the capacity of IDO to modulate the amount of DNA repair enzyme, it would not assess the effect of those amounts on DNA repair activity itself.

6 Chapter 6

6.1 Significance

Data presented in this thesis provides evidence for the identification of a new and previously undescribed function for IDO (*i.e.*, independent of direct function of IDO in or on immune cells). IDO mediates resistance to a number of chemotherapy agents and γ radiation in human tumour cells. Conversely, knockdown of IDO increases the sensitivity of the same cells to these agents. IDO is expressed by most human cancers and cells of the tumour microenvironment, and its role in suppressing cytotoxic anti-tumour immune activity is well-described. I identify IDO as a molecule involved not only in resistance to immunotherapy (as reported before by others), but one that also plays a previously unreported role in resistance to chemotherapy and radiation. The majority of literature reports of *in vivo* IDO characteristics and function involve murine IDO in mouse tumours, in the context of the immune system. In this thesis, human IDO in human tumour cells was assessed. Furthermore, I looked at IDO effects in cancer cells in the absence of a functional immune system. The observations made here provide clear evidence for the benefit of targeting IDO. This not only avoids immunosuppression capable of hindering endogenous immune recognition and destruction of tumour cells, but also sensitizes tumour cells to conventional cancer therapies, including cytotoxic drugs and radiation in a cancer cell-autonomous fashion and independent of immune function. In a preclinical context, IDO in cancer cells can reduce the potential therapeutic effectiveness of anticancer therapies applied singly and in combination, and antisense knockdown of IDO abrogates that reduction in effectiveness – an observation revealing a previously undescribed, cancer cell-autonomous value for therapeutic targeting of IDO. Finally, TDO is overexpressed in brain tumours [293] and is involved in metabolizing tryptophan similar to IDO. Brain tumours are among the most resistance cancers to chemotherapy and radiation [293]. TDO downregulation in glioblastoma can therefore potentially sensitize brain tumours to radiation and some chemotherapy drugs.

6.2 Future Directions

It is valuable to reproduce these *in vitro* results in an *in vivo* model without the immune system. Immunocompromised mice provide a useful tool for this purpose. Searching the available patient databases to examine whether IDO levels were correlated with clinical outcomes from radiation or chemotherapy agents that are tested in this study would also be of great value. Testing the direct effect of IDO on enzymes involved in BER such as DNA glycosylases could provide a clear evidence for IDO being directly involved in an important DNA repair pathway. Adding conditioned media to IDO-negative cells and examining their drug sensitivity can shed light to the potential role of kyneurenine metabolites on IDO-mediated drug resistance. To further examine the underlying mechanism, we can add tryptophan or individual kynurenine metabolites to cultured tumour cells and measure sensitivity to chemotherapy drugs and radiation to provide a detailed insight of IDO's role in drug sensitivity and drug resistance. Finally, comparing the effectiveness of anti-IDO shRNA with conventional IDO inhibitors such as 1-MT in sensitizing cancer cells to chemotherapy agents and radiation would be of outmost importance.

References

1. Nowell, P.C., *The clonal evolution of tumor cell populations.* Science, 1976. **194**(4260): p. 23-8.
2. Boveri, T., *Über mehrpolige mitosen als mittel zur analyse des zellkerns.* Verh. Phys. Med. Ges. Würzburg. **35**: p. 67-90.
3. Loeb, L.A., *Human cancers express mutator phenotypes: origin, consequences and targeting.* Nat Rev Cancer, 2011. **11**(6): p. 450-7.
4. Levine, A.J., J. Momand, and C.A. Finlay, *The p53 tumour suppressor gene.* Nature, 1991. **351**(6326): p. 453-6.
5. Starcevic, D., S. Dalal, and J.B. Sweasy, *Is there a link between DNA polymerase beta and cancer?* Cell Cycle, 2004. **3**(8): p. 998-1001.
6. Stratton, M.R., P.J. Campbell, and P.A. Futreal, *The cancer genome.* Nature, 2009. **458**(7239): p. 719-24.
7. Chabner, B.A. and T.G. Roberts, Jr., *Timeline: Chemotherapy and the war on cancer.* Nat Rev Cancer, 2005. **5**(1): p. 65-72.
8. Hirono, I. and C. Yokoyama, *[Development of the resistance of tumors in chemotherapy; studies on the Yoshida sarcoma]*. Gan, 1954. **45**(2-3): p. 496-8.
9. Law, L.W., *Differences between cancers in terms of evolution of drug resistance.* Cancer Res, 1956. **16**(7): p. 698-716.
10. Rebucci, M. and C. Michiels, *Molecular aspects of cancer cell resistance to chemotherapy.* Biochem Pharmacol, 2013. **85**(9): p. 1219-26.
11. Lesterhuis, W.J., J.B. Haanen, and C.J. Punt, *Cancer immunotherapy--revisited.* Nat Rev Drug Discov, 2011. **10**(8): p. 591-600.
12. Sanford, M., *Trastuzumab: a review of its use in HER2-positive advanced gastric cancer.* Drugs, 2013. **73**(14): p. 1605-15.
13. Maemondo, M., et al., *Gefitinib or chemotherapy for non-small-cell lung cancer with mutated EGFR.* N Engl J Med, 2010. **362**(25): p. 2380-8.
14. Siddik, Z.H., *Cisplatin: mode of cytotoxic action and molecular basis of resistance.* Oncogene, 2003. **22**(47): p. 7265-79.
15. Eastman, A., *The formation, isolation and characterization of DNA adducts produced by anticancer platinum complexes.* Pharmacol Ther, 1987. **34**(2): p. 155-66.
16. Pinto, A.L. and S.J. Lippard, *Binding of the antitumor drug cis-diamminedichloroplatinum(II) (cisplatin) to DNA.* Biochim Biophys Acta, 1985. **780**(3): p. 167-80.
17. Damia, G., et al., *Cisplatinum and taxol induce different patterns of p53 phosphorylation.* Neoplasia, 2001. **3**(1): p. 10-6.
18. Delmastro, D.A., et al., *DNA damage inducible-gene expression following platinum treatment in human ovarian carcinoma cell lines.* Cancer Chemother Pharmacol, 1997. **39**(3): p. 245-53.
19. Smith, M.L., et al., *Interaction of the p53-regulated protein Gadd45 with proliferating cell nuclear antigen.* Science, 1994. **266**(5189): p. 1376-80.
20. Wang, X., J.L. Martindale, and N.J. Holbrook, *Requirement for ERK activation in cisplatin-induced apoptosis.* J Biol Chem, 2000. **275**(50): p. 39435-43.

21. Makin, G.W., et al., *Damage-induced Bax N-terminal change, translocation to mitochondria and formation of Bax dimers/complexes occur regardless of cell fate.* EMBO J, 2001. **20**(22): p. 6306-15.
22. Paz-Ares, L., et al., *Review of a promising new agent--pemetrexed disodium.* Cancer, 2003. **97**(8 Suppl): p. 2056-63.
23. Schultz, R.M., et al., *Role of thymidylate synthase in the antitumor activity of the multitargeted antifolate, LY231514.* Anticancer Res, 1999. **19**(1A): p. 437-43.
24. Shih, C., et al., *LY231514, a pyrrolo[2,3-d]pyrimidine-based antifolate that inhibits multiple folate-requiring enzymes.* Cancer Res, 1997. **57**(6): p. 1116-23.
25. Baldwin, C.M. and C.M. Perry, *Pemetrexed: a review of its use in the management of advanced non-squamous non-small cell lung cancer.* Drugs, 2009. **69**(16): p. 2279-302.
26. Mendelsohn, L.G., et al., *Enzyme inhibition, polyglutamation, and the effect of LY231514 (MTA) on purine biosynthesis.* Semin Oncol, 1999. **26**(2 Suppl 6): p. 42-7.
27. Teicher, B.A., et al., *Treatment regimens including the multitargeted antifolate LY231514 in human tumor xenografts.* Clin Cancer Res, 2000. **6**(3): p. 1016-23.
28. Ullman, B., et al., *Cytotoxicity of 5-fluoro-2'-deoxyuridine: requirement for reduced folate cofactors and antagonism by methotrexate.* Proc Natl Acad Sci U S A, 1978. **75**(2): p. 980-3.
29. Nakagawa, H., et al., *Continuous intrathecal administration of 5-fluoro-2'-deoxyuridine for the treatment of neoplastic meningitis.* Neurosurgery, 2005. **57**(2): p. 266-80; discussion 266-80.
30. van Laar, J.A., et al., *Comparison of 5-fluoro-2'-deoxyuridine with 5-fluorouracil and their role in the treatment of colorectal cancer.* Eur J Cancer, 1998. **34**(3): p. 296-306.
31. Hohn, D.C., et al., *Avoidance of gastroduodenal toxicity in patients receiving hepatic arterial 5-fluoro-2'-deoxyuridine.* J Clin Oncol, 1985. **3**(9): p. 1257-60.
32. Uchida, M., et al., *Transport and intracellular metabolism of fluorinated pyrimidines in cultured cell lines.* Adv Exp Med Biol, 1989. **253B**: p. 321-6.
33. Santi, D.V., C.S. McHenry, and H. Sommer, *Mechanism of interaction of thymidylate synthetase with 5-fluorodeoxyuridylate.* Biochemistry, 1974. **13**(3): p. 471-81.
34. Carmichael, J., *The role of gemcitabine in the treatment of other tumours.* Br J Cancer, 1998. **78 Suppl 3**: p. 21-5.
35. Gmeiner, W.H., *Antimetabolite incorporation into DNA: structural and thermodynamic basis for anticancer activity.* Biopolymers, 2002. **65**(3): p. 180-9.
36. Mini, E., et al., *Cellular pharmacology of gemcitabine.* Ann Oncol, 2006. **17 Suppl 5**: p. v7-12.
37. Blackstock, A.W., et al., *Tumor uptake and elimination of 2',2'-difluoro-2'-deoxycytidine (gemcitabine) after deoxycytidine kinase gene transfer: correlation with in vivo tumor response.* Clin Cancer Res, 2001. **7**(10): p. 3263-8.
38. Huang, P. and W. Plunkett, *Induction of apoptosis by gemcitabine.* Semin Oncol, 1995. **22**(4 Suppl 11): p. 19-25.
39. Begg, A.C., F.A. Stewart, and C. Vens, *Strategies to improve radiotherapy with targeted drugs.* Nat Rev Cancer, 2011. **11**(4): p. 239-53.

40. William B, C., *The treatment of inoperable sarcoma with the mixed toxins of erysipelas and bacillus prodigiosus: immediate and final results in one hundred and forty cases.* JAMA, 1898. **31**: p. 389-395.
41. Baxevanis, C.N., S.A. Perez, and M. Papamichail, *Cancer immunotherapy.* Crit Rev Clin Lab Sci, 2009. **46**(4): p. 167-89.
42. Smith, K.A., *Interleukin-2: inception, impact, and implications.* Science, 1988. **240**(4856): p. 1169-76.
43. Kirkwood, J., *Cancer immunotherapy: the interferon-alpha experience.* Semin Oncol, 2002. **29**(3 Suppl 7): p. 18-26.
44. Castillo, J., E. Winer, and P. Quesenberry, *Newer monoclonal antibodies for hematological malignancies.* Exp Hematol, 2008. **36**(7): p. 755-68.
45. Strome, S.E., E.A. Sausville, and D. Mann, *A mechanistic perspective of monoclonal antibodies in cancer therapy beyond target-related effects.* Oncologist, 2007. **12**(9): p. 1084-95.
46. Iannello, A. and A. Ahmad, *Role of antibody-dependent cell-mediated cytotoxicity in the efficacy of therapeutic anti-cancer monoclonal antibodies.* Cancer Metastasis Rev, 2005. **24**(4): p. 487-99.
47. Weiner, G.J., *Monoclonal antibody mechanisms of action in cancer.* Immunol Res, 2007. **39**(1-3): p. 271-8.
48. Sadelain, M., R. Brentjens, and I. Riviere, *The basic principles of chimeric antigen receptor design.* Cancer Discov, 2013. **3**(4): p. 388-98.
49. Baxevanis, C.N. and M. Papamichail, *Targeting of tumor cells by lymphocytes engineered to express chimeric receptor genes.* Cancer Immunol Immunother, 2004. **53**(10): p. 893-903.
50. Ribas, A., *Update on immunotherapy for melanoma.* J Natl Compr Canc Netw, 2006. **4**(7): p. 687-94.
51. Kanodia, S., D.M. Da Silva, and W.M. Kast, *Recent advances in strategies for immunotherapy of human papillomavirus-induced lesions.* Int J Cancer, 2008. **122**(2): p. 247-59.
52. Pol, S. and M.L. Michel, *Therapeutic vaccination in chronic hepatitis B virus carriers.* Expert Rev Vaccines, 2006. **5**(5): p. 707-16.
53. Cavallo, F., et al., *Vaccination for treatment and prevention of cancer in animal models.* Adv Immunol, 2006. **90**: p. 175-213.
54. Gilboa, E., *DC-based cancer vaccines.* J Clin Invest, 2007. **117**(5): p. 1195-203.
55. Melief, C.J. and S.H. van der Burg, *Immunotherapy of established (pre)malignant disease by synthetic long peptide vaccines.* Nat Rev Cancer, 2008. **8**(5): p. 351-60.
56. Zheng, Z.M., S. Tang, and M. Tao, *Development of resistance to RNAi in mammalian cells.* Ann N Y Acad Sci, 2005. **1058**: p. 105-18.
57. Sharma, P., et al., *Novel cancer immunotherapy agents with survival benefit: recent successes and next steps.* Nat Rev Cancer, 2011. **11**(11): p. 805-12.
58. Higano, C.S., et al., *Sipuleucel-T.* Nat Rev Drug Discov, 2010. **9**(7): p. 513-4.
59. Burch, P.A., et al., *Priming tissue-specific cellular immunity in a phase I trial of autologous dendritic cells for prostate cancer.* Clin Cancer Res, 2000. **6**(6): p. 2175-82.

60. Bellamy, S.R. and G.S. Baldwin, *A kinetic analysis of substrate recognition by uracil-DNA glycosylase from herpes simplex virus type 1.* Nucleic Acids Res, 2001. **29**(18): p. 3857-63.
61. Hewish, M., et al., *Mismatch repair deficient colorectal cancer in the era of personalized treatment.* Nat Rev Clin Oncol, 2010. **7**(4): p. 197-208.
62. Peggs, K.S., et al., *Blockade of CTLA-4 on both effector and regulatory T cell compartments contributes to the antitumor activity of anti-CTLA-4 antibodies.* J Exp Med, 2009. **206**(8): p. 1717-25.
63. Pisco, A.O., et al., *Non-Darwinian dynamics in therapy-induced cancer drug resistance.* Nat Commun, 2013. **4**: p. 2467.
64. D'Andrea, F.P., *Intrinsic radiation resistance of mesenchymal cancer stem cells and implications for treatment response in a murine sarcoma model.* Dan Med J, 2012. **59**(2): p. B4388.
65. Ng, C.P. and B. Bonavida, *A new challenge for successful immunotherapy by tumors that are resistant to apoptosis: two complementary signals to overcome cross-resistance.* Adv Cancer Res, 2002. **85**: p. 145-74.
66. Mumenthaler, S.M., et al., *Evolutionary modeling of combination treatment strategies to overcome resistance to tyrosine kinase inhibitors in non-small cell lung cancer.* Mol Pharm, 2011. **8**(6): p. 2069-79.
67. Lake, R.A. and B.W. Robinson, *Immunotherapy and chemotherapy--a practical partnership.* Nat Rev Cancer, 2005. **5**(5): p. 397-405.
68. Laurence, J., et al., *Apoptotic depletion of CD4+ T cells in idiopathic CD4+ T lymphocytopenia.* J Clin Invest, 1996. **97**(3): p. 672-80.
69. Hannun, Y.A., *Apoptosis and the dilemma of cancer chemotherapy.* Blood, 1997. **89**(6): p. 1845-53.
70. Swann, J.B. and M.J. Smyth, *Immune surveillance of tumors.* J Clin Invest, 2007. **117**(5): p. 1137-46.
71. Iversen, T.Z., et al., *Depletion of T lymphocytes is correlated with response to temozolomide in melanoma patients.* Oncoimmunology, 2013. **2**(2): p. e23288.
72. Zhao, T., et al., *Enhanced antitumor and reduced toxicity effect of Schisanreae polysaccharide in 5-Fu treated Heps-bearing mice.* Int J Biol Macromol, 2013.
73. Klug, F., et al., *Low-Dose Irradiation Programs Macrophage Differentiation to an iNOS(+)/M1 Phenotype that Orchestrates Effective T Cell Immunotherapy.* Cancer Cell, 2013. **24**(5): p. 589-602.
74. Komarova, N.L. and D. Wodarz, *Drug resistance in cancer: principles of emergence and prevention.* Proc Natl Acad Sci U S A, 2005. **102**(27): p. 9714-9.
75. Cole, S.P., et al., *Overexpression of a transporter gene in a multidrug-resistant human lung cancer cell line.* Science, 1992. **258**(5088): p. 1650-4.
76. Slot, A.J., S.V. Molinski, and S.P. Cole, *Mammalian multidrug-resistance proteins (MRPs).* Essays Biochem, 2011. **50**(1): p. 179-207.
77. Kruh, G.D. and M.G. Belinsky, *The MRP family of drug efflux pumps.* Oncogene, 2003. **22**(47): p. 7537-52.
78. Kruh, G.D., et al., *ABCC10, ABCC11, and ABCC12.* Pflugers Arch, 2007. **453**(5): p. 675-84.

79. Saito, J., et al., *Association between DNA methylation in the miR-328 5'-flanking region and inter-individual differences in miR-328 and BCRP expression in human placenta.* PLoS One, 2013. **8**(8): p. e72906.
80. Natarajan, K., et al., *Role of breast cancer resistance protein (BCRP/ABCG2) in cancer drug resistance.* Biochem Pharmacol, 2012. **83**(8): p. 1084-103.
81. Paumi, C.M., et al., *ABC transporters in Saccharomyces cerevisiae and their interactors: new technology advances the biology of the ABCC (MRP) subfamily.* Microbiol Mol Biol Rev, 2009. **73**(4): p. 577-93.
82. Longo-Sorbello, G.S. and J.R. Bertino, *Current understanding of methotrexate pharmacology and efficacy in acute leukemias. Use of newer antifolates in clinical trials.* Haematologica, 2001. **86**(2): p. 121-7.
83. Masters, J.R., et al., *Sensitivity of testis tumour cells to chemotherapeutic drugs: role of detoxifying pathways.* Eur J Cancer, 1996. **32A**(7): p. 1248-53.
84. Tew, K.D., *Glutathione-associated enzymes in anticancer drug resistance.* Cancer Res, 1994. **54**(16): p. 4313-20.
85. Igney, F.H. and P.H. Krammer, *Death and anti-death: tumour resistance to apoptosis.* Nat Rev Cancer, 2002. **2**(4): p. 277-88.
86. Weller, M., et al., *Protooncogene bcl-2 gene transfer abrogates Fas/APO-1 antibody-mediated apoptosis of human malignant glioma cells and confers resistance to chemotherapeutic drugs and therapeutic irradiation.* J Clin Invest, 1995. **95**(6): p. 2633-43.
87. Frosina, G., *DNA repair and resistance of gliomas to chemotherapy and radiotherapy.* Mol Cancer Res, 2009. **7**(7): p. 989-99.
88. Helleday, T., et al., *DNA repair pathways as targets for cancer therapy.* Nat Rev Cancer, 2008. **8**(3): p. 193-204.
89. Taverna, P., et al., *Inhibition of base excision repair potentiates iododeoxyuridine-induced cytotoxicity and radiosensitization.* Cancer Res, 2003. **63**(4): p. 838-46.
90. Chaudhry, M.A., *Base excision repair of ionizing radiation-induced DNA damage in G1 and G2 cell cycle phases.* Cancer Cell Int, 2007. **7**: p. 15.
91. Madlener, S., et al., *Essential role for mammalian apurinic/apyrimidinic (AP) endonuclease Ape1/Ref-1 in telomere maintenance.* Proc Natl Acad Sci U S A, 2013. **110**(44): p. 17844-9.
92. Veuger, S.J., J.E. Hunter, and B.W. Durkacz, *Ionizing radiation-induced NF-kappaB activation requires PARP-1 function to confer radioresistance.* Oncogene, 2009. **28**(6): p. 832-42.
93. Chatterjee, P., et al., *PARP inhibition sensitizes to low dose-rate radiation TMPRSS2-ERG fusion gene-expressing and PTEN-deficient prostate cancer cells.* PLoS One, 2013. **8**(4): p. e60408.
94. Yan, T., et al., *Methoxyamine potentiates iododeoxyuridine-induced radiosensitization by altering cell cycle kinetics and enhancing senescence.* Mol Cancer Ther, 2006. **5**(4): p. 893-902.
95. Kinsella, T.J., *Coordination of DNA mismatch repair and base excision repair processing of chemotherapy and radiation damage for targeting resistant cancers.* Clin Cancer Res, 2009. **15**(6): p. 1853-9.

96. Lim, Y.C., et al., *A role for homologous recombination and abnormal cell-cycle progression in radioresistance of glioma-initiating cells.* Mol Cancer Ther, 2012. **11**(9): p. 1863-72.
97. Brown, E.T. and J.T. Holt, *Rad51 overexpression rescues radiation resistance in BRCA2-defective cancer cells.* Mol Carcinog, 2009. **48**(2): p. 105-9.
98. Hine, C.M., A. Seluanov, and V. Gorbunova, *Rad51 promoter-targeted gene therapy is effective for in vivo visualization and treatment of cancer.* Mol Ther, 2012. **20**(2): p. 347-55.
99. Radvanyi, L., *Immunotherapy exposes cancer stem cell resistance and a new synthetic lethality.* Mol Ther, 2013. **21**(8): p. 1472-4.
100. Marabelle, A., et al., *Depleting tumor-specific Tregs at a single site eradicates disseminated tumors.* J Clin Invest, 2013. **123**(11): p. 4980.
101. Liu, Z., et al., *Tumor regulatory T cells potently abrogate antitumor immunity.* J Immunol, 2009. **182**(10): p. 6160-7.
102. Goel, S., et al., *Normalization of the vasculature for treatment of cancer and other diseases.* Physiol Rev, 2011. **91**(3): p. 1071-121.
103. Munn, D.H. and A.L. Mellor, *Indoleamine 2,3 dioxygenase and metabolic control of immune responses.* Trends Immunol, 2013. **34**(3): p. 137-43.
104. Sugimoto, H., et al., *Crystal structure of human indoleamine 2,3-dioxygenase: catalytic mechanism of O2 incorporation by a heme-containing dioxygenase.* Proc Natl Acad Sci U S A, 2006. **103**(8): p. 2611-6.
105. Shimizu, T., et al., *Indoleamine 2,3-dioxygenase. Purification and some properties.* J Biol Chem, 1978. **253**(13): p. 4700-6.
106. Chen, Y. and G.J. Guillemin, *Kynurenine pathway metabolites in humans: disease and healthy States.* Int J Tryptophan Res, 2009. **2**: p. 1-19.
107. Carmona-Ramirez, I., et al., *Curcumin restores Nrf2 levels and prevents quinolinic acid-induced neurotoxicity.* J Nutr Biochem, 2013. **24**(1): p. 14-24.
108. Grohmann, U., F. Fallarino, and P. Puccetti, *Tolerance, DCs and tryptophan: much ado about IDO.* Trends Immunol, 2003. **24**(5): p. 242-8.
109. Sahm, F., et al., *The endogenous tryptophan metabolite and NAD+ precursor quinolinic acid confers resistance of gliomas to oxidative stress.* Cancer Res, 2013. **73**(11): p. 3225-34.
110. Dai, X. and B.T. Zhu, *Indoleamine 2,3-dioxygenase tissue distribution and cellular localization in mice: implications for its biological functions.* J Histochem Cytochem, 2010. **58**(1): p. 17-28.
111. Yamazaki, F., et al., *Human indolylamine 2,3-dioxygenase. Its tissue distribution, and characterization of the placental enzyme.* Biochem J, 1985. **230**(3): p. 635-8.
112. Sedlmayr, P., et al., *Localization of indoleamine 2,3-dioxygenase in human female reproductive organs and the placenta.* Mol Hum Reprod, 2002. **8**(4): p. 385-91.
113. Yoshida, R., et al., *Induction of indoleamine 2,3-dioxygenase in mouse lung during virus infection.* Proc Natl Acad Sci U S A, 1979. **76**(8): p. 4084-6.
114. Robinson, C.M., P.T. Hale, and J.M. Carlin, *The role of IFN-gamma and TNF-alpha-responsive regulatory elements in the synergistic induction of indoleamine dioxygenase.* J Interferon Cytokine Res, 2005. **25**(1): p. 20-30.

115. Dejean, A.S., S.M. Hedrick, and Y.M. Kerdiles, *Highly specialized role of Forkhead box O transcription factors in the immune system.* Antioxid Redox Signal, 2011. **14**(4): p. 663-74.
116. Orabona, C., et al., *Toward the identification of a tolerogenic signature in IDO-competent dendritic cells.* Blood, 2006. **107**(7): p. 2846-54.
117. Orabona, C., et al., *SOCS3 drives proteasomal degradation of indoleamine 2,3-dioxygenase (IDO) and antagonizes IDO-dependent tolerogenesis.* Proc Natl Acad Sci U S A, 2008. **105**(52): p. 20828-33.
118. Nino-Castro, A., et al., *The IDO1-induced kynurenines play a major role in the antimicrobial effect of human myeloid cells against Listeria monocytogenes.* Innate Immun, 2013.
119. Divanovic, S., et al., *Opposing biological functions of tryptophan catabolizing enzymes during intracellular infection.* J Infect Dis, 2012. **205**(1): p. 152-61.
120. Munn, D.H., et al., *GCN2 kinase in T cells mediates proliferative arrest and anergy induction in response to indoleamine 2,3-dioxygenase.* Immunity, 2005. **22**(5): p. 633-42.
121. Kilberg, M.S., J. Shan, and N. Su, *ATF4-dependent transcription mediates signaling of amino acid limitation.* Trends Endocrinol Metab, 2009. **20**(9): p. 436-43.
122. Sundrud, M.S., et al., *Halofuginone inhibits TH17 cell differentiation by activating the amino acid starvation response.* Science, 2009. **324**(5932): p. 1334-8.
123. Fallarino, F., et al., *The combined effects of tryptophan starvation and tryptophan catabolites down-regulate T cell receptor zeta-chain and induce a regulatory phenotype in naive T cells.* J Immunol, 2006. **176**(11): p. 6752-61.
124. Sharma, M.D., et al., *Plasmacytoid dendritic cells from mouse tumor-draining lymph nodes directly activate mature Tregs via indoleamine 2,3-dioxygenase.* J Clin Invest, 2007. **117**(9): p. 2570-82.
125. Ogata, S., et al., *Apoptosis induced by nicotinamide-related compounds and quinolinic acid in HL-60 cells.* Biosci Biotechnol Biochem, 2000. **64**(2): p. 327-32.
126. Mezrich, J.D., et al., *An interaction between kynurenine and the aryl hydrocarbon receptor can generate regulatory T cells.* J Immunol, 2010. **185**(6): p. 3190-8.
127. Opitz, C.A., et al., *An endogenous tumour-promoting ligand of the human aryl hydrocarbon receptor.* Nature, 2011. **478**(7368): p. 197-203.
128. Nguyen, N.T., et al., *Aryl hydrocarbon receptor negatively regulates dendritic cell immunogenicity via a kynurenine-dependent mechanism.* Proc Natl Acad Sci U S A, 2010. **107**(46): p. 19961-6.
129. Pallotta, M.T., et al., *Indoleamine 2,3-dioxygenase is a signaling protein in long-term tolerance by dendritic cells.* Nat Immunol, 2011. **12**(9): p. 870-8.
130. Munn, D.H., et al., *Prevention of allogeneic fetal rejection by tryptophan catabolism.* Science, 1998. **281**(5380): p. 1191-3.
131. Alexander, A.M., et al., *Indoleamine 2,3-dioxygenase expression in transplanted NOD Islets prolongs graft survival after adoptive transfer of diabetogenic splenocytes.* Diabetes, 2002. **51**(2): p. 356-65.

132. Beutelspacher, S.C., et al., *Function of indoleamine 2,3-dioxygenase in corneal allograft rejection and prolongation of allograft survival by over-expression.* Eur J Immunol, 2006. **36**(3): p. 690-700.
133. Jasperson, L.K., et al., *Inducing the tryptophan catabolic pathway, indoleamine 2,3-dioxygenase (IDO), for suppression of graft-versus-host disease (GVHD) lethality.* Blood, 2009. **114**(24): p. 5062-70.
134. Munn, D.H. and A.L. Mellor, *Indoleamine 2,3-dioxygenase and tumor-induced tolerance.* J Clin Invest, 2007. **117**(5): p. 1147-54.
135. Uyttenhove, C., et al., *Evidence for a tumoral immune resistance mechanism based on tryptophan degradation by indoleamine 2,3-dioxygenase.* Nat Med, 2003. **9**(10): p. 1269-74.
136. Muller, A.J., et al., *Inhibition of indoleamine 2,3-dioxygenase, an immunoregulatory target of the cancer suppression gene Bin1, potentiates cancer chemotherapy.* Nat Med, 2005. **11**(3): p. 312-9.
137. Pan, K., et al., *Expression and prognosis role of indoleamine 2,3-dioxygenase in hepatocellular carcinoma.* J Cancer Res Clin Oncol, 2008. **134**(11): p. 1247-53.
138. Smith, C., et al., *IDO is a nodal pathogenic driver of lung cancer and metastasis development.* Cancer Discov, 2012. **2**(8): p. 722-35.
139. Mansfield, A.S., et al., *Simultaneous Foxp3 and IDO expression is associated with sentinel lymph node metastases in breast cancer.* BMC Cancer, 2009. **9**: p. 231.
140. Brandacher, G., et al., *Prognostic value of indoleamine 2,3-dioxygenase expression in colorectal cancer: effect on tumor-infiltrating T cells.* Clin Cancer Res, 2006. **12**(4): p. 1144-51.
141. Ino, K., et al., *Indoleamine 2,3-dioxygenase is a novel prognostic indicator for endometrial cancer.* Br J Cancer, 2006. **95**(11): p. 1555-61.
142. Liu, P., et al., *Expression of indoleamine 2,3-dioxygenase in nasopharyngeal carcinoma impairs the cytolytic function of peripheral blood lymphocytes.* BMC Cancer, 2009. **9**: p. 416.
143. Inaba, T., et al., *Role of the immunosuppressive enzyme indoleamine 2,3-dioxygenase in the progression of ovarian carcinoma.* Gynecol Oncol, 2009. **115**(2): p. 185-92.
144. Holmgaard, R.B., et al., *Indoleamine 2,3-dioxygenase is a critical resistance mechanism in antitumor T cell immunotherapy targeting CTLA-4.* J Exp Med, 2013. **210**(7): p. 1389-402.
145. Godin-Ethier, J., et al., *Indoleamine 2,3-dioxygenase expression in human cancers: clinical and immunologic perspectives.* Clin Cancer Res, 2011. **17**(22): p. 6985-91.
146. Lob, S., et al., *Inhibitors of indoleamine-2,3-dioxygenase for cancer therapy: can we see the wood for the trees?* Nat Rev Cancer, 2009. **9**(6): p. 445-52.
147. Cady, S.G. and M. Sono, *1-Methyl-DL-tryptophan, beta-(3-benzofuranyl)-DL-alanine (the oxygen analog of tryptophan), and beta-[3-benzo(b)thienyl]-DL-alanine (the sulfur analog of tryptophan) are competitive inhibitors for indoleamine 2,3-dioxygenase.* Arch Biochem Biophys, 1991. **291**(2): p. 326-33.
148. Lob, S., et al., *Levo- but not dextro-1-methyl tryptophan abrogates the IDO activity of human dendritic cells.* Blood, 2008. **111**(4): p. 2152-4.

149. Qian, F., et al., *Efficacy of levo-1-methyl tryptophan and dextro-1-methyl tryptophan in reversing indoleamine-2,3-dioxygenase-mediated arrest of T-cell proliferation in human epithelial ovarian cancer.* Cancer Res, 2009. **69**(13): p. 5498-504.
150. Dolusic, E. and R. Frederick, *Indoleamine 2,3-dioxygenase inhibitors: a patent review (2008 - 2012).* Expert Opin Ther Pat, 2013.
151. Sono, M. and S.G. Cady, *Enzyme kinetic and spectroscopic studies of inhibitor and effector interactions with indoleamine 2,3-dioxygenase. 1. Norharman and 4-phenylimidazole binding to the enzyme as inhibitors and heme ligands.* Biochemistry, 1989. **28**(13): p. 5392-9.
152. Berthon, C., et al., *Metabolites of tryptophan catabolism are elevated in sera of patients with myelodysplastic syndromes and inhibit hematopoietic progenitor amplification.* Leuk Res, 2013. **37**(5): p. 573-9.
153. Temml, V., et al., *Interaction of Carthamus tinctorius lignan arctigenin with the binding site of tryptophan-degrading enzyme indoleamine 2,3-dioxygenase.* FEBS Open Bio, 2013. **3**: p. 450-2.
154. Eguchi, N., et al., *Inhibition of indoleamine 2,3-dioxygenase and tryptophan 2,3-dioxygenase by beta-carboline and indole derivatives.* Arch Biochem Biophys, 1984. **232**(2): p. 602-9.
155. Efimov, I., et al., *The mechanism of substrate inhibition in human indoleamine 2,3-dioxygenase.* J Am Chem Soc, 2012. **134**(6): p. 3034-41.
156. Lancellotti, S., L. Novarese, and R. De Cristofaro, *Biochemical properties of indoleamine 2,3-dioxygenase: from structure to optimized design of inhibitors.* Curr Med Chem, 2011. **18**(15): p. 2205-14.
157. Muller, A.J. and P.A. Scherle, *Targeting the mechanisms of tumoral immune tolerance with small-molecule inhibitors.* Nat Rev Cancer, 2006. **6**(8): p. 613-25.
158. Zheng, X., et al., *Reinstalling antitumor immunity by inhibiting tumor-derived immunosuppressive molecule IDO through RNA interference.* J Immunol, 2006. **177**(8): p. 5639-46.
159. Yen, M.C., et al., *A novel cancer therapy by skin delivery of indoleamine 2,3-dioxygenase siRNA.* Clin Cancer Res, 2009. **15**(2): p. 641-9.
160. Huang, T.T., et al., *Skin delivery of short hairpin RNA of indoleamine 2,3 dioxygenase induces antitumor immunity against orthotopic and metastatic liver cancer.* Cancer Sci, 2011. **102**(12): p. 2214-20.
161. Creelan, B.C., et al., *Indoleamine 2,3-dioxygenase activity and clinical outcome following induction chemotherapy and concurrent chemoradiation in Stage III non-small cell lung cancer.* Oncoimmunology, 2013. **2**(3): p. e23428.
162. Okamoto, A., et al., *Indoleamine 2,3-dioxygenase serves as a marker of poor prognosis in gene expression profiles of serous ovarian cancer cells.* Clin Cancer Res, 2005. **11**(16): p. 6030-9.
163. Sim, S.H., et al., *Influence of chemotherapy on nitric oxide synthase, indole-amine-2,3-dioxygenase and CD124 expression in granulocytes and monocytes of non-small cell lung cancer.* Cancer Sci, 2012. **103**(2): p. 155-60.
164. Sancar, A., et al., *Molecular mechanisms of mammalian DNA repair and the DNA damage checkpoints.* Annu Rev Biochem, 2004. **73**: p. 39-85.

165. Houtgraaf, J.H., J. Versmissen, and W.J. van der Giessen, *A concise review of DNA damage checkpoints and repair in mammalian cells.* Cardiovasc Revasc Med, 2006. **7**(3): p. 165-72.
166. Ljungman, M., *Targeting the DNA damage response in cancer.* Chem Rev, 2009. **109**(7): p. 2929-50.
167. Robertson, A.B., et al., *DNA repair in mammalian cells: Base excision repair: the long and short of it.* Cell Mol Life Sci, 2009. **66**(6): p. 981-93.
168. Petermann, E., M. Ziegler, and S.L. Oei, *ATP-dependent selection between single nucleotide and long patch base excision repair.* DNA Repair (Amst), 2003. **2**(10): p. 1101-14.
169. Kim, K., S. Biade, and Y. Matsumoto, *Involvement of flap endonuclease 1 in base excision DNA repair.* J Biol Chem, 1998. **273**(15): p. 8842-8.
170. Klungland, A. and T. Lindahl, *Second pathway for completion of human DNA base excision-repair: reconstitution with purified proteins and requirement for DNase IV (FEN1).* EMBO J, 1997. **16**(11): p. 3341-8.
171. Kubota, Y., et al., *Reconstitution of DNA base excision-repair with purified human proteins: interaction between DNA polymerase beta and the XRCC1 protein.* EMBO J, 1996. **15**(23): p. 6662-70.
172. Caldecott, K.W., et al., *An interaction between the mammalian DNA repair protein XRCC1 and DNA ligase III.* Mol Cell Biol, 1994. **14**(1): p. 68-76.
173. Wu, X., et al., *Processing of branched DNA intermediates by a complex of human FEN-1 and PCNA.* Nucleic Acids Res, 1996. **24**(11): p. 2036-43.
174. Sharma, R.A. and G.L. Dianov, *Targeting base excision repair to improve cancer therapies.* Mol Aspects Med, 2007. **28**(3-4): p. 345-74.
175. Dianov, G.L., *Base excision repair targets for cancer therapy.* Am J Cancer Res, 2011. **1**(7): p. 845-51.
176. Bapat, A., M.L. Fishel, and M.R. Kelley, *Going ape as an approach to cancer therapeutics.* Antioxid Redox Signal, 2009. **11**(3): p. 651-68.
177. Liuzzi, M. and M. Talpaert-Borle, *A new approach to the study of the base-excision repair pathway using methoxyamine.* J Biol Chem, 1985. **260**(9): p. 5252-8.
178. Montaldi, A.P. and E.T. Sakamoto-Hojo, *Methoxyamine sensitizes the resistant glioblastoma T98G cell line to the alkylating agent temozolomide.* Clin Exp Med, 2012.
179. Bulgar, A.D., et al., *Removal of uracil by uracil DNA glycosylase limits pemetrexed cytotoxicity: overriding the limit with methoxyamine to inhibit base excision repair.* Cell Death Dis, 2012. **3**: p. e252.
180. Fishel, M.L., et al., *Manipulation of base excision repair to sensitize ovarian cancer cells to alkylating agent temozolomide.* Clin Cancer Res, 2007. **13**(1): p. 260-7.
181. Yang, S., et al., *Development and validation of an LC-MS/MS method for pharmacokinetic study of methoxyamine in phase I clinical trial.* J Chromatogr B Analyt Technol Biomed Life Sci, 2012. **901**: p. 25-33.
182. Bulgar, A.D., et al., *Targeting base excision repair suggests a new therapeutic strategy of fludarabine for the treatment of chronic lymphocytic leukemia.* Leukemia, 2010. **24**(10): p. 1795-9.

183. Li, X. and W.D. Heyer, *Homologous recombination in DNA repair and DNA damage tolerance.* Cell Res, 2008. **18**(1): p. 99-113.
184. Moynahan, M.E., A.J. Pierce, and M. Jasin, *BRCA2 is required for homology-directed repair of chromosomal breaks.* Mol Cell, 2001. **7**(2): p. 263-72.
185. Welcsh, P.L. and M.C. King, *BRCA1 and BRCA2 and the genetics of breast and ovarian cancer.* Hum Mol Genet, 2001. **10**(7): p. 705-13.
186. Roy, R., J. Chun, and S.N. Powell, *BRCA1 and BRCA2: different roles in a common pathway of genome protection.* Nat Rev Cancer, 2012. **12**(1): p. 68-78.
187. Rytelewski, M., et al., *Inhibition of BRCA2 and Thymidylate Synthase Creates Multidrug Sensitive Tumor Cells via the Induction of Combined "Complementary Lethality".* Mol Ther Nucleic Acids, 2013. **2**: p. e78.
188. Sung, P. and H. Klein, *Mechanism of homologous recombination: mediators and helicases take on regulatory functions.* Nat Rev Mol Cell Biol, 2006. **7**(10): p. 739-50.
189. Schreiber, V., et al., *Poly(ADP-ribose): novel functions for an old molecule.* Nat Rev Mol Cell Biol, 2006. **7**(7): p. 517-28.
190. de Murcia, J.M., et al., *Requirement of poly(ADP-ribose) polymerase in recovery from DNA damage in mice and in cells.* Proc Natl Acad Sci U S A, 1997. **94**(14): p. 7303-7.
191. Wang, Z.Q., et al., *PARP is important for genomic stability but dispensable in apoptosis.* Genes Dev, 1997. **11**(18): p. 2347-58.
192. Masutani, M., et al., *Poly(ADP-ribose) polymerase gene disruption conferred mice resistant to streptozotocin-induced diabetes.* Proc Natl Acad Sci U S A, 1999. **96**(5): p. 2301-4.
193. Jagtap, P. and C. Szabo, *Poly(ADP-ribose) polymerase and the therapeutic effects of its inhibitors.* Nat Rev Drug Discov, 2005. **4**(5): p. 421-40.
194. Ame, J.C., et al., *PARP-2, A novel mammalian DNA damage-dependent poly(ADP-ribose) polymerase.* J Biol Chem, 1999. **274**(25): p. 17860-8.
195. Menissier de Murcia, J., et al., *Functional interaction between PARP-1 and PARP-2 in chromosome stability and embryonic development in mouse.* EMBO J, 2003. **22**(9): p. 2255-63.
196. Schreiber, V., et al., *Poly(ADP-ribose) polymerase-2 (PARP-2) is required for efficient base excision DNA repair in association with PARP-1 and XRCC1.* J Biol Chem, 2002. **277**(25): p. 23028-36.
197. Javle, M. and N.J. Curtin, *The role of PARP in DNA repair and its therapeutic exploitation.* Br J Cancer, 2011. **105**(8): p. 1114-22.
198. Houtkooper, R.H., et al., *The secret life of NAD+: an old metabolite controlling new metabolic signaling pathways.* Endocr Rev, 2010. **31**(2): p. 194-223.
199. Masson, M., et al., *XRCC1 is specifically associated with poly(ADP-ribose) polymerase and negatively regulates its activity following DNA damage.* Mol Cell Biol, 1998. **18**(6): p. 3563-71.
200. Okano, S., et al., *Spatial and temporal cellular responses to single-strand breaks in human cells.* Mol Cell Biol, 2003. **23**(11): p. 3974-81.
201. Caldecott, K.W., *XRCC1 and DNA strand break repair.* DNA Repair (Amst), 2003. **2**(9): p. 955-69.

202. Heale, J.T., et al., *Condensin I interacts with the PARP-1-XRCC1 complex and functions in DNA single-strand break repair.* Mol Cell, 2006. **21**(6): p. 837-48.
203. Helleday, T., H.E. Bryant, and N. Schultz, *Poly(ADP-ribose) polymerase (PARP-1) in homologous recombination and as a target for cancer therapy.* Cell Cycle, 2005. **4**(9): p. 1176-8.
204. Schultz, N., et al., *Poly(ADP-ribose) polymerase (PARP-1) has a controlling role in homologous recombination.* Nucleic Acids Res, 2003. **31**(17): p. 4959-64.
205. Kummar, S., et al., *Advances in using PARP inhibitors to treat cancer.* BMC Med, 2012. **10**: p. 25.
206. Farmer, H., et al., *Targeting the DNA repair defect in BRCA mutant cells as a therapeutic strategy.* Nature, 2005. **434**(7035): p. 917-21.
207. Ashworth, A., *A synthetic lethal therapeutic approach: poly(ADP) ribose polymerase inhibitors for the treatment of cancers deficient in DNA double-strand break repair.* J Clin Oncol, 2008. **26**(22): p. 3785-90.
208. Ledermann, J., et al., *Olaparib maintenance therapy in platinum-sensitive relapsed ovarian cancer.* N Engl J Med, 2012. **366**(15): p. 1382-92.
209. Evers, B., et al., *Selective inhibition of BRCA2-deficient mammary tumor cell growth by AZD2281 and cisplatin.* Clin Cancer Res, 2008. **14**(12): p. 3916-25.
210. Rottenberg, S., et al., *High sensitivity of BRCA1-deficient mammary tumors to the PARP inhibitor AZD2281 alone and in combination with platinum drugs.* Proc Natl Acad Sci U S A, 2008. **105**(44): p. 17079-84.
211. Fong, P.C., et al., *Inhibition of poly(ADP-ribose) polymerase in tumors from BRCA mutation carriers.* N Engl J Med, 2009. **361**(2): p. 123-34.
212. Fong, P.C., et al., *Poly(ADP)-ribose polymerase inhibition: frequent durable responses in BRCA carrier ovarian cancer correlating with platinum-free interval.* J Clin Oncol, 2010. **28**(15): p. 2512-9.
213. Zhang, Y.W., et al., *Poly(ADP-ribose) polymerase and XPF-ERCC1 participate in distinct pathways for the repair of topoisomerase I-induced DNA damage in mammalian cells.* Nucleic Acids Res, 2011. **39**(9): p. 3607-20.
214. Mendes-Pereira, A.M., et al., *Synthetic lethal targeting of PTEN mutant cells with PARP inhibitors.* EMBO Mol Med, 2009. **1**(6-7): p. 315-22.
215. Khan, J.A., et al., *Nicotinamide adenine dinucleotide metabolism as an attractive target for drug discovery.* Expert Opin Ther Targets, 2007. **11**(5): p. 695-705.
216. Tanaka, T. and W.E. Knox, *The nature and mechanism of the tryptophan pyrrolase (peroxidase-oxidase) reaction of Pseudomonas and of rat liver.* J Biol Chem, 1959. **234**(5): p. 1162-70.
217. Moore, G.P. and D.T. Sullivan, *The characterization of multiple forms of kynurenine formidase in Drosophila melanogaster.* Biochim Biophys Acta, 1975. **397**(2): p. 468-77.
218. Breton, J., et al., *Functional characterization and mechanism of action of recombinant human kynurenine 3-hydroxylase.* Eur J Biochem, 2000. **267**(4): p. 1092-9.
219. Phillips, R.S., B. Sundararaju, and S.V. Koushik, *The catalytic mechanism of kynureninase from Pseudomonas fluorescens: evidence for transient quinonoid and ketimine intermediates from rapid-scanning stopped-flow spectrophotometry.* Biochemistry, 1998. **37**(24): p. 8783-9.

220. Cesura, A.M., et al., *Molecular characterisation of kynurenine pathway enzymes. 3-Hydroxyanthranilic-acid dioxygenase and kynurenine aminotransferase.* Adv Exp Med Biol, 1996. **398**: p. 477-83.
221. Foster, A.C., R.J. White, and R. Schwarcz, *Synthesis of quinolinic acid by 3-hydroxyanthranilic acid oxygenase in rat brain tissue in vitro.* J Neurochem, 1986. **47**(1): p. 23-30.
222. Di Stefano, M. and L. Conforti, *Diversification of NAD biological role: the importance of location.* FEBS J, 2013.
223. Bieganowski, P. and C. Brenner, *Discoveries of nicotinamide riboside as a nutrient and conserved NRK genes establish a Preiss-Handler independent route to NAD+ in fungi and humans.* Cell, 2004. **117**(4): p. 495-502.
224. Magni, G., et al., *Enzymology of NAD+ homeostasis in man.* Cell Mol Life Sci, 2004. **61**(1): p. 19-34.
225. Chambon, P., J.D. Weill, and P. Mandel, *Nicotinamide mononucleotide activation of new DNA-dependent polyadenylic acid synthesizing nuclear enzyme.* Biochem Biophys Res Commun, 1963. **11**: p. 39-43.
226. Hassa, P.O., et al., *Nuclear ADP-ribosylation reactions in mammalian cells: where are we today and where are we going?* Microbiol Mol Biol Rev, 2006. **70**(3): p. 789-829.
227. Burkle, A., *Poly(ADP-ribose). The most elaborate metabolite of NAD+.* FEBS J, 2005. **272**(18): p. 4576-89.
228. Jacobson, E.L., W.M. Shieh, and A.C. Huang, *Mapping the role of NAD metabolism in prevention and treatment of carcinogenesis.* Mol Cell Biochem, 1999. **193**(1-2): p. 69-74.
229. D'Amours, D., et al., *Poly(ADP-ribosyl)ation reactions in the regulation of nuclear functions.* Biochem J, 1999. **342 (Pt 2)**: p. 249-68.
230. Goodwin, P.M., et al., *The effect of gamma radiation and neocarzinostatin on NAD and ATP levels in mouse leukaemia cells.* Biochim Biophys Acta, 1978. **543**(4): p. 576-82.
231. Skidmore, C.J., et al., *The involvement of poly(ADP-ribose) polymerase in the degradation of NAD caused by gamma-radiation and N-methyl-N-nitrosourea.* Eur J Biochem, 1979. **101**(1): p. 135-42.
232. Williams, G.T., et al., *NAD metabolism and mitogen stimulation of human lymphocytes.* Exp Cell Res, 1985. **160**(2): p. 419-26.
233. Chappie, J.S., et al., *The structure of a eukaryotic nicotinic acid phosphoribosyltransferase reveals structural heterogeneity among type II PRTases.* Structure, 2005. **13**(9): p. 1385-96.
234. Garten, A., et al., *Nampt: linking NAD biology, metabolism and cancer.* Trends Endocrinol Metab, 2009. **20**(3): p. 130-8.
235. Kim, M.Y., T. Zhang, and W.L. Kraus, *Poly(ADP-ribosyl)ation by PARP-1: 'PAR-laying' NAD+ into a nuclear signal.* Genes Dev, 2005. **19**(17): p. 1951-67.
236. Tanno, M., et al., *Nucleocytoplasmic shuttling of the NAD+-dependent histone deacetylase SIRT1.* J Biol Chem, 2007. **282**(9): p. 6823-32.
237. Hallows, W.C., S. Lee, and J.M. Denu, *Sirtuins deacetylate and activate mammalian acetyl-CoA synthetases.* Proc Natl Acad Sci U S A, 2006. **103**(27): p. 10230-5.

238. Gagne, J.P., et al., *The expanding role of poly(ADP-ribose) metabolism: current challenges and new perspectives.* Curr Opin Cell Biol, 2006. **18**(2): p. 145-51.
239. Oei, S.L., C. Keil, and M. Ziegler, *Poly(ADP-ribosylation) and genomic stability.* Biochem Cell Biol, 2005. **83**(3): p. 263-9.
240. Pittelli, M., et al., *Inhibition of nicotinamide phosphoribosyltransferase: cellular bioenergetics reveals a mitochondrial insensitive NAD pool.* J Biol Chem, 2010. **285**(44): p. 34106-14.
241. Fu, C.S., et al., *Biochemical markers for assessment of niacin status in young men: levels of erythrocyte niacin coenzymes and plasma tryptophan.* J Nutr, 1989. **119**(12): p. 1949-55.
242. Hasmann, M. and I. Schemainda, *FK866, a highly specific noncompetitive inhibitor of nicotinamide phosphoribosyltransferase, represents a novel mechanism for induction of tumor cell apoptosis.* Cancer Res, 2003. **63**(21): p. 7436-42.
243. Nicotera, P. and M. Leist, *Energy supply and the shape of death in neurons and lymphoid cells.* Cell Death Differ, 1997. **4**(6): p. 435-42.
244. Carreras, C.W. and D.V. Santi, *The catalytic mechanism and structure of thymidylate synthase.* Annu Rev Biochem, 1995. **64**: p. 721-62.
245. Galvani, E., G.J. Peters, and E. Giovannetti, *Thymidylate synthase inhibitors for non-small cell lung cancer.* Expert Opin Investig Drugs, 2011. **20**(10): p. 1343-56.
246. Chen, M., et al., *Transgenic expression of human thymidylate synthase accelerates the development of hyperplasia and tumors in the endocrine pancreas.* Oncogene, 2007. **26**(33): p. 4817-24.
247. Rahman, L., et al., *Thymidylate synthase as an oncogene: a novel role for an essential DNA synthesis enzyme.* Cancer Cell, 2004. **5**(4): p. 341-51.
248. Chu, E., *Ode to 5-Fluorouracil*, in *Clinical Colorectal Cancer*2007. p. 609.
249. Meyerhardt, J.A. and R.J. Mayer, *Systemic therapy for colorectal cancer.* N Engl J Med, 2005. **352**(5): p. 476-87.
250. Scagliotti, G.V., et al., *Phase III study comparing cisplatin plus gemcitabine with cisplatin plus pemetrexed in chemotherapy-naive patients with advanced-stage non-small-cell lung cancer.* J Clin Oncol, 2008. **26**(21): p. 3543-51.
251. Parr, A.L., et al., *5-fluorouracil-mediated thymidylate synthase induction in malignant and nonmalignant human cells.* Biochem Pharmacol, 1998. **56**(2): p. 231-5.
252. Peters, G.J., et al., *Thymidylate synthase inhibition after administration of fluorouracil with or without leucovorin in colon cancer patients: implications for treatment with fluorouracil.* J Clin Oncol, 1994. **12**(10): p. 2035-42.
253. Chu, E., et al., *Identification of an RNA binding site for human thymidylate synthase.* Proc Natl Acad Sci U S A, 1993. **90**(2): p. 517-21.
254. Ferguson, P.J., et al., *Antisense-induced down-regulation of thymidylate synthase and enhanced cytotoxicity of 5-FUdR in 5-FUdR-resistant HeLa cells.* Br J Pharmacol, 2001. **134**(7): p. 1437-46.
255. Di Cresce, C., et al., *Combining small interfering RNAs targeting thymidylate synthase and thymidine kinase 1 or 2 sensitizes human tumor cells to 5-fluorodeoxyuridine and pemetrexed.* J Pharmacol Exp Ther, 2011. **338**(3): p. 952-63.

256. Fuchs, U., C. Damm-Welk, and A. Borkhardt, *Silencing of disease-related genes by small interfering RNAs.* Curr Mol Med, 2004. **4**(5): p. 507-17.
257. Aigner, A., *Applications of RNA interference: current state and prospects for siRNA-based strategies in vivo.* Appl Microbiol Biotechnol, 2007. **76**(1): p. 9-21.
258. Rao, D.D., et al., *siRNA vs. shRNA: similarities and differences.* Adv Drug Deliv Rev, 2009. **61**(9): p. 746-59.
259. Obojes, K., et al., *Indoleamine 2,3-dioxygenase mediates cell type-specific anti-measles virus activity of gamma interferon.* J Virol, 2005. **79**(12): p. 7768-76.
260. Logan, G.J., et al., *HeLa cells cocultured with peripheral blood lymphocytes acquire an immuno-inhibitory phenotype through up-regulation of indoleamine 2,3-dioxygenase activity.* Immunology, 2002. **105**(4): p. 478-87.
261. Chalmers, A.J., *The potential role and application of PARP inhibitors in cancer treatment.* Br Med Bull, 2009. **89**: p. 23-40.
262. Karanikas, V., et al., *Indoleamine 2,3-dioxygenase (IDO) expression in lung cancer.* Cancer Biol Ther, 2007. **6**(8): p. 1258-62.
263. Gottesman, M.M., *Mechanisms of cancer drug resistance.* Annu Rev Med, 2002. **53**: p. 615-27.
264. Nahimana, A., et al., *The NAD biosynthesis inhibitor APO866 has potent antitumor activity against hematologic malignancies.* Blood, 2009. **113**(14): p. 3276-86.
265. Jason, T.L., et al., *ODN 491, a novel antisense oligodeoxynucleotide that targets thymidylate synthase, exerts cell-specific effects in human tumor cell lines.* DNA Cell Biol, 2008. **27**(5): p. 229-40.
266. Ferguson, P.J., et al., *Antisense down-regulation of thymidylate synthase to suppress growth and enhance cytotoxicity of 5-FUdR, 5-FU and Tomudex in HeLa cells.* Br J Pharmacol, 1999. **127**(8): p. 1777-86.
267. Rezaee, M., L. Sanche, and D.J. Hunting, *Cisplatin enhances the formation of DNA single- and double-strand breaks by hydrated electrons and hydroxyl radicals.* Radiat Res, 2013. **179**(3): p. 323-31.
268. Muller, A.J., et al., *Chronic inflammation that facilitates tumor progression creates local immune suppression by inducing indoleamine 2,3 dioxygenase.* Proc Natl Acad Sci U S A, 2008. **105**(44): p. 17073-8.
269. Donovan, M.J., et al., *Indoleamine 2,3-dioxygenase (IDO) induced by Leishmania infection of human dendritic cells.* Parasite Immunol, 2012. **34**(10): p. 464-72.
270. Taylor, M.W. and G.S. Feng, *Relationship between interferon-gamma, indoleamine 2,3-dioxygenase, and tryptophan catabolism.* FASEB J, 1991. **5**(11): p. 2516-22.
271. Mobergslien, A. and M. Sioud, *Optimized protocols for siRNA delivery into monocytes and dendritic cells.* Methods Mol Biol, 2010. **629**: p. 71-85.
272. Sato, N., et al., *Downregulation of indoleamine-2,3-dioxygenase in cervical cancer cells suppresses tumor growth by promoting natural killer cell accumulation.* Oncol Rep, 2012. **28**(5): p. 1574-8.
273. Sorensen, R.B., et al., *Spontaneous cytotoxic T-Cell reactivity against indoleamine 2,3-dioxygenase-2.* Cancer Res, 2011. **71**(6): p. 2038-44.
274. Sorensen, R.B., et al., *Indoleamine 2,3-dioxygenase specific, cytotoxic T cells as immune regulators.* Blood, 2011. **117**(7): p. 2200-10.

275. Munn, D.H., et al., *Inhibition of T cell proliferation by macrophage tryptophan catabolism.* J Exp Med, 1999. **189**(9): p. 1363-72.
276. Curtin, N.J. and C. Szabo, *Therapeutic applications of PARP inhibitors: anticancer therapy and beyond.* Mol Aspects Med, 2013. **34**(6): p. 1217-56.
277. Curtin, N.J., *DNA repair dysregulation from cancer driver to therapeutic target.* Nat Rev Cancer, 2012. **12**(12): p. 801-17.
278. Virag, L., et al., *Poly(ADP-ribose) signaling in cell death.* Mol Aspects Med, 2013. **34**(6): p. 1153-67.
279. von Heideman, A., et al., *Safety and efficacy of NAD depleting cancer drugs: results of a phase I clinical trial of CHS 828 and overview of published data.* Cancer Chemother Pharmacol, 2010. **65**(6): p. 1165-72.
280. Lorenzen, J., et al., *Human tumour-associated NK cells secrete increased amounts of interferon-gamma and interleukin-4.* Br J Cancer, 1991. **64**(3): p. 457-62.
281. Alshaker, H.A. and K.Z. Matalka, *IFN-gamma, IL-17 and TGF-beta involvement in shaping the tumor microenvironment: The significance of modulating such cytokines in treating malignant solid tumors.* Cancer Cell Int, 2011. **11**: p. 33.
282. Barber, L.J., et al., *Secondary mutations in BRCA2 associated with clinical resistance to a PARP inhibitor.* J Pathol, 2013. **229**(3): p. 422-9.
283. Goellner, E.M., et al., *Overcoming temozolomide resistance in glioblastoma via dual inhibition of NAD+ biosynthesis and base excision repair.* Cancer Res, 2011. **71**(6): p. 2308-17.
284. Gordon, M.S., et al., *A phase 1 study of TRC102, an inhibitor of base excision repair, and pemetrexed in patients with advanced solid tumors.* Invest New Drugs, 2013. **31**(3): p. 714-23.
285. Weeks, L.D., P. Fu, and S.L. Gerson, *Uracil-DNA glycosylase expression determines human lung cancer cell sensitivity to pemetrexed.* Mol Cancer Ther, 2013. **12**(10): p. 2248-60.
286. Lau, J.P., et al., *Effects of gemcitabine on APE/ref-1 endonuclease activity in pancreatic cancer cells, and the therapeutic potential of antisense oligonucleotides.* Br J Cancer, 2004. **91**(6): p. 1166-73.
287. Fischer, J.A., S. Muller-Weeks, and S.J. Caradonna, *Fluorodeoxyuridine modulates cellular expression of the DNA base excision repair enzyme uracil-DNA glycosylase.* Cancer Res, 2006. **66**(17): p. 8829-37.
288. Yang, L.Y., et al., *Expression of ERCC1 antisense RNA abrogates gemicitabine-mediated cytotoxic synergism with cisplatin in human colon tumor cells defective in mismatch repair but proficient in nucleotide excision repair.* Clin Cancer Res, 2000. **6**(3): p. 773-81.
289. Shewach, D.S. and T.S. Lawrence, *Antimetabolite radiosensitizers.* J Clin Oncol, 2007. **25**(26): p. 4043-50.
290. Genova, C., et al., *Pemetrexed for the treatment of non-small cell lung cancer.* Expert Opin Pharmacother, 2013. **14**(11): p. 1545-58.
291. Gudmundsdottir, K. and A. Ashworth, *The roles of BRCA1 and BRCA2 and associated proteins in the maintenance of genomic stability.* Oncogene, 2006. **25**(43): p. 5864-74.

292. Chen, Y., L. Zhang, and Q. Hao, *Olaparib: a promising PARP inhibitor in ovarian cancer therapy.* Arch Gynecol Obstet, 2013. **288**(2): p. 367-74.
293. Adams, S., et al., *The kynurenine pathway in brain tumor pathogenesis.* Cancer Res, 2012. **72**(22): p. 5649-57.

Appendix

Copyright and Co-Authorship Statement

 Experiments presented in Figure 1A and 3D were performed by A.N. Shivji, M.A. Yekta, and D.M. Mazzuka. Experiment presented in Figure 4 was carried out by M.J. Harding and S.M.M. Haeryfar. M. Rytelewski was involved in performing experiments presented in Figure 1B and 1C.

American Journal of Transplantation
Wiley Periodicals Inc.

doi: 10.1111/j.1600-6143.2011.03811.x

Differential Regulation of Simultaneous Antitumor and Alloreactive CD8$^+$ T-Cell Responses in the Same Host by Rapamycin

S. Maleki Vareki[a], M. J. Harding[a], J. Waithman[b], D. Zanker[b], A. N. Shivji[a], M. Rytelewski[a], D. M. Mazzuca[a], M. A. Yekta[a], W. Chen[b], T. D. Schell[c] and S. M. M. Haeryfar[a,d,*]

[a] *Department of Microbiology and Immunology, University of Western Ontario, London, ON, Canada*
[b] *T Cell Laboratory, Ludwig Institute for Cancer Research, Melbourne-Austin Branch, Heidelberg, Australia*
[c] *Department of Microbiology and Immunology, Pennsylvania State University, Hershey, PA*
[d] *Centre for Human Immunology, University of Western Ontario, London, ON, Canada*
**Corresponding author: S. M. Mansour Haeryfar,*

Rapamycin is an immunosuppressive agent routinely used in organ transplantation but also paradoxically exerts antiviral and antitumor activities. Pathogen-specific memory CD8$^+$ T-cell (T_{CD8}) responses were recently found to be augmented by rapamycin. However, whether rapamycin influences the magnitude and quality of anticancer T_{CD8} responses is unknown. Importantly, how rapamycin may regulate simultaneous virus/tumor-specific and alloreactive T_{CD8} in the same host remains unexplored. To answer these questions, we primed wild-type mice with allogeneic cells concomitantly expressing simian virus 40 large tumor antigen (T Ag), a viral oncoprotein with well-defined epitopes. Rapamycin selectively enhanced the cross-priming of T_{CD8} specific for T Ag's most immunodominant epitope called site IV but not T_{CD8} alloreactivity. Rapamycin-treated mice also had a high percentage of splenic CD127^{high}KLRG1^{low} T_{CD8} and an increased frequency of site IV-specific T cells long after the peak of their primary response. When site IV was presented as a cytosolic minigene encoded by a recombinant vaccinia virus, rapamycin failed to boost the site IV-specific response. Therefore, the nature and presentation mode of antigen determine the susceptibility to the adjuvant effect of rapamycin. Our findings reveal the unexpected benefit of rapamycin treatment in recipients of allografts co-expressing tumor/viral Ags.

Key words: Alloreactivity, antitumor response, CD8$^+$ T cells, memory, mTOR, rapamycin

Abbreviations: B6, C57BL/6; FBS, fetal bovine serum; ICS, intracellular cytokine staining; IFN, interferon; KLRG1, killer cell lectin-like receptor G1; LCMV, lymphocytic choriomeningitis virus; MFI, mean fluorescence intensity; mTOR, mammalian target of rapamycin; mTORC, mTOR complex; T_{CD8}, CD8$^+$ T cell; rVV, recombinant vaccinia virus; SV40, simian virus 40; T Ag, large tumor antigen.

Received 20 April 2011, revised and accepted for publication 02 September 2011

Introduction

Allograft rejection by immunological mechanisms constitutes a formidable obstacle to life-saving organ transplantation. Initially discovered as an antifungal macrolide produced by *Streptomyces hygroscopicus*, rapamycin is an immunosuppressive agent commonly used in the clinic to hamper alloaggressive T cells in renal graft recipients (1). It potently and specifically inhibits the mammalian target of rapamycin (mTOR), an intracellular serine/threonine protein kinase that controls cellular metabolism, growth and survival. Various aspects of innate and adaptive immune responses are modulated by mTOR (2). The inhibition of the mTOR signaling pathway by rapamycin leads to altered T-cell trafficking (3), attenuated effector T-cell proliferation and enhanced regulatory T-cell function (4,5), all of which are likely to contribute to rapamycin-induced immunosuppression.

Recent studies have revealed that rapamycin surprisingly improves, rather than weakens, the memory CD8$^+$ T-cell (T_{CD8}) responses to lymphocytic choriomeningitis virus (LCMV) in mice (6) and vaccinia virus (VV) in rhesus macaques (6,7). However, several important questions remain regarding T_{CD8} immunomodulation by rapamycin. First, it is not clear whether T_{CD8} specific for tumor antigens (Ags) are controlled by mTOR. This is particularly important given the increased risk of malignancy in allograft recipients. Second, to what degree rapamycin treatment influences T_{CD8} cross-priming is unknown. Cross-priming is spearheaded by professional Ag-presenting cells (pAPCs), particularly dendritic cells (DCs), which acquire antigenic materials from client cells (e.g. an allogeneic graft cell) that are incapable of activating naïve T_{CD8} on their own (8). Cross-priming is a robust pathway for inducing T_{CD8}

responses to tumors of nonhematopoietic origin and to viruses that paralyze the MHC class I pathway in infected host cells. Although Ags displayed by allografted tissues may trigger T_{CD8} cross-priming, T_{CD8} alloreactivity may also result from direct priming. Third, whether rapamycin affects the epitope breadth of T_{CD8} responses is not understood. Of thousands of potentially immunogenic peptides harbored by complex Ags, only a handful elicit detectable T_{CD8} responses of varying magnitude, thus creating an immunodominance hierarchy among Ag-specific T_{CD8} clones (9). Immunodominance may influence the effectiveness of T_{CD8} responses to tumors, pathogens and transplants. Last, but certainly not least, it is not known how rapamycin may regulate concurrent T_{CD8} responses mounted toward allografts and other Ags in the same host at the same time. This is a relevant question in light of the clinical facts that: (i) current organ deficit may justify the usage of allografts prepared from "high-risk" kidneys containing tumor masses for recipients with limited life expectancy (10), which could introduce tumor Ags to the recipients' immune system; (ii) donor-derived infections with a variety of microbes (e.g. cytomegalovirus and BK polyoma virus) still occur with significant frequency (11) and (iii) community-acquired and nosocomial infections or reactivation of endogenous latent viruses are common in immunocompromised allograft recipients.

To address all the above questions in a nontransgenic, physiologically relevant setting, we primed wild-type mice with allogeneic kidney epithelial cells expressing a clinically relevant tumor Ag, the simian virus 40 (SV40) large tumor Ag (T Ag), which is in fact homologous to the BK virus T Ag detected in human kidneys. We demonstrate that rapamycin selectively improves the T_{CD8} response elicited by cross-priming against the most immunodominant epitope of T Ag (site IV) although not affecting or slightly attenuating alloreactive T_{CD8} present in the same host. In addition, rapamycin failed to boost the T_{CD8} response to site IV in mice infected with a recombinant VV (rVV) expressing site IV. Therefore, the mode of T_{CD8} priming and the immunodominance status of targeted epitopes determine susceptibility to the immunostimulatory effect of rapamycin on T_{CD8}. Our findings have clear clinical implications in allotransplantation and in therapeutic vaccine design.

Materials and Methods

Mice

Adult female C57BL/6 (B6; H-2^b) mice were purchased from Charles River Canada Inc. (St. Constant, QC, Canada), housed at the University of Western Ontario animal care facility under specific pathogen-free conditions and cared for in accordance with institutional and national guidelines.

Cell lines

The SV40-transformed cell lines KD2SV (H-2^d) and C57SV (H-2^b) were grown in Dulbecco modified Eagle medium supplemented with 5% fetal bovine serum (FBS). The mouse mastocytoma cell line P815 (H-2^d) was maintained in complete RPMI 1640 medium containing 10% FBS, nonessential amino acids, 2 mM L-glutamine, 1 mM sodium pyruvate and 50 μM 2-mercaptoethanol.

Immunization and rapamycin treatment

Age- and gender-matched mice received daily intraperitoneal (i.p.) injections of freshly prepared rapamycin (LC Laboratories, Woburn, MA, USA) at 1.5 μg/dose in PBS or of vehicle (phosphate-buffered saline [PBS] containing Phosal 50 PG and Tween 80). This regimen provides a blood rapamycin concentration of approximately 5–20 ng/mL (6), which is consistent with its clinical dosing in humans. Treatment with rapamycin or vehicle started 1 day before i.p. immunization with 2×10^7 allogeneic KD2SV cells or 5×10^6 plaque-forming units of a rVV expressing the T Ag's immunodominant peptide site IV (rVV-IV) and ended 1 day before the animals were euthanized.

Intracellular cytokine staining (ICS) and cytofluorimetric analyses

Unless otherwise indicated, mice were euthanized 9 or 7 days after immunization with KD2SV cells or rVV-IV, respectively, time points at which corresponding primary T_{CD8} responses reach their peak (12). Erythrocyte-depleted splonocytes and peritoneal exudate cells were then stimulated *ex vivo*, as appropriate, with C57SV cells, KD2SV cells, P815 cells or the following synthetic peptides corresponding to T Ag- and VV-derived epitopes (12,13): T Ag peptides: SAINNYAQKL (site I), CKGVNKEYL (site II/III), VVYDFLKC (site IV), QGINNLDNL (site V); VV peptides: TSYKFESV ($B8R_{20}$), AAFEFINSL ($A47L_{138}$), YSLPNAGDVI ($K3L_6$), YAPVSPIVI ($A42R_{88}$), VSLDYINTM ($A19L_{47}$). An H-2^b-restricted peptide derived from HSV-1, gB_{498} (SSIEFARL), served as an irrelevant control. All these peptides were >95% pure and generously provided by Drs. Jonathan Yewdell and Jack Bennink (National Institutes of Health). All peptides were used at a 500 nM final concentration. After 2-h incubation at 37°C, brefeldin A was added at 10 μg/mL and cultures were continued for an additional 3 h. Cells were then washed, stained for surface CD8α, CD127 (IL-7Rα), killer cell lectin-like receptor G1 (KLRG1), fixed and permeabilized to enable staining for intracellular interferon (IFN)-γ and Bcl-2. All fluorochrome-labeled Abs were from eBioscience (San Diego, CA, USA) except for anti-KLRG1-FITC (Southern Biotech, Birmingham, AL, USA) and anti-Bcl-2-FITC (BD Pharmingen, San Jose, CA, USA). Isotype controls were purchased from eBioscience or BD Pharmingen. MHC class I tetramers were prepared and used as we described previously (14). A BD FACSCanto II flow cytometer and FlowJo software (Tree Star, Ashland, OR, USA) were used for data acquisition and analysis. The percentage of IFN-γ^+ or tetramer$^+$ cells was determined after live gating on $CD8^+$ events and Ag-specific T_{CD8} were enumerated accordingly.

Statistical analysis

Statistical comparisons were performed using Student's t-test with the aid of GraphPad Prism software (GraphPad Prism Software, Inc., La Jolla, CA, USA). Significant values $p < 0.05$, $p < 0.01$ and $p < 0.001$ are denoted by *,** and ***, respectively.

Results and Discussion

mTOR regulation of concomitant tumor-specific and alloreactive T_{CD8} responses

It was recently demonstrated that the antipathogen T_{CD8} can be augmented by rapamycin treatment (6,7,15). An important and elegant study by Ferrer et al. found that rapamycin enhances the responsiveness of adoptively transferred ovalbumin-specific T_{CD8} in mice infected with recombinant *Listeria monocytogenes* encoding ovalbumin but not in recipients of an ovalbumin-expressing skin allograft (15). This study examined transgenic T_{CD8} responses in parallel, not in the same host. Therefore, we set to

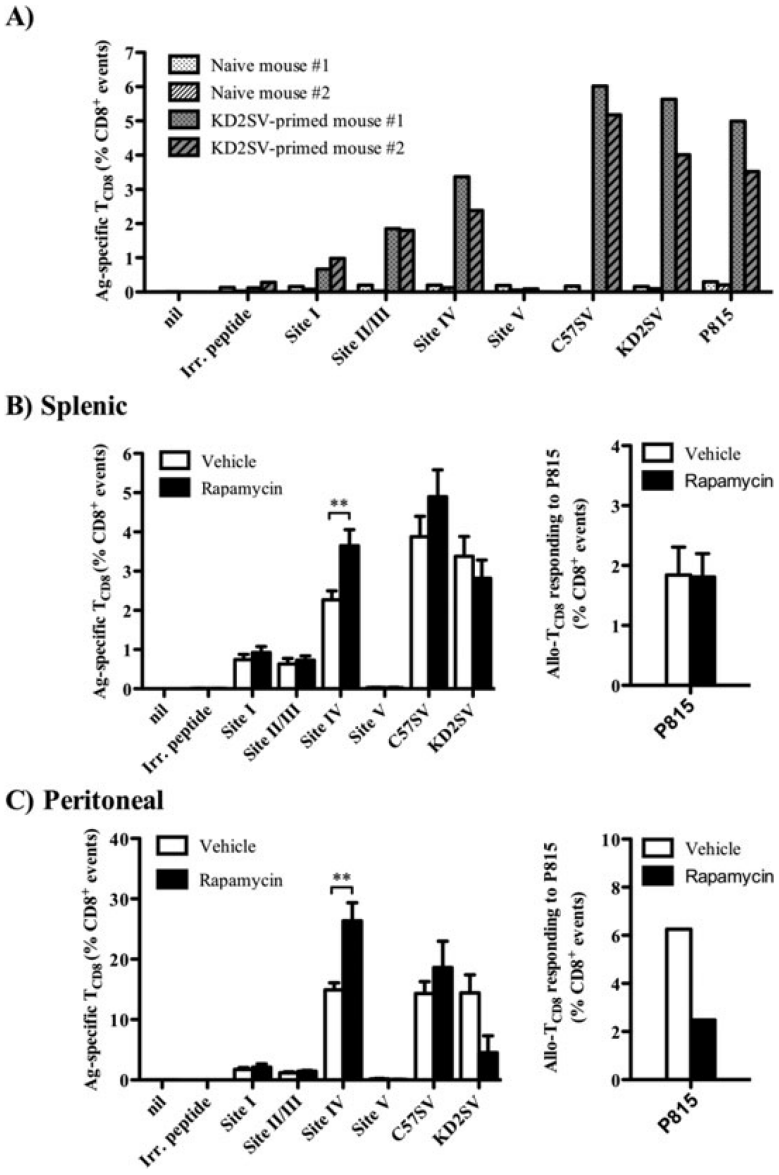

Figure 1: Treatment with rapamycin increases the frequency of functional T_{CD8} specific for the T Ag immunodominant epitope (site IV) but not that of alloreactive T_{CD8}. To confirm the requirement for *in vivo* priming in the generation of T Ag-specific and alloreactive T_{CD8} responses, splenocytes from naïve B6 mice or B6 mice immunized with allogeneic (H-2^d) T Ag^+ KD2SV cells were restimulated *ex vivo* with T Ag-derived peptides (sites I, II/III, IV or V), syngeneic (H-2^b) T Ag^+ C57SV cells, allogeneic KD2SV cells or allogeneic P815 cells used at 2×10^5 cells/well. The frequency of cognate T_{CD8} was calculated as the percentage of IFN-γ^+ cells after live gating on $CD8^+$ events. (A) Individual mouse data are shown. To assess the effect of rapamycin, (B) splenocytes and (C) peritoneal exudate cells from vehicle- and rapamycin-treated B6 mice that were immunized with KD2SV cells were restimulated *ex vivo* with T Ag-derived peptides, C57SV, KD2SV or P815 cells. The frequency of cognate T_{CD8} was determined as described earlier. Data are shown as mean ± SEM obtained from 19 mice/group pooled from five independent experiments except in the case of the T_{CD8} response to P815 cells that was assessed in two experiments.

explore the effect of rapamycin on simultaneously ongoing T_{CD8} responses against tumor/viral Ags and alloantigens within the same wild-type animal. To do so, we injected B6 mice (H-2^b) with KD2SV cells (H-2^d) that are transformed with SV40 and, as such, express T Ag, a viral oncoprotein with well characterized T_{CD8} epitopes (14). T_{CD8} responses in this model mimic the "real life" situation because they are elicited against two types of clinically relevant Ags (i.e. alloantigens and T Ag) expressed by kidney epithelial cells (a known target of T cells in renal allograft recipients) in wild-type animals harboring a natural T-cell repertoire.

We first confirmed that in our model, T Ag-specific and alloreactive T_{CD8} responses require *in vivo* priming with KD2SV cells and are not detectable in naïve animals (Figure 1A). Treatment with rapamycin increased the frequency of both the splenic and peritoneal T_{CD8} specific for site IV, the most immunodominant epitope of T Ag (14), as judged by intracellular staining for IFN-γ (Figures 1B and C). Peritoneal and splenic T_{CD8} represent local and systemic responders to site IV, respectively (8,12). There was also a trend for an enhanced T_{CD8} response to C57SV cells, T Ag^+ fibroblastic cells of B6 origin, when they were used in

doi: 10.1111/j.1600-6143.2011.03811.x

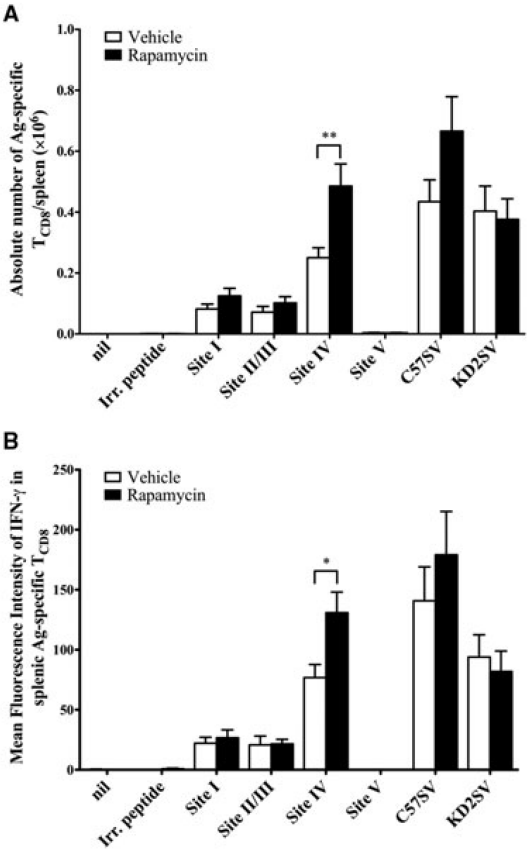

Figure 2: Treatment with rapamycin increases the absolute number and mean IFN-γ production (on a per cell basis) of splenic site IV-specific T_{CD8} but not those of alloreactive T_{CD8}. Splenocytes from vehicle- and rapamycin-treated B6 mice that were immunized with KD2SV cells were restimulated *ex vivo* with peptides corresponding to T Ag epitopes (sites I, II/III, IV or V), syngeneic T Ag^+ C57SV cells or allogeneic KD2SV cells. (A) The frequency of cognate IFN-γ^+ T_{CD8} was used to enumerate the absolute number of these cells within each spleen, and (B) their MFI for IFN-γ was also determined using FlowJo software. Data are shown as mean ± SEM obtained from 19 mice/group pooled from five independent experiments.

lieu of T Ag-derived peptides for *ex vivo* T_{CD8} restimulation. We found a similar increase in both the absolute number and mean fluorescence intensity (MFI) of site IV-specific IFN-γ^+ T_{CD8} in the spleens of rapamycin-treated animals (Figures 2A and B). Contrary to T Ag-specific T_{CD8}, the frequency of alloreactive T_{CD8}, defined by their *ex vivo* responsiveness to KD2SV cells, was unaltered or decreased to varying degrees upon rapamycin treatment (Figure 1). This decrease was most pronounced within the peritoneal cavity (Figure 1C). This response is of allogeneic nature and independent of T Ag expression by KD2SV cells because these cells express H-2^d allomorphs and cannot be directly recognized by T Ag-specific T_{CD8} that are H-2^b-restricted. This notion is supported by our observation that rapamycin treatment of KD2SV-primed mice failed to increase the frequency of alloreactive cells restimulated with P815 cells, a T Ag^- H-2^{d+} cell line (Figures 1B and C).

Our finding that site IV-specific T_{CD8} in rapamycin-treated mice produce more IFN-γ on a per cell basis—hence their higher MFI—indicates that rapamycin improves the functional fitness of these T_{CD8}. This is consistent with our unpublished observation that treatment with rapamycin also amplifies cytotoxic responses of cross-primed, T Ag-specific T_{CD8} (data not shown).

Previous studies have documented the positive effect of rapamycin on memory but not primary T_{CD8} responses. Rapamycin treatment reportedly failed to increase LCMV-specific T_{CD8} numbers at the peak of their primary response (6). In contrast, the primary T_{CD8} response to VV in rhesus macaques and that to a heat shock protein-based vaccine in mice were boosted by the inhibition of mTOR (7,16). These discrepancies may have stemmed from different readouts used in these studies. The former study enumerated LCMV-specific T_{CD8} by tetramer staining whereas the latter two studies used functional assays similar to ours. In fact, when we detected site IV-specific T_{CD8} by tetramer staining in a head-to-head comparison with ICS, we did not find any difference between mice receiving rapamycin or vehicle by tetramer staining (Figure S1).

It was of interest to determine whether rapamycin affects the quality of primary T Ag-specific T_{CD8} and their progression to a memory state. We found that the site IV-specific T_{CD8} pool in rapamycin-treated animals had a higher proportion of $CD127^{high}KLRG1^{low}$ cells and a lower proportion of $CD127^{low}KLRG1^{high}$ cells, which are considered memory T_{CD8} precursors and short-lived effectors, respectively (Ref. 6; Figures 3A and B). Rapamycin treatment also increased the expression of the prosurvival protein Bcl-2 in site IV-specific T_{CD8} at the peak of their primary response (Figure 3C). Importantly, treatment with rapamycin during the initial priming phase (i.e. during the first 9 days) led to a higher frequency of site IV-specific T_{CD8} detected at a later time point (day 27; Figure 3D). In a different setting that simulates clinical conditions requiring continuous treatment, daily administration of rapamycin up until day 27 resulted in a higher proportion of T Ag-specific (but not alloreactive) T_{CD8} (Figure S2). These results collectively show that rapamycin ameliorates the functional fitness of primary antitumor T_{CD8} and raises both their primary and long-term frequencies.

Inhibition of mTOR affects T_{CD8} cross-priming and immunodominance

The T Ag-specific response in our model occurs exclusively through cross-priming (8,12). This is because: (i) KD2SV

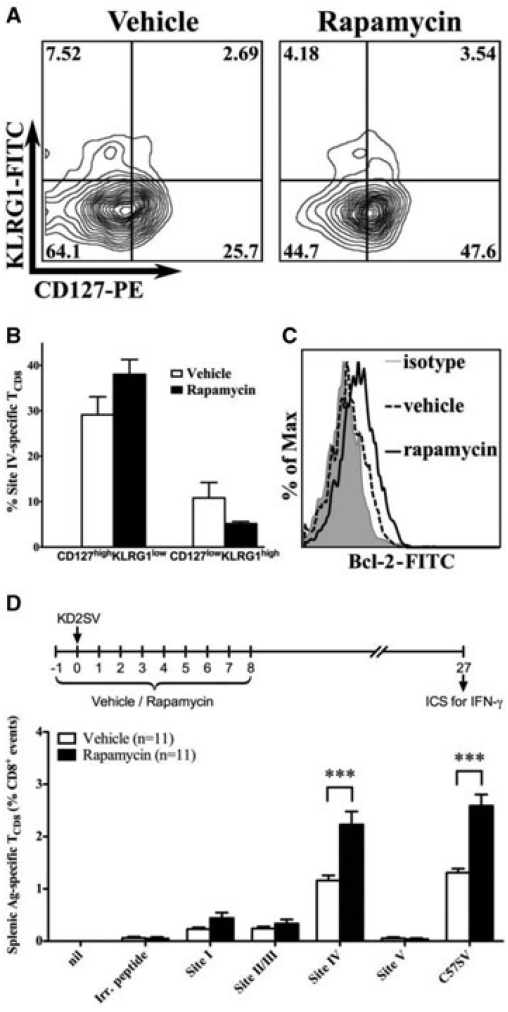

Figure 3: Rapamycin treatment improves the quality of primary T Ag-specific T_{CD8} and promotes their progression to memory cells. Site IV-specific T_{CD8} identified by ICS for IFN-γ were gated upon and assessed for their expression of (A, B) CD127 and KLRG1 and (C) intracellular Bcl-2. Representative FACS plots for these markers are shown. In addition, (B) the frequencies of $CD127^{high}KLRG1^{low}$ (memory T_{CD8} precursors) and $CD127^{low}KLRG1^{high}$ (short-lived effectors) are shown for 6 mice/group. Statistical comparisons revealed that rapamycin-treated mice had a higher proportion of $CD127^{high}KLRG1^{low}$ cells compared with vehicle-treated animals (38 ± 3.3 vs. 29.1 ± 4, $p = 0.11$) and a lower proportion of $CD127^{low}KLRG1^{high}$ cells (5.1 ± 0.4 vs. 10.8 ± 3.4, $p = 0.15$). (D) In separate experiments, B6 mice were immunized with KD2SV cells and treated with rapamycin or vehicle during the initial priming phase as illustrated. Mice were left untreated until day 27, at which point the frequency of T Ag-specific T_{CD8} was determined by ICS for IFN-γ. Data are shown as mean ± SEM obtained from 11 mice/group pooled from three independent experiments.

cells are of kidney epithelial origin, not pAPCs, and lack B7 costimulatory molecules, a prerequisite for naïve T_{CD8} activation; (ii) they are allogeneic to B6 mice and unable to directly prime T_{CD8} in this strain according to the rule of MHC restriction and (iii) they are transformed with subgenomic fragments of SV40 and fail to produce SV40 virions, thus eliminating any possibility that the ensuing T_{CD8} responses are due to the infection of host pAPCs (8). Therefore, our finding that the T_{CD8} response to T Ag in this model is improved by rapamycin constitutes the initial report describing the effect of this agent on cross-priming. This is important for allotransplantation because T_{CD8} responses to microbial and tumor Ags of donor origin, which are believed to occur at least partially through cross-priming, are likely to be heightened by rapamycin. We have recently found that anti-influenza T_{CD8} responses can also be augmented by rapamycin in a cross-priming model (8; unpublished data).

We found that rapamycin strengthens the T_{CD8} response to site IV, but typically not those targeting subdominant epitopes (sites I, II/III and V). This indicates that even among T_{CD8} clones recognizing the same Ag, some are more prone than others to the immunostimulatory effect of rapamycin. We previously reported that site IV-specific T_{CD8} are sufficient for the eradication of T Ag-induced choroid plexus brain tumors in irradiated mice (17). However, it is noteworthy that T_{CD8} clones specific for immunodominant epitopes are not always necessarily the most protective T_{CD8} against all forms of cancer and infectious diseases. Therefore, the selective adjuvanticity of rapamycin for some but not all T_{CD8} clones need to be taken into consideration in therapeutic vaccine design.

Mode of Ag presentation determines the susceptibility of T_{CD8} responses to rapamycin adjuvanticity

Next, we asked whether rapamycin affects T_{CD8} responses to antigenic peptides encoded by a viral vector. We infected vehicle- and rapamycin-treated mice with a rVV that expresses site IV as a cytosolic minigene (12). Direct priming is presumed to be the predominant pathway in activating naïve T_{CD8} recognizing peptides encoded by such minigenes. This experiment also enabled us to examine the effect of rapamycin on mouse T_{CD8} responses to VV epitopes that we previously characterized (13). T_{CD8} responses to both site IV and the VV-derived epitopes $B8R_{20}$, $A47L_{138}$, $K3L_6$, $A42R_{88}$ and $A19L_{47}$ remained unaltered upon rapamycin treatment (Figure 4 and data not shown). Therefore, we conclude that: (i) regardless of whether site IV-specific T_{CD8} activation after rVV-IV infection can be dubbed as direct priming, the mode of Ag presentation can clearly dictate the susceptibility of T_{CD8} responses to rapamycin and (ii) the adjuvanticity of rapamycin cannot be generalized to all pathogen-specific T_{CD8} responses and even to T_{CD8} responses against the same pathogen in different host species. This is because mouse T_{CD8} responses to VV epitopes are resistant to rapamycin treatment whereas the

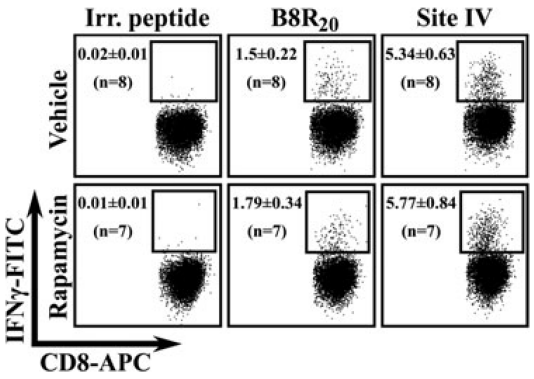

Figure 4: VV- and site IV-specific T_{CD8} induced through infection with rVV-IV are not affected by rapamycin. Splenocytes from rVV-IV-infected mice that received daily treatment of rapamycin or vehicle were restimulated *ex vivo* with VV-derived peptides (including $B8R_{20}$) or the T Ag site IV peptide. The frequencies of epitope-specific T_{CD8} are shown as mean ± SEM obtained from 7 to 8 mice/group pooled from two independent experiments that yielded almost identical results. Representative dot plots are also shown.

bulk VV-specific T_{CD8} response is reportedly augmented in rapamycin-treated rhesus macaques (7). It will be important to explore the susceptibility of VV-specific T_{CD8} to rapamycin in humans because rVVs are pursued as suitable vectors in therapeutic vaccination.

How rapamycin modulates T_{CD8} responses is unclear. Using RNA interference to knock down mTOR, raptor (an important component of the mTOR complex 1 [mTORC1]) or FKBP12 (a binding partner of rapamycin) exclusively in LCMV-specific transgenic T_{CD8}, a previous study found that rapamycin operates in a T-cell-intrinsic fashion to accelerate memory T_{CD8} differentiation (6). Whether this is true also for wild-type T_{CD8} is currently unknown. The role of mTORC2, whose activity may be reduced in some cell types after prolonged exposure to rapamycin (18), remains to be elucidated. mTOR is known to modulate autophagy in DCs and rapamycin-induced autophagy in these cells enhances their ability to prime T cells *in vitro* (19). We favor the possibility that APCs may participate in modulation of T_{CD8} by rapamycin. This is because: (i) tumor-specific and alloreactive T_{CD8} primed in the same host behave differently in response to rapamycin; (ii) T_{CD8} clones recognizing various epitopes of the same Ag show variation in response to the immunostimulatory effect of rapamycin (site IV vs. other epitopes); (iii) the T_{CD8} priming route for the same epitope determines the response to rapamycin (site IV expressed by allogeneic non-APCs as opposed to site IV encoded by a rVV), potentially implicating various APC subsets in the observed effect and (iv) T_{CD8} found in different environments exhibit varying degrees of susceptibility to rapamycin (splenic vs. peritoneal alloresponses). The activity of mTORC1 and/or mTORC2 and the specialized functions of distinct APC subsets (e.g. autophagy) may be subject to differential rapamycin regulation. Infection with replicating viral vectors (e.g. rVV) expressing tumor Ags may yield a high Ag load and simultaneously trigger viral pattern recognition receptors within APCs. This would be absent in responses to cell-associated Ags.

In summary, we show for the first time that rapamycin augments the vigor, fitness and quality of T_{CD8} responses induced by cross-priming against a clinically relevant viral oncoprotein but not the alloreactive T_{CD8} response occurring in the same host. The ultimate question is whether human T_{CD8} are prone to the adjuvant effect of rapamycin. Rapamycin is not only used in allograft recipients but is also an approved therapeutic agent for advanced renal cell carcinoma. How T_{CD8} in allograft recipients and cancer patients under rapamycin therapy respond to viruses and tumor Ags warrants further investigation.

Acknowledgments

This work was supported by grants to S.M.M.H. from the Canadian Institutes of Health Research (CIHR grant MOP 86601), The Cancer Research Society Inc. and the Multi-Organ Transplant Program, London Health Sciences Centre, and to T.D.S. by grant CA025000 from the National Cancer Institute/National Institutes of Health. S.M.M.H. holds a Canada Research Chair in Viral Immunity & Pathogenesis. S.M.V. was a recipient of a CIHR Training Grant in Cancer Research & Technology Transfer and M.R. was a recipient of a Canada Graduate Scholarship from Natural Sciences and Engineering Research Council of Canada. The authors wish to thank Dr. Rafi Ahmed and Dr. Koichi Araki (Emory Vaccine Center) and Dr. Joaqúin Madrenas (McGill University) for their critical review of this work.

Disclosure

The authors of this manuscript have no conflicts of interest to disclose as described by the *American Journal of Transplantation*.

References

1. Wullschleger S, Loewith R, Hall MN. TOR signaling in growth and metabolism. Cell 2006; 124: 471–484.
2. Thomson AW, Turnquist HR, Raimondi G. Immunoregulatory functions of mTOR inhibition. Nat Rev Immunol 2009; 9: 324–337.
3. Sinclair LV, Finlay D, Feijoo C, et al. Phosphatidylinositol-3-OH kinase and nutrient-sensing mTOR pathways control T lymphocyte trafficking. Nat Immunol 2008; 9: 513–521.
4. Sauer S, Bruno L, Hertweck A, et al. T cell receptor signaling controls Foxp3 expression via PI3K, Akt, and mTOR. Proc Natl Acad Sci USA 2008; 105: 7797–7802.
5. Haxhinasto S, Mathis D, Benoist C. The AKT-mTOR axis regulates de novo differentiation of CD4+Foxp3+ cells. J Exp Med 2008; 205: 565–574.
6. Araki K, Turner AP, Shaffer VO, et al. mTOR regulates memory CD8 T-cell differentiation. Nature 2009; 460: 108–112.

7. Turner AP, Shaffer VO, Araki K, et al. Sirolimus enhances the magnitude and quality of viral-specific CD8(+) T-cell responses to vaccinia virus vaccination in rhesus macaques. Am J Transplant 2011; 11: 613–618.
8. Chen W, Masterman KA, Basta S, et al. Cross-priming of CD8+ T cells by viral and tumor antigens is a robust phenomenon. Eur J Immunol 2004; 34: 194–199.
9. Yewdell JW, Bennink JR. Immunodominance in major histocompatibility complex class I-restricted T lymphocyte responses. Annu Rev Immunol 1999; 17: 51–88.
10. Sener A, Uberoi V, Bartlett ST, Kramer AC, Phelan MW. Living-donor renal transplantation of grafts with incidental renal masses after ex-vivo partial nephrectomy. BJU Int 2009; 104: 1655–1660.
11. Grossi PA, Fishman JA. Donor-derived infections in solid organ transplant recipients. Am J Transplant 2009; 9(Suppl 4): S19–S26.
12. Haeryfar SM, DiPaolo RJ, Tscharke DC, JR Bennink, JW Yewdell. Regulatory T cells suppress CD8+ T cell responses induced by direct priming and cross-priming and moderate immunodominance disparities. J Immunol 2005; 174: 3344–3351.
13. Tscharke DC, Karupiah G, Zhou J, et al. Identification of poxvirus CD8+ T cell determinants to enable rational design and characterization of smallpox vaccines. J Exp Med 2005; 201: 95–104.
14. Mylin LM, Schell TD, Roberts D, et al. Quantitation of CD8(+) T-lymphocyte responses to multiple epitopes from simian virus 40 (SV40) large T antigen in C57BL/6 mice immunized with SV40, SV40 T-antigen-transformed cells, or vaccinia virus recombinants expressing full-length T antigen or epitope minigenes. J Virol 2000; 74: 6922–6934.
15. Ferrer IR, Wagener ME, Robertson JM, et al. Cutting edge: Rapamycin augments pathogen-specific but not graft-reactive CD8+ T cell responses. J Immunol 2010; 185: 2004–2008.
16. Wang Y, Wang XY, Subjeck JR, Shrikant PA, Kim HL Temsirolimus, an mTOR inhibitor, enhances anti-tumour effects of heat shock protein cancer vaccines. Br J Cancer 2011; 104: 643–652.
17. Tatum AM, Mylin LM, Bender SJ, et al. CD8+ T cells targeting a single immunodominant epitope are sufficient for elimination of established SV40 T antigen-induced brain tumors. J Immunol 2008; 181: 4406–4417.
18. Sarbassov DD, Ali SM, Sengupta S, et al. Prolonged rapamycin treatment inhibits mTORC2 assembly and Akt/PKB. Mol Cell 2006; 22: 159–168.
19. Jagannath C, Lindsey DR, Dhandayuthapani S, Xu Y, Hunter RL Jr., Eissa NT. Autophagy enhances the efficacy of BCG vaccine by increasing peptide presentation in mouse dendritic cells. Nat Med 2009; 15: 267–276.

Supporting Information

Additional supporting information may be found in the online version of this article.

Figure S1: Depicts a head-to-head comparison of ICS for IFN-γ and tetramer staining for detection of site I- and site IV-specific T_{CD8} at the peak of their primary response.

Figure S2: Demonstrates the effect of continuous rapamycin treatment on long-term frequencies of T Ag-specific and alloreactive T_{CD8}.

Please note: Wiley-Blackwell is not responsible for the content or functionality of any supporting materials supplied by the authors. Any queries (other than missing material) should be directed to the corresponding author for the article.

JOHN WILEY AND SONS LICENSE TERMS AND CONDITIONS

Feb 10, 2014

This is a License Agreement between Saman Maleki Vareki ("You") and John Wiley and Sons ("John Wiley and Sons") provided by Copyright Clearance Center ("CCC"). The license consists of your order details, the terms and conditions provided by John Wiley and Sons, and the payment terms and conditions.

All payments must be made in full to CCC. For payment instructions, please see information listed at the bottom of this form.

License Number	3325500286682
License date	Feb 10, 2014
Licensed content publisher	John Wiley and Sons
Licensed content publication	American Journal of Transplantation
Licensed content title	Differential Regulation of Simultaneous Antitumor and Alloreactive CD8 T-Cell Responses in the Same Host by Rapamycin
Licensed copyright line	©Copyright 2011 The American Society of Transplantation and the American Society of Transplant Surgeons
Licensed content author	S. Maleki Vareki,M. J. Harding,J. Waithman,D. Zanker,A. N. Shivji,M. Rytelewski,D. M. Mazzuca,M. A. Yekta,W. Chen,T. D. Schell,S. M. M. Haeryfar
Licensed content date	Oct 25, 2011
Start page	233
End page	239
Type of use	Dissertation/Thesis
Requestor type	Author of this Wiley article
Format	Print and electronic
Portion	Full article
Will you be translating?	No
Title of your thesis / dissertation	Indoleamine 2,3-dioxygenase confers resistance to chemotherapy and γ radiation to cancer cells, independent of direct immune involvement
Expected completion date	Mar 2014
Expected size (number of pages)	280
Total	0.00 USD

Curriculum Vitae

Saman Maleki Vareki, MS.c.

Education:

Candidate in the Doctor of Philosophy program (since September 2008 to present)

Dept. of Microbiology & Immunology, Schulich School of Medicine & Dentistry

Western University, London, Canada

Master of Science (July, 2008)

Department of Biology, Faculty of Sciences, University of Isfahan, Isfahan, Iran

Bachelor of Science (July, 2004)

Department of Microbiology, Faculty of Sciences, Arak Azad University, Arak, Iran

Honors, Distinctions & Awards

1- Schulich Scholarship For Medical Research. UWO.
-September 2012-August 2013

- Value $7900

2- Canadian Institute of Health Research (CIHR)-Institute of Cancer Research (ICR), Travel Award- Institute Community Support to attend AACR Tumor Immunology: Multidisciplinary Science Driving Basic and Clinical Advance. Miami, Florida December 2-5, 2012
-December 2012

- National Competitive Award

- Value $1000

3- CIHR Training Program in Cancer Research and Technology Transfer (CaRTT, a CIHR Strategic Training Initiative in Health Research [STIHR] program).
-September 2012-August 2013

-Institutional competitive award

-Awarded without stipend (full program participation in all other respects, as per program requirements that restrict stipend allocation only for the first 5 years of enrolment in graduate programs, including non-Canadian programs)

4- Poster award, Oncology Research and Education Day, UWO

-June 2012

-Value $100

5- Nominated by the department of Microbiology & Immunology for the Nellie Farthing Fellowship in Medical Sciences from the Schulich School of Medicine and Dentistry at the Western University.

-June 2012

6- UWO Division of Experimental Oncology Graduate Student Travel Award to attend 2011 AACR-NCI-EORTC International conference on Molecular Targets and Cancer Therapeutics: Discovery, Biology and Clinical Applications. San Francisco, USA,

-April 2012

-Institutional competitive award

-Value $1500

7- Department of Microbiology and Immunology graduate student travel award to attend AACR-NCI-EORTC International conference on Molecular Targets and Cancer Therapeutics: Discovery, Biology and Clinical Applications. San Francisco, USA,

-November 2011

-Departmental level award based on academic merit

-Value $1000

8- CIHR Training Program in Cancer Research and Technology Transfer (CaRTT, a CIHR Strategic Training Initiative in Health Research [STIHR] program); as an international student.

-September 2011-August 2012

-Institutional competitive award

-Awarded without stipend (full program participation in all other respects, as per program requirements that restrict stipend allocation only for the first 5 years of enrolment in graduate programs, including non-Canadian programs)

9- CIHR Training Grant in Cancer Research and Technology Transfer (CaRTT, a CIHR Strategic Training Initiative in Health Research [STIHR] program); as an international student.

-September 2010-August 2011

-Institutional competitive award

-Stipend awarded: $26,700

10- Poster award, Oncology Research and Education Day, UWO

-June 2010

-Value $100

11- Graduate Entrance Scholarship, Dept. of Microbiology and Immunology, UWO

-September 2008

-Awarded to the top 4 students in the department

-Value $5000

12- Schulich Graduate Enhancement Scholarship (SGE), UWO

-September 2008-2011

-Awarded based on the academic merit

-Value $5000/year

13- Western Graduate Research Scholarship

-September 2008-present

-Awarded to students with an 80%+ entrance average

-Value $7400/year

14- Scholarship of the city of Freiburg for the summer term from Albert-Ludwigs University, Freiburg, Germany

-March 2008-August 2008

-Institutional competitive award

-Value 2000 euros

Invited Talks:

1) Lay presentation of research. Title: The immune system and cancer. Presented at the Canadian cancer society (CCS) Essex County Unit. Annual volunteer driver workshop. September 26th 2013. London. ON. Canada

2) Lay presentation of research. Title: Cancer research-hope for the future. Presented at the Canadian cancer society (CCS) Essex County Unit. Fueling the Mission Volunteer Leadership Meeting February 4th 2012. Oldcastle, ON, Canada.

3) Lay presentation of research. Title: Cancer research-hope for the future. Presented at the Canadian cancer society (CCS) South Western Ontario all staff meeting. October 19th 2011. London, ON, Canada

4) Rogers daytime live TV show about cancer research and CCS YouTube videos. http://www.rogerstv.com/page.aspx?lid=237&rid=9&gid=108223

5) Lay presentation of research. Title: Cancer Research. April 20th 2013. Theater for cure (A fundraising program). London. ON. Canada

Invited articles:

1) Jensen M, Yeung T, Coschi C, and **Maleki Vareki S.** Progress and promise in cancer research. *The Londoner*. December 2012
http://eedition.thelondoner.ca/doc/The-Londoner/londoner_1227_vp/2012122701/10.html#10

2) **Maleki Vareki S.** Beating cancer by improving anti-cancer immunity. *The Londoner.* August 2012.
http://eedition.thelondoner.ca/doc/The-Londoner/londoner_0816_vp/2012081401/26.html#26

Teaching Assistantships:

1) Microbiology and Immunology 3600G, Laboratory Techniques in Microbiology and Immunology, lab course for 8-12 undergraduate students (third year), 3 hours lab per week. Fall-Winter 2010

2) Microbiology and Immunology 3300A, Immunology, 275 undergraduate students (third year), 2 hours per week. Fall-Winter 2009

Publications

Patents:

1) **Maleki Vareki S,** Vincent M, Koropatnick J. Chemo- and Radiation sensitization of cancer by indoleamine-2, 3 dioxygenase (IDO) inhibitors. USA patent office number 753-128pr, field on May 31, 2013

Books Authored:

1) Kermanshahi RK, and **Maleki Vareki S**: *Microbiology for Everyone* (2009). Dibagaran Tehran publishing group. Tehran. Iran. Library of Congress publication number: 1864877-Total number of pages 238. I have written 6 chapters of this book. From page 11-154. This is a textbook used for teaching general microbiology to undergraduate students in Iran.

Chapters in Books:

1) Christine Di Cresce, Colin Way, Mateusz Rytelewski, **Saman Maleki Vareki**, Supritha Nilam, Mark D. Vincent, James Koropatnick, and Peter Ferguson. *Antisense Technology: From Unique Laboratory Tool to Novel Anticancer Treatments.* 2012. In press. Numbers cited: 2.

Articles in Peer-reviewed Journals:

1) **Maleki Vareki S**, Rytelewski M, Figueredo R, Chen D, Ferguson PJ, Vincent M, Min WP, Zheng X Koropatnick J. Indoleamine 2,3-dioxygenase mediates immune-independent human tumor cell resistance to olaparib, γ radiation, and cisplatin. *Oncotarget*. 2014. *In Press*

2) Rytelewski M, Ferguson PJ, **Maleki Vareki S**, Figueredo R, Vincent M, Koropatnick J. Inhibition of BRCA2 and Thymidylate Synthase Creates Multidrug Sensitive Tumor Cells via the Induction of Combined "Complementary Lethality". *Molecular Therapy — Nucleic Acids*. 2013. doi:10.1038/mtna.2013.7

3) **Maleki Vareki S**, Zarkesh-Esfahani H, Behjati M: H.pylori's evasion of the immune system could establish an inflammatory environment that potentially induces the development of coronary artery disease. *Jundishapur J Microbiol.* 2013. In press

4) Hayworth JL, Mazzuca DM, **Maleki Vareki S**, Welch I, McCormick JK, Haeryfar, SMM: CD1d-independent activation of mouse and human invariant NKT cells by bacterial superantigens. *Immunology and Cell Biology.* 2011. doi: 10.1038/icb.2011.90. (Numbers article cited in other peer-reviewed journals: 4).

5) **Maleki Vareki S**, Harding MJ, Waithman J, Zanker D, Shivji AN, Rytelewski M, Mazzuca DM, Yekta MA, Chen W, Schell TD, Haeryfar SMM: Differential regulation of simultaneous anti-tumor and alloreactive CD8+ T cell responses in the same host by rapamycin. *Americal Journal of Transplantation.* 2011. doi: 10.1111/j.1600-6143.2011.03811.x. (AJT impact factor on March 2012: 6.394. Ranking: 1/24 Transplantation journals. 2/198 Surgery journals). Numbers article cited in other peer-reviewed journals: 1

6) Hashemi Jazi SM, Shafiei S, Zarkesh-Esfahani SH, **Maleki Vareki S**, Haghjooy Javanmard S: The effects of bare metal versus drug-eluting stent implantation on circulating endothelial cells following percutaneous coronary intervention. *Journal of Research in Medical Sciences.* 2011. 16(5): 605-610

7) Stuart JK, Bisch SP, Leon-Ponte M, Hayatsu J, Mazzuca DM, **Maleki Vareki S**, Haeryfar SMM: Negative modulation of invariant natural killer T cell responses to glycolipid antigens by p38 MAP kinase. *International Immunopharmacology* 2010. 10(9): 1068-1076 (Numbers article cited in other peer-reviewed journals: 4)

Abstracts and Poster Presentations:

1) **Maleki Vareki S,** Rytelewski M, Figueredo R, Chen D, Ferguson PJ, Vincent M, Min W, Koropatnick J. Indoleamine 2,3-dioxygenase mediates immune-independent human tumor cell resistance to olaparib, γ radiation, and cisplatin. Proc. Of the AACR Annual meeting. *International conference*. San Diego, USA April 2014

2) Rytelewski M, Tong J, Buensucesco A, **Maleki Vareki S**, Ferguson P, Figueredo R, Vincent M, Shepherd T, Deroo B, Koropatnick J. A BRCA2-targeting antisense oligodeoxynucleotide enhances cisplatin-induced decreases in human tumor cell proliferation, metastatic frequency, and metabolic response. Proc. Of the AACR Annual meeting. *International conference*. San Diego, USA April 2014

3) Rytelewski M, Tong J, Buensucesco A, **Maleki Vareki S**, Ferguson P, Figueredo R, Vincent M, Shepherd T, Deroo B, Koropatnick J. A novel BRCA2 targeting antisense oligonucleotide sensitizes human tumor cells to chemotherapy and radiotherapy - the induction of 'complementary lethality' by targeting DNA repair. Proc. Of the AACR *International conference* on Molecular targets and cancer therapeutics. Boston, USA 2013

4) **Maleki Vareki S,** Chen D, Rytelewski M, Ferguson P, Min W, Vincent M, Koropatnick J. IDO confers chemo-and radiation resistance to cancer cells independent of immune function. Proc. Of the CIHR – Strategic training program in cancer research & technology transfer (CaRTT) and the department of oncology – research & education

day, UWO, 2013.

5) Rytelewski M, Ferguson P, Tong J, Buensucesco A, **Maleki Vareki S**, Figueredo R, Vincent M, Koropatnick J. A second-generation antisense oligodeoxynucleotide targeting BRCA2 sensitizes human tumour cells to chemotherapy and radiotherapy – The induction of "complementary lethality" by targeting DNA repair. Proc. Of the CIHR – Strategic training program in cancer research & technology transfer (CaRTT) and the department of oncology – research & education day, UWO, 2013

6) **Maleki Vareki S** and Koropatnick J. Enhancing Chemotherapy Efficacy and Antitumor Immune Activity by Combined Antisense Downregulation of TS and IDO. Proc. Of the AACR *International conference* on Tumor Immunology: Multidisciplinary Science Driving Basic and Clinical Advance. Miami, USA 2012

7) Rytelewski M, Vincent MD, Ferguson PJ, **Maleki Vareki S**, Figueredo R, Koropatnick J. Downregulation of BRCA2 and Thymidylate Synthase (TS) Sensitizes Human Tumour Cells to Chemotherapy: Induction of 'Complementary Lethality'by Targeting DNA Repair. Proc. Of the EORTC-NCI-AACR *International conference* on Molecular Targets and Cancer Therapeutics. Dublin, Ireland 2012

8) **Maleki Vareki S** and Koropatnick J: Combined antisense downregulation of TS and IDO for better cancer treatment. Proc. Of the CIHR – Strategic training program in cancer research & technology transfer (CaRTT) and the department of oncology – research & education day, UWO, 2012

9) **Maleki Vareki S**, Harding MJ, Shivji AN, Rytelewski M, Mazzuca DM, Yekta MA, Schell TD, Haeryfar SMM: Differential regulation of simultaneous anti-tumor and alloreactive CD8+ T cell responses in the same host by rapamycin. Proc. Of the 6th Infection and Immunity Research Forum (IIRF), UWO, 2011

10) **Maleki Vareki S**, Harding MJ, Waithman J, Zanker D, Shivji AN, Rytelewski M, Mazzuca DM , Yekta MA, Chen W, Schell TD, Haeryfar SMM: Differential regulation of simultaneous anti-tumor and alloreactive CD8+ T cell responses in the same host by rapamycin. Proc. Of the AACR-NCI-EORTC *International conference* on Molecular Targets and Cancer Therapeutics: Discovery, Biology and Clinical Applications. San Francisco, USA, 2011

11) **Maleki Vareki S**, Harding MJ, Rytelewski M, Haeryfar, SMM: Rapamycin differentially modulates anticancer and alloreactive CD8+ T cell responses generated in the same host. Proc. Of the 2nd *International conference* on Cancer Immunotherapy and Immunomonitoring. Budapest, Hungary, 2011

12) **Maleki Vareki S**, Harding MJ, Rytelewski M, Haeryfar, SMM: Targeting mTOR differentially regulates antiviral and allogeneic CD8+ T cell responses elicited in the same host. Proc. Of the 24th Annual Canadian Society for Immunology Conference. Lake Louise, Canada, 2011 *(National conference)*

13) **Maleki Vareki S**, Harding MJ, Rytelewski M, Schell TD, Haeryfar, SMM: Differential regulation of simultaneous tumor-specific and alloreactive CD8+ T cell responses in the same host by targeting mTOR. Proc. Of the CIHR – Strategic training program in cancer research & technology transfer (CaRTT) and the department of oncology – research & education day, UWO, 2011

14) **Maleki Vareki S**, Haeryfar SMM**:** Concurrent activation of iNKT and CD8+ T cell subsets by α-GalCer-pulsed tumor cells boosts the CD8+ T response to the most immunodominant epitope of SV40 large T antigen. Proc. Of the CIHR – Strategic training program in cancer research & technology transfer (CaRTT) and the department of oncology – research & education day, UWO, 2010

15) **Maleki Vareki S**, Haeryfar SMM: *i*NKT cells suppress T_{CD8+} response to the most immunodominant epitope of T Ag. Proc. Of the 4th Infection and Immunity Research Forum (IIRF), UWO, 2009

16) **Maleki Vareki S**, Zarkesh H and Emami H: Comparison of *S. aureus* and *E. coli* effects on CD11b expression and human peripheral blood stimulation. Proc. of the 9th Iranian congress of microbiology, Kerman Medical University, 2008 *(National conference)*

17) **Maleki Vareki S,** Zarkesh H and Emami H, Lak M and Babaie A: Study of peripheral blood neutrophil's biological response to *Helicobacter pylori* stimulation using flow cytometry technique. Proc. of the 162nd Society of General Microbiology, Edinburgh, United Kingdom (2008) *(International conference)*

18) Hashemi M, Shafiei S, Zarkesh H, **Maleki Vareki S** and Haghjooy-Javanmard S: Comparison of the effects of bare metal versus drug-eluting stent implantation on circulating endothelial cells following precutaneous coronary intervention for non-ST-elevation acute coronary syndrome**.** Proc of the 15th *International Vascular Biology Meeting*. Sydney, Australia, 1-5 June 2008, Sydney, Australia.

19) **Maleki Vareki S**, Zarkesh H, and Emami H: Study of Peripheral blood neutrophil's biological response to *Helicobacter.pylori* stimulation using flow cytometry technique. Proc of the 5th *National Biotechnology Congress of Iran* (2007)

20) **Maleki Vareki S**, Zarkesh H. and Emami H: Study of *h.pylori* effects on human neutrophil CD11b expression, Proc of the 10th research week of The University of Isfahan (2007)

21) Ahmadzadeh E, Zarkesh H, Roghanian R and **Maleki Vareki S**: Comparison of *H.pylori* & *E.coli* in expression of mRNA of inflammatory cytokines from human mononuclear cells. Proc of the 9th research week of The University of Isfahan (2006)